

The Modular Synthesis of Rigid Rod-like Scaffolds Towards Artificial Ion Channels

Emma K. Muehlberg

B.Sc. (Forensic and Analytical Chemistry), B.Sc. (Honours),
Flinders University

A thesis submitted in fulfilment of the requirements for the degree
Doctor of Philosophy

School of Chemical and Physical Sciences
Flinders University, Australia
September 2015

CONTENTS

Summary	v
Declaration	viii
Acknowledgments	ix
List of abbreviations	x
1. Introduction	
1.1 Introduction to Artificial Ion Channels	1
1.2 Artificial Ion Channel Design	2
1.3 The Lipid Bilayer	3
1.4 Ion Channel Conceptualisation - Head Groups	4
1.5 Introduction to Crown Ethers and their Synthesis	5
1.6 Architectural Variations within Cation Channels	9
1.6.1 Cation Channels incorporating more than one ionophore for transport <i>via</i> a relay approach	11
1.6.2 Cation Channels Incorporating One Central Ionophore for Transport	13
1.6.3 Cation ion channels constructed of α -helical amphiphilic peptide nanostructure	16
1.7 Rigid Rod-like Ion Channels	21
1.8 Summary of Transport Mechanisms	28
1.9 Introduction to Polycyclic Frameworks	28
2.0 Project Aims	31
<i>References</i>	32
2. Synthesis of the Hedaya Block with an Ethylene Linker	
2.1 Introduction	37
2.2 Design of an Artificial Ion Channel Based on A Polynorbornyl Framework	38
2.3 Synthesis of Polycyclic Norbornyl Linear Framework for Crown Ether Attachment (Hedaya Diene)	41

CONTENTS

2.4 Synthesis of Dopamine Derived Substituted Aromatic Crown Ethers	43
2.5 Synthesis and Reactivity of Acid Chloride Polycyclic (Hedaya Diene) Substrates	49
2.6 Investigations into the Decomposition of Dopamine	51
2.7 Imide Synthesis of Polynorbornyl Frameworks for the Attachment of Functionalised Alkyl Halides	53
2.8 Alternative Pathways to an Ethylene Linker	60
2.9 Wilgerodt-Kindler Reactions Towards an Ethylene Linker	64
2.9.2 Conclusions	71
<i>References</i>	72
3. Synthesis of the Hedaya Block with a Methylene Linker	
3.1 Introduction	76
3.2 Modelling of a Methylene Linked System	76
3.3 Substituted Aromatic Crown Ether Preparation and Attachment to the Polynorbornyl Imide	78
3.4 Variations in Coupling Reactions to Extend Polynorbornyl Frameworks	81
3.5 ACE Coupling Reactions of the Methylene linked Block	91
3.6 Crown Ethers and ^t BuOOH, ^t BuOK in THF	97
3.7 Epoxidation Reagents for Synthesis of Methylene Linked Polynorbornyl Blocks	98
3.8 Conclusions	101
<i>References</i>	102

CONTENTS

4. Synthesis of a Rigid System Based on a Direct Attachment	
4.1 Introduction	105
4.2 Molecular Modelling of the Polynorbornyl Scaffold with a Direct Attachment to the Benzocrown Ether	106
4.3 Aromatic Amine Crown Ether Preparation	107
4.4 Linking of the Backbone with Crown Ether with Model <i>endo</i> -Carbic Anhydride	109
4.5 Amalgamation of the Backbone with Crown Ether with Anhydride, 42 .	113
4.6 ACE Coupling Reactions to form Tricrown A	115
4.7 ACE Coupling Reactions to form Tricrown B	121
4.7.1 Tricrown Systems with Varying Crown Ether Sizes	126
4.8 Extension of Tricrown A to a Pentacrown System	129
4.9 End Block Functionality and Potential Pathways for Additional Pentacrown Systems	132
4.9.1 Conclusions	138
<i>References</i>	139
5. Monomer and Tricrown Transport Analysis	
5.1 Introduction	141
5.2 Electrochemical Impedance spectroscopy of Polycyclic Crown Ether Compounds	141
5.3 ¹ H NMR Titrations of Synthesised Crown Ether Systems	159
5.3.1 NMR Titrations with Potassium Salts	164
5.4 Black Lipid Membrane Analysis of Polycyclic Crown Ether Compounds	168
5.5 Calcein Release Studies from POPC (1-palmitoyl-2-oleoyl-sn-glycero-3-phosphatidylcholine) Vesicles	171
5.7 Conclusions	173
<i>References</i>	175

CONTENTS

6. Conclusions and Future Directions	177
7. Experimental	
7.1 General experimental Details	181
7.2 Experimental Procedures	182
7.3 Analytical Procedures	218
<i>References</i>	220
8. Appendix	
A.1 Bode plot of the bilayer recovery when TMAC is added to the tBLM with tricrown A	222

SUMMARY

Nature has developed a large number of ion channels and carriers which are complex systems that alter membrane permeability and allow the transport of alkali metal ions. This supramolecular process is of interest in the development of new transport systems to alter natural channel function for disease investigation.

Artificial ion channels with attached crown ethers as ionophores for cation transportation across lipid membranes have been extensively studied. Both semi- and fully synthetic channels have been investigated leading to a greater understanding of genetic diseases. The development and utilisation of new synthetic rigid rod channel systems have not been fully investigated.

The work presented in this thesis details the synthesis of rigid polycyclic frameworks with appended crown ethers for potential trans-membrane transport of alkali metal cations. The focus of this research is the development of new rigid-rod like compounds from the modular synthesis of polycyclic structures appended with crown ethers, with a high level of structural control. This research extends the established work on polycyclic norbornyl systems into creating new polycyclic compounds with appended crown ethers through a building block approach. The research carried out is most easily categorised by the number of carbon atoms linking the crown ether and the imide functionality (Figure I). Three systems were investigated using an ethylene (A), methylene (B) and a direct carbon link (C) described in Chapters 2, 3, and 4 respectively (Figure I).

The first stage of the research investigated a rigid polycyclic block with an ethylene attachment to a benzo-15-crown-5 ether as discussed in Chapter 2 (Figure I, A). Due to difficulties associated with this synthesis the ethylene attachment progressed towards a methylene connection (Figure I, B) of the polycyclic block and crown ether, discussed in Chapter 3.

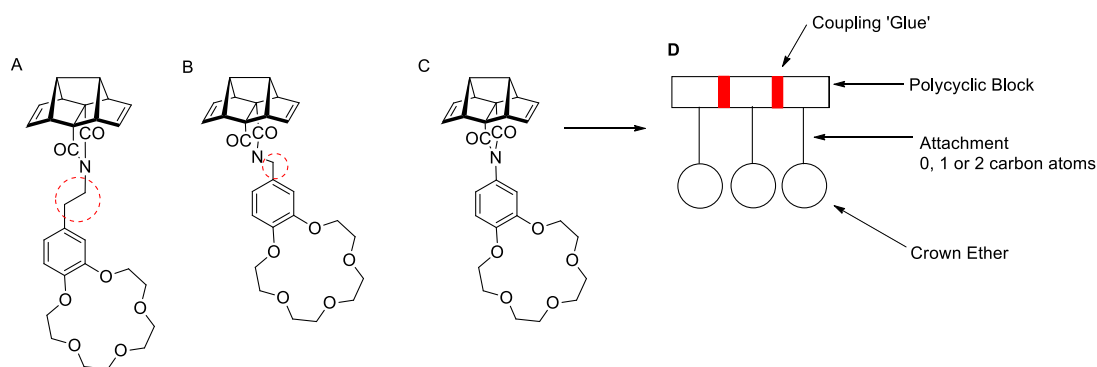


Figure I New polycyclic blocks with varying attachments between the imide and benzocrown ether, and their extension towards longer systems.

Although there was initial success in the synthesis of the compounds A and B outlined in Figure I, further synthetic procedures and methods were unable to yield coupled blocks which would see these systems extended as depicted in Figure I, D.

A new synthetic approach was required which saw all carbon units between the polycyclic norbornyl block and the crown ether removed (Figure I, C). This enabled the coupling of synthesised blocks into extended systems that were similar in length to a bilayer, and are discussed in Chapter 4.

Two tricrown systems, A and B (Figure II) were successfully synthesised and characterised by 1 and 2D NMR spectroscopy and HR-MS. Both of these tricrown systems, and similar monomer units, were analysed for complexation and transport with alkali metal ions through EIS, NMR and BLM as discussed throughout Chapter 5. Calcein release experiments were also undertaken.

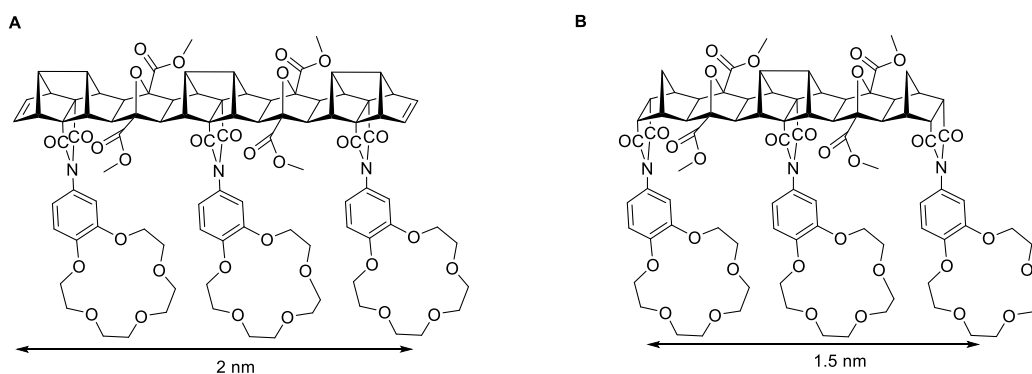


Figure II Two new polycyclic blocks with crown ethers appended for alkali metal ion transport.

The main results from these studies showed a significant trend, for both tricrown and monomer systems tested, to be the selectivity of potassium ions over sodium ions. Transport of potassium ions was monitored by the decrease in electrical resistance in EIS when the concentration of monomer was greater than 12×10^{-5} M. However the threshold concentration for transport of potassium ions with tricrown systems varied between 7×10^{-5} M and 14×10^{-5} M depending on the overall tricrown structure. These results are unusual given the preference for 15-crown-5 to complex with sodium ions rather than the larger potassium ions. However NMR complexation studies reinforced the selectivity of potassium ions (forming higher order complexes) as well as the complexation of sodium ions (1:1 and 1:2 complexes). These results are rather intriguing which require further investigation to gain a greater understanding of the potassium ion complexation as well as the mechanism of ion transport.

DECLARATION

I certify that this thesis does not incorporate without acknowledgement any material previously submitted for a degree or diploma in any university; and that to the best of my knowledge and belief does not contain any material previously published or written by another person except where due reference is made in the text.

.....
Emma Muehlberg

Dated:.....

ACKNOWLEDGMENTS

Firstly I would like to express my sincere thanks to both of my supervisors, Martin Johnston and Peter Duggan for the opportunity to undertake this PhD project and for their invaluable assistance and support along the way.

Next to my partner in crime Sam, who has been by my side every step of the way. The continued encouragement, support and understanding you have shown me along this journey has been truly invaluable. I look forward to starting the next chapter of our lives together with the new addition to our family.

Thanks to my ever supporting parents, who have been with me every step of the way, encouraging me to do my best at everything I undertake both professionally and personally.

Throughout the period of my candidature I have had the pleasure of working with a number of people within the organic chemistry department whom have had an influence on my life over the time spent undertaking this PhD. These people include:

My constant lab companions, Will Gibbs, Andrew Blok, and Gen Dennison, whom have made it easier coming into work every day with your continuous amusement, guidance and friendship.

A special mention to Thomas Hensel, for being one of my closest and best friends, your constant reassurance, assistance and understanding over the last few years has been admirable. Cheers for the never ending supply of Haighs chocolate and morning coffee.

Lastly, to Rebecca Norman and David Passande, for being great friends, I feel privileged to have met you along the way.

LIST OF ABBREVIATIONS

Abbreviation	Description
15C5	15-crown-5
AC	alternating current
Ac ₂ O	acetic anhydride
ACE	alkene and cyclobutene epoxide
ACN	acetonitrile
AcOH	acetic Acid
ATR	attenuated total reflectance
B15C5	benzo-15-crown-5
BLM	black lipid membrane
Bn	benzyl
BnBr	benzyl bromide
Boc	<i>tert</i> -butyloxycarbonyl
Boc ₂ O	<i>tert</i> -butyl dicarbonate
bs	broad singlet
CAN	ceric ammonium nitrate
Cbz	benzyloxycarbonyl
CE	crown ether
CF	5(6)-carboxyfluorescein
COSY	correlation spectroscopy
CPD	cyclopentadiene
d	doublet
DCC	N,N-dicyclohexylcarbodiimide
DCM	dichloromethane
dd	doublet of doublets
DMAD	dimethyl acetylenedicarboxylate
DMAP	4-dimethylaminopyridine

LIST OF ABBREVIATIONS

DMDO	dimethyl dioxirane
DMF	dimethylformamide
DMSO	dimethyl sulfoxide
DPTL	2,3-di- <i>O</i> -phytanyl- <i>sn</i> -glycerol-1-tetraethyleneglycol-D,L- α -lipoic acid ester
EDC	1-Ethyl-3-(3-dimethylaminopropyl)carbodiimide
EIS	electrochemical impedance spectroscopy
ESI	electrospray ionisation
EtOAc	ethyl acetate
EYPC	egg yolk phosphatidycholine
HCl	hydrochloric acid
HMQC	heteronuclear multiple quantum correlation
HOBt	1-hydroxybenzotriazole
HPTS	hydroxyrene-1,3,6-trisulfonic acid, tri-sodium salt
HRMS	high resolution mass spectrometry
Hz	hertz
IR	Infrared
J	coupling constant (Hz)
KOH	potassium hydroxide
LDA	lithium diisopropylamine
m	multiplet
MeLi	methyllithium
MeO	methoxy
MeOH	methanol
MS	mass spectrometry
MW	microwave
NaH	sodium hydride
NMR	nuclear magnetic resonance

LIST OF ABBREVIATIONS

NOESY	nuclear Overhauser effect spectroscopy
OD	oxadiazole
PC	phosphatidycholine
PCl ₅	phosphorus pentachloride
PEG	polyethylene glycol
PLB	planar lipid bilayer
PMB	<i>p</i> -mehoxybenzyl
POPC	1-palmitoyl-2-oleoyl-sn-glycero-3-phosphatidylcholine
ppm	parts per million
PTC	phase transfer catalyst
q	quartet
RT	room temperature
s	singlet
SUV	small unilamellar vesicles
t	triplet
TBAI	tetrabutylammonium iodide
tBLM	tethered bilayer membrane
^t BuOK	potassium <i>tert</i> -butoxide
^t BuOOH	<i>tert</i> -butyl hydroperoxide
TEA	triethylamine
TFA	trifluoroacetic acid
THF	tetrahydrofuran
TLC	thin layer chromatography
TMAC	tetramethylammonium chloride
Troc	2,2,2-Trichlorethoxycarbonyl chloride

CHAPTER 1

INTRODUCTION

1.1 Introduction to Artificial Ion Channels

The concept of ion channels and their role in the cell membrane was proposed in the late 1800's,^[1] before it was possible to examine their properties and structural identity. In the early 1950's Hodgkins and Huxley provided the mathematical basis for the flow of both sodium and potassium ions through axonal membranes identifying the movement of charged ions.^[2] Following this, Hodgkins and Keynes (1955), demonstrated that radioactive potassium ions could permeate the axon nerve membrane, allowing ions to move through the membrane in a "single file" described as a "channel".^[2] Since then there have been numerous sophisticated approaches and investigations into natural and synthetic ion channels. The design and synthesis of new compounds has led to advances in the development of artificial ion channels and carriers (cationic and anionic) to facilitate therapies and cures related to channelopathies.^[3]

The study of natural transmembrane ion channels is one of the most investigated areas in modern biochemistry.^[4-6] Ion channels are comprised of vital membrane proteins which form aqueous pores with the potential to open and close - allowing the flow of ions through the cell membrane. This is commonly referred to as ion channel translocation.^[7] Ion channels are selective for the transport of particular ions across the cell membrane.^[7] The flow of ions is dependent on the electrochemical gradients within the cell which are also ion-specific,^{[8],[9]} thus facilitating cation or anion exchange across a membrane.

Natural ion channels can be formed from a number of non-protein natural compounds, for example Gramicidin. Gramicidin is a heterogeneous mixture of several antibiotic compounds isolated from *Bacillus Brevis* and is active against gram-positive bacteria.^[10,11] This is achieved by the 'formation of membrane channels that are specific for monovalent cations such as H⁺ and alkali metals'.^[10] Formation of the Gramicidin ion channel has been explained *via* the barrel stave model shown in Figure 1.1.1. Gramicidins are believed to function by the formation of an internal channel within the hydrophobic section of the lipid bilayer (Figure 1.1.1).

Scientists have attempted to incorporate aspects of natural ion channel-forming compounds like Gramicidin into new artificial channels^[12-17] that may be useful for diseases in which ion channel function has been disrupted e.g. cystic fibrosis.^[18,19]

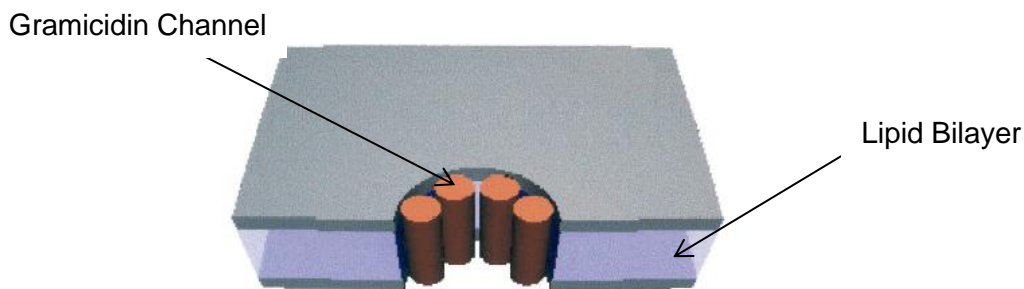


Figure 1.1.1 Yang's barrel-stave model of Gramicidin incorporated into the lipid bilayer.^[20]

The central issues around artificial ion channel design as well as some literature examples will now be discussed.

1.2 Artificial Ion Channel Design

One of the most important aspects of artificial ion channel synthesis is the design. It is essential to incorporate appropriate structural properties such as channel size, shape and orientation within the lipid bilayer (Table 1.2.1).^[21]

Table 1.2.1 Gokel's criteria for ion channel conceptualisation.^[21]

Feature	Criteria
Bilayer membrane	Thickness, typical composition, headgroups
Donor groups within the channel	Identity, cation affinities, strong vs weak, number and placement within the channel
Headgroup	Entry portal function, anchoring function, selectivity function
'Central Relay'	Structural, functional, interaction with cation or water or both
Other Issues	Overall length, extension past headgroups, direct interaction with aqueous environment, role of water, association of water with cations

These design principles have been utilised in the preparation of many new channel systems.^[22–26] In addition to these principles Fyles proposed that ‘the ion channel should have a polar core which is surrounded by a non-polar exterior layer for simultaneous stabilisation of an ion in transit and have favourable interactions with membrane lipids’.^[17] This allows the channel to self-assemble within the membrane rather than on the surface, thus permitting ions to traverse the bilayer.

Secondly Fyles placed emphasis on the overall length and shape of the ion channel so that it is suitable to align within the lipid bilayer (approximately 40 Å in thickness).^[17] An in-depth discussion of these principles in relation to previously designed systems and their use in the development of the proposed novel rigid ion channel will follow.

1.3 The Lipid Bilayer

It is known that all biological membranes are based on the lipid bilayer, which is composed of phospholipids with hydrophobic properties.^[27] The hydrophobic effect is one of the most important influences on biological macromolecular structures in that the bilayer is arranged so that polar head groups interact with water and the non-polar tails do not, as shown below in Figure 1.3.1.^[27]

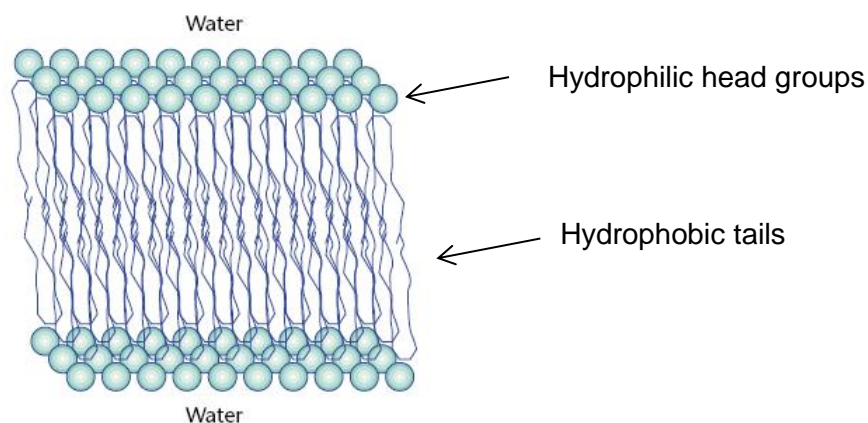


Figure 1.3.1 Yeagle and co-workers lipid bilayer arrangement composed of phospholipids.^[27]

The lipid bilayer forms a continuous barrier around cells, keeping ions and proteins in position by preventing diffusion across the membrane. Three polarity regimes of the phospholipid bilayer have been identified. These are; polar head groups, the hydrocarbon insulator regime and the mid-polar regime (Figure 1.3.2). Through electrophysiological measurements of the structure outlined in Figure

1.3.2, the thickness of the insulator regime (hydrocarbon chain), was found to be typically 30-40Å.^{[21],[28]}

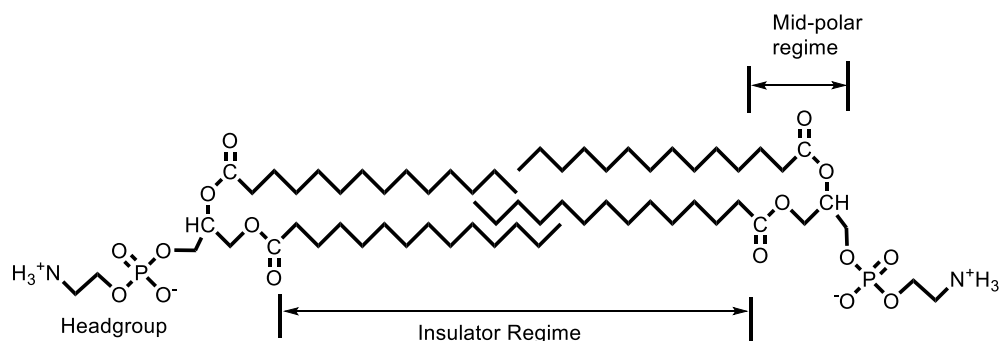


Figure 1.3.2 The three polarity regimes of the phospholipid bilayer – headgroup, insulator and mid-polar.^{[21],[29]}

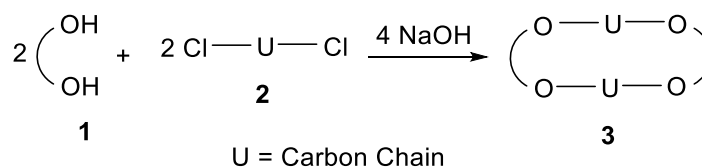
1.4 Ion Channel Conceptualisation - Head Groups

Head groups are an important aspect in the design and synthesis of ion channels due to their ability to help anchor channels within lipid bilayers. A flexible ion channel structure would require an anchoring group that has specific properties to hold the compounds position in relation to the bilayer.^[21] The most active materials have hydrophilic head groups where transport activity is controlled by structural variables.^[17] Therefore, a balance of hydrophilic and lipophilic groups in the wall units and a total length which is compatible with the bilayer thickness is required for successful transportation of ions. Incorporation of head groups at the end of the channel may help facilitate the channel's incorporation into the bilayer, thus allowing for successful ion translocation.

However, an ionophore, such as a lipid-soluble molecule such as a crown ether, must align itself from the interior to exterior of a membrane to allow the flow of ions.^[30] Thus, the receptor and the ionophore are functionally linked. There are a number of ionophores which have been described within the literature such as, peptide, steroid, calixarene and sugar based systems, including general macrocycles (crown ethers).^[24,31–35] Herein the following discussion will focus largely on crown ethers as ionophores, with limited discussion of other types of channels.

1.5 Introduction to Crown Ethers and their Synthesis

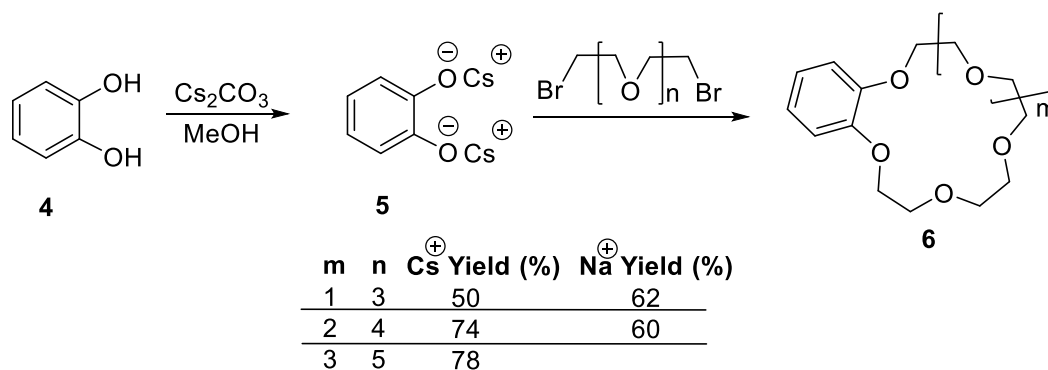
Crown ethers are one of the most commonly used family of host compounds in supramolecular chemistry.^[36] In 1967, Pedersen reported the synthesis of a class of macrocyclic polyether's labelled 'crown ethers',^[36] which were shown to have selective complexation affinities with metal cation, neutral and anionic species.^[37] It was demonstrated that the particular metal ions could be used as templates for the formation of crown ethers. Crown ethers can be prepared *via* numerous pathways which rely upon the Williamson ether synthesis, Scheme 1.5.1.^[36,38]



Scheme 1.5.1 Synthesis of crown ethers *via* Williamson ether synthesis.^[36]

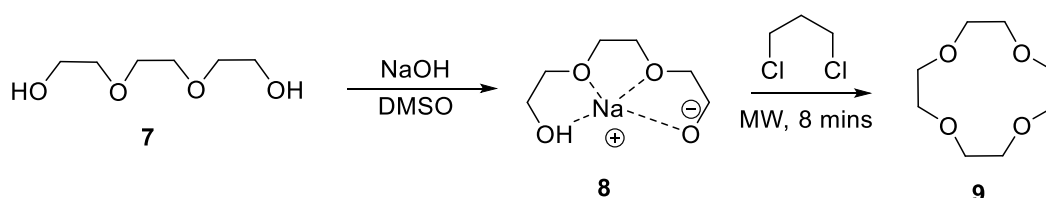
The preparation of crown ethers is widely reported throughout the literature.^[36,39–44] Crown ether synthesis can utilise a range of cyclisation strategies including the template and cesium effect, the high dilution principle and phase transfer catalysts.^[39–43,45–50]

The 'cesium effect' has been used by a number of groups to synthesise large macrocycles in high yields, reducing side reactions.^[41,51,52] This approach involves the use of cesium carbonate and/or cesium fluoride in an organic solvent such as MeOH, ACN or DMF to synthesise dibenzocrown ethers or ring compounds bearing 8-12 atoms. The synthesis of smaller macrocyclic systems with cesium salts has also been reported by Kellogg and co-workers (Scheme 1.5.2) and has been achieved with similar or decreased yields.^[42,51] The cesium effect directly relates to the 'template effect', which employs alkali metal hydroxides or smaller metal carbonates such as sodium or potassium which are highly suited for the synthesis of smaller crown systems.



Scheme 1.5.2 Synthesis of aromatic crown ethers of varying size.^[51]

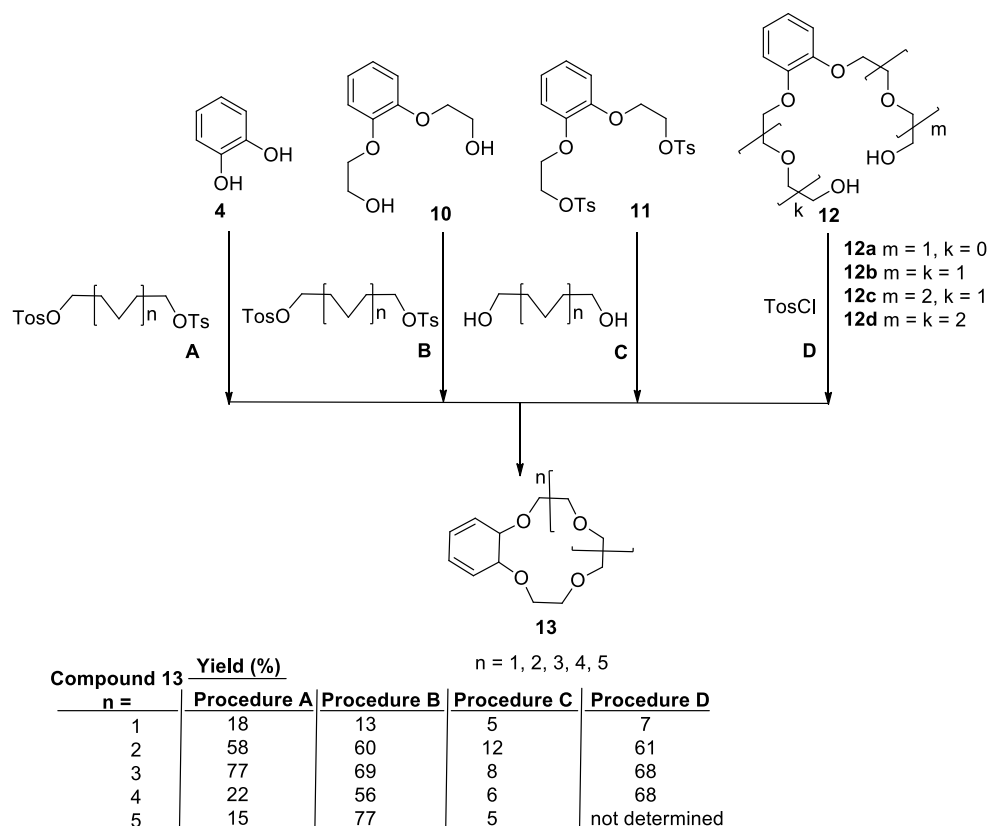
In addition to the cesium and template effects, an alternative approach can be taken using the high dilution principle. The high dilution principle is based upon a large increase in solvent (high dilution) versus crown ether reagents, decreasing dimerisation and increasing ring formation. The dilution technique requires increased addition rates of the monomer to decrease the formation of dimer at a maximum concentration between 10^{-2} - 10^{-3} mol/L. This leads to the favourable intramolecular cyclisation over the intermolecular reaction.^[43] Issues that may accompany the use of the high dilution technique which include dimerization may be reduced when the template effect is used in conjunction with this principle. The template effect relies on pre-organisation with alkali metals with oligomers as shown in Scheme 1.5.3.



Scheme 1.5.3 An example of the template effect associated with the use of the alkali metal ion Na⁺ from NaOH.^[50]

Crown ethers can additionally be synthesised *via* the templating of alkali metals *via* phase transfer catalyst (PTC) reactions.^[39] These types of reactions also rely on the addition of alkaline solutions. In PTC reactions the rate of the nucleophilic reaction increases, therefore increasing macrocyclic ring formation, leading to higher yields.^[24] In Scheme 1.5.4, four different routes demonstrate PTC reactions to generate benzocrown ethers. Route A is the most convenient for crown synthesis, as the macrocycle is produced in one step. The remaining routes (B-D) entail variations in starting materials, requiring multiple steps and

therefore a reduction in the overall yield. These PTC reaction conditions are used in this thesis to synthesise the crown ether ionophores (see Chapter 4, Section 4.3).



Scheme 1.5.4 Bogaschenko and co-workers pathways for the synthesis of aromatic crown ethers using PTC conditions.^[39]

Crown ethers are neutral colourless low molecular weight polyethers with sharp melting points,^[46] which display some solubility in water, alcohols and aromatic solvents and are very soluble in methylene chloride and chloroform.^[46] Crown ethers are susceptible to the substitution reactions that are characteristic for aromatic ethers.^[46]

Crown ethers are highly popular for use in supramolecular chemistry due to their ion channelling abilities and host capabilities,^[36] and as such have been used in many ion channel designs, where metal ions are complexed by the crown ethers.^[46] For instance sodium ions are bound in the cavity of the crown ether by electrostatic attraction between its positive charge and the dipolar charge on the six oxygen atoms on the polyether ring.^[46]

It is important to have an understanding of the crown ether structure, cavity size and diameters for the complexation of various alkali metals. The structures of simple and synthetically accessible crown ethers with various cavity diameters and ionic diameters for complexing with alkali metals are shown in Figure 1.5.1. The selectivity of metal binding with crown ethers has been described as the 'lock and key' approach where 18-crown-6 has cavity dimensions which are similar to the dimensions of the potassium ion.^[36] This is similar for the 15-crown-5 and 12-crown-4 where the cavity sizes are more suited to the sodium and lithium ions respectively. This suggests that particular crowns are more selective for particular alkali metal ions than others. The 18-crown-6 can form complexes with both potassium ions and sodium ions.^[36]

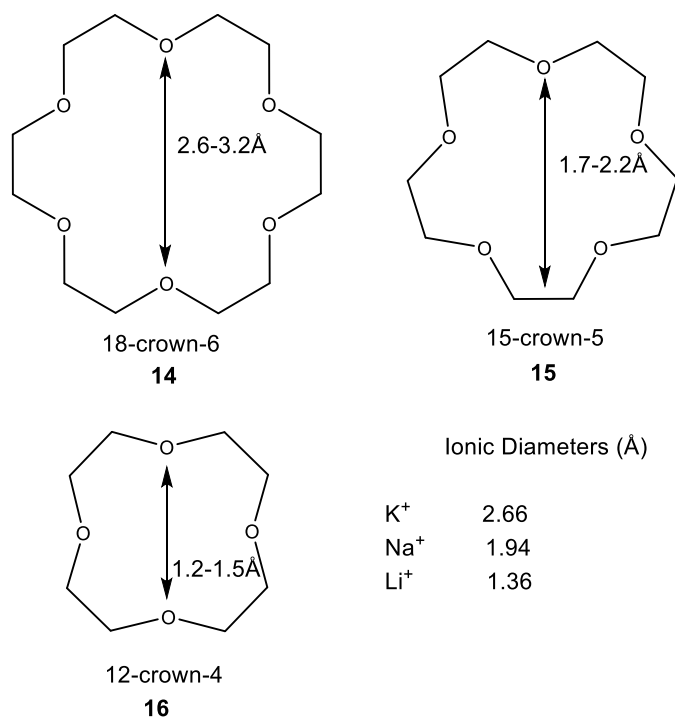


Figure 1.5.1 Structures of simple crown ether cavity diameters and alkali metal diameters.^[36]

Crown ethers are also able to solubilise metal ions in solvents they would be traditionally insoluble in. The crown ethers solubilisation process is shown in Figure 1.5.2. The 18-crown-6 has the ability to effectively coordinate with a potassium ion within the polyether ring (Figure 1.5.2). Given that the complex has a hydrophobic ('greasy') exterior it is not surprising that it has been found to be readily soluble in nonpolar or dipolar aprotic solvents.^[36] However to achieve

electrical neutrality the anion must accompany the crown ether complex into solution.

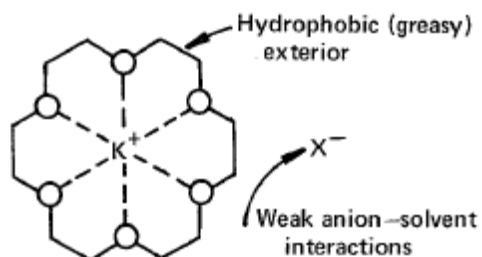


Figure 1.5.2 Binding of 18-crown-6 with potassium ions in solution.^[36]

1.6 Architectural Variations within Cation Channels

Having now looked at crown ethers and their properties, artificial ion channels will be investigated, focussing mainly on systems containing crown ethers.

The first synthetic ion channel was prepared by Tabushi and co-workers in 1982, using a substituted β -cyclodextrin **17** (Figure 1.6.1B).^[53,54] This substituted β -cyclodextrin molecule was designed to be a barrel-shaped entity spanning a single side (leaflet) or half of a lipid bilayer (Figure 1.6.1A). The “half channel” was found to be soluble in typical organic solvents (chloroform, methanol), however the channel was insoluble in water even though it had strong hydrophilicity from the cyclodextrin.^[53] The “half channel” showed a moderate association constant ($K_{\text{ass}} > 10^4 \text{ M}^{-1}$) for both Cu^{2+} and Co^{2+} allowing the substituted β -cyclodextrin to be investigated further as a channel forming compound.

The β -cyclodextrin ion channel becomes “active” when two molecules in opposite leaflets self-assemble in an end-to-end configuration. Once the β -cyclodextrin molecules are established in an end-to-end arrangement, ions can flow freely from one side of the bilayer to the other (Figure 1.6.1A). The estimated length of the overall dimer was determined to be 48\AA .^[53] The length was designed in this form to align with lecithin molecules of the bilayer and utilise a number of equally spaced binding sites for metal ion transport.

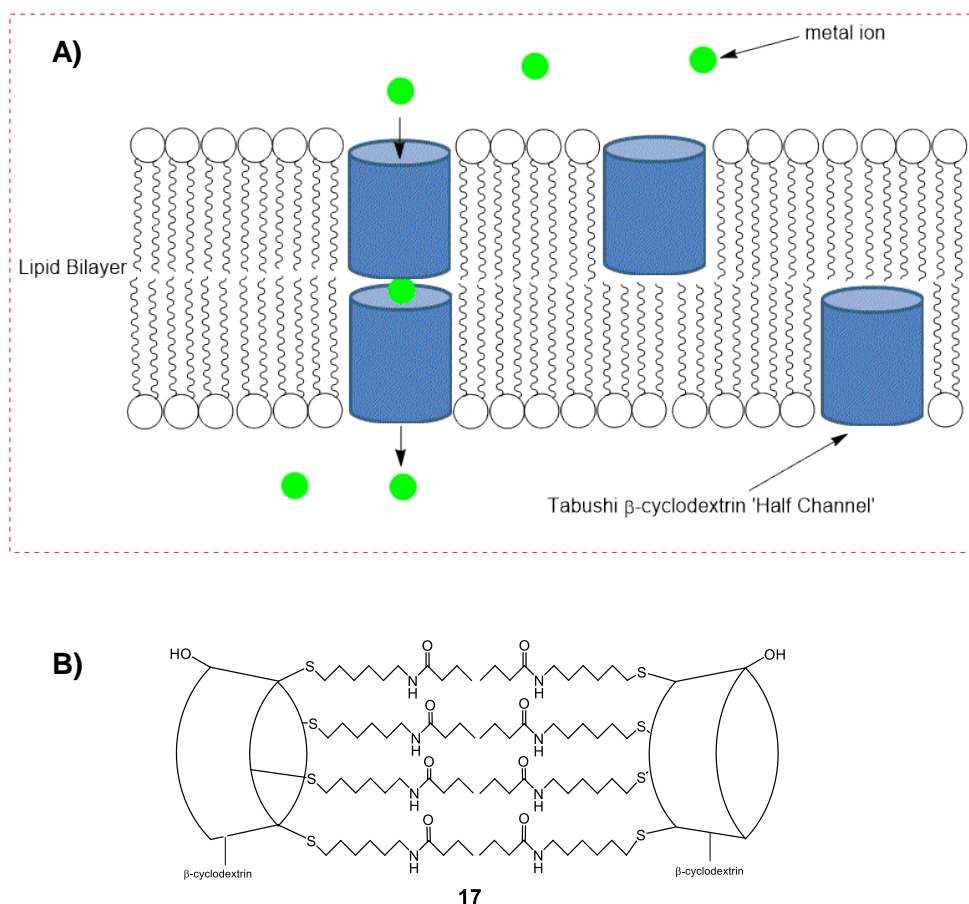


Figure 1.6.1 Tabushi and co-workers (1982) representative synthetic ion channel based upon a substituted β -cyclodextrin. **A)** Illustration of the "half channel" forming in opposite sides of the lipid bilayer, **B)** Structure and alignment of the complete channel.^[53]

The transport of Cu^{2+} and Co^{2+} ions across egg lecithin membranes was evaluated by incorporating the "half channel" into a lipid bilayer.^[29] Aqueous solutions of CoSO_4 or CuSO_4 were used to measure the rate of metal ion transport across the membrane.^[53] An increase in characteristic absorption for both solutions at 310 nm of artificial liposome incorporating Tiron (4,5-Dihydroxy-1,3-benzenedisulfonic acid disodium salt, a complexing agent) and Co^{2+} was observed.

An artificial liposome was prepared with Tiron incorporated in the interior. To this purified liposome the channel was added forming the liposome containing both Tiron and the artificial "half channel".^[53] This liposome was then combined with the aqueous alkali metal salt solutions. The rate of alkali metal ion transport was monitored from the outside to the interior aqueous solution across the liposome with the incorporated "half channel".^[53] This was monitored by following the increase in absorption of Tiron and the alkali metal complex.

The rate of the Co^{2+} followed second order kinetics in relation to channel concentration while rates for Cu^{2+} transport followed first order kinetics.^[29,53] The channel transport rate was reported to be $4.5 \times 10^{-4} \text{ s}^{-1}$ at $55 \mu\text{M}$ for the Co^{2+} ion.^[53] It was identified that the channel transport rate was 'much faster than with the specific carriers; e.g. $5.4 \times 10^{-5} \text{ s}^{-1}$ under the corresponding conditions for 18-azacrown-6'.^[53]

1.6.1 Cation Channels incorporating more than one ionophore for transport via a relay approach

Following the first example, more sophisticated artificial ion channels have been developed. Since the mid 1990's research into synthetic ion channels has broadened to include various new molecular architectures including, central relay, central core and rigid systems such as cation pi-sliders.^[29,55] In 2001 Gokel and co-workers designed a synthetic ion channel **18** based on a central relay mechanism (Figure 1.6.1.1).^[21] This particular ion channel was designed with distal macrocyclic crown ether headgroups which also served as entry portals for transport across the lipid bilayer.^[21] The third crown ether in the central hydrophobic region acted as a relay moiety to help with polar stabilisation and cation transport across increased distances (such as 30 \AA). Initial design studies suggested that the crown ether residues would stabilise the position of the channel structure within the bilayer.^[21]

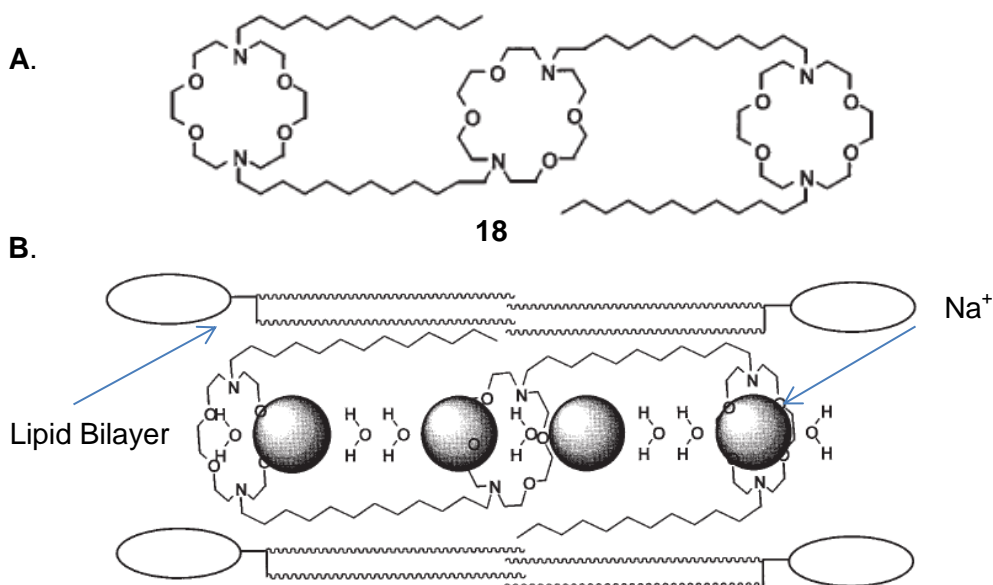


Figure 1.6.1.1 A) Gokel and co-workers proposed central relay ion channel based upon 18-crown-6 azacrown with C_{12} hydrocarbon chains. B) Proposed incorporation of the central ion channel into the lipid bilayer.^[21]

The additional hydrocarbon chains were thought to align in the lipid bilayer with the fatty acid chains (Figure 1.6.1.2). It was expected that the channel would insert into the lipid bilayer whereby a partially hydrated sodium ion would enter the bilayer *via* the distal macrocycle. This would eventually form a chain with water and sodium ions (Figure 1.6.1.1B).^[21] When the pores were filled the addition of another sodium ion at the distal macrocycle would force out a cation on the opposite side of the membrane as shown in Figure 1.6.1.1B.

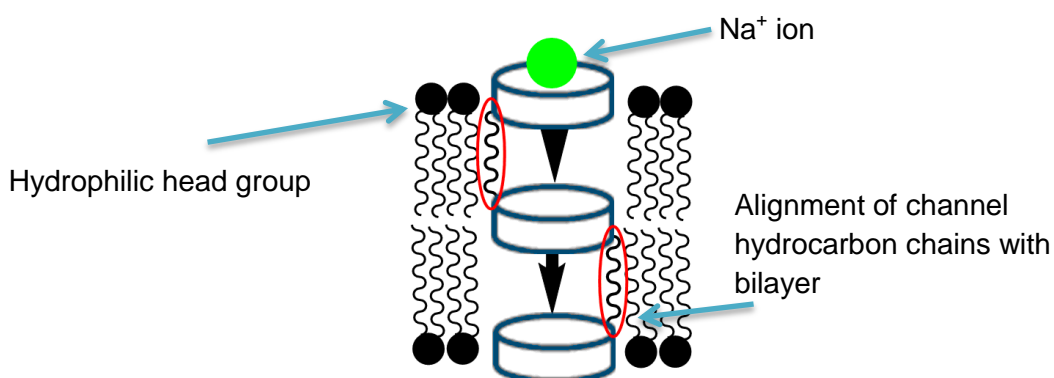


Figure 1.6.1.2 Gokel and co-worker's channel with hydrocarbon chains aligned with the hydrophobic section of the lipid bilayer.^[21]

The headgroups of the channel were designed to be spaced approximately 30-35 Å apart to be consistent with the width of the insulator regime of a typical phospholipid bilayer. This spacing was established with the use of covalent dodecyl spacers (in alignment with fatty acid chains of lipid bilayer) separating the distal macrocycles by 30 Å (Figure 1.6.1.3).^[21] Attachment of dodecyl spacers opposite to the covalently attached chains were secured at the ends of the molecule (Figure 1.6.1.3). This allowed for any adjustment necessary in regards to size, shape and function of the channel. However further research revealed that the dodecyl spacers were not necessary and that the channel was more active having CH₂Ph side chain substituents attached.^[21]

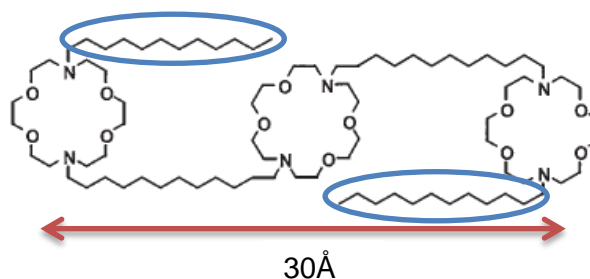


Figure 1.6.1.3 Gokel and co-workers channel with hydrocarbon chains with an overall length of 30 Å.^[56]

The synthetic ion channel was tested for cation (Na⁺) transport by ²³Na nuclear magnetic resonance (NMR). The Na⁺ exchange rate, *K*, based on Na⁺ in and out of the liposome was shown to be 50 s⁻¹ and was compared to that of Gramidicin (175 s⁻¹), a natural ion channel.^[21] These results demonstrated that the artificial ion channel was 30% less active than Gramidicin. This has relevance for this work because it revealed that the spacing between the aza-crown ethers and the carbon chains has a strong influence on the overall transport ability of the system.

1.6.2 Cation Channels Incorporating one Central Ionophore for Transport

A different approach to Gokel's artificial channels was to have only one central ionophore. Molecules based around a central scaffold have also been used for ion translocation through lipid bilayers.^[57] In the central scaffold strategy a cyclic structural unit (such as a cyclodextrin or crown ether) acts as a building block to which the channel walls are attached.

Julien and Lehn reported one of the first 'full span channel models' built around a central scaffold of a tartaric acid based crown ether **19**.^[57] The design was

described as ‘a molecular sheaf formed by bundles of oligo(oxyethylene) chains grafted on a macrocyclic polyether’.^{[29],[57]} The design of the structure was referred to as a ‘chundle’ and described as a mixture of a channel and a bundle of axial chains containing oxygen groups for cation binding sites. These long chains, as shown in Figure 1.6.2.1, allow the molecule to span the length of a typical lipid bilayer. It was estimated that the overall length of the ‘chundle’ channel was 45-50Å.^[57] The channel was thought to assemble within the lipid bilayer through the interactions between the carboxylate groups (on the eight oxygen containing chains) and the water/membrane interface.^[57] No transport data was reported for the channel.

In later studies the central scaffold was changed to a β -cyclodextrin structure **20**, termed the ‘Bouquet’ approach for artificial ion channels. In the ‘Bouquet’ approach, the overall strategy was similar to the ‘chundle’^[58] with poly(ethylene oxide) chains appended to a central scaffold derivative of β -cyclodextrin. Transport studies, however, indicated poor translocation of alkali metal ions.^[29,58]

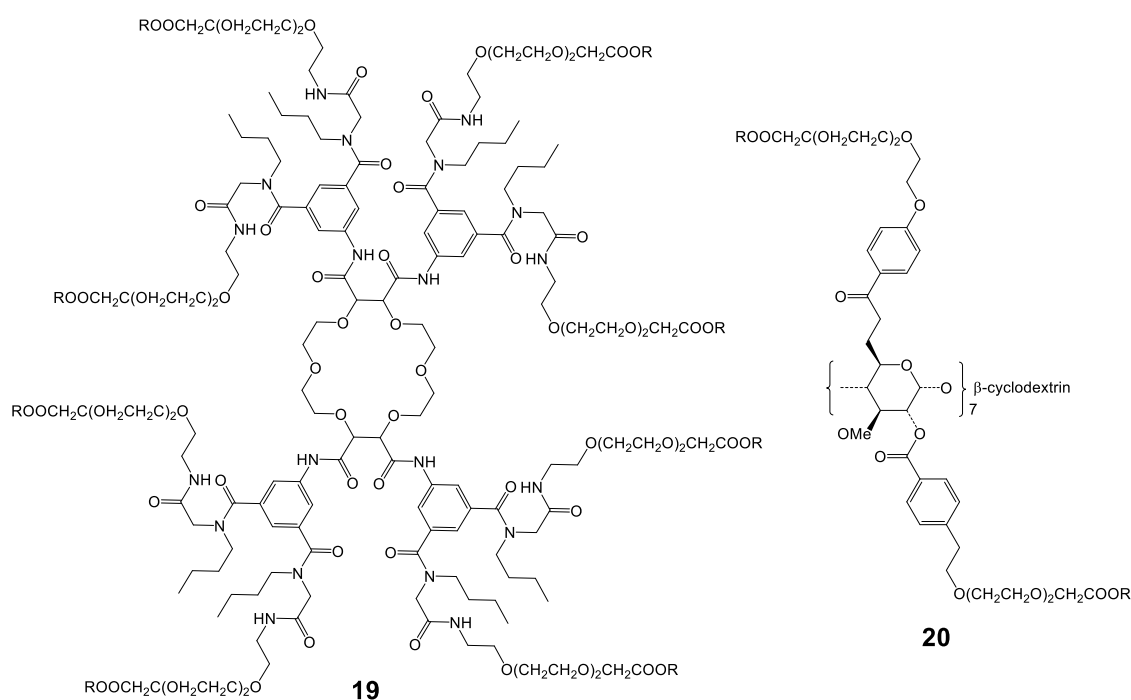


Figure 1.6.2.1 The ‘Chundle’ and ‘Bouquet’ ion channels incorporating central crown ether and β -cyclodextrins.^[29]

Building on the work of Julien and Lehn, Frye and co-workers attached six cholesterol units to a tartaric acid-18-crown-6 central macrocycle shown in Figure 1.6.2.2.^[29,59]

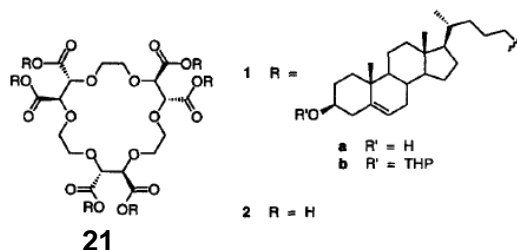


Figure 1.6.2.2 Frye and co-workers tartaric acid based 18-crown-6 ether with six cholesterol units attached.^[59]

The structure was designed so that three of the cholesterol units faced in one direction whilst the other three faced in the opposite direction, forming a cylindrical shape. The walls of the channel were comprised of the cholesterol units which could interact with the fatty acid chains of the bilayer.^[59] The 3-hydroxyl groups situated in the cholesterol attached to the macrocycle were expected to serve as headgroup anchors aligning the channel within the bilayer.^[29] The ion channel transport efficiency was analysed *via* Riddell and Hayer's dynamic NMR method for Li^+ and Na^+ translocation.^[59]

This process of Li^+ and Na^+ NMR involves direct monitoring of the signals of the transported species on either side of the membrane. In ^{23}Na NMR, liposomes from phospholipids are produced in the presence of dilute NaCl. This is to ensure that sodium ions are present both inside and outside the vesicles. Due to similar magnetic environments there is only one signal observed for Na^+ . However upon addition of Dy^{3+} an NMR shift reagent, both external and internal sodium signals were observed.^[60] Once the channel inserts into the liposomes, equilibration of Na^+ ions in and Na^+ ions out commences and the exchange rate can then be monitored. In this instance from Frye, the cation transport efficiency was demonstrated to be low suggesting there may be other 'interactions between the crown ethers and the alkali metal cations'.^[29,59]

Using the same central relay approach based on the tartaric acid-18-crown-6 motif, Fyles and co-workers designed a tunnel incorporating twin bola-amphiphiles as the walls.^[9,17,29] The twin bola-amphiphiles are defined as macrocycles which consist of two head groups and two hydrocarbon linking chains. The amphiphiles are linked to the central scaffold *via* ester linkages

forming channel **22** as shown in Figure 1.6.2.3. The carboxyl groups at the end of each amphiphile were proposed to act as the headgroups and help arrange the channel in the lipid bilayer by interacting with the hydrophilic fatty acid chains and the polar exterior.^[17] Various twin bola-amphiphiles were assessed and their transport efficiency analysed *via* dynamic NMR. Dynamic NMR (variable temperature) is used to obtain information in regards to time-dependent phenomena. The transport efficiency for the channels which had non-polar ‘walls’ was found to be greater than those constructed from ethyleneoxy units.^[29] It was rationalised that the hydrophobic lining causes an unreactive surface to a diffusing ion over a considerable length of the channel, suggesting that the polarity may be increased and in turn enhance transport efficiency. Whilst, it was identified that ‘half of the synthesised channels were ion carriers (i.e. bind ions and carry across the bilayer) rather than ion channels (opens in the presence of specific ions to flow through the membrane)’.^[29] There were two channel structures which showed greater selectivity for potassium ions than any other metal cations.

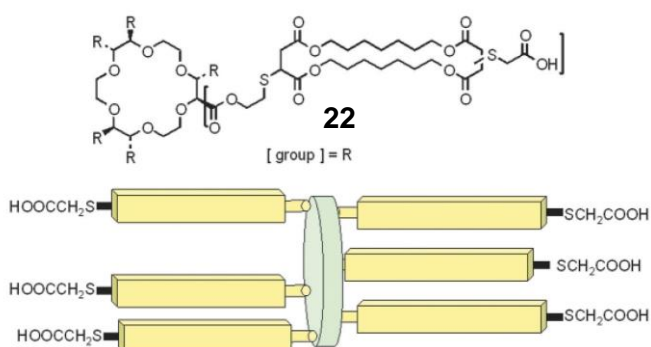


Figure 1.6.2.3 Fyles and co-workers ‘Hydrapile’ ion channel design.^[29]

1.6.3 Cation Ion Channels Constructed of a α -helical Amphiphilic Peptide Nanostructure

In addition to both the central relay and central scaffold ion channels discussed previously, α -helical amphiphilic peptide nanostructures have been used for cation translocation through lipid bilayers.^[61] An example of an α -helical amphiphilic peptide nanostructure **23** was designed and synthesised by Voyer and co-workers in 1995.^[61] These nanostructures have considerable relevance to this thesis and will be discussed in some detail.

Voyer and Robitaille reported a fast, simple and efficient approach for the synthesis of a novel artificial ion channel based upon a 21 amino acid peptide incorporating 15 L-leucines and six 21-crown-7 L-phenylalanine groups (Figure 1.6.3.1).^[61] The amino acids, leucine and alanine were chosen in the structural design due to their hydrophobic nature. Therefore incorporating these amino acids into a peptide should impart lipophilicity and facilitate interactions with the lipid bilayer. Leucine and alanine are also known to have a strong propensity to orientate in an α -helical conformation.^[61] The amphiphilic peptide nanostructure was synthesised *via* solid phase peptide synthesis using an oxime resin.^[61,62]

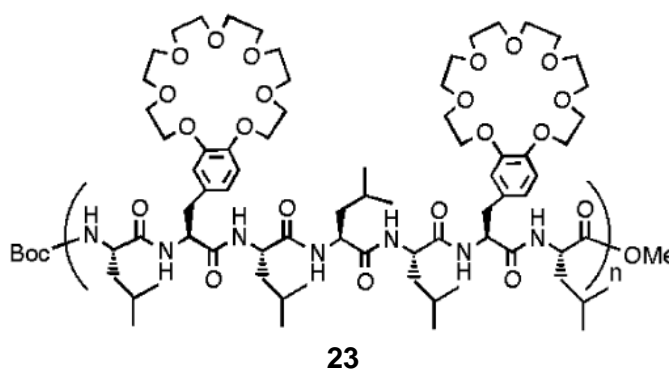


Figure 1.6.3.1 Voyer and co-workers schematic representation of the α -helical amphiphilic peptide nanostructure ($n = 1$ 7-mer, $n = 2$ 14-mer, $n = 3$ 21-mer).^[63]

The 21-crown-7 artificial ion channel was analysed for membrane conductivity by PLB (planar lipid bilayer/ black lipid membrane)^[64] which indicated that the peptide was orientated into the lipid bilayer, as demonstrated by the observations of various amplitudes of transmembrane currents.^[64]

Following on from previous work, in 2002 Voyer and co-workers investigated amphiphilic helical peptide membrane disruption using a 21-mer (3 repeating sequence of seven amino acids) and a 14-mer (2 repeating units of seven amino acids) channel.^[63] It was identified *via* calcein leakage studies that the 14 residue peptide containing four 'benzo-21-crown-7 side chains aligned along one face induced significantly more vesicle leakage than analogues 21-mer or 7-mer peptides'.^[63] This is due to the difference in overall length of the peptide in comparison to the hydrophobic section of the bilayer - what the authors have designated a 'hydrophobicity mismatch effect'.^[65] Due to the length of the 14-mer peptide (21Å), the 'hydrophobicity mismatch effect' and the cross-sectional shape determines whether the prepared peptides interact with the lipid bilayer hence

determining their ion transport ability.^[63] In this instance both the 7-mer (11Å) and 14-mer lacked sufficient length to span the bilayer and transport as an ion channel compared to the 21-mer (31Å). In comparison the 7-mer acted as an ion carrier, whereas the 14-mer was neither a carrier nor a channel, but rather disrupts vesicles.

Later studies showed that the synthesised 21-mer peptides bearing the six 21-crown-7 moieties were able to transport ions in a similar manner to that of natural ion channels.^[62] Further investigations into the modification of C- and N-terminal groups of the 21-mer peptide were undertaken to optimise cation transport and orientation within the bilayer. The study incorporated hydrophilic non-ionic units to allow for stabilisation and incorporation of the ion channels within the lipid bilayer.^[66] Hydrophilic groups at both C and N termini in this example led to more efficient incorporation into the lipid bilayer. Increasing the number of terminal hydrophilic groups gave improved water solubility with slight inhibition of membrane incorporation.^[66]

Further investigations into the mechanism of action of the synthetic peptide involved circular dichroism, ²³Na NMR, ³¹P and ²H solid state NMR.^[65,67] The modes of action for the 14-mer were determined by NMR (³¹P and ²H solid state) to be at the surface of the bilayer in an in-plane orientation minimising the hydrophobic mismatch effect allowing for the peptide to interact with the polar head groups of the bilayer (Figure 1.6.3.2). In comparison, the 21-mer peptide does not encourage the hydrophobic mismatch between the peptide and bilayer therefore indicating that there is a transmembrane topology. Previous ATR (attenuated total reflectance) studies have suggested that the peptide may be in equilibrium between the in-plane and transmembrane orientations as shown below in Figure 1.6.3.2.^[65]

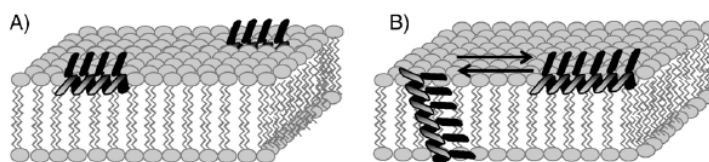


Figure 1.6.3.2 Models proposed for the binding of 14-mer (A) and 21-mer (B) peptides in DMPC lipid bilayers.^[65]

In 2007 Voyer and co-workers investigated the cytolytic activity of the α -helical peptide nanostructures (14-mer, 21-mer) *via* the incorporation of varying acidic dipeptide groups at both the C- and N-termini.^[68] It was noted that the addition of hydrophilic or hydrophobic C- or N- terminal groups had a significant impact on the ion channels lysing ability.

In 2011 Voyer and co-workers looked at using analogues of an α -helical synthetic peptide ion channel to study the mechanism of cation transport within the lipid bilayer.^[22] Derivatives of the synthetic ion channel varied with two, three, four and six 21-crown-7 ether relay sites (Figure 1.6.3.3).

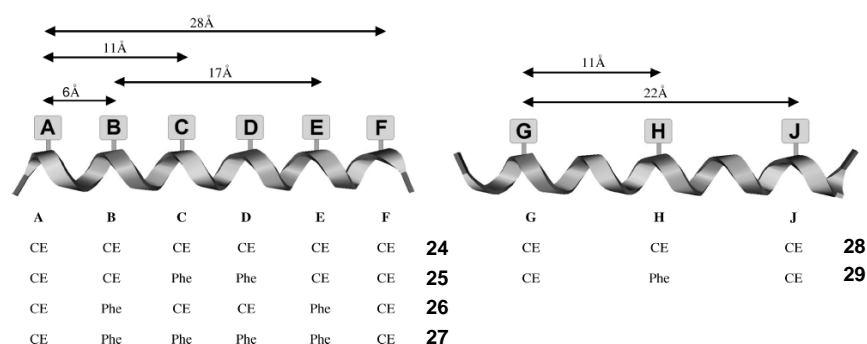


Figure 1.6.3.3 Voyer and co-workers list of various peptides and crown ether distances which were used in the analysis of sodium transport across the lipid bilayer.^[22]
(CE = crown ether).

The transportation of Na^+ across the lipid membrane for all 6 peptides (**24-29**), (Figure 1.6.3.4) was measured *via* fluorescence assays using pyranine as a pH dependant fluorescent probe. The probe was covered in phosphatidylcholine (PC) at a pH of 6.2 inserted into a Na^+ ion solution at pH 7.2.^[22] The channel transport was observed when cations enter the vesicles, forcing protons to escape to maintain ionic equilibrium (Figure 1.6.3.4). For each peptide the membrane transport was measured for 400 s, with an increase in fluorescence observed over time.

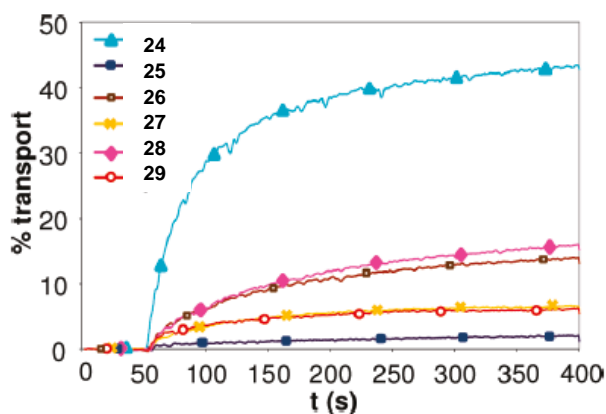


Figure 1.6.3.4 Voyer and co-workers fluorescent experiments of Na^+ ion transport with peptides **24-29** added at 50s and terminated at 400s with Triton X-100.^[22]

The results indicated (Table 1.6.3.1) that the maximum distance a Na^+ ion can travel between two relay sites in a lipid bilayer was 11Å . Thus, peptide **24** (Table 1.6.3.1, Figure 1.6.3.3) was observed to be the most efficient Na^+ ion transporter with a distance between relay sites of only 6Å . Peptides **26** and **28** had relay site distances of 11Å and hence reasonable Na^+ ion transport was observed.^[22]

Table 1.6.3.1 Voyer and co-workers results of Na^+ transport at 400s with relative initial rates for peptides **24-29** with various crown substituents.^[22]

Compound	% Transport	Relative initial rate
24	43	1
25	2	0.21
26	14	0.54
27	7	0.26
28	16	0.46
29	6	0.24

Calcein leakage experiments were performed to confirm that the fluorescence results corresponded with the transportation of Na^+ ion and not membrane perturbation.^[22] Additionally, peptide **24**, with crown ethers spaced 6Å apart was investigated to determine if the cations travelled through the crown ethers or through undefined pores.^[22]

The K^+ ion transport was shown to be efficient with 21-crown-7 and 18-crown-6 bearing peptides but not so for 15-crown-5 and 13-crown-4 analogues. This was

due to the K^+ ion being larger than the cavity of the 15-crown-5. Similarly the Na^+ ion transport efficiency was greater for larger crown ethers but inefficient for small crown ethers such as 13-crown-4 (Table 1.6.3.2).^[22]

Table 1.6.3.2 Voyer and co-workers observed transport with different crown ethers and different metal cations.^[22]

Crown Ether	% Transport		
	Na^+	K^+	Cs^+
21C7	33	53	62
18C6	28	38	13
15C5	12	7	8
13C4	2	2	2
Measured at 400s.			

The performance of these artificial ion channels is key for the design of systems presented in this thesis. In particular, the importance of a relay site distance $<11\text{\AA}$ apart for effective ion transport is vital.

1.7 Rigid Rod-like Ion Channels

Another class of non-peptide ion channel model is based on rigid rod molecules. These are a class of molecules that cannot be bent or compressed easily.^[26] Current and ongoing research in this area looks at whether rigid rod molecules have the ability to provide, in life sciences, what they have in material science and be as rewarding.^[69-71] Again this work is relevant to this thesis since the rigid backbones made of polynorbornyls are utilised (see Chapter 4, Section 4.3).

Research undertaken by Matile and co-workers have focused on rigid rod-like molecules (polyols, π -slides, rigid push-pull rods) that function as synthetic ion channels and pores in lipid bilayers. Their results indicated that rod length and bilayer thickness are key functional concerns for successful ion transport.^[72]

The polyols synthesised (e.g. Figure 1.7.2) were prepared to exploit these rigid structures and to give a hydrogen bonded chain which allows protons to be transported. The mechanism of transportation (Figure 1.7.1) was proposed to be a two-step hop-and-turn mechanism.^[26,73]

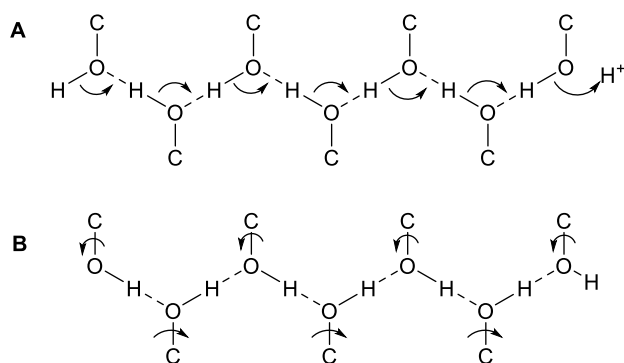


Figure 1.7.1 Matile and co-workers proposed hop-and-turn mechanism for transport across the polyol, **A)** 'hop' and **B)** 'turn'.^[73]

Studies by Matile and co-workers have shown that the polyol structure acts as a selective unimolecular proton channel.^[26] The polyol outlined (Figure 1.7.2) has an approximate length of (34 Å) which almost covers the hydrophobic part of the egg yolk PC bilayer.

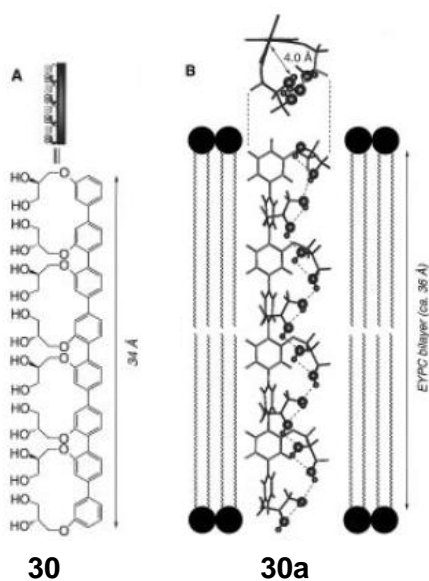


Figure 1.7.2 Matile and co-workers representative polyol structure **30**. **A)** 3D drawing using molecular modelling (Cerius 2). **B)** The proposed active conformer (**30a**) within the lipid bilayer (inside and top views).^[73]

Further studies by Matile and co-workers evaluated mechanisms of bilayer incorporation and proton selective transport. Overall the active conformer **1a** adopted a transmembrane orientation (Figure 1.7.2) which coincided with the length of the hydrophobic section of the bilayer. The proton selectivity is identified through the active conformer **30a** where the hydroxyl groups form hydrogen bonded chains that are shielded by hydrophobic carbon chains and the rigid backbone (oligophenylene). As depicted the conformer **30a** contains a central

channel of 4 Å in diameter which has both oxygen atoms and aromatic rings in close proximity allowing for selective transport of metal cations.

Initial black lipid membrane (BLM) studies of polyol **30** were undertaken. BLM is a technique based on electrophysiology used to monitor the transport of alkali metal ions across membranes with ion channels (described in detail in Chapter 5, section 5.4).^[74] The transport of these ions is monitored with the charges, potentials and voltages they possess applied across lipid membranes. The BLM is based upon two separate *cis* and *trans* compartments where upon a small aperture containing the membrane separates the two chambers.^[75] Each chamber has separated input and reference electrodes connected through a salt bridge. A potential is applied and amplified and the stochastic (activity shown in Figure 1.7.3) output monitored with small increments in current to identify channel activity.^[74]

The BLM procedure focussed on polyol **30** where a voltage was applied after 1 hour of incubation with 5 µM of **30**.^[76] In instances where a voltage greater than 50 mV was applied, large currents with a short duration were observed (Figure 1.7.3). It was suggested that these observed currents were the result of polyol **1** having a short active structural lifetime < 0.1 ms, therefore the nanopores are short lived.^[76] When the applied voltage was increased the probability of observing an open channel increased rapidly as indicated in Figure 1.7.3 (100 mV). The results of BLM suggested that the voltage directed self-assembly of polyol **30** within the bilayer was more likely to result in short life-time currents.

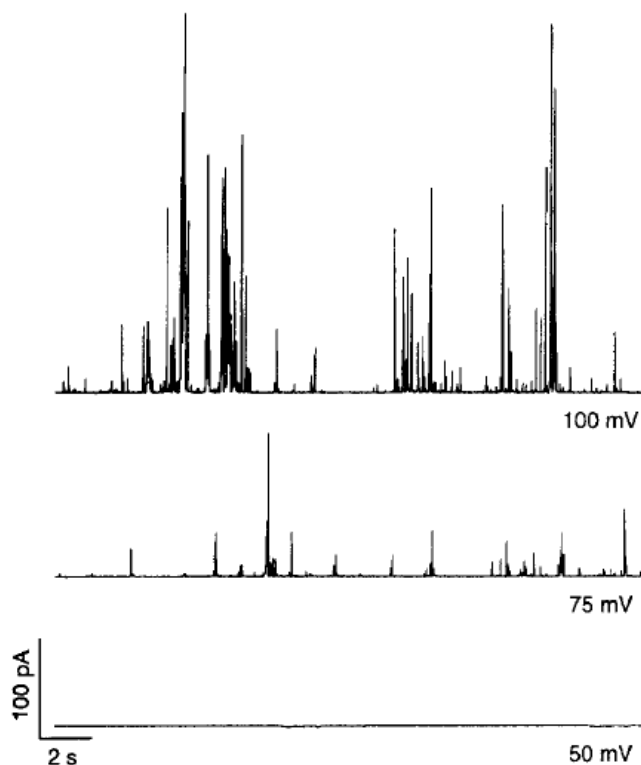


Figure 1.7.3 Matile and co-workers Black Lipid Membrane trace for polyol **30** with increased applied voltages.^[76]

Matile and co-workers also developed rigid ligand gated K^+ ion π -slides with flexible arene – arene distances which were designed to facilitate selective potassium ion transport across a lipid membrane.^[26] This is a new interaction discussed in this thesis based on a cation- π interaction using potassium ions and arenes. This is a noncovalent interaction between the arene (or π -systems) and the corresponding potassium cation. The positive charge from the potassium is attracted to the negative electrostatic potential at the centre of the face of the aromatic ring.^[77] The structure of **31** (Figure 1.7.4)^[77] consists of a binding site at the terminus of the system followed by polyethylene spacers with attachment to the arene π -slide. Initial studies of the π -slide *via* fluorescence quenching gave some indication that the orientation of the receptor was in alignment with the bilayer.^[78]

The ion transport of the ligand receptor system (Figure 1.7.4) was investigated by using egg yolk phosphatidylcholine small unilamellar vesicles (EYPC- SUV's) with a pH sensitive fluorophore. The transport activity of the π -slide was compared to amphotericin B similar to the polyol system discussed previously.

The π -slide system with external electrolyte solutions (Rb^+ , Cs^+ , Li^+ and Cs^+) gave three times lower rates than the K^+ ion. The π -slide has shown 'greater selectivity for K^+ ions in comparison to Na^+ ions and is reported to be amongst the highest observed in synthetic models to date'.^[55]

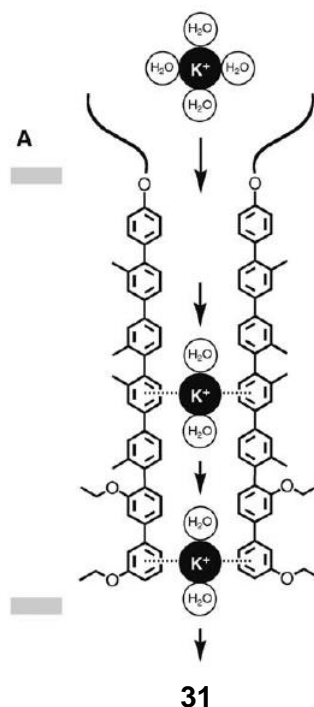


Figure 1.7.4 Artificial rigid rod π -slide for K^+ transport across bilayers.^[55]

However, Matile and co-workers found that the cation- π interactions to be the origin of channel blockages by tetraethylammonium cations, TEA.^[78] Therefore the channel can be inhibited by the common K^+ ion channel blocker (TEA), suggesting the concept of using these chemically appealing selective aromatic molecules for cation- π interactions in nature is likely to be impractical and or ineffective.

In further channel developments Matile and co-workers expanded their research to include a rigid push-pull rod system (Figure 1.7.5).^[79] These rods are composed of an electron donor at one terminus and an electron acceptor at the opposing terminus^[26,69]. As shown in Figure 1.7.5 the sulphide group is used as the π -donor and the sulfone as the π -acceptor^[26]. Therefore these compounds could potentially provide an electron transport system through a lipid bilayer.

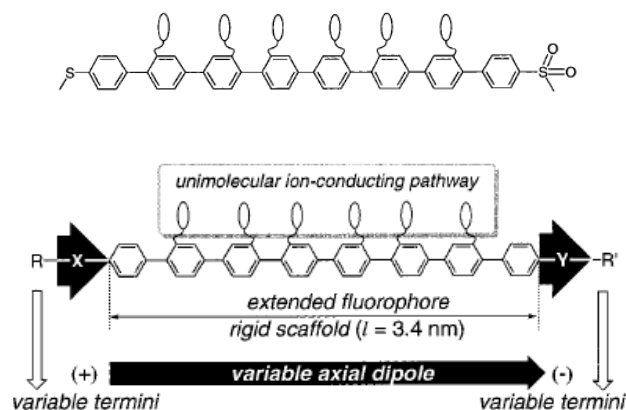


Figure 1.7.5 Matile and co-workers rigid rod design of push pull rod with variable axial dipoles.^[80]

A variety of rigid rod systems based on the above scaffold with differing terminal groups were assessed *via* unpolarised bilayers, EYPC – SUV with an internal fluorescent pH sensitive probe (HPTS- 8-hydroxypyrene-1,3,6-trisulfonic acid, tri-sodium salt) in the vesicle.^[80] Changes in fluorescence intensity of the probe were monitored after the ionophore was added as a function of time and lysed with Triton X-100 after 600 seconds (Figure 1.7.6). The activity of neutral rods with four lateral aza-crowns in comparison to neutral scaffolds with six aza-crowns revealed little effect on the activity of the system.^[80] Scaffolds with larger numbers of aza-crowns were expected to increase the activity of the system. However it was observed that these scaffolds had poor water-solubility and limited incorporation into the lipid bilayer.

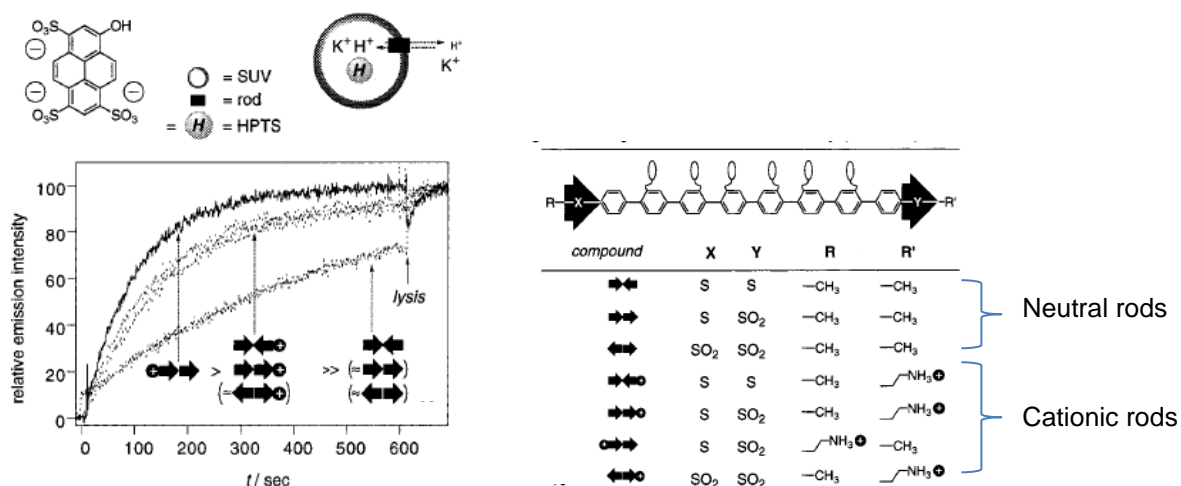


Figure 1.7.6 Matile and co-workers assay of ion transport activity for neutral and cationic rods in unpolarised EYPC-SUV's.^[80]

However when the rods were assessed under polarised EYPC-SUV's the cationic rods did not hold the highest fluorescent activity. Both neutral and cationic rods (Figure 1.7.6) had similar fluorescent activities.

Calcein leakage studies were also investigated for many of the rods, with dye leakage experiments from EYPC-SUV's loaded with CF (5(6)-carboxyfluorescein).^[80] The CF fluorescence was monitored as a function of time following the addition of the ionophore rods. As depicted in Figure 1.7.7 there was no detectable efflux of CF with the ionophore rods assessed. Therefore no leakage of the CF was displayed and transport was through the rods (channel function) rather than pores from membrane perturbation.

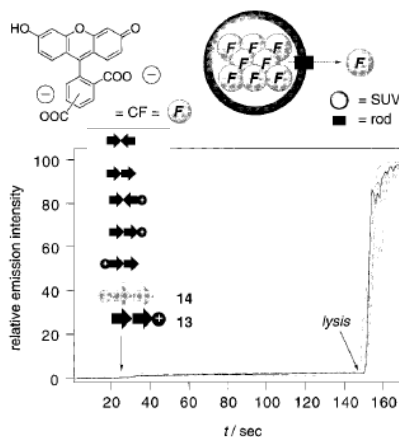


Figure 1.7.7 Matile and co-workers calcein leakage assay of neutral and cationic rods in unpolarised bilayer membranes with CF.^[80]

The investigation of these 'electrostatically asymmetric nanorods' has shown 'direct experimental evidence for cell membrane recognition'.^[80] This is particularly important in regards to understanding antibiotic resistance, which is of significant importance.

The research undertaken by Matile co-workers suggests that rigid-rod molecules such as those described previously are scaffolds of elevated interest in bioorganic chemistry. Most certainly these types of scaffolds are of interest due to their ability to address problems in bioorganic chemistry and further afield. This thesis makes use of rigid rods (albeit different from those employed by Matile) in constructing artificial ion channels. The focus has moved towards improving the design and synthesis of rigid-rod molecules for effective transport in biological membranes.

1.8 Summary of Transport Mechanisms

As described in previous sections there are a number of different mechanisms in which ions can be transported across a lipid membrane. Figure 1.8.1a below shows a summary of the different types of approaches for the transport of alkali ions across lipid membranes. In conjunction with these mechanisms, an alternative transport mechanism is a carrier method (1.8.1b), where small molecules can transport alkali metals across the membrane interface. There have been a number of small compounds identified within the literature which have demonstrated this ability.^[81,82]

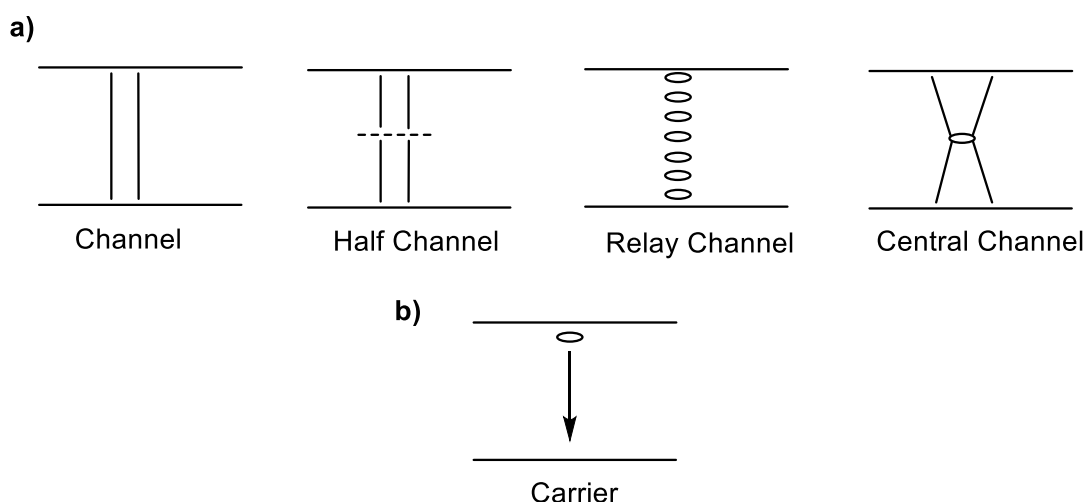


Figure 1.8.1 a) Various channel systems which were reviewed in Chapter 1, b) small molecule carrier of alkali metals

This area becomes important in Chapter 5 when examining the synthesised systems described in this thesis.

1.9 Introduction to Polycyclic Frameworks

Rigid rods have been previously reviewed by Michl and co-workers with reference to various modules such as cubane, porphyrin and bicyclo[2.2.2]octane.^[71] Such rigid multicyclic structures are referred to as molecular racks because of their resemblance to a rack structure. Polynorbornyl and polycyclic frameworks are also included in this type of molecular construct. These types of scaffolds and the extension of these frameworks have been described within the literature for applications in a variety of areas including anion recognition,^[83] custom functional structures for bioactive compounds,^[84] as well as molecular clefts^[85] and tweezers.^[86]

The rigidity and functionalization of these polynorbornyl systems was employed in the study described in this thesis for the construction/development of new, rigid artificial ion channels. In Figure 1.9.1 a small sample of rigid polycyclic scaffolds are depicted. These scaffolds can adopt either a curved topology (polynorbornane, [n]laddernane) or straight framed blocks, the latter being derived from the Hedaya diene or the Cram diene.^[87] This thesis focusses on the straight framed analogues since they represent the simplest way of spanning the lipid bilayer. These systems can be constructed in a sequential way but also through the use of building blocks and coupling strategies.^[88–93]

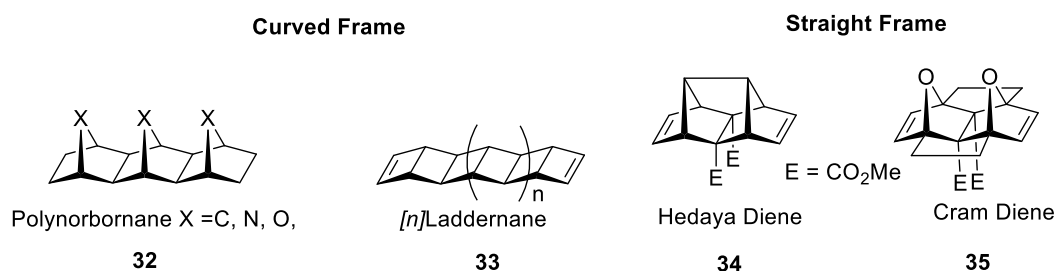


Figure 1.9.1 Polycyclic rigid scaffolds for building block extensions towards novel frameworks.^[87]

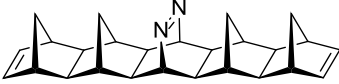
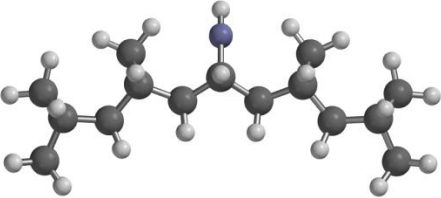

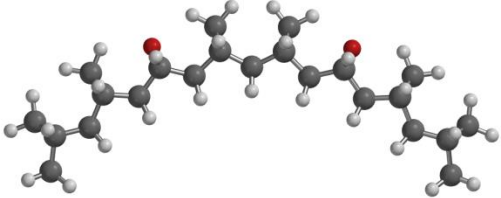


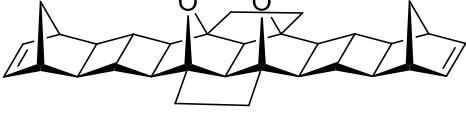
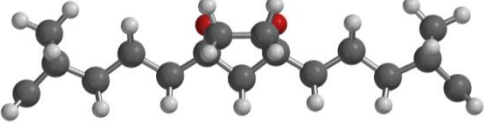



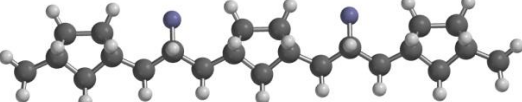
Warrener and co-workers in 2006 investigated a number of blocks coupled together using different coupling techniques (s-tetrazine coupling, alicyclic cyclobutene epoxide coupling (ACE), oxadiazole coupling) with the blocks outlined in Figure 1.9.1. The coupled products **36** and **37** (Table 1.9.1)^[87] gave a curved extended framework. In comparison the use of [n]laddernanes, the Hedaya diene and the Cram diene produced rod-like linear scaffolds (**38–41**).

The ability to couple multiple blocks together through a building block approach is of interest in the development of an artificial ion channel incorporating relay sites at set distances as indicated by Voyer's work. Cram's diene was avoided due to the instability it has shown during the synthesis of extended linear frameworks. The Hedaya diene could therefore be utilised in the synthesis of rigid-rod like frameworks allowing for functionalised systems and the attachment of ionophores for cation translocation. The coupling of Hedaya diene blocks has been reported by Warrener and co-workers but with only ester functionality.^[87]

Analysis *via* molecular modelling (Spartan Software, AM1) has provided an in-depth look into the different types of rigid blocks, their topology and the

consequence of the coupling between blocks for the extension of the rigid frameworks.^[87]

Table 1.9.1 Novel polycyclic extended frameworks highlighting the extent of curvature and linearity between various structures identified by Warrenner and co-workers.^[87]

 <p>s-tetrazine coupling 36</p>	
 <p>ACE Coupling 37</p>	
 <p>(2π+2π) reactions 38</p>	
 <p>Cram diene 39</p>	
 <p>Hedaya diene with ACE coupling 40</p>	
 <p>Hedaya diene with s-tetrazine coupling 41</p>	

2.0 Project Aims

The aim of this research is to bring together several properties of previously developed ion channel models detailed within this chapter, including, crown ethers, relay site spacing, and rigidity of the backbone, to create a new class of ion channel, Figure 2.0.1. To achieve this, a number of steps are required;

- The synthesis of small polycyclic block structures with ion binding capabilities, i.e. blocks with crown ethers attached (15-crown-5).
- Extend these frameworks into systems that are consistent with the length of lipid bilayers.
- Perform ion channel testing to determine ion transport capabilities and selectivity.

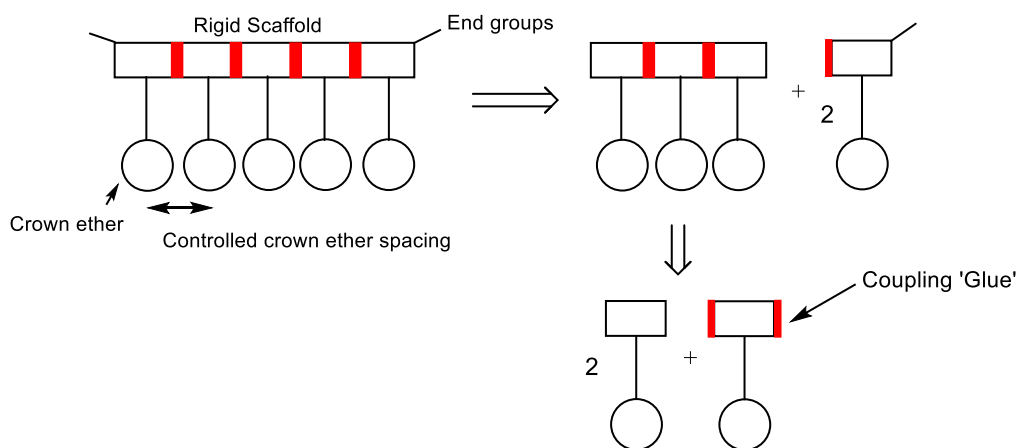


Figure 2.0.1 Schematic breakdown of the building block approach to an artificial ion channel based on a polycyclic framework.

More specific chemical detail and synthetic strategies are outlined in the following chapters.

REFERENCES

- [1] J. Behrends, *Chem. Rev.* **2012**, 6218–6226.
- [2] D. Aidley, *Ion Channels : Molecules in Action*, Press Syndicate, University Of Cambridge, **1996**.
- [3] M. S. Gin, E. G. Schmidt, P. Talukdar, in *Nanobiotechnology II More Concepts Appl.* (Eds.: C.A. Mirkin, C.M. Niemeyer), Wiley-VCH, **2007**, pp. 3–12.
- [4] E. Abel, G. E. M. Maguire, O. Murillo, I. Suzuki, S. L. De Wall, G. W. Gokel, *J. Am. Chem. Soc.* **1999**, *121*, 9043–9052.
- [5] G. W. Gokel, in *Adv. Supramol. Chem.*, JAI Press Inc, Stamford, **2001**, pp. 3–11.
- [6] F. M. Ashcroft, *Ion Channels and Disease: Channelopathies*, Academic Press, San Diego, **2000**.
- [7] F. Stephenson, *Curr. Opin. Struct. Biol.* **1991**, *1*, 569–574.
- [8] C. Miller, *Curr. Opin. Chem. Biol.* **2000**, *4*, 148–151.
- [9] T. M. Fyles, *Chem. Soc. Rev.* **2007**, *36*, 335–347.
- [10] B. M. Burkhart, R. M. Gassman, D. a Langs, W. a Pangborn, W. L. Duax, V. Pletnev, *Biopolymers* **1999**, *51*, 129–144.
- [11] D. W. Urry, *Proc. Natl. Acad. Sci.* **1971**, *68*, 810–814.
- [12] F. W. Kotch, *Artificial Ion Channels*, **1997**.
- [13] M. R. Ghadiri, J. R. Granja, L. K. Buehler, *Nature* **1994**, *369*, 301–304.
- [14] V. Sidorov, F. W. Kotch, J. T. Davis, M. El-Kouedi, *Chem. Commun.* **2000**, 2369–2370.
- [15] K. S. Akerfeldt, J. D. Lear, Z. R. Wasserman, L. A. Chung, W. F. DeGrado, *Acc. Chem. Res.* **1993**, *26*, 191–197.
- [16] M. F. M. Roks, R. J. M. Nolte, *Macromolecules* **1992**, *25*, 5398–5407.
- [17] T. M. Fyles, T. D. James, K. C. Kaye, *J. Am. Chem. Soc.* **1993**, *115*, 12315–12321.
- [18] S. Licen, F. D. Riccardis, *Curr. Drug Discov. Technol.* **2008**, *5*, 86–97.
- [19] R. S. Kass, *J. Clin. Invest.* **2005**, *115*, 1986–1989.
- [20] L. Yang, T. A. Harroun, T. M. Weiss, L. Ding, H. W. Huang, *Biophys. J.* **2001**, *81*, 1475–1485.

- [21] G. W. Gokel, *Cell Biochem. Biophys.* **2001**, *35*, 211–231.
- [22] F. Otis, C. Racine-Berthiaume, N. Voyer, *J. Am. Chem. Soc.* **2011**, 6481–6483.
- [23] C. G. Espínola, R. Pérez, J. D. Martín, *Org. Lett.* **2000**, *2*, 3161–3164.
- [24] F. De Riccardis, I. Izzo, D. Montesarchio, P. Tecilla, *Acc. Chem. Res.* **2013**, *46*, 2781–2790.
- [25] P. Reiß, U. Koert, *Acc. Chem. Res.* **2013**, *46*, 2773–2780.
- [26] N. Sakai, J. Mareda, S. Matile, *Acc. Chem. Res.* **2005**, *38*, 79–87.
- [27] P. L. Yeagle, *Encycl. Life Sci.* **2001**, 1–7.
- [28] G. Von Heijne, D. Rees, *Curr. Opin. Struct. Biol.* **2008**, *18*, 403–405.
- [29] G. W. Gokel, A. Mukhopadhyay, *Chem. Soc. Rev.* **2001**, *30*, 274–286.
- [30] G. Harrison, R. Lunt, *Biological Membranes Their Structure and Function*, John Wiley And Sons, Published USA Halsted Press, **1975**.
- [31] S. Matile, A. Vargas Jentzsch, J. Montenegro, A. Fin, *Chem. Soc. Rev.* **2011**, *40*, 2453–2474.
- [32] D. Montesarchio, C. Coppola, M. Boccalon, P. Tecilla, *Carbohydr. Res.* **2012**, *356*, 62–74.
- [33] N. Maulucci, F. De Riccardis, C. B. Botta, A. Casapullo, E. Cressina, M. Fregonese, P. Tecilla, I. Izzo, *Chem. Commun. (Camb)*. **2005**, *10*, 1354–1356.
- [34] M. Di Filippo, I. Izzo, L. Savignano, P. Tecilla, F. De Riccardis, *Tetrahedron* **2003**, *59*, 1711–1717.
- [35] A. Satake, M. Yamamura, M. Oda, Y. Kobuke, *J. Am. Chem. Soc.* **2008**, *130*, 6314–6315.
- [36] D. Parker, *Macrocyclic Synthesis - A Practical Approach*, Oxford University Press, United States, New York City, **2002**.
- [37] M. Kralj, L. Tusek-Božić, L. Frkanec, *ChemMedChem* **2008**, *3*, 1478–1492.
- [38] J. W. Steed, J. L. Atwood, *Supramolecular Chemistry*, John Wiley And Sons, **2009**.
- [39] T. Bogaschenko, S. Basok, C. Kulygina, A. Lyapunov, N. Lukyanenko, *Synthesis (Stuttg)*. **2002**, 2266.
- [40] X. Jiang, X. Yang, C. Zhao, L. Sun, *J. Phys. Org. Chem.* **2009**, *22*, 1–8.

- [41] N. Gerbeleu, V. Arion, J. Burgess, *Template Synthesis of Macrocyclic Compounds*, Wiley VCH, **1999**.
- [42] A. Ostrowicki, E. Koepp, F. Vogtle, in *Macocycles*, Springer Berlin Heidelberg, **1991**, pp. 37–67.
- [43] P. Knops, N. Sendhoff, H. Mekeiburger, F. Vogtle, in *Macocycles*, Wiley VCH, **1991**, pp. 1–36.
- [44] M. Hiraoka, *Crown Ethers and Analogous Compounds*, Elsevier Science, Amsterdam, **2013**.
- [45] B. Czech, A. Czech, B. Son, H. Lee, R. Bartsch, *J. Hetero. Chem.* **1986**, *23*, 465–471.
- [46] C. J. Pedersen, in *Nobel Lect.*, **1987**.
- [47] B. R. Bowsher, A. J. Rest, *Inorg. Chim. Acta* **1981**, *53*, 175–176.
- [48] P. Taylor, L. Mandolini, B. Masci, C. N. R. Centro, *C. Organica, Synth. Commun.* **1979**, *9*, 851–856.
- [49] C. J. Pedersen, *Angew. Chem* **1988**, *100*, 1053–1059.
- [50] A. Ziafati, H. Eshghi, O. Sabzevari, *Chin. Chem. Lett.* **2009**, *20*, 924–926.
- [51] B. V Van Keulen, R. Kellogg, O. Pirpers, *J. Chem. Soc., Chem. Comm* **1979**, 285–286.
- [52] R. Hanes, J. Lee, S. Ivy, A. Palka, R. Bartsch, *Arkivoc* **2010**, 238–248.
- [53] I. Tabushi, Y. Kuroda, K. Yokota, *Tetrahedron Lett.* **1982**, *23*, 4601–4604.
- [54] N. Sakai, S. Matile, *Langmuir* **2013**, *29*, 9031–9040.
- [55] J. Mareda, S. Matile, *Chem. Eur. J.* **2009**, *15*, 28–37.
- [56] G. W. Gokel, S. Negin, *Adv. Drug Deliv. Rev.* **2012**, *64*, 784–96.
- [57] L. Jullien, J. Lehn, *Tetrahedron Lett.* **1988**, *29*, 3803–3806.
- [58] M. J. Pregel, L. Jullien, J. Canceill, L. Lacombe, J. Lehn, *J. Chem. Soc. Perkins Trans. 2* **1995**, 417–426.
- [59] A. D. Pechulis, R. J. Thompson, J. P. Fojtik, H. M. Schwartz, C. A. Lisek, L. L. Frye, *Bioorg. Med. Chem.* **1997**, *5*, 1893–1901.
- [60] F. G. Riddell, M. K. Hayer, *Transport* **1985**, *817*, 313–317.
- [61] N. Voyer, M. Robitaille, *J. Am. Chem. Soc.* **1995**, *117*, 6599–6600.

- [62] E. Biron, F. Otis, J. C. Meillon, M. Robitaille, J. Lamothe, P. Van Hove, M.-E. Cormier, N. Voyer, *Bioorg. Med. Chem.* **2004**, *12*, 1279–1290.
- [63] Y. R. Vandenburg, B. D. Smith, E. Biron, N. Voyer, *Chem. Commun.* **2002**, 1694–1695.
- [64] N. Voyer, L. Potvin, É. Rousseau, *J. Chem. Soc. Perkin Trans. 2.* **1997**, 1469–1472.
- [65] M. Ouellet, F. Otis, N. Voyer, M. Auger, *Biochim. Biophys. Acta* **2006**, *1758*, 1235–1244.
- [66] F. Otis, N. Voyer, A. Polidori, B. Pucci, *New J. Chem.* **2006**, *30*, 185.
- [67] E. Biron, N. Voyer, J. C. Meillon, M. È. Cormier, M. Auger, *Pept. Sci.* **2000**, *55*, 364–372.
- [68] P. L. Boudreault, N. Voyer, *Org. Biomol. Chem.* **2007**, *5*, 1459–1465.
- [69] S. Matile, *Chem. Rec.* **2001**, *1*, 162–172.
- [70] N. Sakai, J. Mareda, S. Matile, *Mol. BioSyst.* **2007**, *3*, 658–666.
- [71] P. F. H. Schwab, M. D. Levin, J. Michl, *Chem. Rev.* **1999**, *99*, 1863–1934.
- [72] A. V. Jentsch, A. Hennig, S. Matile, J. Mareda, *Acc. Chem. Res.* **2013**, *46*, 2791–2800.
- [73] L. A. Weiss, N. Sakai, *J. Am. Chem. Soc.* **1997**, *7863*, 12142–12149.
- [74] S. Matile, N. Sakai, in *Anal. Methods Supramol. Chem.* (Ed.: C. Schalley), Wiley-VCH, Weinheim, **2012**, pp. 711–742.
- [75] B. Rudy, L. E. Iverson, *Ion Channels: Methods in Enzymology*, Academic Press, New York, **1992**.
- [76] N. Sakai, C. Ni, S. M. Bezrukov, S. Matile, *Bioorganic Med. Chem. Lett.* **1998**, *8*, 2743–2746.
- [77] D. A. Dougherty, *J. Nutr.* **2007**, *137*, 1504–1508.
- [78] M. M. Tedesco, B. Ghebremariam, N. Sakai, S. Matile, *Angew. Chem. Int. Ed.* **1999**, *38*, 540–543.
- [79] N. Sakai, S. Matile, *Chem. Eur. J.* **2000**, *6*, 1731–1737.
- [80] N. Sakai, D. Gerard, S. Matile, *J. Am. Chem. Soc.* **2001**, *123*, 2517–2524.
- [81] W. Walkowiak, C. a. Kozlowski, *Desalination* **2009**, *240*, 186–197.
- [82] A. L. Sisson, M. R. Shah, S. Bhosale, S. Matile, *Chem. Soc. Rev.* **2006**, *35*, 1269–86.

- [83] F. M. Pfeffer, T. Gunnlaugsson, P. Jensen, P. E. Kruger, *Org. Lett.* **2005**, *7*, 5357–5360.
- [84] R. Warrener, A. Schultz, *Chem. Commun.* **1997**, 1023–1024.
- [85] R. Warrener, D. Margetic, A. Amarasekara, D. Butler, I. Mahadevan, R. Russel, *Org. Lett.* **1999**, *1*, 199–202.
- [86] R. B. Murphy, D. T. Pham, S. F. Lincoln, M. R. Johnston, *Eur. J. Org. Chem.* **2013**, 2985–2993.
- [87] M. Golić, M. R. Johnston, D. Margetić, A. C. Schultz, R. N. Warrener, *Aust. J. Chem.* **2006**, *59*, 899–914.
- [88] R. N. Warrener, G. Abbenante, C. H. L. Kennard, *J. Am. Chem. Soc.* **1994**, *116*, 3645–3646.
- [89] G. Mehta, M. B. Viswanath, A. C. Kunwar, *J. Org. Chem.* **1993**, *59*, 6131–6132.
- [90] G. Mehta, M. B. Viswanath, A. C. Kunwar, *Synlett* **1995**, 317–318.
- [91] G. Mehta, M. B. Viswanath, *J. Braz. Chem. Soc.* **1996**, *7*, 219–224.
- [92] R. N. Warrener, G. Abbenante, S. R. G. R. A. Russell, *Tetrahedron Lett.* **1994**, *35*, 7639–7642.
- [93] M. N. Paddon-Row, J. W. Verhoeven, *New J. Chem.* **1991**, *15*, 107–116.

CHAPTER 2

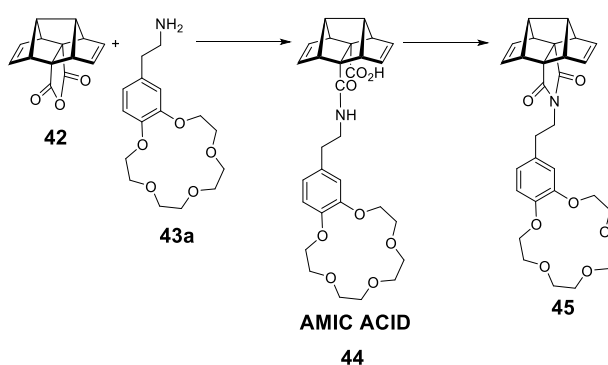
SYNTHESIS OF THE HEDAYA BLOCK WITH AN ETHYLENE LINKER

2.1 Introduction

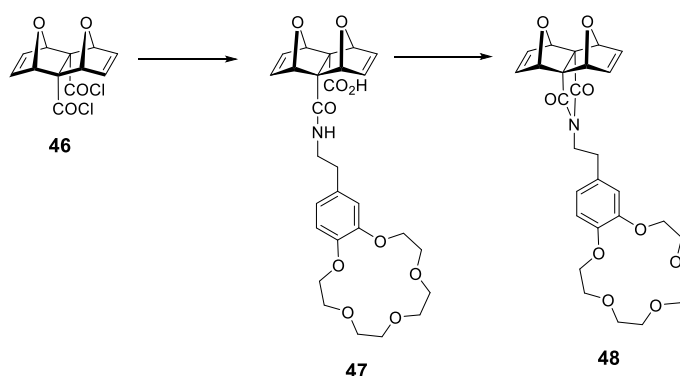
The aim of this study was to construct a rigid molecule with crown ether relay sites, set at regular distances in a parallel alignment, leveraging on the work described in Chapter 1 from Voyer and Matile. Initial studies investigated the reactivity of polynorbornyl systems with aliphatic amino crown ethers.

In essence, there exists a number of possible routes to append aliphatic and/or aromatic amines to polynorbornyl architectures. However, there are limited routes to form systems that are symmetrical, and easily accessible. The approaches which will be discussed are;

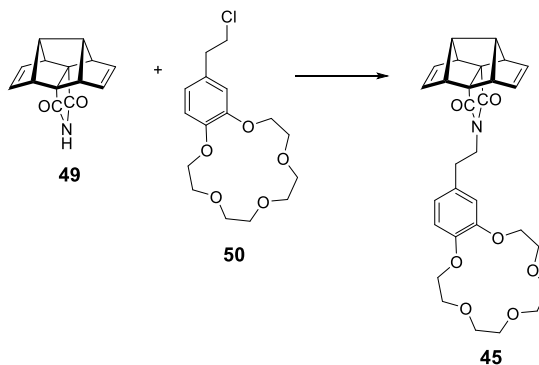
- i) a two-step procedure involving reaction of an anhydride with an aliphatic amine to initially form an amic acid, followed by dehydration to the imide.



- ii) the reaction of a *bis*-acyl chloride with a primary amine, followed by ring closure to the imide, promoted by amide-forming coupling reagents.



- iii) the reaction of a polynorbornyl imide with aliphatic halides *via* nucleophilic substitution reaction.



Herein the target structure was the Hedaya block (see Fig 1.8.1)^[1] with an ethylene linker between the imide and the aromatic crown ether. Synthesis of this target started through pathway I.

2.2 Design of an Artificial Ion Channel Based on a Polynorbornyl Framework

The initial design of the proposed artificial ion channel was based around rigidity and the ability of the system to promote the passage of ions across a lipid membrane. These aspects were investigated using a polynorbornyl block with the attachment of a crown ether.

As discussed in Chapter 1, there are two types of architectures for polynorbornyl blocks i.e. curved and straight. In this study polynorbornyl blocks with a linear alignment will be used in order facilitate direct transport across the bilayer and to provide equal spacing between relay sites.

Computational modelling of the polynorbornyl (Hedaya) framework bearing crown ethers **51** (Fig 2.2.1A) was undertaken before synthetic work was initiated. Modelling of a polynorbornyl framework bearing five aromatic side chains (the crown ethers removed to simplify modelling) was performed using Spartan 10' software. The result is shown in Figure 2.2.1, which illustrates the amine attachment through the imide. From the modelling it could be concluded that the ethylene linker between the imide and the benzocrown ether was key to the

alignment of ionophores and their relative spacing. If the ethylene groups were initially in different conformations, free rotation around the carbon atoms would allow the crown ethers to align, due to their flexible nature. The orientation and the spacing between relay sites are important properties that influence ion transport. As described previously by Voyer and co-workers, distances greater than 11 Å between relay sites resulted in decreased transport rates. The relative distance between relay sites in the proposed structure was measured at ~6.5-8.0 Å (measured between 3,4 aromatic carbon atoms) with an overall length of 35 Å. Modelling predicts that the structure has the desired properties to span and facilitate the transport of ions across a bilayer with the relative distances calculated in between ionophores and the overall span of the system. The modelling results indicated that the framework (Figure 2.2.1A) has the desired properties such as; rigid linear framework, ionophore spacing, crown alignment and overall span to be the first synthetic target within this thesis. As described in Chapter 1, the overall length is also a significant feature in relation to membrane assembly and transport (Section 1.2).

Note, the models generated by Spartan 10' throughout this thesis show alignment of the aromatic rings. This may be due to each aromatic ring acting independently from each other when there is no ether ring attached. Even when the modelling is undertaken with the aromatic rings at different initial positions, the model generated still led to a similar overall geometry.

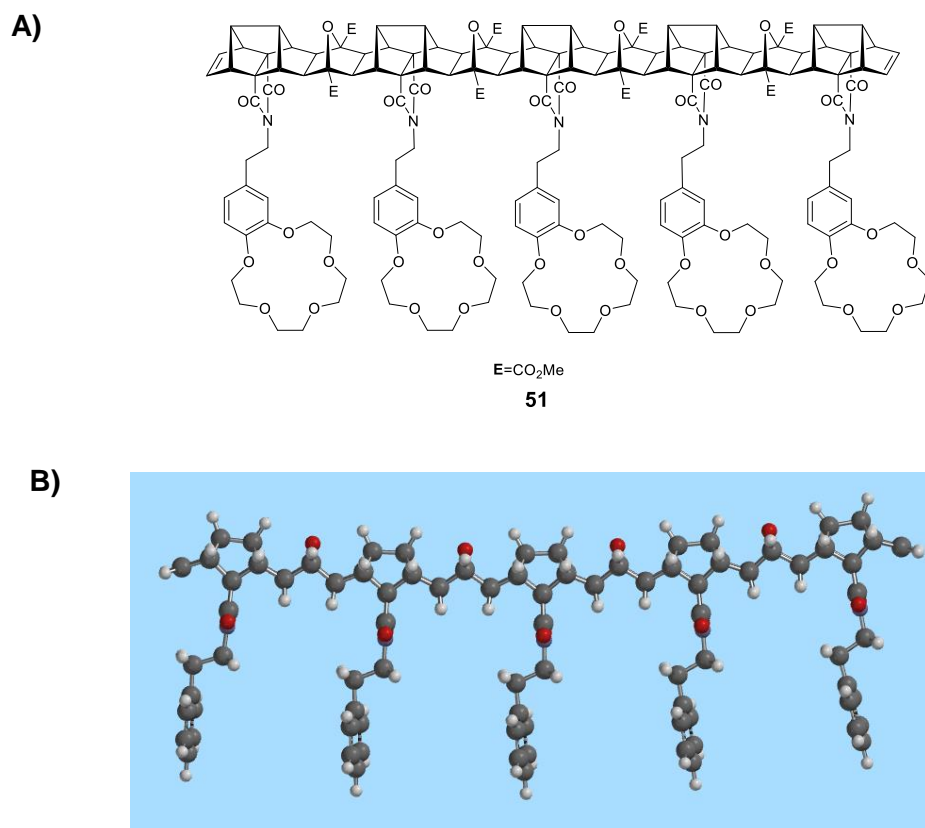


Figure 2.2.1 **A)** Schematic representation of the fused polycyclic norbornyl system, **B)** Proposed polycyclic norbornyl linear framework with an ethylene linker for channel transportation and orientation (crown ethers removed for ease of modelling), (Modelled by Spartan 10').

A retrosynthetic analysis of the synthesis of the proposed artificial ion channel is shown in Figure 2.2.2. This scheme shows the initial formation of the polynorbornyl crown ether block **45** from a dopamine-derived crown ether and the polycyclic norbornyl block (Hedaya anhydride **42**). The formation of this block is then followed by numerous coupling reactions of the same block to extend the framework to the overall five crown system **51**. Dopamine has previously been shown to have the required orientation; it is highly accessible and has functional groups amenable to crown ether synthesis.

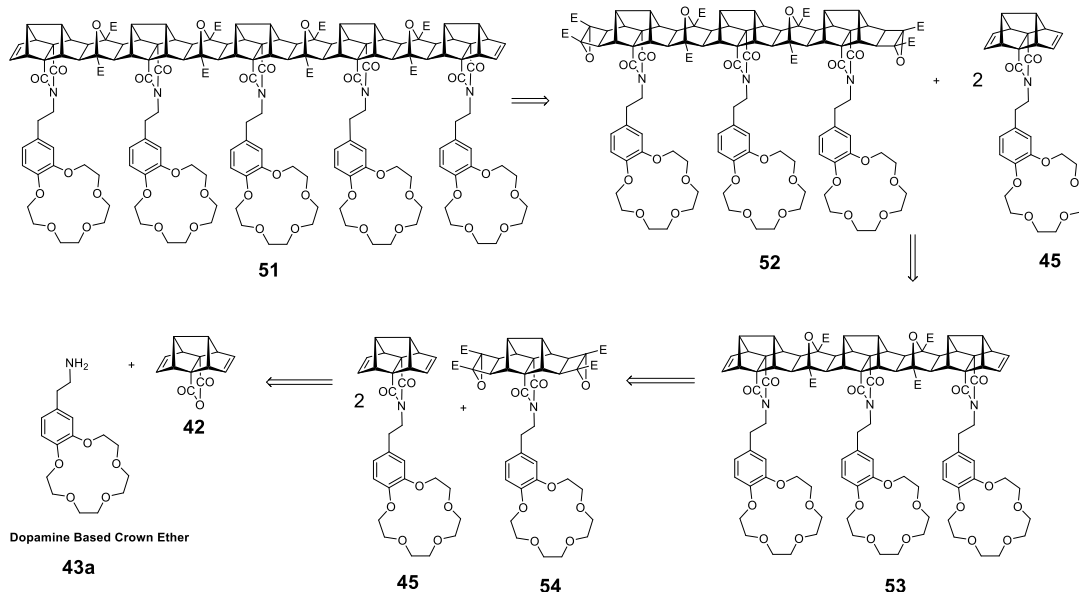


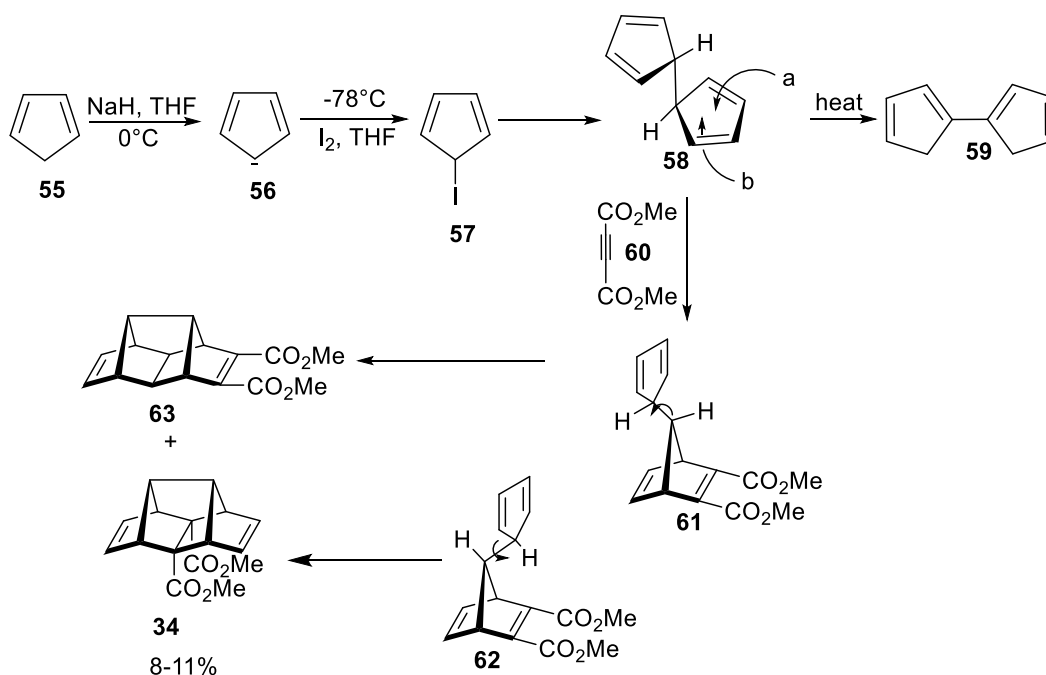
Figure 2.2.2 Retrosynthetic analysis of the synthesis of a polynorbornyl based artificial ion channel.

2.3 Synthesis of Polycyclic Norbornyl Linear Framework for Crown Ether Attachment (Hedaya Diene)

The key structural unit in the target structure is the Hedaya diene appended with a crown ether. The Hedaya diene was initially synthesised by Hedaya and co-workers in 1974 before Paquette and co-workers updated the method with minor changes.^[2–5] The synthesis of the Hedaya diene proceeds *via* 9,10-dihydrofulvalene **58** (Scheme 2.3.1) which in previous times has been produced *via* flash vacuum pyrolysis of nickelocene.^[3,5] However there are numerous limitations and expenses related to the process which led Paquette and co-workers to utilize Doering and Matzner's observations of the reaction where sodium cyclopentadiene is oxidatively coupled in the presence of 0.5 equivalents of iodine in THF at -78°C (Scheme 2.3.1).^[5] Initially the cyclopentadiene anion **56** was formed by the deprotonation of cyclopentadiene using sodium hydride in THF at 0°C (Scheme 2.3.1). Following which the cyclopentadiene anion nucleophilically attacks iodine (loss of I^-) at -78°C in THF. The second mole of cyclopentadiene anion attacks the iodo species yielding **58** *in situ*. It is important to note that the temperature was kept below -70°C , since higher temperatures favoured the formation of 1,5-dihydrofulvalene **59**.^[5]

The 9,10-dihydrofulvalene system **58** has C_{2v} symmetry and can adopt a C_{2h} conformation as depicted in Scheme 2.3.1.^[5] This is where the cyclopentadiene

rings are characterised by two angles where if both angles are of the same sign and degree the molecule is likely to have C_{2h} symmetry. With this conformational change, it was possible that a dienophile such as dimethyl acetylenedicarboxylate (DMAD) can react on the inside or the outside of the cyclopentadiene rings as shown in Scheme 2.3.1.^[5] Attack of the dienophile, (DMAD, **60**) at position **a** produces the intermediate compound **61** however attack of DMAD at the opposing face of one of the cyclopentadiene rings produces the intermediate compound **62** (Scheme 2.3.1). Compound **63** and **34** are further formed *via* subsequent bond rotations and intramolecular Diels Alder of compound **61** and **62** respectively.^[5]



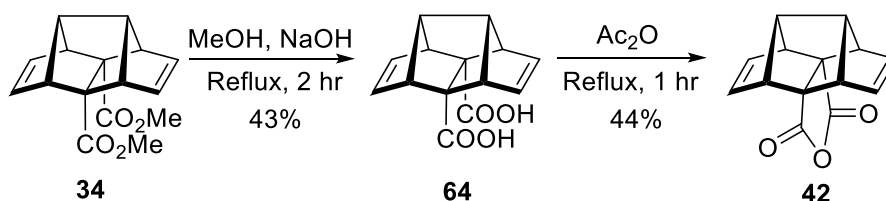
Scheme 2.3.1 Pathway towards the synthesis of the Hedaya polycyclic block **34**.^[5]

Compounds **63** and **34** can be separated *via* base hydrolysis of the more accessible esters in **63**. Thus, undesired compound **63** was removed with potassium hydroxide (KOH) in methanol at room temperature to hydrolyse the esters to the *bis*-acid, leaving the remaining *endo* diesters of **34** intact. Block **34** was synthesised in 8-11% yield and characterised by nuclear magnetic resonance spectroscopy (NMR spectroscopy) and high resolution mass spectrometry with electrospray ionisation (HRMS-ESI) which was consistent with literature values.^[5,6] The Hedaya diene **34** synthesis was successful with the observation of new resonances at 6.06 ppm which is consistent with the chemical

shift for the *bis*-alkene. In addition, the observed resonance at 3.58 ppm was consistent for the methyl esters. The structure was further confirmed by HRMS-ESI calculated for $C_{16}H_{16}O_4Na$, 295.0946, found 295.0939 $[M+Na]^+$.

The Hedaya anhydride **42** was prepared by hydrolysis of the *endo* diester **34** with 10% NaOH in MeOH, to obtain *bis*-acid **64** in moderate yield (43%), (Scheme 2.3.2). NMR spectroscopy and mass spectroscopy electrospray ionisation (MS-ESI) data of the product were consistent with the reported literature values^[6]. The 1H NMR spectrum indicated a loss of the dimethylester resonance at 3.58 ppm from the initial Hedaya diene **34**. The structure was further confirmed by MS-ESI calculated for $C_{14}H_{11}O_4$, 243.07, found 243.06 $[M-H]^-$.

The *bis*-acid **64** was then subjected to ring closure conditions with acetic anhydride to afford **42** (Scheme 2.3.2) in moderate yield (44%).^[1] NMR spectroscopy and HRMS-ESI confirmed the structure which was consistent with the reported literature values.^[1] The ^{13}C NMR spectrum was recorded and showed the carbonyl resonance at 170.1 ppm, significantly upfield from the *bis*-acid **64** carbonyl resonance at 179.4 ppm. The structure was further confirmed by HRMS-ESI calculated for $C_{14}H_{11}O_3$, 227.0708, found 227.0709 $[M+H]^+$.



Scheme 2.3.2 Preparation of Hedaya anhydride **42** from the Hedaya diene diester **34** and *bis*-acid **64**.^[1,5]

The Hedaya anhydride **42** was now ready for the attachment of an amine-derivatised crown ether.

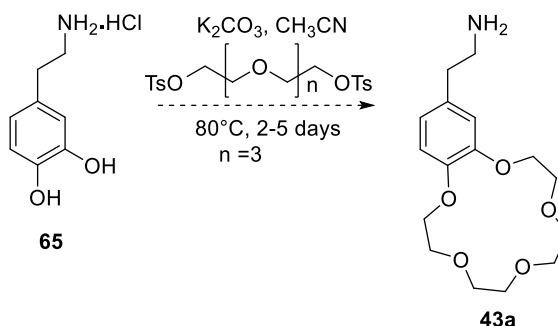
2.4 Synthesis of Dopamine Derived Substituted Aromatic Crown Ethers

The aliphatic amine **43a** was derived from dopamine, which is a commonly known hormone and neurotransmitter from the catecholamine family.^[7] Dopamine is usually supplied as the hydrochloride salt **65** and is affordable in large quantities. Dopamine is used extensively in synthesis specifically but not limited to, applications in polymer chemistry and pharmaceuticals.^[8-10]

Substituted crown ethers were synthesised by reactions of the 3,4-dihydroxy functional groups of dopamine. Crown ethers were prepared *via* the Williamson

ether synthesis as discussed in Chapter 1. The crown ether synthesis required two substrates, an alkoxide nucleophile and an alkyl electrophile, such as tosyl or halide species. Different size crown ethers are synthesised by varying the size of the polyethylene glycol units (PEG). In this research tetraethylene glycol, pentaethylene glycol and hexaethylene glycol were converted with tosyl chloride and or thionyl chloride to their respective alkyl electrophiles for crown ether preparation. NMR spectroscopy of all tosylated PEG substrates resulted in new aromatic resonances within the ^1H NMR spectrum with doublets observed between 7.77-7.79 ppm and 7.33-7.34 ppm. Additionally a methyl ester resonance was observed upfield at 2.44 ppm for all tosylated PEG compounds.

The variations discussed in Chapter 1 for macrocyclic synthesis were explored throughout this research. The desired amino crown ether system was prepared by reaction of dopamine hydrochloride with tetraethylene glycol bistosylate (TEGOTS₂) (Scheme 2.4.1). However starting material and decomposition products were the main components of the crude material analysed by NMR spectroscopy.



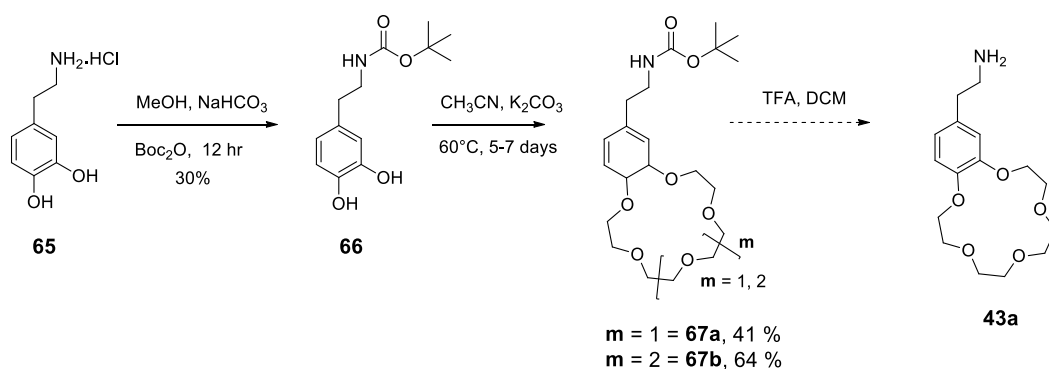
Scheme 2.4.1 Initial synthetic pathway to dopamine derived crown ethers.

Reaction with the free base of dopamine was also examined using three different methods with varying strengths of base for deprotonation of the hydroxyl groups. In all reactions the mixture turned brown, potentially a sign of decomposition where upon no product was isolated from the aqueous extracts. To prevent decomposition that was potentially occurring at the amine functionality a Boc protecting group was added at the primary amine to reduce the possibility of decomposition during synthesis of the crown ether.

The Boc protecting group was installed by a procedure outlined by the McGarvey research group.^[11] Using aqueous conditions with excess Boc anhydride, **66** was prepared in 30% yield after purification *via* trituration (THF:hexane) as shown in

Scheme 2.4.2. NMR spectroscopy of **66** observed new methyl resonances within the ^1H NMR spectrum with a singlet observed at 1.37 ppm. The structure was further confirmed by MS-ESI calculated for $\text{C}_{13}\text{H}_{19}\text{NO}_4$ 253, found 252 $[\text{M}-\text{H}]^-$.

Compound **66** was used to synthesise both the 15-crown-5 **67a** and 18-Crown-6 **67b** ethers with the use of K_2CO_3 and/or Cs_2CO_3 for the templating and deprotonation of the hydroxyl groups. The respective PEG ditosylates were reacted with substrate **66** in acetonitrile over several days. Purification *via* trituration afforded the corresponding crown ethers in 41% and 64% respectively. Crown ether **67a** was synthesised successfully with the new crown ether resonances observed between 4.10-4.13, 3.89-3.91, and 3.68-3.69 ppm. High resolution MS calculated for $\text{C}_{21}\text{H}_{33}\text{NO}_7\text{Na}$, 434.2155, found 434.2149 $[\text{M}+\text{Na}]^+$. The 18-crown-6 ether **67b** was also successfully synthesised with new crown ether resonances observed between 4.11-4.14, 3.86-3.87, 3.69-3.70, 3.67-3.68, and 3.64-3.65 ppm. Mass spectroscopy ESI calculated for $\text{C}_{23}\text{H}_{37}\text{NO}_8\text{Na}$, 478, found 478 $[\text{M}+\text{Na}]^+$.

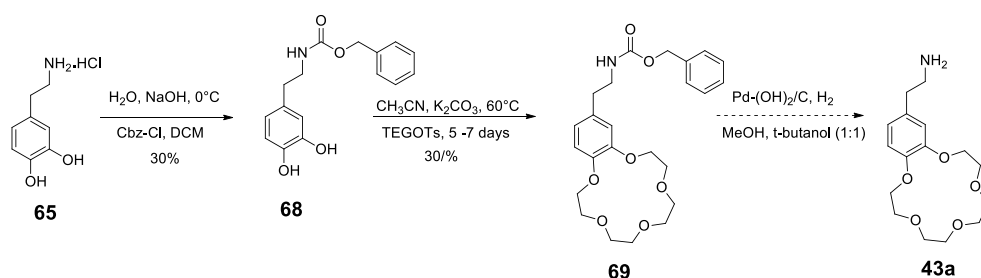


Scheme 2.4.2 Synthetic pathway for the synthesis of crown ether **43a** with Boc protection of the amine derived from dopamine.

To obtain the free amine for attachment to the Hedaya anhydride block **42**, it was necessary to remove the Boc protecting group. Deprotection conditions such as TFA:DCM proved to be problematic. On addition of the deprotection reagents the reaction altered colour, from yellow to purple to brown. The ^1H NMR analysis of the crude product indicated there was no starting material or product present. Further investigation into the removal of the Boc protecting group through varying reaction time, and reagent equivalents proved to be ineffective. It was thought that **43** were unstable under acidic conditions and the removal of the Boc protecting group is carried out under the described conditions in Scheme 2.4.2.

Due to the relatively harsh conditions used to remove the Boc protecting group an alternative protecting group, benzyloxycarbonyl, Cbz was used in an attempt to synthesise **43a** (Scheme 2.4.3). The Cbz protecting group can be removed *via* mild conditions, i.e. hydrogenolysis. The Cbz protected dopamine **68** was synthesised by a procedure outlined by the McGarvey research group,^[11] under aqueous conditions with Cbz-chloride, and isolated *via* column chromatography in 30% yield. A subsequent crown ether reaction as described previously was employed to generate the benzo-15-crown-5 ether **69** in 29% yield.

The Cbz protecting group was removed *via* a hydrogenolysis reaction with Pd(OH)₂/C. Deprotection using the palladium catalyst afforded initially a beige solid however upon drying, *in vacuo* the material liquefied. The product could not be isolated due to decomposition, as indicated by NMR spectral analysis, with no representative resonances consistent with product **43a** being observed.

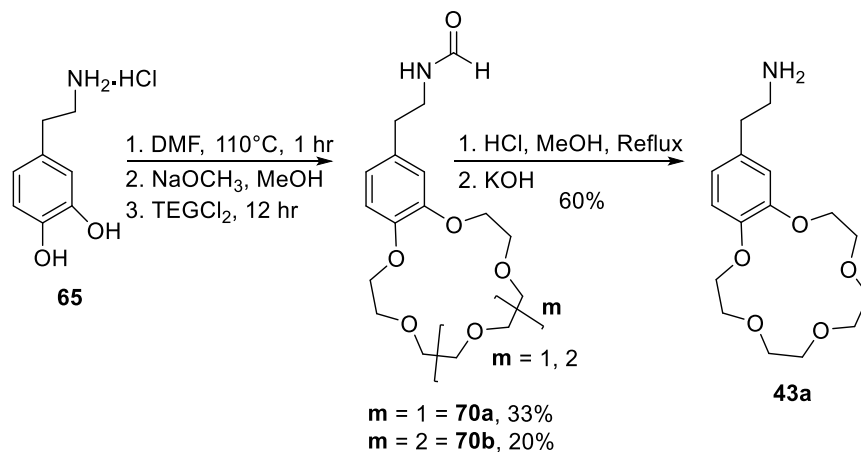


Scheme 2.4.3 Synthetic pathway towards the synthesis of crown ether **43a** with Cbz protection of the amine derived from dopamine.

As the use of Cbz and Boc protecting groups did not facilitate the preparation of **43a**, a review of already established methods for the preparation of catecholamine derived crown ethers was undertaken. Both epinephrine and dopamine crown ether derivatives have been synthesised.^[12,13] In one example, reported by Vögtle and co-workers, no yields were reported. Dettelier and Stover used Pedersen's approach to repeat Vögtle and co-workers research, however yields were reported to be very poor (2%).^[14,15] Dettelier and Stover synthesised **43a** in two steps *via* a reaction in DMF to protect the amine functionality of dopamine, as shown in Scheme 2.4.4. Crown ether cyclisation was then performed. The formidyl group was removed by reflux in dilute hydrochloric acid (5%) in methanol (1:1) to afford **43a** in moderate yield.

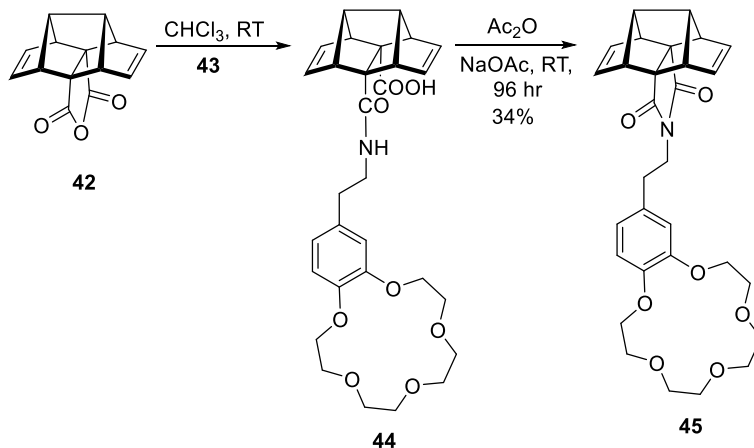
Following Dettelier and Stovers method with minor modifications, using the hydrochloride salt of dopamine rather than bromide salt, the dopamine derived benzo-15-crown-5 ether **43a** was synthesised in 60 % yield. The successful

synthesis of **43a** was confirmed by NMR spectroscopy with the removal of the formidyl group and proton resonance at 8.12 ppm, consistent with reported literature values.^[15] It should also be noted that further work with the larger 18-crown-6 formidyl compound **70b** did not progress beyond this point due to the preliminary results of **43a** with anhydride **42** (see Scheme 2.4.5).



Scheme 2.4.4 Dettelier and Stover's method for the synthesis of crown ethers derived from dopamine hydrochloride.^[15]

The dopamine derived crown ether **43a** was allowed to react with the anhydride **42**, the synthesis of which is described in Section 2.3. These two analogues were combined to afford the imide **45** as shown in Scheme 2.4.5. This procedure involved the use of a primary amine which ring opens the anhydride to afford an amic acid **44**. This is followed by dehydration and ring closure of the intermediate amic acid to form the imide product **45**.



Scheme 2.4.5 Synthesis of the initial polycyclic norbornyl block **45** for future ion channel transport.

Upon addition of substrates, **43a** and **42** the amic acid **44** was isolated with the solvent removed and the residue used in the subsequent ring closure reaction to the imide without purification or characterisation. Analysis of a sample of **45** after 48 hrs *via* ^1H NMR spectroscopy indicated that a significant portion of the reaction mixture was derived from the decomposition of **43a**, with no observed resonances consistent with the starting material within the spectrum. The formation of the amic acid **44** took up to 3 – 4 days and after this time the amine was observed to be fully decomposed with multiple aromatic and crown ether resonances within the ^1H NMR spectrum. Increasing the temperature (to 60°C) of the reaction did not increase amide formation, however contributed to increased rates of amine decomposition. Small amounts of the amic acid were subjected to ring closure conditions to form the imide **45**. Compound **45** was isolated *via* column chromatography (DCM/MeOH, silica) in a moderate yield (34 %).

Compound **45** was characterised by ^1H NMR spectroscopy, with aromatic doublet resonances at 6.74 ppm ($J = 8.04$ Hz) for the *ortho* positioned protons. The other doublet of doublets and small doublet are overlapped within the spectra which were split by *ortho* and *meta* protons. The representative alkene resonance was observed at 5.89 ppm. The crown ethers were characterised *via* multiple resonances between 4.12-3.74 ppm integrating for 16H. Two triplet resonances at 3.60 ppm ($J = 7.68$ Hz) and 2.68 ppm ($J = 7.80$ Hz) were identified for the protons (CH_2) between the imide and the aromatic crown ether. The norbornyl bridgeheads and *endo* protons are characterised by resonances at 3.41 (4H) and 2.85 ppm (2H).

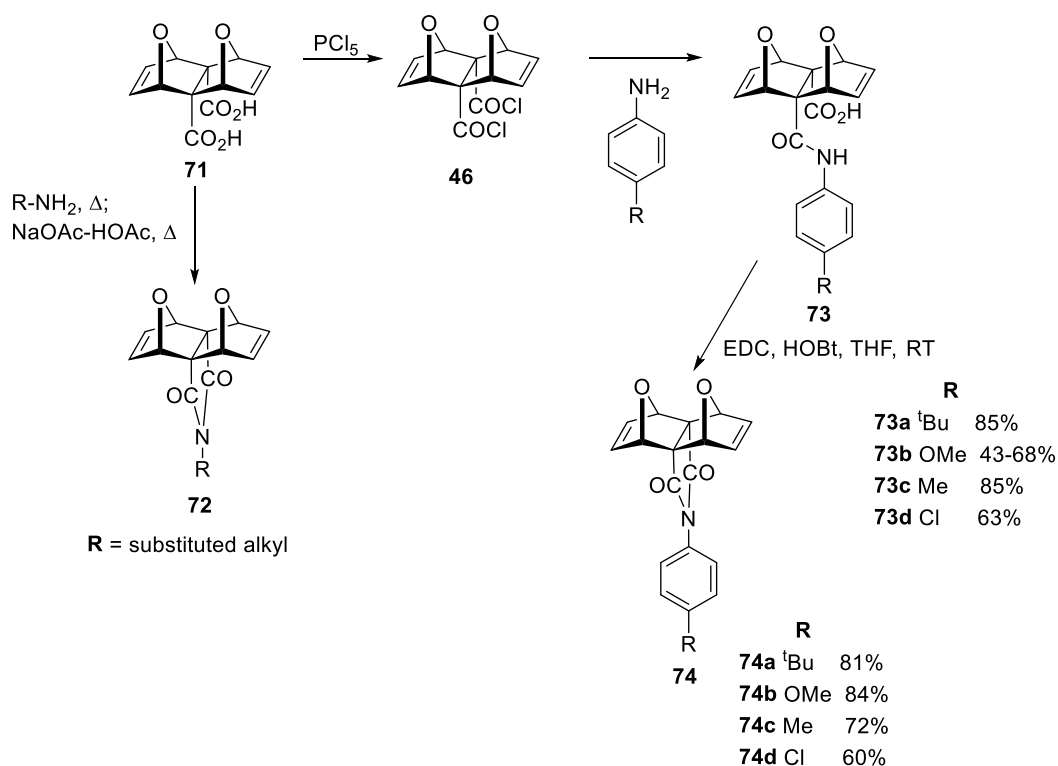
Compound **45** was additionally characterised by ^{13}C NMR spectroscopy where the alkene resonance was observed at 132.1 ppm. Crown ether resonances within the ^{13}C NMR spectroscopy ranged between 70.0-61.0 ppm with peak overlap visible. This was due to small differences between each proton and carbon chemical environment on the crown ether. Therefore different numbers of resonances were observed with numerous compounds with crown ethers attached. The ^{13}C NMR spectrum was consistent with the appearance of the carbonyl resonances from the imide at 175.3 ppm. High resolution mass spectroscopy ESI confirmed the structure, calculated for $\text{C}_{30}\text{H}_{33}\text{NO}_7\text{Na}$, 542.2155, found 542.2146 $[\text{M}+\text{Na}]^+$.

Although **45** was obtained in a moderate yield, the compound was difficult to produce, with the most troublesome steps being the initial amic acid formation

and the purification of the cyclised imide. Due to these concerns further synthetic pathways were explored.

2.5 Synthesis and Reactivity of Acid Chloride Polycyclic (Hedaya Diene) Substrates

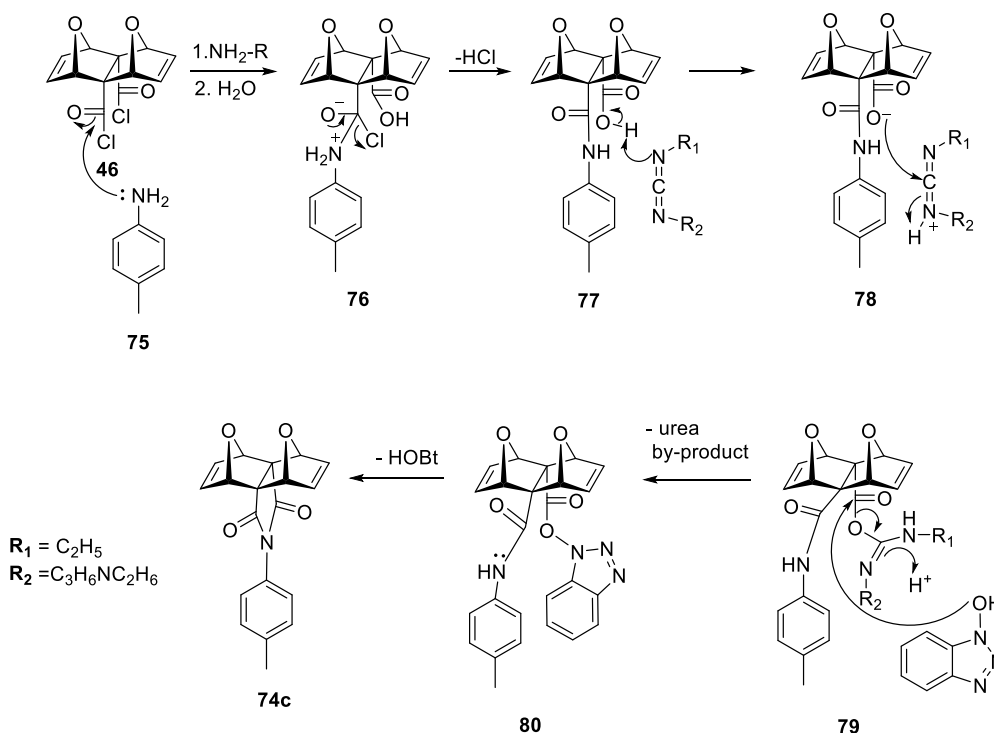
The synthesis of alkyl-substituted imides with polynorbornyl systems has been explored previously.^[1,16-18] As outlined in this thesis (Section 2.4) and in previous works,^[19-24] the reaction of aliphatic amines with anhydrides proceeds through a two-step process, involving formation of amic acid followed by dehydration to the corresponding imides in moderate yields as outlined in Scheme 2.5.1.



Scheme 2.5.1 Gaynor and co-workers' approach to the synthesis of polycyclic aryl-substituted systems.^[25]

Reactions of anilines with anhydrides positioned beneath polycyclic backbones under both mild and harsh reaction conditions have failed to produce acceptable yields of the amic acid or imide.^[25] This led to the synthesis of more reactive substrates such as that outlined by Gaynor and co-workers and their work with *exo,exo*-fused-oxabridged norbornene *bis*-acyl chloride. The *bis*-acyl chloride **46** was found to show increased reactivity towards aryl amine substrates (Scheme 2.5.1).

In Gaynor and co-workers' research the acid chloride **46** was generated from the *bis*-acid **71** by treatment with phosphorus pentachloride (PCl_5), although the acid chloride is moderately unstable (Scheme 2.5.1). *Para* substituted aromatic amines such as 4-methylaniline, reacted with the *bis*-acylchloride and on work up, formed the amic acid in moderate yields (Scheme 2.5.2). Coupling reagents, EDC and HOBt aid in ring closure of the amic acid to the imide **74c**.

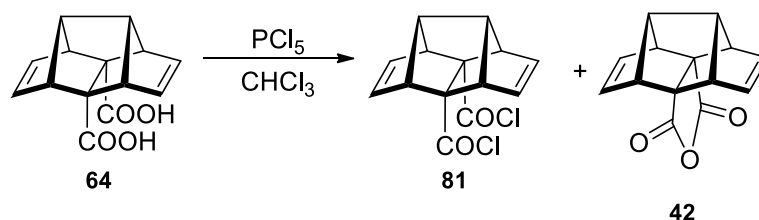


Scheme 2.5.2 Mechanism for the formation of the imide **74c** with coupling reagents EDC and HOBt.

Following the success of Gaynor and co-workers' synthesis of the *bis*-acyl chloride derivative **46**, and its increased reactivity towards aromatic amines, an investigation into the synthesis of the corresponding Hedaya diene *bis*-acylchloride **81** was initiated. This route was anticipated to involve reduced reaction times, due to the increased reactivity of the *bis*-acyl chloride Hedaya block, and hence was expected to lead to much more limited decomposition of the dopamine crown **43a**. This is important because **43a** showed significant decomposition when treated with the corresponding anhydride systems, as described in Section 2.4.

Bis-acyl chloride **81** was synthesised under the conditions outlined by Gaynor and co-workers, (Scheme 2.5.3). Analysis of the ^1H NMR spectrum of the crude

material showed that the stability of the acid chloride was poor. Three compounds were observed in the ^1H NMR spectrum namely, starting *bis*-acid **64**, anhydride **42** and *bis*-acyl chloride **81** (Scheme 2.5.3). This was evident from the alkene resonances for the anhydride and *bis*-acid, which were observed at 6.09 and 6.16 ppm respectively. In addition a new alkene resonance was observed at 6.23 ppm which was ascribed to the *bis*-acyl chloride. The stability of the *bis*-acyl chloride was investigated *via* ^1H NMR spectroscopy by analysis of the reaction mixture by dissolving in reagent grade CDCl_3 . The spectra showed a decrease in **81**, and an increase in **42** over time. This indicates that the *bis*-acyl chloride **81** preferred to ring close to the anhydride as time progressed, presumably because the anhydride is more stable. This suggests that one of the acid chloride groups had hydrolysed to a carboxylic acid which subsequently reacts with the remaining acid chloride to produce the anhydride. It is also possible that the acid chloride, carboxylic acid intermediate prefers to undergo intramolecular ring closure over the intermolecular reaction with PCl_5 .



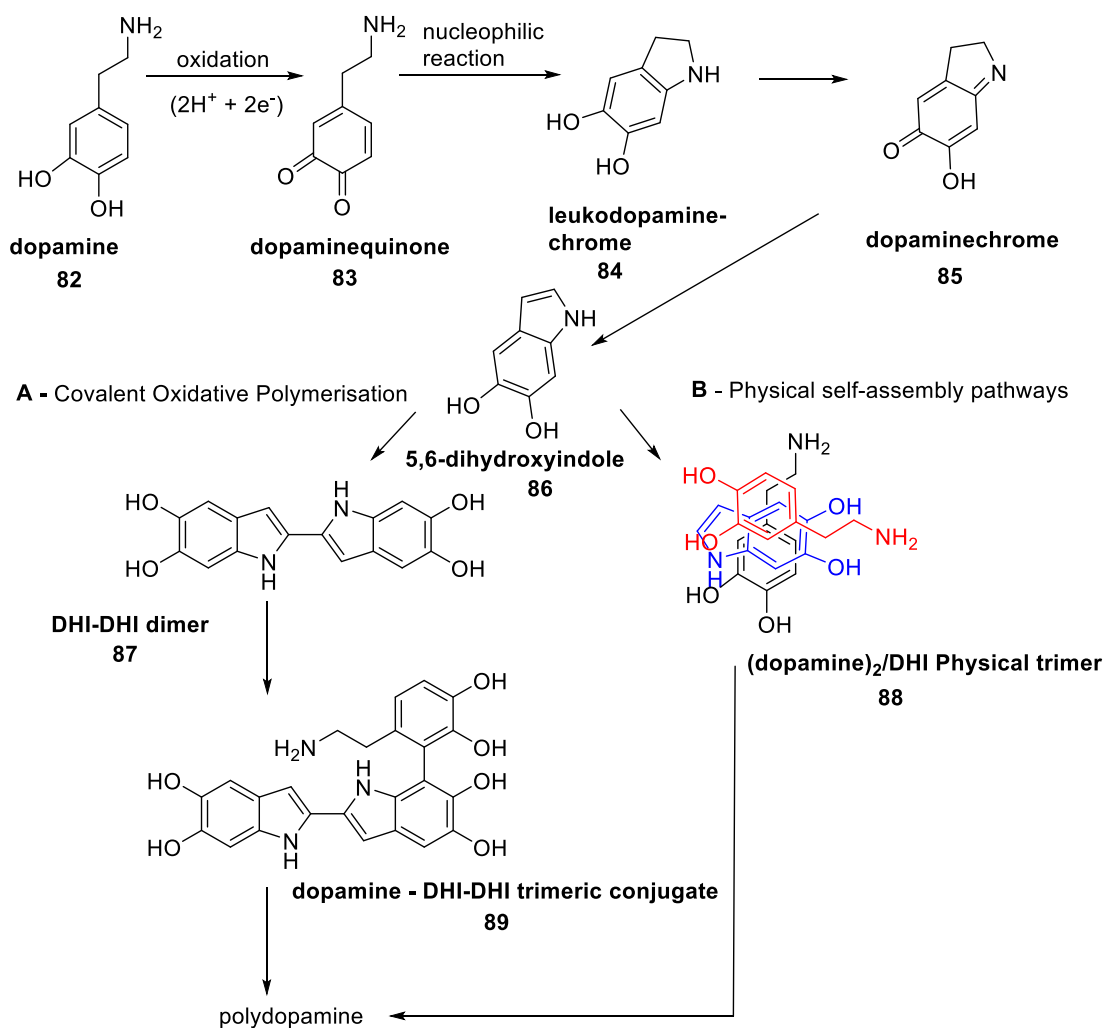
Scheme 2.5.3 Synthesis of the novel Hedaya *bis*-acyl chloride **81**.

The route involving the reaction of the dopamine derivative **43a** with the *bis*-acyl chloride **81** was abandoned due to the instability of both compounds. In addition further analysis of the literature gave insight into the potential decomposition products of dopamine.

2.6 Investigations into the Decomposition of Dopamine

In recent years there has been an interest in the attachment and self-assembly of catechols and derived compounds in various inorganic and organic materials^[26] due to their useful properties with respect to surface modification.^[27,28] Polydopamine coatings were first reported by Messersmith and co-workers in 2007 and were inspired by the adhesive properties of marine mussels.^[27] Polydopamine is spontaneously formed from dopamine hydrochloride in alkaline solutions, undergoing oxidative polymerization.^[28] There is widespread use of polydopamine^[29–33] however the mechanism by which it forms is not fully

understood, nor has it been investigated. Suggestions have been made that polydopamine forms *via* a biosynthetic pathway similar to that of melanin biosynthesis.^[8,27,28,34] The melanin biosynthetic pathway comprises an oxidative process in which dopamine is converted into L-dopaquinone from L-tyrosine, similar to the dopamine transformation to 5,6-dihydroxyindole (DHI, **86**) outlined in Scheme 2.6.1 through oxidation and other polymerisation stages.^[27] The polydopamine synthetic pathway is shown in Scheme 2.6.1.

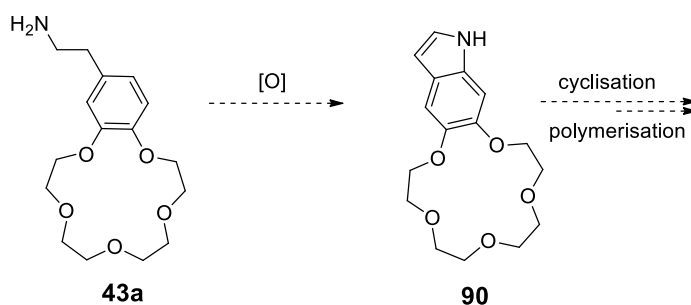


Scheme 2.6.1 Lee's proposed mechanism of polydopamine synthesis.^[27]

The proposed pathway suggests that catecholamine compounds such as dopamine are susceptible to oxidation to *o*-quinones, such as dopaminequinone **83** which eventually leads to a nucleophilic cyclisation of the amine onto the ring to form leukodopaminechrome **84**.^[35] This synthetic process eventually leads towards the formation of polydopamine through 5,6-dihydroxyindole **86**.^[27,28,34,35] Therefore in previously synthetic approaches, dopamine 15-crown-5 **43a** may

potentially have been oxidised then cyclised to produce **90** in a similar manner to dopamine itself (Scheme 2.6.2). Although this is not mechanistically viable, it is a possible pathway for **43a** decomposition.

If this is the case, long reaction times and varying reaction conditions (i.e. heat) will favour the formation of compounds similar to quinone **83** rather than reaction of the amine with electrophiles such as anhydrides and acid chlorides.



Scheme 2.6.2 Potential method of dopamine 15-crown-5 oxidation and cyclisation towards polymerisation.

Due to the abovementioned concerns and observations it was decided that other synthetic strategies were required.

2.7 Imide Synthesis of Polynorbonyl Frameworks for the Attachment of Functionalised Alkyl Halides

Attachment of functionalised aromatic crown ethers to an imide was a possible synthetic approach (Section 2.1. pathway III) for the incorporation of an ethylene linker, as described for dopamine. Examination of the literature has identified various synthetic procedures for preparing polynorbonyl imides. These procedures will be reviewed and used in order to gain a greater understanding of imide functionalities. Model systems will also be considered.

A number of polynorbonyl frameworks have used a readily available imide for the synthesis of new functionalised systems. Polynorbonyl imides in various rigid arrangements such as the *endo*-carbocyclic anhydride **91**,^[36] *bis*-oxa **92b** and the Hedaya **49**^[37] motifs will be discussed briefly (Figure 2.7.1).

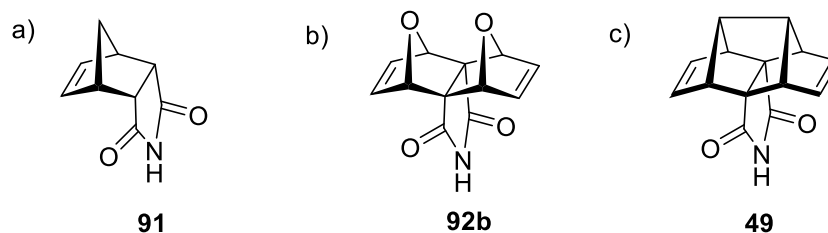
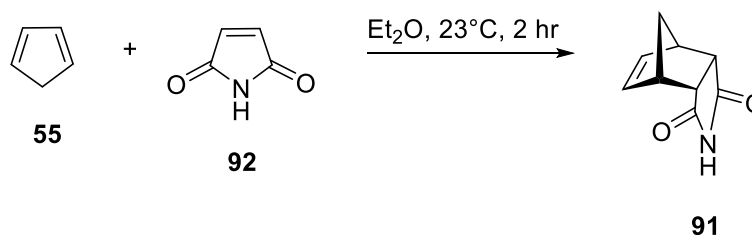


Figure 2.7.1 Imide containing building blocks for attachment of functionalised aromatic crown ethers with an ethylene spacer.

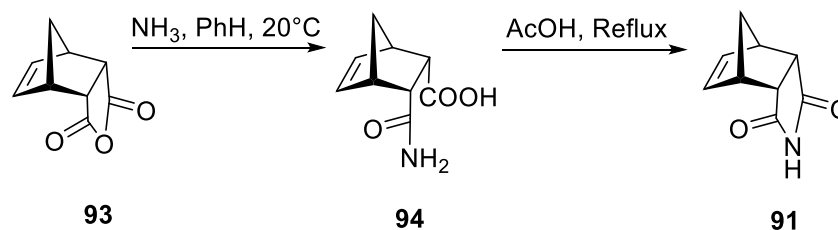
Literature studies investigated the synthesis and use of the *endo*-carbocyclic imide **91** through a number of processes. One of the first procedures explored within the literature was by Blechert and co-workers, where **91** was synthesised by Diels Alder reaction of cyclopentadiene and maleimide.^[36] This procedure required cyclopentadiene and maleimide to react at 23°C for 2 hrs (Scheme 2.7.1) after which a solid precipitate was removed by filtration and dried to afford the imide **91** in 96 % yield.



Scheme 2.7.1 Blechert and co-workers synthesis of *endo* imide.^[36]

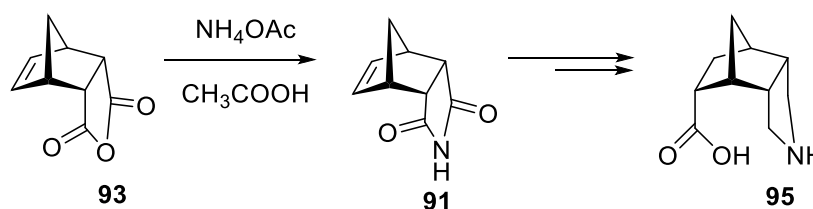
However, as the *endo*-carbocyclic anhydride **93** (Scheme 2.7.2) had been prepared in the current project, for use in anhydride reactivity studies with aliphatic and aromatic amines, imide formation from anhydrides was investigated here.

Literature has revealed the preparation of imide **91** from the already established anhydride functionality. Kas'yan and co-workers discovered an aminolysis approach with ammonia (NH₃). In this procedure the anhydride **93** was stirred in a solution of benzene whereupon a 25% ammonia solution was added dropwise, to afford the amic acid **94** in good yields (82%).^[38,39] Kas'yan and co-workers subjected the amic acid to dehydration under reflux in acetic acid for 6 hr to afford the imide **91** in good yields (78%, Scheme 2.7.2). Although successful, this approach requires two synthetic steps, as opposed to other procedures outlined in the literature.



Scheme 2.7.2 Kas'yan and co-workers synthesis of *endo* imide **91**.^[39]

In 2009, Breuning and co-workers investigated the enantioselective synthesis of tricyclic amino acid derivatives based upon a central polynorbornyl framework. A pyrrolidine ring was installed in the 2,3 *endo* positions with a methylene or ethylene carbon chain (shown in Scheme 2.7.3). The compounds synthesised with the amino acid functionality were promising derivatives for β -turn inducing peptide motifs in peptidomimetics as well as *bi*-functional organocatalysts. The imide **91** was synthesised in one step from the readily prepared *endo*-carbic anhydride **93** with NH_4OAc in acetic acid, with heating under reflux at 140°C for 4 days.



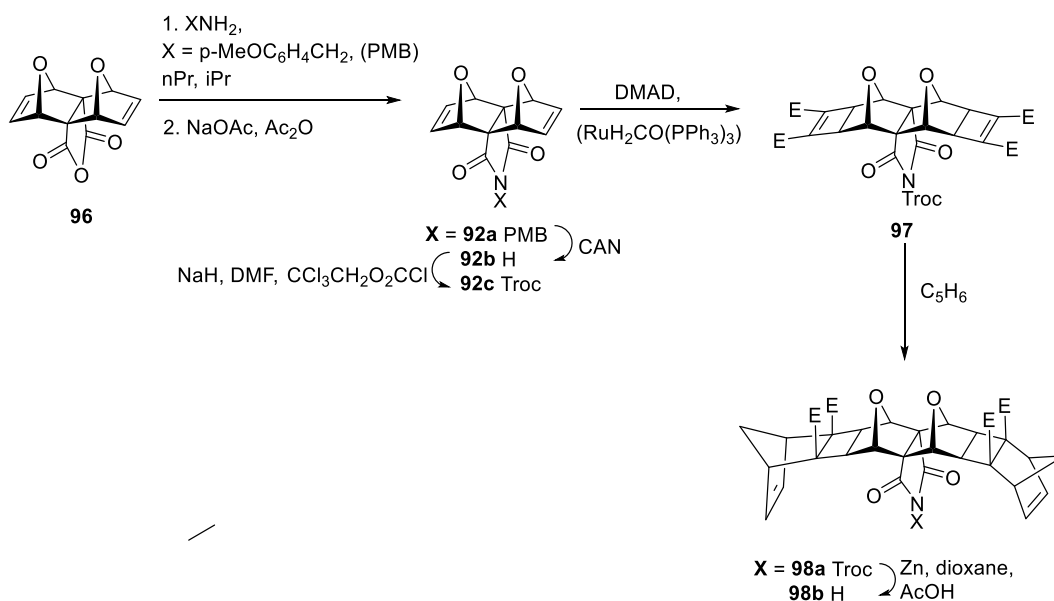
Scheme 2.7.3 Breuning and co-workers synthesis of imide **91**.^[40]

More recently Combe and co-workers used a similar procedure to that outlined above, in their investigations towards the synthesis of co-polymers using a ring opening metathesis procedure. However in their method the imide was synthesised in a quantitative yield under reflux for 16 h^[41] in comparison to the 4 days described by Breuning and co-workers. Both procedures are high yielding and either procedure was adequate in the synthesis of imide **91**. Application of their methods allowed the imide to be synthesised in this project (Breuning's synthesis, quantitative yield) in 84% yield. This was an important compound which was further used in this thesis as a model substrate for additional studies detailed in Chapter 3.

In comparison to these straightforward synthetic procedures for the synthesis of imide **91**, the *bis*-oxa polynorbornyl imide **92b** synthesis was slightly more

complex. This was due to the heat sensitivity of the *bis*-oxa system, which readily undergoes a retro Diels Alder reaction, resulting in the the loss of furan.

Paddon-Row and co-workers investigated the synthesis of novel U-shaped systems which contain the imide functional group for the investigation with solvent and neighbouring group interactions. This system required the installation of the imide with a protecting group such as *p*-methoxybenzene (PMB) which was removed with cerium (IV) ammonium nitrate (CAN) to afford the imide **92b** in a moderate to poor yield^[19] shown in Scheme 2.7.4.



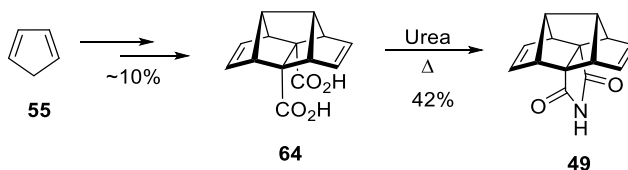
Scheme 2.7.4 Preparation of *Bis*-oxa norbornyl imide motifs with the use of both PMB and Troc protecting groups.^[19]

The early removal of the PMB group was critical as it was described by Paddon-Row and co-workers to be problematic when removed later in the synthesis.^[19] The PMB group was then replaced with a trichloroethoxycarbonyl (Troc) group which was much more readily removable with zinc. The Troc group remained in place until all cycloaddition reactions were complete.^[19] Upon removal of Troc the free imide (NH) could be functionalised accordingly.

This approach was considered for the synthesis of imide **49** (Scheme 2.7.5), however the additional protection stage with PMB was viewed negatively, due to a decrease in yield. This method towards the formation of the imide was set aside as an alternative approach if all other procedures proved to be problematic for the synthesis of **49**.

The synthesis of imide **49** was brought to our attention from the recent studies of Vazquez and co-workers, who investigated a series of polycyclic compounds based on analogues of adamantane to inhibit Influenza A virus replication.^[42] Amantadine and Rimantadine are both FDA approved antiviral drugs that inhibit a viral protein, M2, a proton channel. In recent times the use of adamantane analogues for the treatment of influenza A has ceased due to the resistance of the virus to the drug. Vazquez's research explored novel drugs that were effective against new types of influenza Am-resistant strains.^[42] In the process, polynorbornyl motifs were synthesised, derivatised and tested against new strains of influenza virus, for example H1N1 swine flu. During the course of their synthetic pathways, imide **49** became a valuable target and was synthesised from the *bis*-acid **64** via the decomposition of urea to ammonia and CO₂ at high temperatures.

Herein exploration of the synthesis of imide **49** with both NH₄OAc, used for *endo*-carbic imide **91** synthesis' as well as the use of urea at high temperatures as outlined by Vazquez and co-workers was undertaken (Scheme 2.7.5).



Scheme 2.7.5 Synthesis of Imide **61** via Vazquez and co-workers method.^[42]

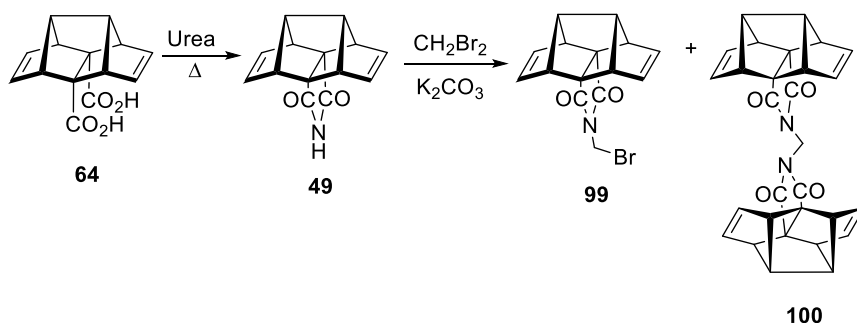
The *bis*-acid **64** was allowed to react neat with urea at high temperature. Initially the material was heated from room temperature to melt urea (135°C) then the temperature was slowly increased to 180°C over a period of 30 min. The urea continued to melt and decompose around the *bis*-acid to afford the imide **49** in a moderate yield (42%).

Characterisation of the imide *via* ¹H and ¹³C NMR spectroscopy indicated resonances which were consistent with literature values.^[42] However upon characterisation *via* HRMS, in both positive and negative ionisation modes resulted in a mass to charge ratio (*m/z*) of 225.1027 [M+H]⁺, [M+H]⁻, C₁₄H₁₃N₂O which was not consistent with the calculated *m/z*, 225.0790, C₁₄H₁₁NO₂. The MS identification of two nitrogens is strange and is inconsistent with the imide structure **49**. However, quite similar *m/z* ratio's the formula is not exactly correct. This led to further characterisation *via* infrared spectroscopy (IR) to identify the

removal of the OH peaks at 3477 cm^{-1} from the *bis*-acid and the additional C-N stretch at 1069 cm^{-1} in comparison to the starting material. Subsequent products synthesised using **49** showed correct MS values, thus **49** was determined to be the correct structure.

Additional analysis of the imide was initiated with trial reactions with alkyl halides and then further analysed *via* HRMS. This synthetic strategy also gave insight into the nucleophilicity of the imide which from our understanding had not been explored within the [n]norbornyl type frameworks.

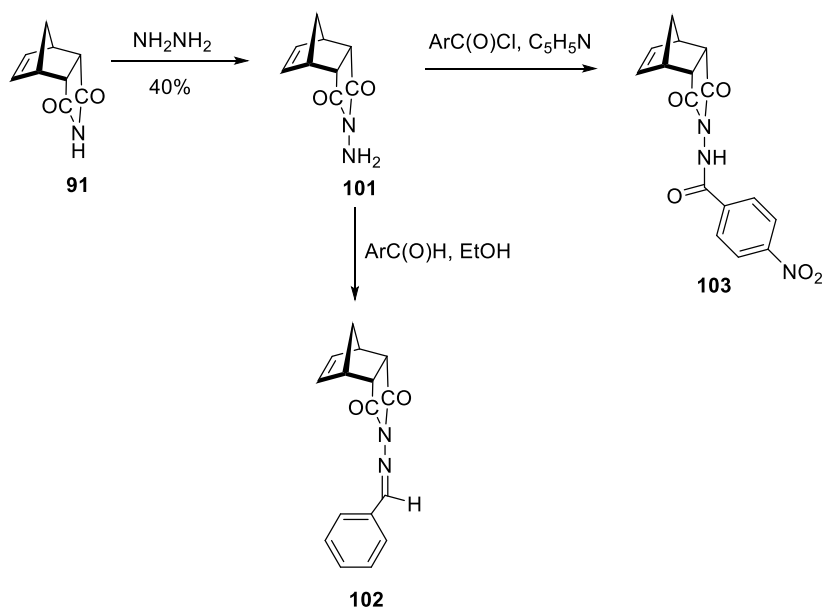
The imide **49** was treated with dibromomethane (CH_2Br_2) and potassium carbonate (K_2CO_3) in acetone at reflux for 7 hr, affording a mixture (Scheme 2.7.6). The crude ^1H NMR spectrum of the mixture suggested two products **99** and **100**, which were isolated *via* column chromatography (hexane: ethyl acetate on silica) to afford the mono adduct **99** (15%) and the dimer **100** (49%). The ^1H and ^{13}C NMR spectra for both the monomer and dimer were consistent with the proposed structures. Doubling in the integration of the proton resonances were observed for the dimer except for the adjoining CH_2 group between the [n]polynorbornyl blocks, observed at 2.84 ppm. The HRMS-ESI data were also consistent with the structure for the monomer **99**, HRMS-ESI calculated for $\text{C}_{15}\text{H}_{12}\text{BrNO}_2\text{Na}$, 339.9949, found 339.9961 $[\text{M}+\text{Na}]^+$. The dimer **100** was also confirmed *via* HRMS-ESI calculated for $\text{C}_{29}\text{H}_{22}\text{N}_2\text{O}_4\text{Na}$ 485.1477, found 485.1483 $[\text{M}+\text{Na}]^+$.



Scheme 2.7.6 Nucleophilic substitution reactions of alkyl halide with imide **49**.

Further analysis of varying attachments of the crown ether to the polynorbornyl imide were examined within the literature. One synthetic pathway which may have overcome the difficulties in attachment of the crown system to the imide, is with the reaction of the **91** with hydrazine (Scheme 2.7.7).^[43–45] This reaction led to the attachment of aromatic rings through Kas'yan and co-workers' acid

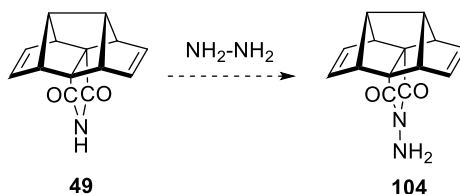
chloride^[38] synthesis with **101** as outlined in Scheme 2.7.7. In addition the aldehyde^[46] functionality may be attached to the hydrazine adduct **101** through a reaction outlined by Gul and co-workers in Scheme 2.7.7. The aromatic ring in these procedures could be substituted to allow for crown ethers to be attached using this methodology.



Scheme 2.7.7 Hydrazine reactions with *endo* imide **91** for further attachment of various functional groups.^[38,46]

However the use of the hydrazine reaction does not facilitate an ethylene linker, a three carbon unit linker is likely. Molecular modelling of both systems indicated slight twists in both linkages to the [n]polynorbornyl scaffold which may compromise the translocation of ions in a final artificial ion channel system functionalised with crown ethers.

This synthetic approach was explored for the Vazquez imide **49** (Scheme 2.7.8), however all attempts to synthesise **104** were unsuccessful.



Scheme 2.7.8 Attempted synthesis of hydrazine derivative **104** for further attachment of functional groups.

It was unclear as to the reasons associated with the unsuccessful synthesis of **104**. One possible explanation may be due to the steric bulk of the system, specifically the polycyclic structure in comparison to the model system **101** outlined in Scheme 2.7.7.

It may also be related to decreased reactivity of the nucleophile towards hydrazine and the solubility of the system. The preparation of the above key compound **104** for the attachment of functionalised crown ethers was problematic. Therefore alternative methods were required, for the synthesis of a functionalised crown ether system to attach to the polynorbornyl molrac.

2.8 Alternative Pathways to an Ethylene Linker

As a result of the instability of dopamine, other means of synthesising an ethylene linker between the polynorbornyl and aromatic crown ether were explored. The issues that surround an ethylene linker between the aromatic crown and polynorbornyl may potentially be overcome by using hydroxytyrosol, a metabolite of dopamine. This compound contains functionality to allow for the benzocrown ether synthesis as well as attachment to the polynorbornyl imide. Hydroxytyrosol is a natural phenylethanoid which is commonly found in olive oil and leaf with a cost of \$1000 per 100 mg.^[47] It is known to have pharmacological properties such as but not limited to antimicrobial and anti-inflammatory activity. Hydroxytyrosol can be accessed through molecular engineering more specifically using amino acids for example L-tyrosine.^[48,49] Although hydroxytyrosol can also be extracted from plants on a small scale, a low cost and effective synthetic route is desirable to obtain this pharmaceutical and valuable food additive in high yields.

Pathways which have been explored in this study to synthesise ethylene chain bearing linkers (Figure 2.8.1) around hydroxytyrosol **105** involve various chain extension reactions. This would extend the alkyl chain with end group functionality to attach to the rigid block through the already established imide **49** synthesised previously. An alternate pathway would see the crown hydroxyl react with the imide under Mitsunobu reaction conditions (not pictured) or through the chlorinated substrate **107** with imide **49** shown in Figure 2.8.1.

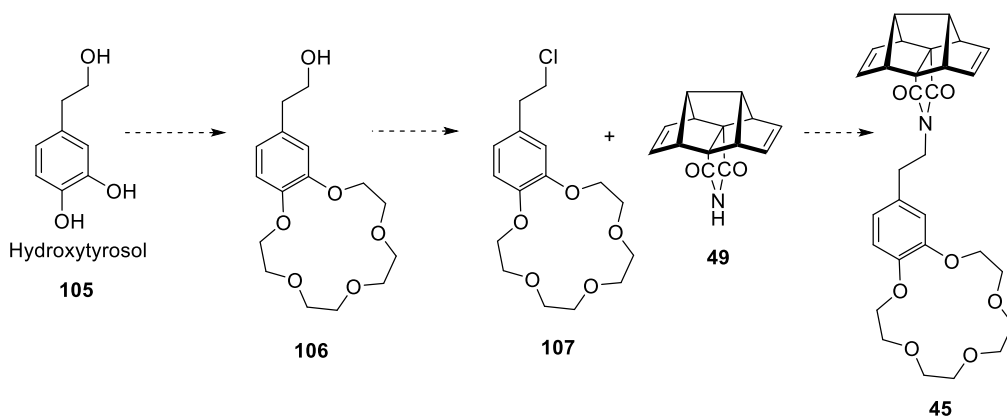


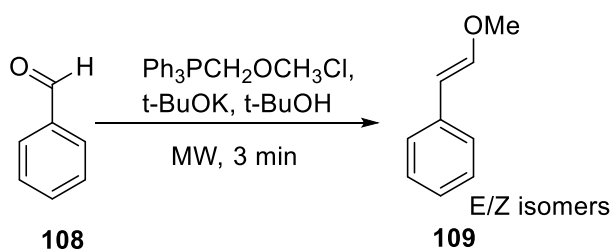
Figure 2.8.1 Hydroxytyrosol pathway to fused ethylene polynorbornyl block systems.

The preparation of hydroxytyrosol *via* various different synthetic routes has been described in the literature. Many pathways use varying hydroxytyrosol derivatives, for example the first reported synthesis performed by Schopf and co-workers in 1949, which hydroxytyrosol was prepared from 3,4-dihydroxyphenylacetic acid.^[50] Other pathways to hydroxytyrosol have included synthetic procedures using metal catalysts^[51,52], Grignard reactions^[53] using ethylene oxide, synthesis of α -cyanoenamines^[51] and reactions with readily available compounds such as euganol.^[54,55]

However, many of these synthetic pathways use reagents that can be expensive, highly toxic or not easily accessible. This research aimed to synthesise hydroxytyrosol from readily available laboratory reagents and accessible catechol derivatives, thus no further mention of the synthetic procedures outlined above will be further discussed in this thesis.

One approach to the synthesis of hydroxytyrosol from readily available laboratory reagents was through a Wittig reaction using substituted aromatics. The Wittig reaction, a transformation involving an ylide reacting with a ketone or aldehyde, was first described in 1953 by George Wittig and George Geissler.^[56] The Wittig reaction installs functionality *via* carbonyl olefination, however the functionality introduced depends on the triphenylphosphonium ylide employed in the synthesis. There are two types of ylides, stabilised and non-stabilised. Ylides that are stabilised are referred to as having an R group which is anion stabilizing, for example CN, or ester (CO₂CH₃), and therefore less reactive. In comparison, ylides that bear alkyl substituents are anion destabilising and therefore tend to have greater reactivity towards aldehydes and ketones.^[57]

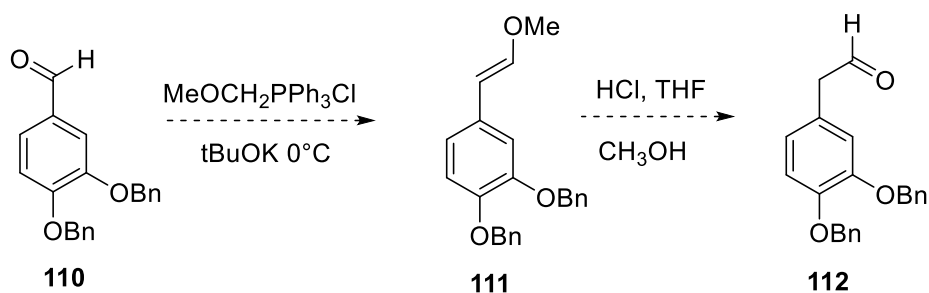
The ylide initially investigated in this study was prepared from the phosphonium salt, methoxymethyl triphenylphosphonium chloride, which undergoes a homologation reaction to extend the alkyl chain by a methylene unit, disclosed by Saidi and co-workers as shown in Scheme 2.8.2.^[58]



Scheme 2.8.2 Saidi and co-workers methylene unit extension of benzaldehyde.^[58]

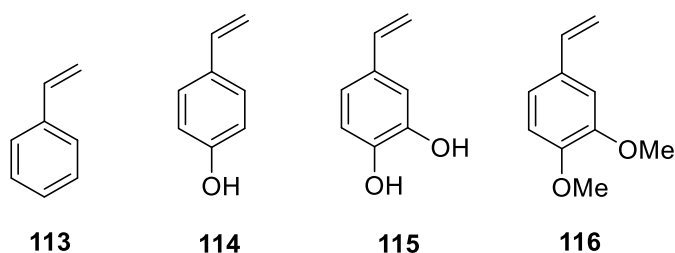
There have been examples described in the literature where aromatics substituted in all 1', 3', and 5' positions on the ring with nitro, dimethylamine and or methoxy groups have proven to yield the corresponding homologated methoxy derivative. However there has been limited evidence of this ylide reacting with dihydroxy substituted aromatic rings. Primarily within this research a derivative with both 3,4-dihydroxy substitution was required, with a view to the formation of crown ethers later in the synthesis.

Initial synthesis towards the homologation reaction involved the benzyl protected substituted aromatic aldehyde shown in Scheme 2.8.3. The use of methoxymethyl triphenylphosphonium chloride proved fruitless with varying reaction temperatures and reaction times, yielding only recovered starting material. The lack of reactivity may be due to the stabilisation of the ylide as well as the reduced reactivity of the aromatic with the benzyl groups attached in the *meta* and *para* positions therefore not allowing reactivity at the aldehyde.



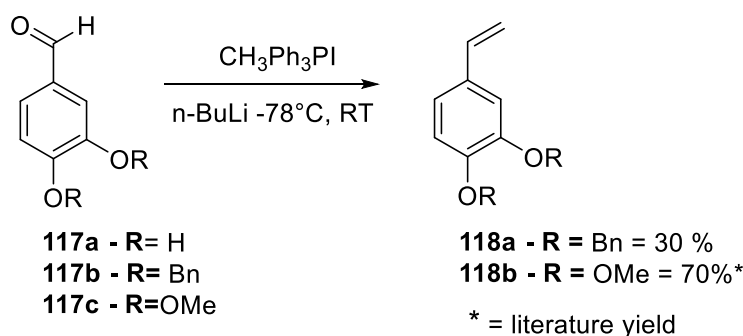
Scheme 2.8.3 Wittig reaction pathway with the addition of an additional carbon unit in **112**.

Due to the lack of reactivity of the previous ylide (anion stabilising) and substrate, a common Wittig reagent was used, methyltriphenylphosphonium iodide to synthesise the alkene based products (Scheme 2.8.4). Wittig reactions with methyltriphenylphosphonium iodide have greater reactivity towards aldehydes and ketones attached to an aromatic ring in comparison to the methoxymethyl triphenylphosphonium chloride ylide.^[57]



Scheme 2.8.4 Various products from Albert *et al.* of Wittig reactions with methyltriphenylphosphonium iodide.^[59]

Albert and co-workers in 2011 discussed the synthesis of the above compounds, however their purpose was to synthesise stilbenes from the Mizoroki-Heck reaction.^[59] Herein, the objective was to synthesise the 3,4 substituted aryl alkene with the intention to apply a hydroboration reaction to the olefin to afford the primary alcohol. However, there has been limited evidence to suggest this occurring with the free hydroxyl groups present.^[60,61] This led to the protection of the hydroxyl groups as benzyl ethers, and allowing reaction with the Wittig reagent, shown in Scheme 2.8.5. The reaction to produce **118a** was analysed *via* ¹H NMR spectroscopy, and found to be very low yielding, recovering large quantities of starting aldehyde **117b**. The reaction conditions were altered leaving the reaction to proceed for extended periods of time, however the amount of product recovered after purification was moderate to poor (30% yield) on all occasions. Analysis of the ¹H NMR spectra indicated the loss of aldehyde resonance at 9.81 ppm from the starting aldehyde with the addition of new double bond resonances observed at 6.66 ppm, 5.62 ppm and 5.18 ppm. Gas chromatography mass spectroscopy data were consistent with the structure C₂₂H₂₀O₂ (calculated 316.14 m/z) at a retention time of 13.9 min and observed mass of 316.2 m/z.



Scheme 2.8.5 The Wittig reaction of both benzyl and methoxy substituted aromatics.^[59]

The protection of the 3,4-dihydroxy groups with methoxy functionality was not investigated in these reactions due to the difficulties associated in their removal later in the synthetic plan. However Albert and co-workers have investigated the use of methoxy groups (Scheme 2.8.5) in the Wittig reactions with good yields above 70% obtained.^[59] This may suggest in the above reactions with the installed benzyl group that steric bulk may be a factor in the low yields observed. However it was necessary to have these hydroxyls protected and easily deprotected for further crown ether attachment after the styrene conversion to the alcohol by hydroboration procedures.^[61]

Due to the low yields isolated for **118a**, the hydroboration was not carried out, and the alcohol **105** (Figure 2.8.1) was not produced. This led to an alternative synthetic approach for the synthesis of an ethylene linker molecule for the preparation of the crown ether polycyclic block in reasonable yields. Thus, our attention turned to the chain extension of catechol derivatives through the Wilgerodt-Kindler reaction, which will now be discussed in detail.

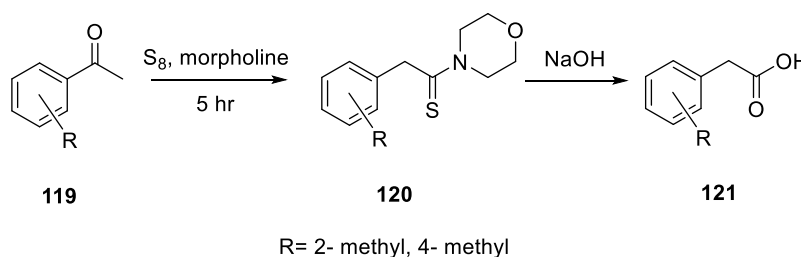
2.9 Wilgerodt-Kindler Reactions Towards an Ethylene Linker

The Wilgerodt reaction was first discovered by Conrad Wilgerodt in 1887, and involves the conversion of carbonyl compounds to terminal amides through an oxidative rearrangement procedure with aqueous ammonium polysulfide.^[62] The result of the reaction is the migration of the functional group to the terminus of the chain. In later years, 1923, Karl Kindler extended this reaction to involve elemental sulphur and a secondary amine such as morpholine, with the addition of heat to afford the corresponding thioamide derivative.^[63]

The Wilgerodt-Kindler reaction can be carried out in a one-pot process with the above reagents. The thioamides can be readily converted to carboxylic acids or

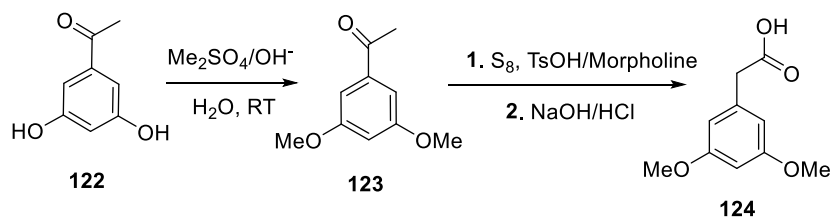
thioesters, however within this project conversion to carboxylic acids was investigated.

There is a widespread use of the Wilgerodt-Kindler reaction, within the pharmaceutical industry for the synthesis of stilbene derivatives as well as the manufacture of methamphetamines.^[62,64] The reaction for methamphetamine synthesis involves heating under reflux with sulphur, morpholine and methylacetophenone, as shown in Scheme 2.9.1 for five hours. Fergusson and co-workers have discussed the implications of the sulphur equivalents in reference to yield and purification issues determining the appropriate ratios to be 1:2.5:2 (acetophenone:morpholine:sulphur).



Scheme 2.9.1 Wilgerodt-Kindler reactions on substituted aromatic acetophenones towards their corresponding phenylacetic acids.^[65]

More importantly there are very few examples of 3,4-di-substituted acetophenones within the literature, more specifically with hydroxyl substituents. The most relevant derivative 3,5-dimethoxyacetophenone **123** was used by Sun and co-workers to synthesise the corresponding thiomorpholide and subsequently produce the phenylacetic acid derivative **124** (Scheme 2.9.2).^[66]

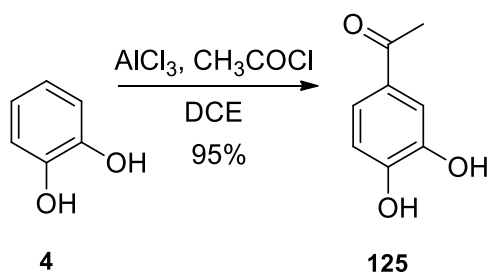


Scheme 2.9.2 Synthetic route towards chain extension of 3,5-disubstituted acetophenone.^[66]

Firstly, attempts at the preparation of 3,4-dihydroxyacetophenone are to be discussed with the substrate to be further used in the Wilgerodt-Kindler reaction. Synthesis of the 3,4-dihydroxyacetophenone *via* an acid catalysed reaction were

unsuccessful and or low yielding (Scheme 2.9.3) and further synthesis was required.^{[67][68]}

In mid-2012 a paper published by Payne and co-workers^[69] used a different synthetic method for the synthesis of the acetophenone which was used in an attempt to synthesise the desired compound shown in Scheme 2.9.3. Numerous efforts were made to reproduce the experiments outlined; however replication of the yields reported for this reaction was not possible. Specifically Payne and co-workers report a yield of 95% however the best reproduced was between 40-50%. One finding identified from subsequent repetitions is that when an NMR spectrum is acquired in deuterated chloroform there are numerous peaks evident, certain chemical shifts correspond to the product and others relate to the acylation of the hydroxyl groups to form the diester. However when the reaction mixture is taken for NMR spectroscopy in deuterated acetone, which is used as the NMR spectroscopy solvent in the described work by Payne and co-workers the NMR spectrum shows largely shifts for the product and some baseline impurities. It is unknown as to the circumstances surrounding the issues in replicating the reaction outlined by Payne and co-workers. In the process of acquiring yields as described by Payne and co-workers a number of different reaction conditions were used, for example, different reaction temperatures (-15°C to 0°C), purification of starting reagents and variations between inert gases, argon and nitrogen. However these reaction conditions did not significantly improve the yield above 30%.



Scheme 2.9.3 Payne's synthesis of 3,4-dihydroxyacetophenone **125**.^[69]

Figure 2.9.1 shows the NMR spectra of the 3,4-dihydroxyacetophenone in deuterated acetone in comparison to that in deuterated chloroform in Figure 2.9.2. The NMR spectra are of the same sample analysed in different deuterated solvents peaks at 1.26, 2.05, 4.12ppm are due to residual ethyl acetate.

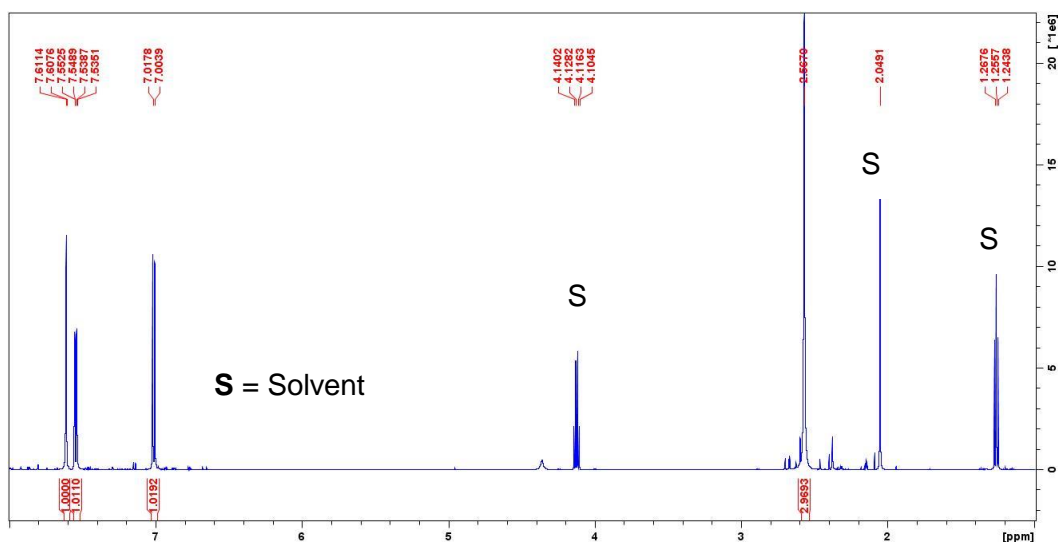


Figure 2.9.1 NMR Spectrum of 3,4-dihydroxyacetophenone **98** in deuterated acetone.

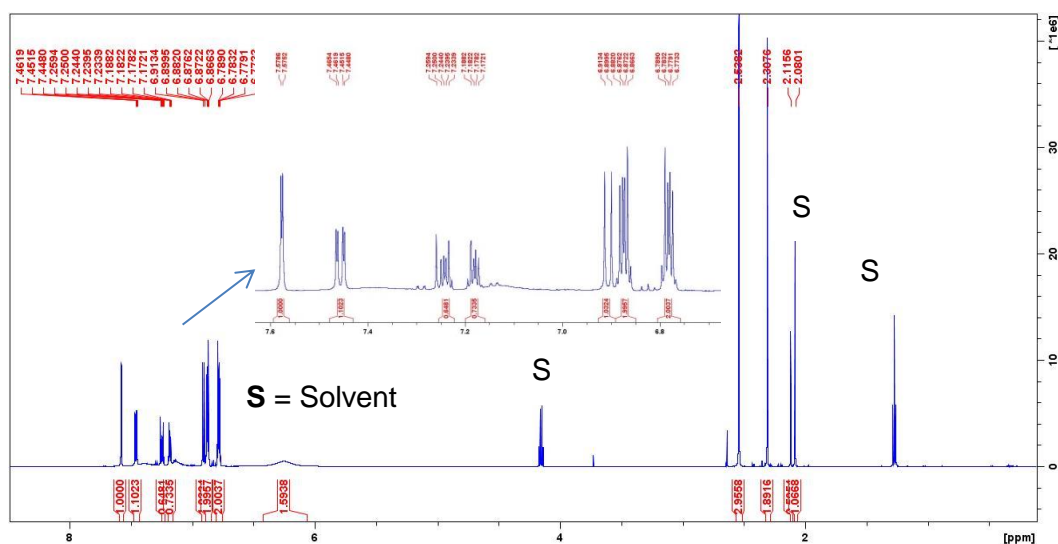


Figure 2.9.2 NMR Spectrum of 3,4-dihydroxyacetophenone **98** in deuterated chloroform.

As shown in the NMR Spectrum (Figure 2.9.2) with deuterated chloroform it suggests that there is a large amount of starting catechol, **4** (6.8-6.7 ppm) and also the possibility of retro acetylation at the alcohol groups (Figure 2.9.3), **126** (7.3-7.1 ppm). In addition the product, **125** was confirmed with a doublet resonance at 7.58-7.57 ppm, doublet of doublets observed at 7.46-7.44 ppm and large doublet at the observed resonance of 6.91-6.89 ppm.

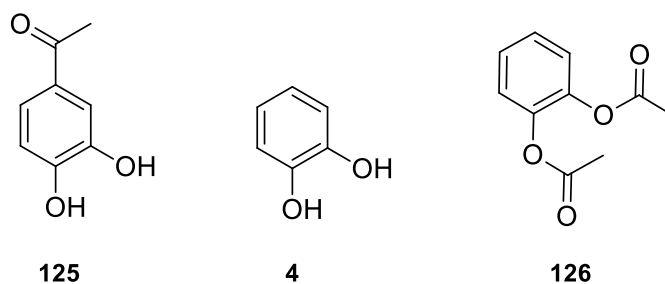
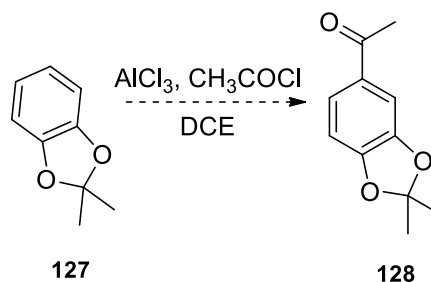


Figure 2.9.3 Three components of the ^1H NMR spectrum from the synthesis of **125**.

Due to the difficulties associated in synthesising **125** through the previously mentioned procedures, attention was turned to the protection of the hydroxyl groups as an acetonide.

A similar method by Iwagami and co-workers^[70] was also exhausted with the protection of catechol using an acetonide (Scheme 2.9.4) followed by addition of the acid catalyst and acetyl chloride. However, the conditions for this reaction in particular are reasonably acidic and this is apparently why, in our hands, no product was formed and NMR spectroscopy indicated that the acetonide protection had been removed. Given the difficulty of starting with catechol in these procedures attention was turned to the utilisation of different starting materials.

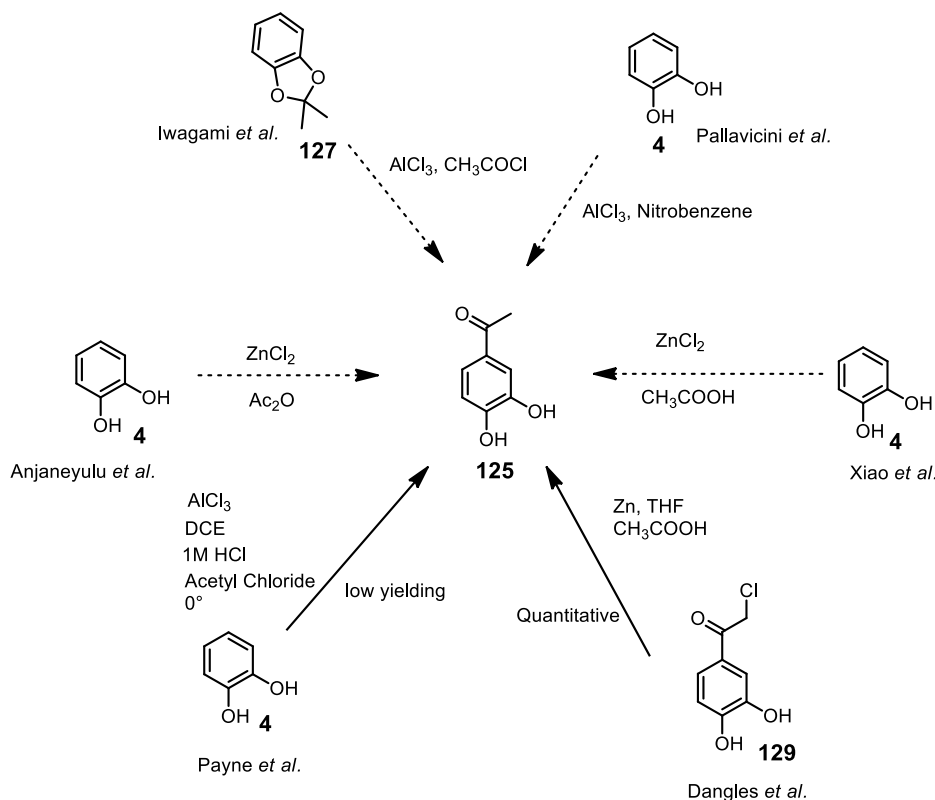


Scheme 2.9.4 Attempted synthesis of acetophenone **128** with acetonide protection.^[61]

Scheme 2.9.5 depicts the procedures and process investigated to acquire the acetophenone **125**. The experimental procedure that was successful in producing **125** in good yields followed the process outlined by Dangles and co-workers (2013).^[71]

The synthesis of acetophenone **125** was straightforward using activated zinc powder in THF and acetic acid with the commercially available 2-chloro-3',4'-dihydroxyacetophenone **129**. The reported yield for the acetophenone was 90%

and was obtained as a white solid. These conditions were repeated and resulted in the isolation of the desired acetophenone **125** in a quantitative yield. NMR spectroscopy confirmed the structure **125** with the loss of CH₂ resonance at 4.8 ppm and new observed resonances at 2.56 ppm for the methyl ketone.



Scheme 2.9.5 Various reported synthetic pathways towards the synthesis of 3,4-dihydroxyacetophenone **125**.

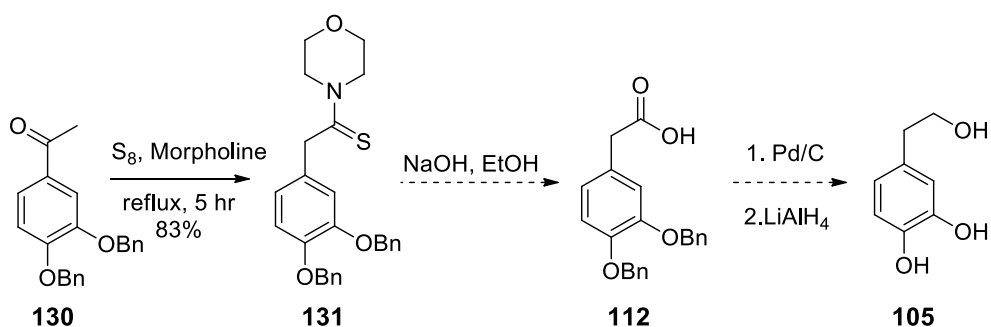
After the successful synthesis of the acetophenone **125** additional investigations towards the synthesis of 3,4-dihydroxyphenylacetic acid involved the initial protection of the hydroxyl groups using benzyl bromide, for ease of removal at a later stage. Thus **125** was allowed to react with benzyl bromide to give **130** in quantitative yield (Scheme 2.9.6).

The benzyl protected substrate was then used in the Wilgerodt-Kindler reaction (Scheme 2.9.6). The preparation of the thiomorphilide compound was undertaken through various reaction pathways. Firstly procedures were undertaken *via* the conventional heating under reflux procedure. Replication of the experiment on numerous occasions showed the reaction results to be quite varied, unable to produce the same outcome. From a visual observation of the crude ¹H NMR a mixture of starting materials and decomposition material was present. Therefore other experimental methods were examined, i.e. sonication^[72]

and with the inclusion of a 1-Butyl-3-methylimidazolium tetrafluoroborate ionic medium^[73] however the conditions used were unsuccessful. Therefore general reflux conditions were used to generate a small amount of the morpholide product **131**.

In addition however complications were encountered during the purification of the thiomorpholide **131**. NMR spectroscopic analysis of the crude product **131** suggested approximately an 80% yield, however upon purification *via* column chromatography (hexane: ethyl acetate on silica) only 30% was recovered. This may be due the stability of thioamides or in addition to adhesion to the silica gel during column chromatography. NMR spectroscopy of the purified product identified the removal of the methyl ketone at 2.56 ppm in the proton spectra. In addition new resonances were observed for the morpholide group with four multiplet resonances between 4.25 and 3.22 ppm and CH₂ group observed at 4.20 ppm. HRMS confirmed the structure C₂₆H₂₇NO₃S calculated 456.1609, found 456.1609 [M+Na]⁺.

It has been identified with the samples analysed *via* Ferguson and co-workers^[64,65] that before purification of a *meta*-methylphenylacetothiomorpholide a yield of 78% was acquired and after recrystallization only 25% was isolated. This was very similar to that of **131** shown in Scheme 2.9.6.



Scheme 2.9.6 Wilgerodt-Kindler reaction with 3,4-disubstituted aromatic system.

The following step in the synthesis was to take a small amount of **131** and subject this morpholide derivative to hydrolysis conditions with sodium hydroxide (7M) and ethanol.^[64] It was found by Ferguson and co-workers that 7M sodium hydroxide was required, any lower in concentration and no reaction occurs.^[64] It was also identified that the amount of ethanol added to the reaction was also critical for different acetophenone derivatives. Varying quantities of ethanol was used however the process of synthesising **112** was still unsuccessful, due to no

reaction taking place and decomposition being observed. The synthesis of **112** would have been very useful for the conversion to hydroxytyrosol by removal of the benzyl groups and reduction of the carboxylic acid. Hydroxytyrosol as discussed in previous work, is difficult to synthesise and very expensive to purchase. Nonetheless, the main requirement for **112** was for acquiring the targeted block structure **45** with an ethylene unit for the initial ion channel design for cation transportation shown in Figure 2.9.4. Given the synthetic difficulties encountered in pursuing block structure **45**, it was decided to halt investigations towards this compound.

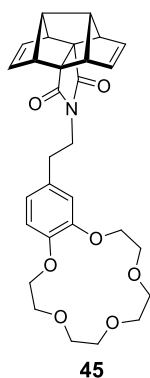


Figure 2.9.4 Desired block structure **45** for further block extension work towards artificial ion channel.

2.9.2 Conclusions

Herein we have described the successful synthesis of block **45** *via* the reaction of amines with anhydrides based on dopamine derivatives. However as described this synthetic approach has proved problematic, with increased decomposition of the aromatic amino crown ether derived from dopamine with low yielding and difficult purification processes.

This instigated new synthetic approaches towards the ethylene block system. Numerous methods such as the Wittig and Wilgerodt-Kindler reactions were employed to synthesise the desired block **45**. However all of these experimental processes in one way or another failed to produce the desired polycyclic block **45**.

This led to a modification in the target system which required less reactivity for the fusion of the anhydride to react with the aromatic amine as well as improved yields. These new processes and experimental approaches will be outlined in the commencing chapter.

REFERENCES

- [1] M. Golić, M. R. Johnston, D. Margetić, A. C. Schultz, R. N. Warrener, *Aust. J. Chem.* **2006**, *59*, 899–914.
- [2] D. McNeil, B. R. Vogt, J. J. Sudol, S. Theodoropoulos, E. Hedaya, *J. Am. Chem. Soc.* **1974**, *96*, 4673.
- [3] L. A. Paquette, M. J. Wyratt, *J. Am. Chem. Soc.* **1974**, *96*, 4673–4674.
- [4] L. A. Paquette, M. J. Wyratt, *J. Am. Chem. Soc.* **1974**, *42*, 4671–4673.
- [5] L. A. Paquette, M. J. Wyratt, H. C. Berk, R. E. Moerck, *J. Am. Chem. Soc.* **1978**, *100*, 5845–5855.
- [6] R. T. Taylor, M. W. Pelter, L. A. Paquette, *Org. Synth.* **1990**, *68*, 198.
- [7] J. Cui, J. Iturri, J. Paez, Z. Shafi, C. Serrano, M. Ischia, A. Campo, *Macromol. Chem. Phys.* **2014**, 2403–2413.
- [8] R. P. Liang, X. N. Wang, C. M. Liu, X. Y. Meng, J. D. Qiu, *J. Chromatogr.* **2014**, *1323*, 135–142.
- [9] Y. Li, Y. Zhou, B. Qi, T. Gong, X. Sun, Y. Fu, Z. Zhang, *Mol. Pharm.* **2014**, *11*, 3174–3185.
- [10] V. K. Thakur, M.-F. Lin, E. J. Tan, P. S. Lee, *J. Mater. Chem.* **2012**, *22*, 5951–5959.
- [11] G. McGarvey, “Synthetic Procedures,” can be found under <http://www.faculty.virginia.edu/mcgarveylab/>, **2004**.
- [12] D. Fenton, D. Parkin, R. Newton, *J. Chem. Soc., Perkin Trans. 1* **1981**, 449–454.
- [13] V. F. Vögtle, B. Jansen, *Tetrahedron Lett.* **1976**, 4895–4898.
- [14] C. Pedersen, *J. Am. Chem. Soc.* **1967**, 7017–7036.
- [15] C. Detellier, H. D. H. Stover, *Synthesis (Stuttg.)* **1983**, 990–992.
- [16] K. Hermann, M. Nakhla, J. Gallucci, E. Dalkilic, A. Dastan, J. D. Badjić, *Angew. Chem. Int. Ed. Engl.* **2013**, *52*, 11313–11316.
- [17] L. D. Van Vliet, T. Ellis, P. J. Foley, L. Liu, F. M. Pfeffer, R. A. Russell, R. N. Warrener, F. Hollfelder, M. J. Waring, *J. Med. Chem.* **2007**, *50*, 2326–2340.
- [18] P. Troselj, I. Dilovic, D. Matkovic-Calogovic, D. Margetic, *J. Hetero. Chem.* **2013**, *50*, 83–90.

- [19] M. N. Paddon-Row, N. J. Head, A. M. Oliver, K. Look, N. R. Lokan, G. A. Jones, *Angew. Chem. Int. Ed.* **1999**, *38*, 3219–3222.
- [20] R. B. Murphy, D. T. Pham, S. F. Lincoln, M. R. Johnston, *Eur. J. Org. Chem.* **2013**, 2985–2993.
- [21] R. N. Warrener, S. Wang, R. a. Russell, *Tetrahedron* **1997**, *53*, 3975–3990.
- [22] T. C. Chou, K. C. Lin, C. A. Wu, *Tetrahedron* **2009**, *65*, 10243–10257.
- [23] S. Chakrabarti, M. Liu, D. H. Waldeck, A. M. Oliver, M. N. Paddon-Row, *J. Am. Chem. Soc.* **2007**, *129*, 3247–3256.
- [24] D. Margetić, D. N. Butler, R. N. Warrener, Y. Murata, *Tetrahedron* **2011**, *67*, 1580–1588.
- [25] S. P. Gaynor, M. J. Gunter, M. R. Johnston, R. N. Warrener, *Org. Bio. Mol. Chem.* **2006**, *4*, 2253–2266.
- [26] Q. Ye, F. Zhou, W. Liu, *Chem. Soc. Rev.* **2011**, *40*, 4244–4258.
- [27] S. Hong, Y. S. Na, S. Choi, I. T. Song, W. Y. Kim, H. Lee, *Adv. Funct. Mater.* **2012**, *22*, 4711–4717.
- [28] S. Kang, N. Hwang, J. Yeom, S. Y. Park, P. B. Messersmith, I. S. Choi, R. Langer, D. G. Anderson, H. Lee, *Adv. Funct. Mater.* **2012**, 2949–2955.
- [29] A. J. Blok, R. Chhasatia, J. Dilag, A. V. Ellis, *J. Memb. Sci.* **2014**, *468*, 216–223.
- [30] H. Chu, C.-W. Yen, S. C. Hayden, *Biotechnol. Prog.* **2015**, *31*, 299–306.
- [31] P. Yan, J. Wang, L. Wang, B. Liu, Z. Lei, S. Yang, *Appl. Surf. Sci.* **2011**, *257*, 4849–4855.
- [32] H. Shen, J. Guo, H. Wang, N. Zhao, J. Xu, *ACS Appl. Mater. Interfaces* **2015**, 150224074733007.
- [33] S. Huang, L. Yang, M. Liu, S. L. Phua, W. A. Yee, W. Liu, R. Zhou, X. Lu, *Langmuir* **2013**, *29*, 1238–1244.
- [34] N. Della Vecchia, R. Avolio, M. Alfe, M. E. Errico, A. Napolitano, M. D’Ischia, *Adv. Funct. Mater.* **2012**, 1–10.
- [35] B. Murphy, T. Schultz, *J. Org. Chem.* **1985**, *2245*, 2790–2791.
- [36] S. Michaelis, S. Blechert, *Chem. Eur. J.* **2007**, *13*, 2358–2368.
- [37] E. Torres, M. D. Duque, P. Camps, L. Naesens, T. Calvet, M. Font-Bardia, S. Vázquez, *ChemMedChem* **2010**, *5*, 2072–2078.

- [38] L. I. Kas'yan, I. N. Tarabara, Y. S. Bondarenko, S. V. Shishkina, O. V. Shishkin, V. I. Musatov, *Russ. J. Org. Chem.* **2005**, *41*, 1122–1131.
- [39] I. N. Tarabara, A. O. Kas'yan, O. V. Krishchik, A. V. Shishkina, O. V. Shishkin, L. I. Kas'yan, *Russ. J. Org. Chem.* **2002**, *38*, 1299–1308.
- [40] M. Breuning, T. Häuser, C. Mehler, C. Däschlein, C. Strohmam, A. Oechsner, H. Braunschweig, *Beilstein J. Org. Chem.* **2009**, *5*, 1–5.
- [41] C. M. S. Combe, K. Biniek, B. C. Schroeder, I. McCulloch, *J. Mater. Chem.* **2014**, *2*, 538–541.
- [42] M. Duque, C. Ma, E. Torres, J. Wang, L. Naesens, J. Juarez-Jimenez, P. Camps, F. Luque, W. DeGrado, R. Lamb, et al., *Med. Chem. (Los Angeles)*. **2011**, *54*, 2646–2657.
- [43] N. R. Patel, J. L. Rutter, *N-(arylthiocarbamoyl)-2-Amino-1H-Isoindole-1,3-(2H)diones and Use as Plant Growth Regulators*, **1980**, 19065.
- [44] J. L. Kirkpatrick, N. R. Patel, J. L. Rutter, *Isothioereido Isoindolediones and Use as Plant Growth Regulators*, **1980**, 35875.
- [45] S. Dey, D. Lightner, *J. Org. Chem.* **2007**, *1*, 9395–9397.
- [46] M. Gul, N. Ocal, *Can. J. Chem.* **2010**, *88*, 323–330.
- [47] Aldrich, “3-Hydroxytyrosol,” can be found under <http://www.sigmaaldrich.com/catalog/product/sigma/h4291?lang=en®ion=AU>, **2015**.
- [48] J. Espín, C. Soler-Rivas, *J. Agric. Food Chem.* **2001**, *49*, 1187–1193.
- [49] Y. Satoh, K. Tajima, M. Munekata, J. D. Keasling, T. S. Lee, *Metab. Eng.* **2012**, *14*, 603–610.
- [50] C. Schöpf, G. Göttmann, E. Meisel, L. Neuroth, *Justus Liebigs Ann. Chem.* **1949**, *563*, 86–93.
- [51] M. Breuninger, M. Joray, *Process for the Preparation of Hydroxytyrosol*, **2008**, WO2008/107109.
- [52] M. Breuninger, M. Joray, *Process for the Preparation of Phenolic Compounds*, **2007**, WO2007/009590.
- [53] Z. Yang, F. Tan, H. Wong, *Process for Production of Hydroxytyrosol Using Organometallic Compounds*, **2012**, WO2012/006783.
- [54] D. Deffieux, P. Gossart, S. Quideau, *Tetrahedron Lett.* **2014**, *55*, 2455–2458.
- [55] D. Deffieux, P. Gossart, S. Quideau, *Method of Preparation of Hydroxytyrosol*, **2012**, EP 2620424A1.

- [56] M. Edmonds, A. Abell, in *Mod. Carbonyl Olefin*. (Ed.: T. Takeda), Wiley-VCH Verlag GmbH & Co.KGaA, Weinheim, **2004**, pp. 1–17.
- [57] F. A. Carey, R. J. Sundberg, in *Adv. Org. Chem. Part B React. Synth.*, Springer Science & Business Media, New York, **2007**, p. 159.
- [58] M. R. Saidi, M. M. Mojtahedi, M. Bolourtchian, *J. Sci. I. R. Iran* **2000**, *11*, 217–219.
- [59] S. Albert, R. Horbach, H. B. Deising, B. Siewert, R. Csuk, *Bioorganic Med. Chem.* **2011**, *19*, 5155–5166.
- [60] H. S. Lee, K. Isagawa, H. Toyoda, Y. Otsuji, *Chem. Lett.* **1984**, 673–676.
- [61] A. S. B. Prasad, J. V. B. Kanth, M. Periasamy, *Tetrahedron* **1992**, *48*, 4623–4628.
- [62] D. L. Priebbenow, C. Bolm, *Chem. Soc. Rev.* **2013**, *42*, 7870–7880.
- [63] W. C., *Berichte der Dtsch. Chim. Geesellschaft* **1887**, *20*, 2467–2470.
- [64] J. N. Fergusson, The Synthesis and Characterisation of Methamphetamines Using the Willgerodt Kindler Reaction, Flinders University, Honours Thesis, **2011**.
- [65] J. N. Fergusson, M. R. Johnston, B. Painter, P. E. Pigou, *Utilising the Wilgerodt-Kindler Reaction in the Production of Methamphetamine from Methylacetophenones*, **2011**.
- [66] H. Sun, C. Xiao, Y. Cai, Y. Chen, *Chem. Pharm. Bull.* **2010**, *58*, 1492–1496.
- [67] Z. Xiao, D. Shi, H. Li, L. Zhang, C. Xu, H. Zhu, *Bioorg. Med. Chem.* **2007**, *15*, 3703–3710.
- [68] A. S. R. Anjaneyulu, U. V Mallavahani, Y. Venkateswarlu, A. V Rama Prasad, *Indian J. Chem.* **1987**, *26*, 823–826.
- [69] A. Tran, N. West, W. Britton, R. Payne, *ChemMedChem* **2012**, *7*, 1031–1043.
- [70] H. Iwagami, M. Yatagai, M. Nakazawa, H. Orita, T. Honda, Yutaka, Ohnuki, T. Yukawa, *Bull. Chem. Soc. Jpn.* **1991**, *64*, 175–182.
- [71] N. Mora-Soumille, S. Al Bittar, M. Rosa, O. Dangles, *Dye. Pigment.* **2013**, *96*, 7–15.
- [72] M. M. Mojtahedi, T. Alishiri, M. S. Abaee, *Phosphorus. Sulfur. Silicon Relat. Elem.* **2011**, *186*, 1910–1915.
- [73] J. S. Yadav, B. V. S. Reddy, G. Kondaji, J. S. S. Reddy, K. Nagaiah, *J. Mol. Catal. A Chem.* **2007**, *266*, 249–253.

CHAPTER 3

SYNTHESIS OF THE HEDAYA BLOCK WITH A METHYLENE LINKER

3.1 Introduction

As discussed in Chapter 2, a number of difficulties were encountered in the isolation of a rigid polynorbornyl block linked to a 3,4 dihydroxylated aromatic *via* a methylene chain (Figure 2.9.1.3). This prompted a review of the proposed artificial ion channel system due to the limitations of dopamine and its derivatives used in attempted reactions.

Due to its ease of synthesis and reactivity towards alkyl halides the imide functional group of the polynorbornyl system was of synthetic interest as it negated the synthesis of amino crown derivatives known to have decomposition potential. Therefore a system with one carbon atom between the imide group and the crown ether was investigated.

Herein, the exploration of a methylene linker is discussed. This was achieved *via* crown ether attachment at the polynorbornyl imide. These polynorbornyl systems were then extended to the preparation of coupled blocks, with crown ethers for cation binding imparting ion channel functionality.

3.2 Modelling of a Methylene Linked System

Building on the initial design of the block motif with an ethylene chain linker (Chapter 2), new synthetic pathways were explored with both the rigid block and attachment of the crown ether. In particular, preliminary modelling using Spartan (AM1), of the methylene linked system (Figure 3.2.1) predicted an sp^3 carbon with an orientation between the crown ether and the imide of $\sim 120^\circ$. This was not considered ideal when an extended framework was considered due to the angle of the crown ether which may effect a reaction to take place at the norbornyl double bond due to steric issues. However, it was hoped that free rotation around the methylene carbon in the linker may reduce steric issues in regards to block extension to a larger system. In Scheme 3.2.1 a possible route to the synthesis of the methylene linked block is shown with the use of the polynorbornyl block and functionalised crown ether unit.

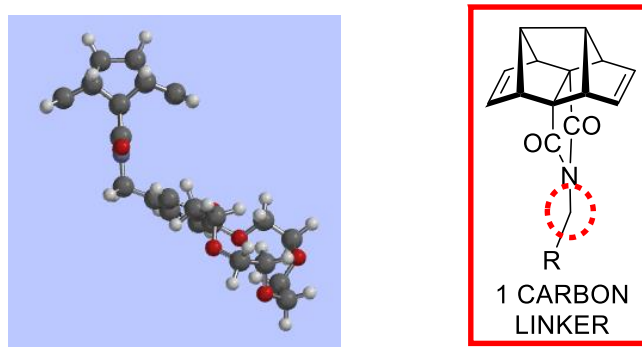
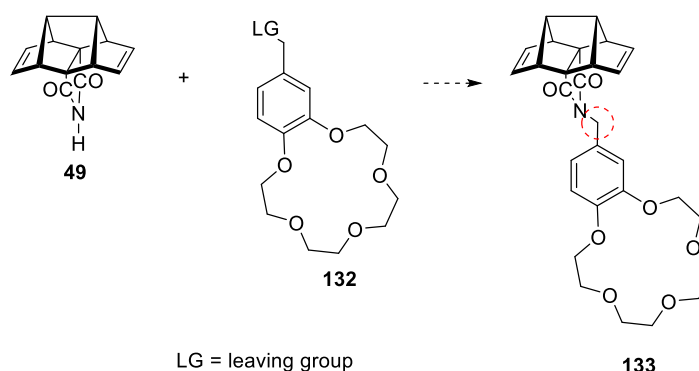


Figure 3.2.1 Molecular model and structure of Hedaya diene block with one carbon attachment at the imide.



Scheme 3.2.1 Possible synthesis of methylene linked block and crown ether.

Molecular modelling (AM1) of the extended polynorbornyl blocks were performed as previously outlined and an image of the output is shown in Figure 3.2.2. In this model the crown ethers have been removed for ease of modelling. However the attachment of the crown ethers would be through the imide moiety coupled to subsequent blocks with crown ethers in the 3,4 positions on the appended aromatic ring.

The methylene linker between the imide and the crown ether does not allow for significant alignment of the crown ethers as was seen in Chapter 2. However, if the mechanism for ion transport is *via* hopping where ions ‘hop’ between various sites to cross the membrane as outlined by Voyer and co-workers, ion transport rates may not be significantly perturbed by the lack of perfect alignment of the crown ethers.^[1]

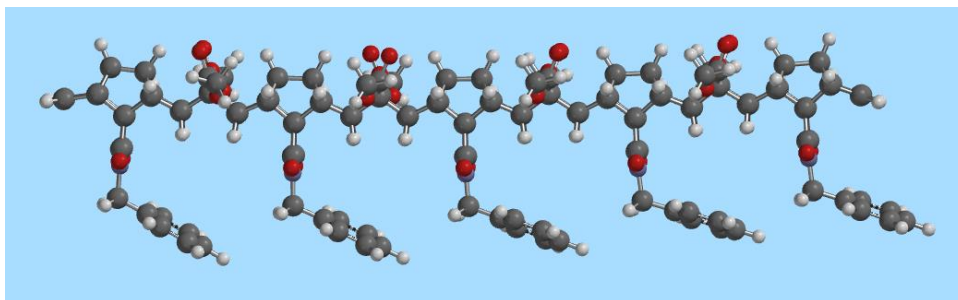
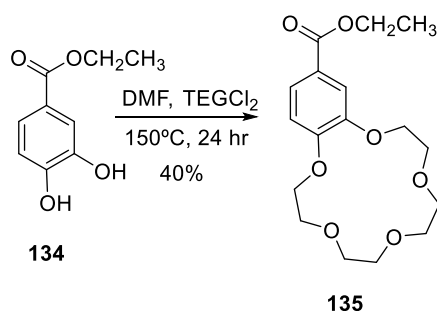


Figure 3.2.2 Proposed polycyclic norbornyl linear framework with a methylene linker for channel transportation (Crown ethers removed for ease of modelling), Spartan 10⁷.

Additionally, crown ethers are well known to be quite flexible in their free/non-complexed state, not remaining in the one conformation for long periods.^[2-4] Complexation with cations forces the crown ether to adopt a rigid assembly. The relative distance between the aromatic sites was measured to be 6.5-8.0 Å with the polynorbornyl framework having an overall length of 35 Å, which is consistent with the previous model (Figure 2.2.1). Thus it was decided that a methylene linker was worthy of synthetic investigation.

3.3 Substituted Aromatic Crown Ether Preparation and Attachment to the Polynorbornyl Imide

The benzocrown ether synthesis was achieved using established literature methods.^[5] The ethyl ester of 3,4-dihydroxybenzoic acid **134** was prepared using standard esterification conditions in excellent yields. Crown ether **135** was prepared by literature methods (Scheme 3.3.1).^[5] The prepared ethyl ester **134**, was allowed to react with potassium carbonate and tetraethylene glycol dichloride (TEGCl₂) to obtain the 15-crown-5 ether in a moderate yield (40%).^[5]



Scheme 3.3.1 Preparation of crown ether **135** from ethyl 3,4-dihydroxybenzoate **134**.

The ^1H NMR spectra of **135** matched that of the literature.^[5] However it was noted that the ^{13}C NMR spectrum contained an additional resonance observed at 60.92 ppm which was not reported by Garcia and co-workers. Heteronuclear Multiple-Quantum Correlation (HMQC) analysis determined that this ^{13}C correlated to the methylene of the ethyl moiety. Accurate analysis of **135** was consistent with an observed mass of 363.1409 $[\text{M}+\text{Na}]^+$, corresponding to the calculated mass, 363.1420, from the literature.^[5]

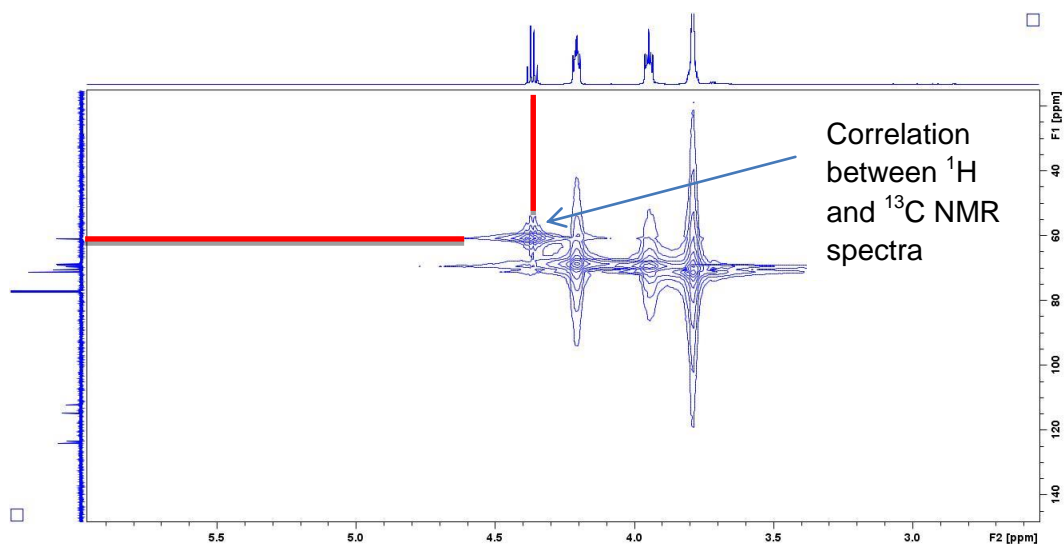
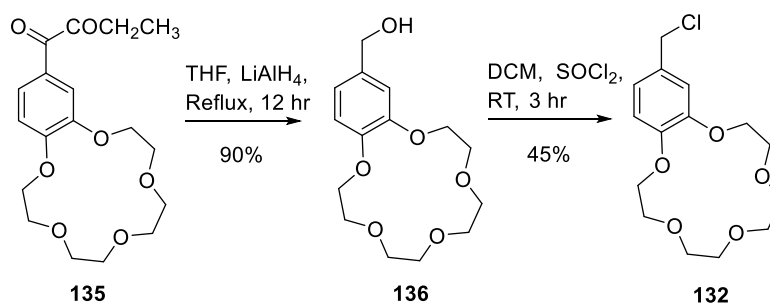


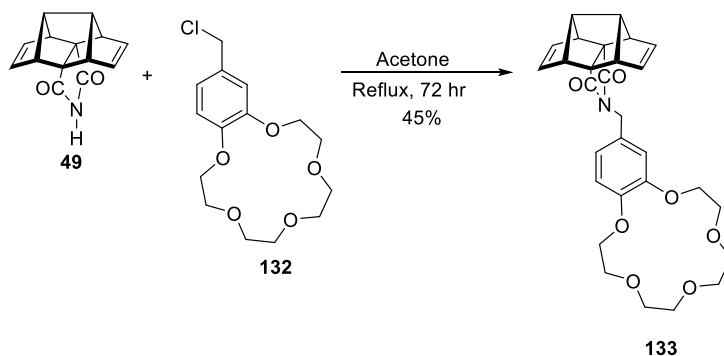
Figure 3.3.1 HMQC of compound **135** for assignment of the carbon resonance at 60.92 ppm.

Preparation of the chloride **132** was achieved *via* literature methods^[6,7], Scheme 3.3.2. The hydroxyl derivative **136** was obtained by reduction of **135** with lithium aluminium hydride (LiAlH_4) in excellent yields (90%). Chlorination was achieved by treatment with thionyl chloride (SOCl_2) in moderate yields (45%). Larger scale reactions generated mixtures of hydroxyl and chlorinated compounds and required extended reaction times to achieve complete conversion.



Scheme 3.3.2 Preparation of functionalised crown ethers for attachment to Hedaya diene block **49**.

Investigation of the nucleophilic reactivity of the polynorbornyl imide **49** with the prepared halogenated crown ether **132** was explored using a process similar to that of the Gabriel synthesis where an imide, usually a phthalamide, is deprotonated with base (e.g. OH⁻). The imide proton has increased acidity due to the two adjacent carbonyl groups generating resonance stability of the imide anion. This anion is sufficiently nucleophilic to participate in S_N2 substitution reactions such as the proposed reaction outlined in Scheme 3.3.3.



Scheme 3.3.3 Reaction for the formation of the fused Hedaya block **133**.

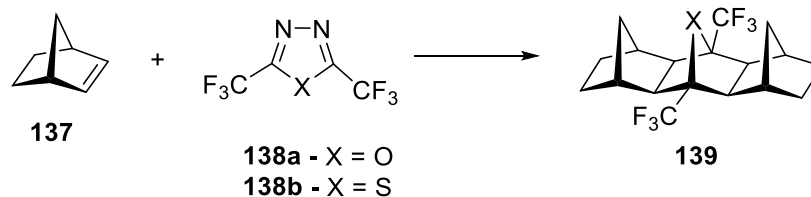
In the block system (Scheme 3.3.3) the imide **49** was deprotonated with potassium carbonate to form the nucleophilic nitrogen centre which further reacted with the alkyl halide of the crown ether as described previously to form the fused block **133** (Scheme 3.3.3) in moderate yields (45%).

NMR spectroscopy and MS analysis was consistent with the structure of **133**. It is important to note for numerous compounds containing crown ethers, multiple resonances were observed within the ¹³C NMR spectra between 40-70 ppm with some of the unique signals overlapping complicating assignment. This is due to slight changes in the chemical shift of the carbon atoms in the crown ether with respect to the block structure placing all of them in slightly different environments.

The synthesised polynorbornyl system **133** was then subsequently used in coupling reactions to generate longer frameworks that could potentially span the bilayer for ion transport. The extension of these rod-like motifs can be achieved through various types of coupling reactions. There are several different types of coupling reactions reported in the literature for norbornyl-based systems and a brief discussion of each follows.

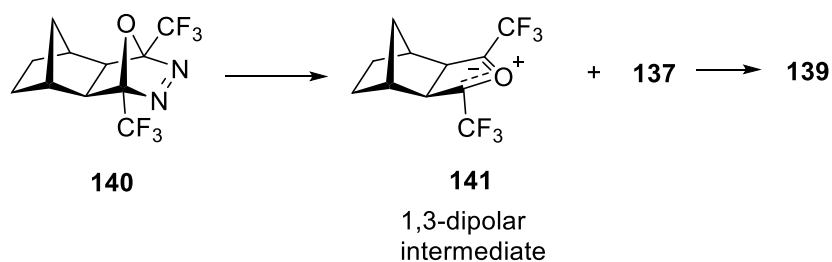
3.4 Variations in Coupling Reactions to Extend Polynorbornyl Frameworks

Linking of norbornene units has been extensively described in the literature through various types of coupling reactions.^[8] These coupling reactions extended rigid systems, and can also apply to functionalised norbornyl units.^[9] Seitz and Wassmuth^[10] first explored the coupling of norbornene units with 1,3,4-oxadiazole or 1,3,4-thiadiazoles to afford the coupled cycloaddition products shown in Scheme 3.4.1.



Scheme 3.4.1 Oxadiazole coupling of norbornene units.^[11]

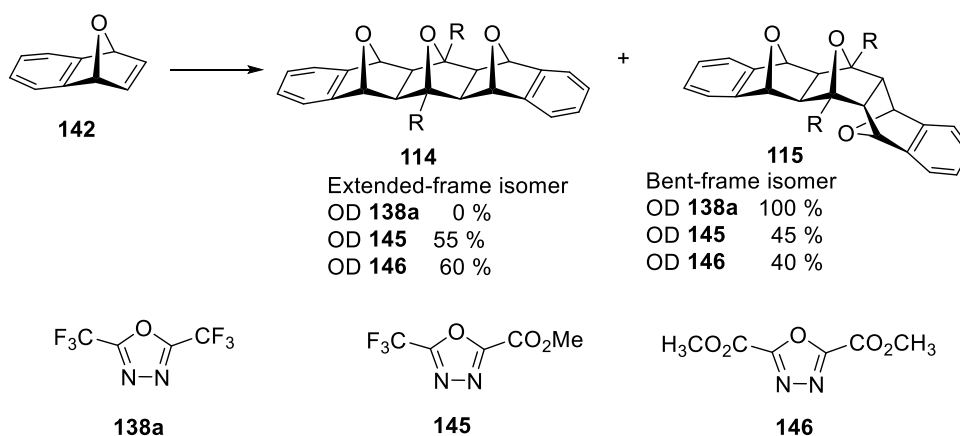
These coupled systems were described further in the literature for the preparation of functionalised polynorbornanes and this reagent is still used to couple blocks together currently.^[11–22] Initially there was limited evidence for the mechanism of the coupling until Warrenner and co-workers proposed the two-step mechanism outlined in Scheme 3.4.2.^[23,24] Investigation *via* coupling reactions demonstrated the first step to be a Diels Alder cycloaddition between norbornene **137** and the oxadiazole (or thiazole) diene to afford the intermediate **140**. A loss of dinitrogen (N_2) generates the 1,3-dipolar intermediate **141** which further reacts with another alkene (same or different) to afford fused [n]polynorbornanes.



Scheme 3.4.2 Formation of the 1,3-dipolar intermediate.^[24]

Interestingly, reactions of 1,3,4-oxadiazole (OD) with 7-oxabenzonorbornenes are stereoselective. This leads to bent frame isomers, used for U-shaped type stepped structures illustrated in the literature.^[11]

In more recent investigations, different 1,3,4-oxadiazoles were used to reveal differences within the stereoselective coupling, replacing CF_3 moieties with one or two ester (CO_2CH_3) moieties (Scheme 3.4.3).^[25] The change in substituent impacts the stereoselectivity of the coupled product. The steric bulk of the CF_3 groups resulted in the formation of bent-framed systems only. As a result of the smaller moieties substituents the major isomer of the syn-facially coupled products **145** and **146** provided the extended frame rather than the bent frame oxabenzonorbornyl structures.

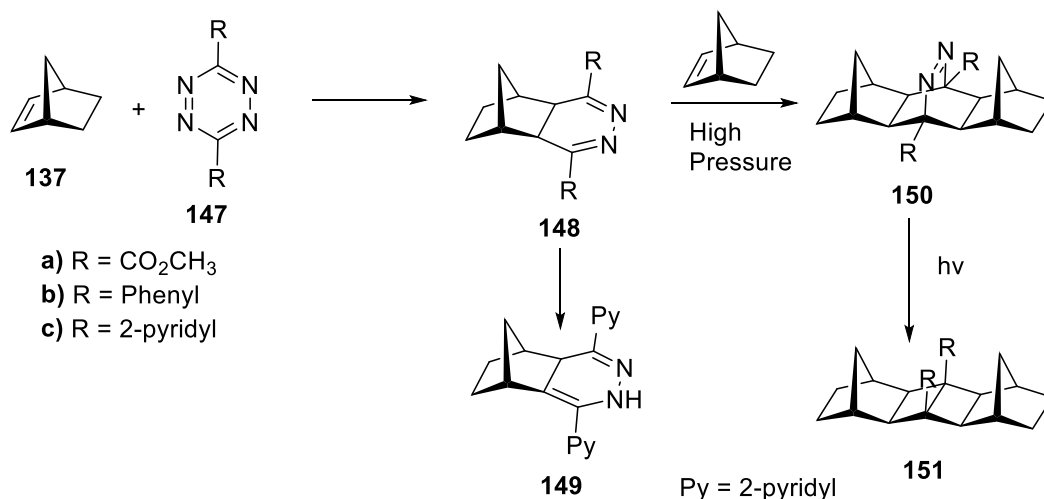


OD = Oxadiazole

Scheme 3.4.3 Variations in oxadiazole coupling with differing side functionalities for extended and bent frame systems.^[25]

The oxadiazole coupling reactions can be quite useful in the synthesis of large [n] polynorbornane derivatives allowing access to extended frameworks. However the use of oxadiazole coupling uses trifluoromethyl groups in comparison to other coupling reactions which will be further discussed. The trifluoromethyl groups are difficult to remove and functionalise in order to instil more hydrophilic character and hence solubility in biological systems. In comparison to the ester substituted oxadiazoles, which are difficult to synthesise, their stability is limited. Therefore other coupling techniques were investigated.

Another unique coupling reaction uses s-tetrazine derivatives to synthesise new [n]polynorbornane frameworks.^[8,26–28] The s-tetrazine coupling reactions rely on the interaction of alicyclic alkenes and s-tetrazine reagents to afford fused aza-dienes. The aza-dienes are further reacted with alkenes under high pressures (14 kbar)^{[29],[30]} to form aza-bridged Diels-Alder products as shown in Scheme 3.4.4.

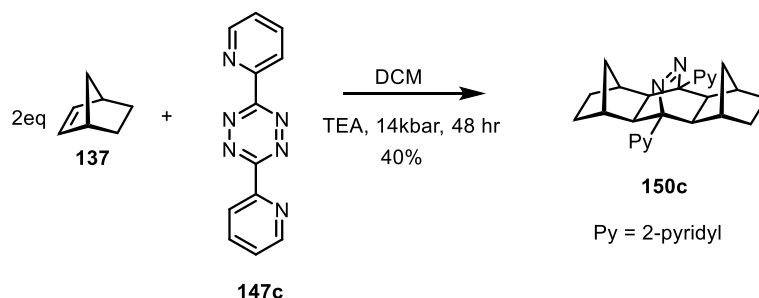


Scheme 3.4.4 Preparation of *s*-tetrazine fused polycyclic frameworks.^[31]

The *s*-tetrazine coupling reactions, unlike the oxadiazole coupling reactions, are highly stereoselective and exclusively form symmetrical *exo-exo*-coupled products (resulting from reactions at the *exo*-face). The azo-bridged product **150** can undergo photochemical deazertization (removal of dinitrogen) to afford the binane **151** as described by Sauer.^[27]

Further studies investigating *s*-tetrazine coupling led the Warrenner group to explore reactions with the more accessible 3,6-di(2'-pyridyl)-*s*-tetrazine^[32], however initial studies proved problematic with the dihydropyridazine rearranging to the unreactive isomer **149** (Scheme 3.4.4). Suppression of the reaction that forms **149** was achieved with the addition of small amount of triethylamine during the *s*-tetrazine cycloaddition under high pressure conditions. Similar dihydropyridazine formation was observed under thermal conditions.^[32]

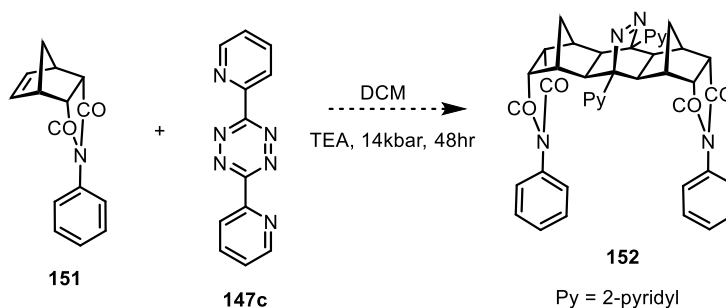
This type of coupling reaction for the linking of block substituents was considered in the preliminary stages of synthesis in this work. A trial reaction coupling two equivalents of norbornene with a 2-pyridyl tetrazine derivative was performed. Norbornene was treated with 3,6-di(2'-pyridyl)-*s*-tetrazine in TEA/CH₂Cl₂ under high pressure for 24-48 hr as shown below in Scheme 3.4.5.



Scheme 3.4.5 Preparation of norbornene *s*-tetrazine fused polycyclic framework **150c**.

NMR analysis of the products of trial experiments indicated the formation of small amounts of the desired block system **150c**. Variation of the reaction conditions (including extended reaction times) resulted in the successful synthesis of the aza-bridged compound **150c** (40%). However the results of this investigation were not consistently reproducible. The ^1H NMR and mass spectroscopic analysis for the successful reaction product was consistent with the structure of **150c** as outlined by Warrenner and co-workers.^[32]

Similar attempts were made to synthesise block structures with appended groups using the *s*-tetrazine aza-bridge linkers. However all attempts with compound **151** (Scheme 3.4.6) were unsuccessful. This may be due to the steric bulk of the starting materials with close proximity of the phenyl substituents appended from the block scaffold (see Figure 3.4.1) causing issues with the reactivity of the double bond.



Scheme 3.4.6 Preparation of endo functionalised norbornene *s*-tetrazine fused polycyclic framework **152**.

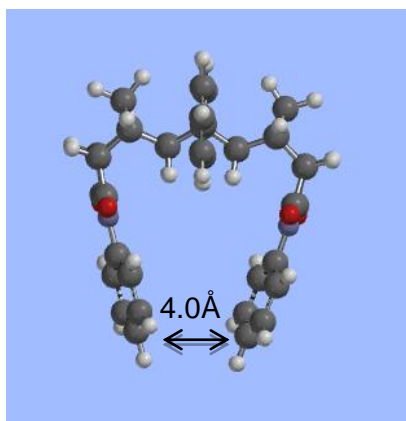
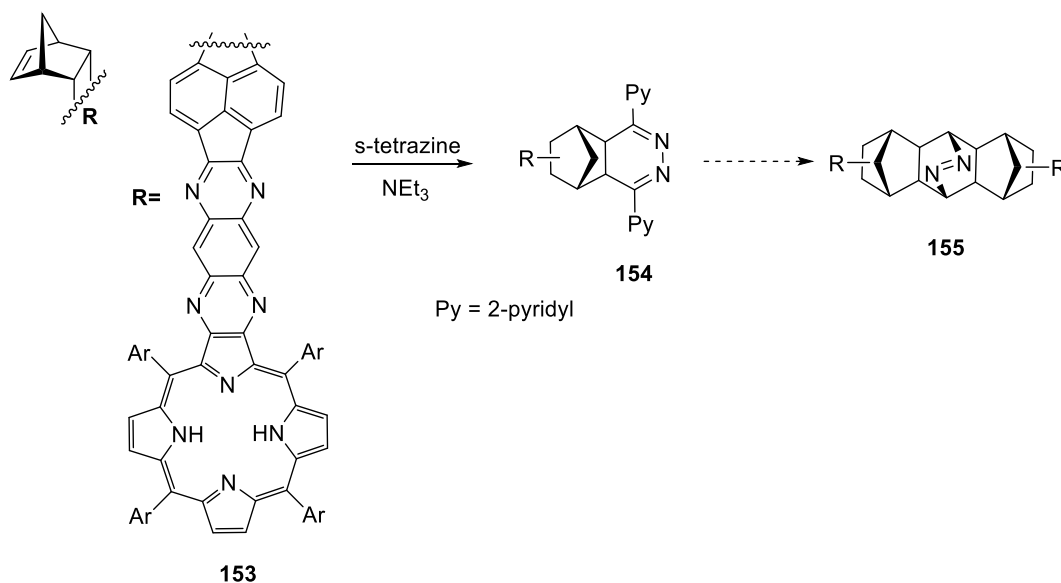


Figure 3.4.1 Molecular modelling of the proposed fused polycyclic framework **152**.

One example outlined by Warrener and co-workers highlighted the problematic nature of polynorbornyl block systems resembling **155** (Scheme 3.4.7, Figure 3.4.2), coupled with *s*-tetrazine derivatives.^[31] Although this system is quite different to **152** discussed previously, the results of Warrener's investigations indicate that similar end group functionalities projected 'back' in underneath the norbornyl type scaffold detracted from the formation of the coupled product.



Scheme 3.4.7 Attempted preparation of porphyrin functionalised *endo*-norbornene *s*-tetrazine fused polycyclic framework **155**.

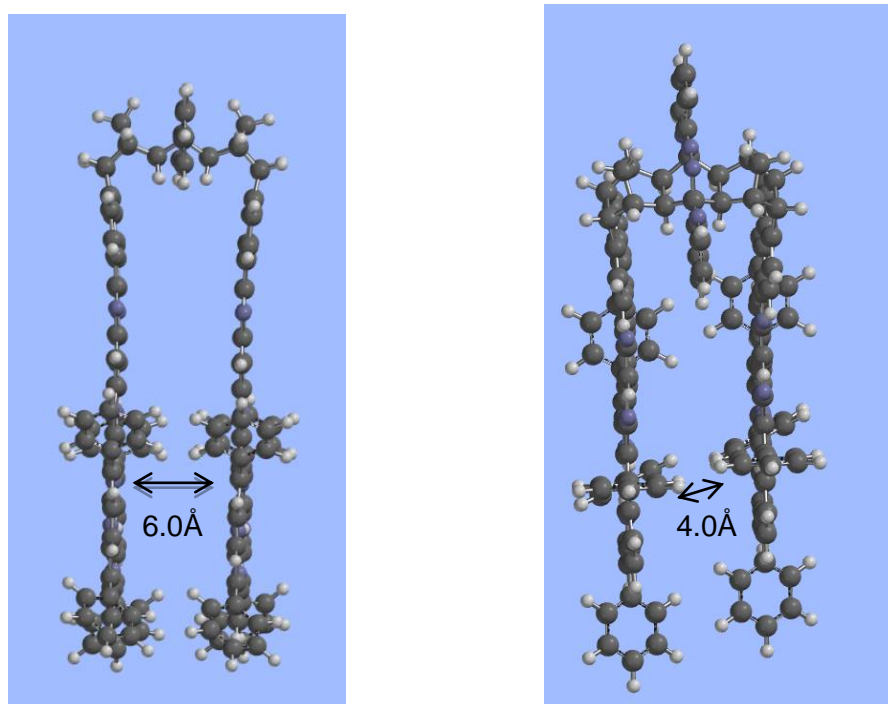


Figure 3.4.2 Molecular modelling (AM1) of the proposed fused polycyclic framework **155**.

The aforementioned complications arising from the *s*-tetrazine reaction with norbornene **137** proved this type of coupling to be unsuitable for endo norbornyl systems with bulky attachments.

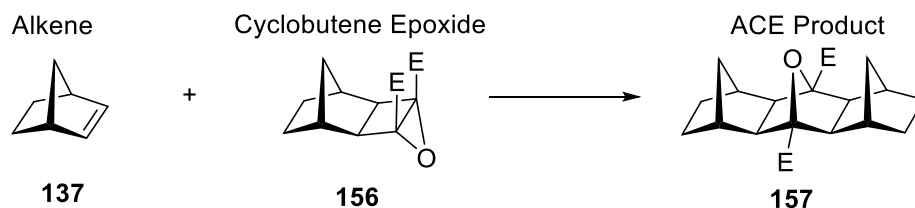
The disadvantages identified in using the *s*-tetrazine coupling reactions are linked to the formation of the dihydropyridazine adduct. If the adduct is formed, no coupling reactions can take place. The reactions were unreproducible with large variations in the success of coupling as well as inconsistent yields. In addition to the high pressures required, only small scale reactions were possible (< 2 mL) due to equipment limitations. Thus, multiple reactions were needed to synthesise the large amounts of material required for further synthetic modifications. Furthermore, *s*-tetrazine coupling reactions can require extended reaction times as well as lengthy purification processes which were undesirable.

In addition, the system outlined in Section 3.3 was proposed for straightforward incorporation into the lipid bilayer. For this to be successful it was essential that the functional groups associated with coupling reagents when fused were able to be readily manipulated into systems with increased aqueous solubility. Unlike the pyridyl group, which requires stringent conditions for removal, ester moieties are

highly desired for functional group derivatisation. An *s*-tetrazine derivative (dimethyl 1,2,4,5-tetrazine-3,6-dicarboxylate, **147a**) with ester moieties has been synthesised.^[33] However it was found to be unstable to silica gel chromatography and susceptible to decomposition. In addition the intermediate products were found to undergo an acid-promoted rearrangement.^[34] Therefore the incorporation of dimethyl 1,2,4,5-tetrazine-3,6-dicarboxylate, **147a** into coupling reactions was unlikely to produce the desired products in this work. To overcome the multitude of issues surrounding *s*-tetrazine reactions, further coupling reactions were considered.

Coupling of an alkene and a cyclobutane epoxide, commonly referred to as ACE (alkene plus cyclobutene epoxide) coupling was developed by Warrener, Butler and Russell.^[35] This type of coupling is one of the most commonly described coupling processes in the literature for the extension of [n]polynorbornyl frameworks.^[17,30,35–42] In comparison to *s*-tetrazine coupling, ACE coupling requires thermal conditions, rather than high pressures. The ACE coupling reaction allows for ester linkages to be incorporated at the sides of the system which can be manipulated, whether it be through hydrolysis reactions or by other means (e.g. reduction to the primary alcohol). In addition, ACE reactions can be performed on larger scales when compared to the *s*-tetrazine coupling.

A generalised reaction for ACE coupling is outlined for fused [n]polynorbornane frameworks below (Scheme 3.4.8).

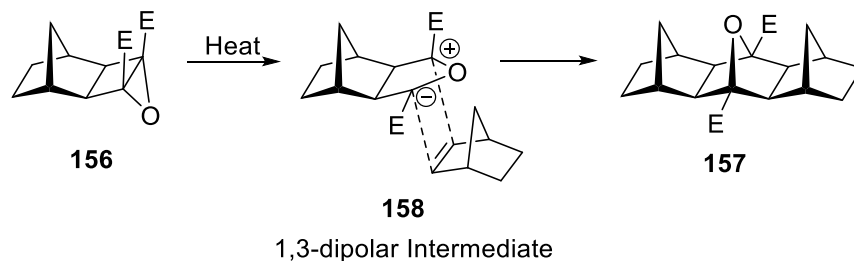


Scheme 3.4.8 Preparation of ACE fused polycyclic framework **157**.^[31]

As described for the oxadiazole coupling, the mechanism of ACE product formation proceeds through a 1,3-dipolar intermediate.^[30] Evidence of the formation of these dipoles has been discussed by Huisgen^[43] and throughout a small number of related studies.^[44–47]

ACE coupling is a stereoselective reaction in which the epoxide ring opens to form a carbonyl ylide which then is able to undergo a reaction with a norbornene alkene (Scheme 3.4.9). This is a [3+2] cycloaddition which generates a 5

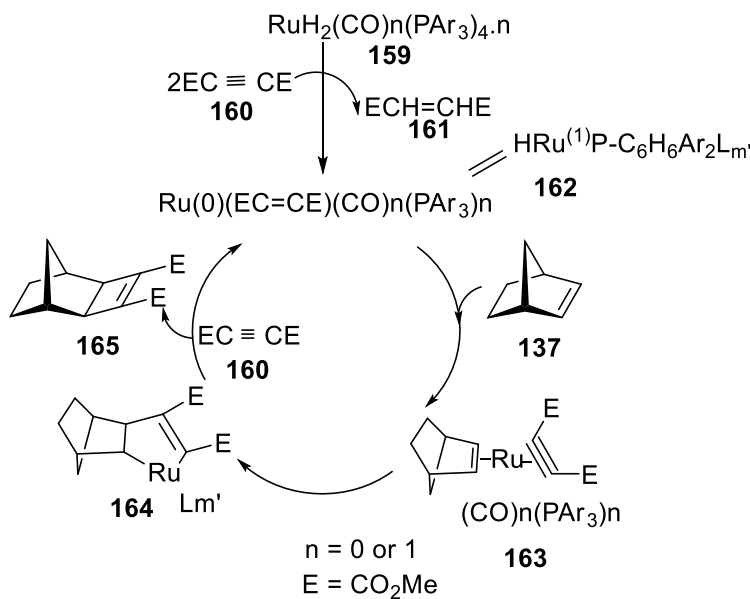
membered ring from a reaction between the 1, 3-dipole and a dipolarophile.^[35] The electron withdrawing nature of the ester groups helps stabilise the 1,3-dipole.



Scheme 3.4.9 Proposed mechanism of ACE reaction for the preparation of fused polycyclic framework **157**.^[48]

The ACE reaction is versatile and amenable to numerous functional groups for example, esters, crown ethers and porphyrins. The early examples of the ACE reaction^[26] utilised sealed tube thermal conditions, however the Pfeffer group in 2009 introduced a new microwave- accelerated 1, 3-dipolar cycloaddition which reduced reaction times and levels of decomposition.^[48]

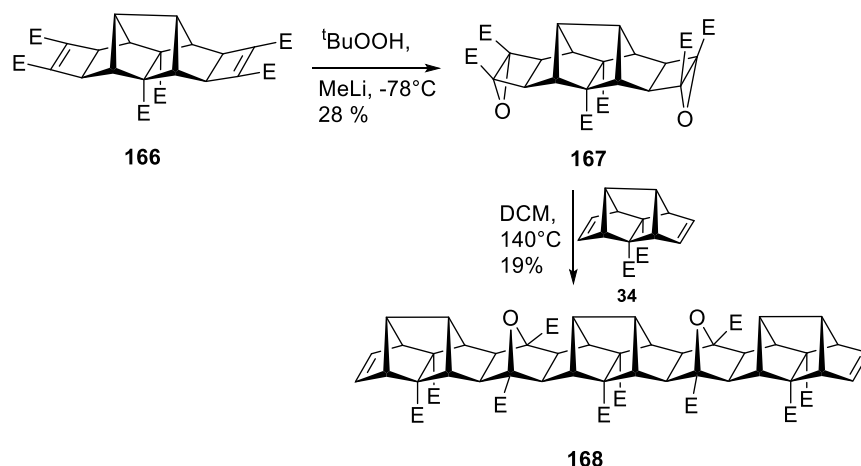
The cyclobutene epoxide used in these ACE reactions is normally synthesised from a norbornene system which firstly involves a ruthenium catalysed $[2\pi+2\pi]$ Mitsudo cycloaddition. This reaction has been used extensively in the past for reactions appending polynorbornane systems to cyclobutene-1,2-diesters.^[49,50] The $[2\pi+2\pi]$ cycloaddition of alkynes is stereospecific and generates four membered rings from one alkene and one alkyne. The mechanism proposed for the $[2\pi+2\pi]$ cycloaddition is shown in Scheme 3.4.10.



Scheme 3.4.10 Mitsudo and co-workers proposed cyclobutene 1,2-diester **165** formation.^[50]

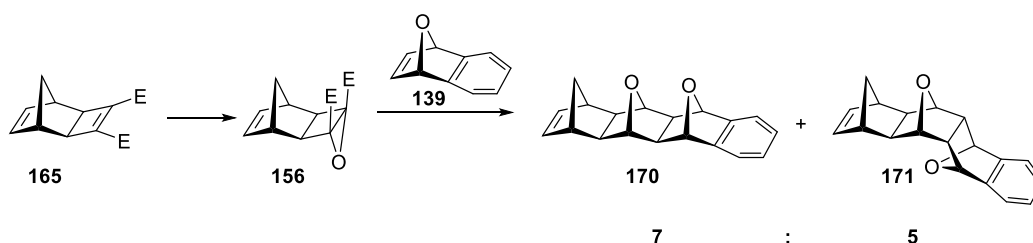
The mechanism proposed by Mitsudo and co-workers is based around the $[2\pi+2\pi]$ cycloaddition of $\text{RuH}_2(\text{CO})_n(\text{PAr}_3)_{4-n}$ ($n = 0$ or 1) with an alkene to form a ruthenium zero valence complex. This leads to the consecutive formation of metallacyclopentene complex followed by a reductive elimination reaction to afford the corresponding polynorbornyl cyclobutene 1,2-diester **165**.

Subsequent conversion of the cyclobutene-1,2-diester to the corresponding epoxide was explored *via* nucleophilic epoxidation, a two-step reaction which forms epoxides from electron deficient alkenes with nucleophilic oxidising agents.^[51] Electrophilic epoxidising reagents such as *m*-CPBA are a poor choice for epoxidation at electron deficient alkenes conjugated with electron withdrawing groups.^[51] The most common reagents used in the epoxidation of electron deficient alkenes is that of anhydrous *tert*-butyl hydroperoxide in conjunction with a strong base to deprotonate the peroxide, Scheme 3.4.11. Upon epoxide formation **167** can be subsequently used with other alkenes in ACE coupling reactions for block extension.^[30,52] This coupling reaction forms extended linear (*exo-exo*-) polynorbornyl adducts.



Scheme 3.4.11 Nucleophilic epoxidation of electron deficient alkenes **167** with tert-butyl hydroperoxide, and subsequent ACE reaction with **34** to form an extended framework.^[30]

A complication with the ACE reaction occurs when heteronorborene materials are used. The use of 1,3-dipolar cycloadditions when fusing norbornene to 7-heteronorborene produces both syn-facial and exo-facial adducts^[25]. Hetero-bridged norbornenes can act as dipolarophiles in the ACE reaction to afford hetero-bridged [n]polynorbornanes. 7-azanorborenes are described as being stereoselective for syn-facial adducts exclusively.^[25] On the other hand the reaction of 7-oxanorborene is stereoselective and this is indicated in the reaction Scheme 3.4.12 with the cyclobutene epoxide of **156** reacting with the 7-oxabenzonorbornadiene affording an isomeric mixture of **170** and **171** (7:5).^[25] The isomers are distinguished using nOe based NMR spectroscopy due to the proximity of the endo protons.^[25] This stereoselectivity provides access to U-shaped systems, rather than extended linear systems described previously.

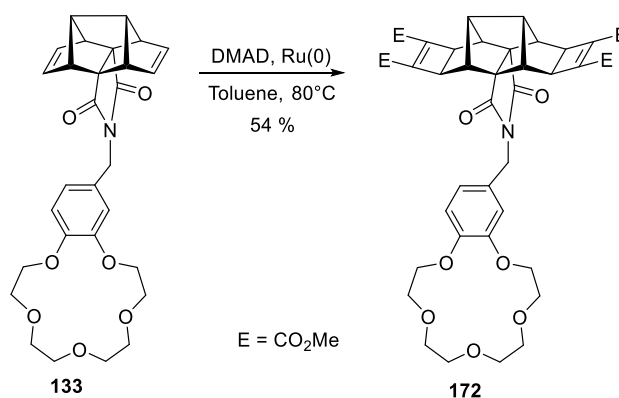


Scheme 3.4.12 ACE coupling reactions used for U-shaped systems.^[25]

The ACE reaction was settled on as being suitable for use in this project for the synthesis of the large ion channel backbones. Herein this study focuses on extended linear [n]polynorbonyl frameworks only. This is due to the limitations in the overall length of the system needed to span the lipid membrane (40-50 Å).

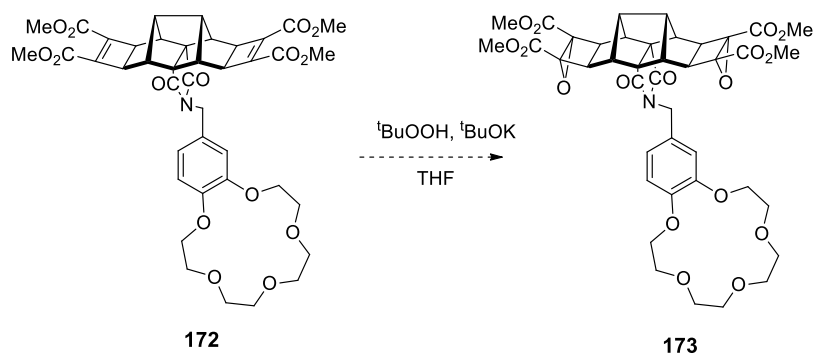
3.5 ACE Coupling Reactions of the Methylene Linked Block

The methylene linked block **133** that was synthesised as described in Section 3.3 was the starting point for further derivatisation so that an ACE coupling reaction could be used. This was achieved by the Mitsudo reaction where compound **133**, DMAD, and ruthenium catalyst ($\text{RuH}_2\text{CO}(\text{P}(\text{Ph})_3)_3$) were stirred at 80°C overnight in toluene. The product **172** was isolated in moderate yield (54%) with NMR spectroscopy and MS analysis consistent with the structure of **172**. In particular the disappearance of the olefinic resonance observed for the starting material at 5.92 ppm and the addition of the new methyl ester resonance at 3.79 ppm. Furthermore bridgehead resonances in the starting material observed at 2.85 ppm were shifted upfield to 2.48 ppm. These chemical shifts are consistent with the addition of the cyclobutene 1,2-diester to the diene.



Scheme 3.5.1 Preparation of cyclobutene 1,2-diester **172** under general Mitsuno conditions.

The next step in the synthesis was epoxidation of **172** to yield the cyclobutene epoxide. Thus compound **172** was treated under standard nucleophilic epoxidation conditions, with $^t\text{BuOOH}$ and $^t\text{BuOK}$ (Scheme 3.5.2), however initial experiments did not lead to compound **173**. The presence of starting material and a large amount of decomposed material were identified in the reaction mixture *via* both ^1H and ^{13}C NMR spectroscopy. Peaks resulting from decomposed crown ether were present between 4-5 ppm and 6-7.5 ppm in the ^1H NMR spectrum indicating that the aromatic and the crown ether were decomposing. Variation of reaction conditions (i.e. reaction times, temperature and reagent equivalents) failed to generate the desired compound **173**.

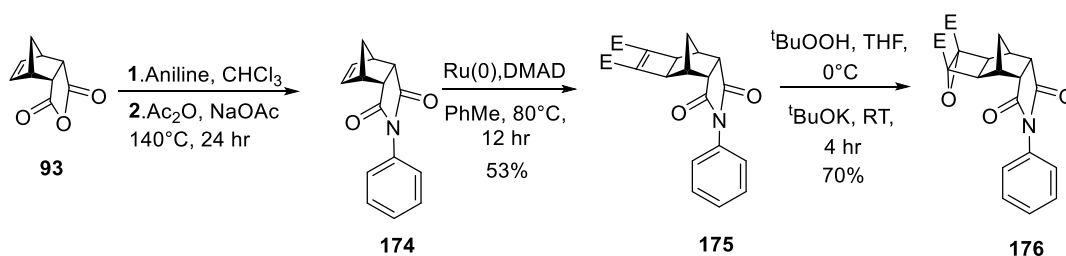


Scheme 3.5.2 Attempted preparation of epoxide **173** under general nucleophilic epoxidation conditions.

It was unclear as to whether there was interference from the crown ether which hindered the production of diepoxide **173**. In addition there may be potential reactions occurring at the methylene linking group contributing to the unsuccessful synthesis of **173**.

Following these attempts to prepare diepoxide **173** via this method the same conditions were applied to various model systems, commonly described in the literature to help understand possible reaction improvements. These included imide-phenyl, imide-Boc and imide-benzyl systems which will be discussed in turn.

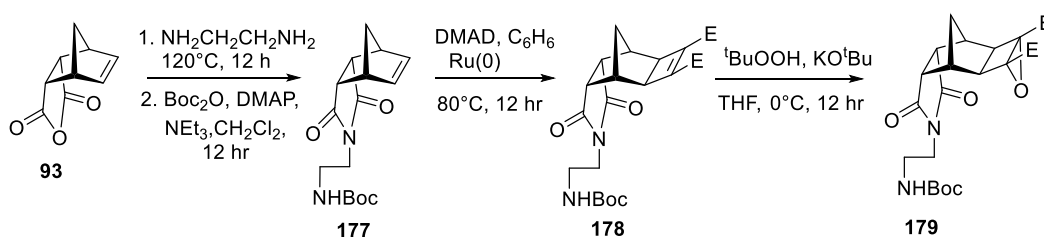
In the first model system, endo carbic anhydride **93** was treated with aniline to form the amic acid which was subsequently ring closed to the imide, to form the product **174**, (Scheme 3.5.3).^[53] The alkene of **174** was allowed to react under the general Mitsudo reaction conditions to generate the cyclobutene 1,2-diester, **175** in moderate yield (53%). Similar to the previous Mitsudo reaction, the olefin resonances observed within the ¹H NMR spectrum of the starting material at 6.30 ppm disappear. New methyl ester (OCH₃) resonances were observed at 3.77 ppm with the addition of another new resonance at 2.99 ppm for the endo protons closest to the cyclobutene ring.



Scheme 3.5.3 Synthesis of a simple substrate **174** in preparation for the formation of epoxide **176** for ACE coupling reactions.

Similar conditions used in the previous example for the nucleophilic epoxidation of **173** were utilised in this model system with the use of $t\text{BuOOH}$ and $t\text{BuOK}$. This time application of the prescribed reagents with compound **175** demonstrated that the nucleophilic epoxide can be prepared in moderate yields (70%).

The epoxidation is a critical component of the overall synthetic strategy for the preparation of the ion channel since there are limited reagents that are applicable for use with electron deficient alkenes. The epoxide is essential for the subsequent steps involving ACE coupling of blocks and further extension towards lengthy polynorbornyl frameworks. Thus, further investigations into the epoxidation using model systems were undertaken. Various substrates incorporating protecting groups and in the absence of crown ethers were used to gain insight into the nucleophilic epoxidation reaction. The model compound, *endo*-carbic anhydride **93**, with imide synthesis and Boc protection were investigated, initially due to its similarity to systems used by Pfeffer and co-workers (Scheme 3.5.4).^[39]

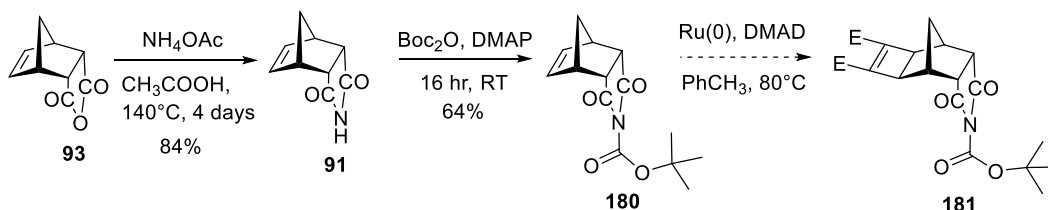


Scheme 3.5.4 Pfeffer and co-workers Boc protection of primary amine polycyclic systems.^[39]

Pfeffer and co-workers demonstrated that the Mitsunobu reaction conditions as well as the general epoxidation conditions shown in Scheme 3.5.4 were effective. In Pfeffer's system, the Boc protecting group was installed at the amine position on

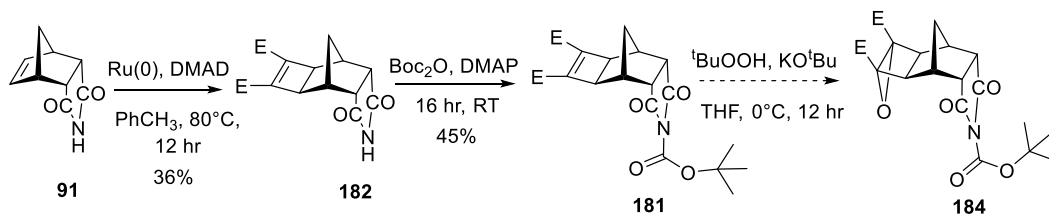
ethylamine rather than a direct attachment to an imide, proposed in our system. Therefore these similar conditions were applied to model compounds (Scheme 3.5.5).

As previously outlined in Chapter 2, the imide **91** has been synthesised in a quantitative yield from the *endo* carbic anhydride **93**.^[54] Initial attachment of the Boc protecting group to the imide afforded **180** in moderate yield (64%) evidenced in ¹H NMR spectroscopy by the new methyl resonances at 1.46 ppm and new carbonyl resonance at 173.8 ppm in the ¹³C NMR spectrum. Mass spectroscopy was consistent with the structure of **180** C₁₄H₁₇O₄N calculated, 263.1158, found 163.0628 [M-BOC+2H]⁺. Synthesis of the cyclobutene 1,2-diester, following the general Mitsudo conditions was unsuccessful, with no product formation identified within the ¹H NMR spectrum of the crude mixture. It is possible that the desired reaction was limited by the coordination of ruthenium catalyst with the carbonyl groups of the imide Boc group, leading to limited reactivity and precluding the formation of the Mitsudo product **181**.



Scheme 3.5.5 Boc protecting pathway employed in order to gain an understanding of the required nucleophilic epoxidation conditions.

Due to the complications in forming adduct **181**, an alternative synthetic strategy was investigated, where the Boc group was installed prior to the Mitsudo reaction (Scheme 3.5.6). It was hoped that this would overcome the possible ruthenium co-ordination and lead to the formation of the cyclobutene 1,2-diester and furthermore facilitate the nucleophilic epoxidation to form the desired compound **184**. This synthetic route enabled the formation of the Boc protected Mitsudo product **183** as evidenced in ¹H NMR spectroscopy by the new methyl resonances at 1.55 ppm and new carbonyl resonance at 172.7 ppm in the ¹³C NMR spectrum. Mass spectroscopy was consistent with the structure of **183** C₂₀H₂₃O₈N calculated, 405.1424, found 305.0894 [M-BOC+2H]⁺. Unfortunately, exposure of **183** to the strongly basic epoxidation conditions resulted in the decomposition of **183**.

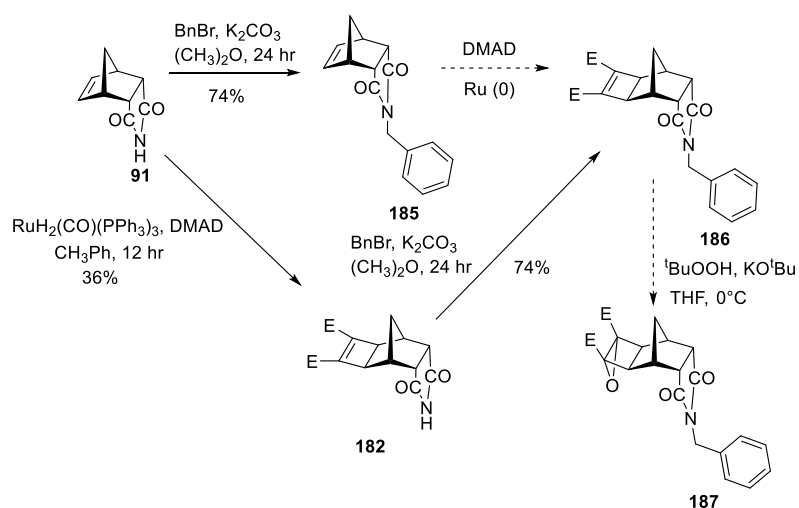


Scheme 3.5.6 Alternative Boc protecting pathway with initial formation of imide **91** before the addition of the cyclobutene 1,2-diester to afford **182**.

Due to the aforementioned difficulties encountered with the Boc group, investigations with an alternative protecting group, namely benzyl were undertaken. The benzyl group played a similar role to the Boc protecting group giving access to both functional groups (imide and epoxide). The imide **91** was protected with the benzyl group eliminating potential side reactions from the epoxidation conditions.

The benzyl protecting group is similar in structure to the methylene crown block **133** examined previously. The benzyl group is unable to co-ordinate to the catalyst as implicated for the previous Boc system. However the formation of the $[2\pi+2\pi]$ Mitsunobu adduct was again unsuccessful (Scheme 3.5.7). The utilisation of this system provided information about both the methylene unit and aromatic decomposition observed for the earlier crown system.

It is unclear why the formation of product **186** did not occur from **185** since there is limited steric hinderance and free rotation around the methylene unit should allow for the catalyst to react with the alkene.



Scheme 3.5.7 Benzyl protecting pathway to gain an understanding of the required nucleophilic epoxidation conditions for systems with methylene units between the imide and aromatic ring.

As described with the previous model system that employed Boc protection, access to the benzyl protected substrate **185** was gained through the imide **91**. Similar results were obtained for the epoxidation of the benzyl protected block as were observed for Boc protected block, with small amounts of starting material and decomposition shown mainly in the aromatic region when compared to that of the starting material. Therefore unfortunately the desired product was unobtainable.

Overall the results from both the Boc and benzyl protections in conjunction with the phenylamine block derivative **176** discussed have given in sight into the imide protection and functionalisation that then directly effects the epoxidation under standard conditions. Under the standard epoxidation conditions (^tBuOOH and ^tBuOK) the epoxide has only formed in one example, compound **176** summarised in Figure 3.5.1. The use of both carbon linkers and protecting groups attached to the imide of the polycyclic blocks are detrimental to the formation of the epoxide.

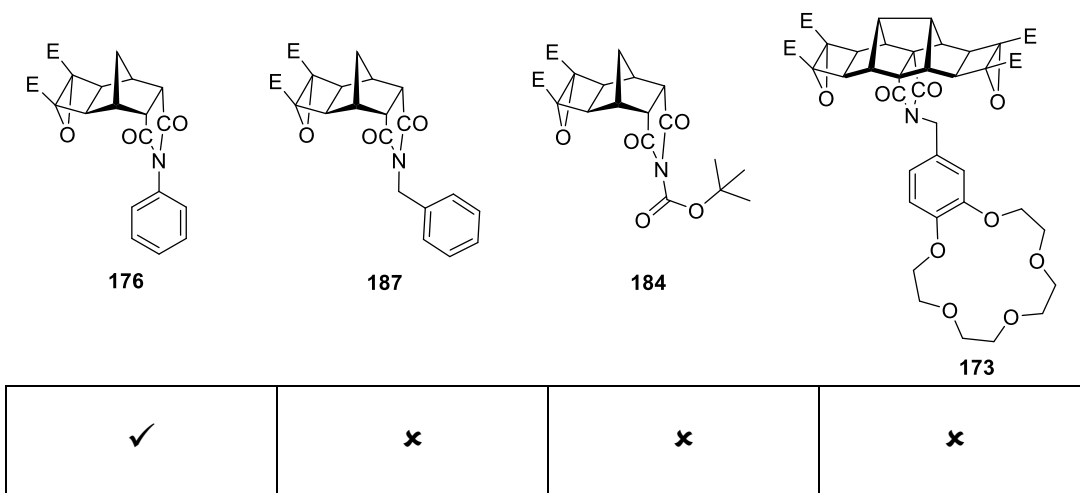


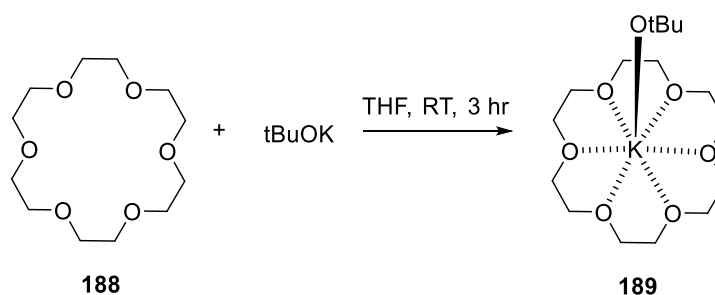
Figure 3.5.1 Nucleophilic epoxidation of variations of Mitsunobu compounds (**173**, **176**, **184**, **187**) and their reaction outcome.

Further investigations of the standard epoxidation conditions (^tBuOOH and ^tBuOK) and its effects on crown ethers, namely coordination were explored in order to circumvent the aforementioned synthetic drawbacks.

3.6 Crown Ethers and ^tBuOOH, ^tBuOK in THF

There have been several articles illustrating the use of potassium tert-butoxide with crown ethers, particularly 18-crown-6 ethers in THF.^[55,56] Potassium tert-butoxide is mainly used by organic chemists as a strong base, however it has the potential for increased nucleophilic character, when used in the presence of 18-crown-6.^[55] In the process of identifying the problems associated with the nucleophilic epoxidation reaction with the use of potassium tert-butoxide in THF, the idea arose that there may potentially be interactions between the crown ether and the potassium tert-butoxide. Exploration of the literature found a number of papers that considered the basicity versus the nucleophilicity of the potassium tert-butoxide in varying solvents, one being THF.^[55]

In the work performed by Gokel and co-workers, it appears that the use of potassium tert-butoxide in a solution of THF with crown ethers is both a potent nucleophile and base.^[55] However the extent of the enhancement of nucleophilicity appears to exceed that of the basicity in THF, and resulting in a powerful nucleophile. In additional work demonstrated by Kleeberg in 2011, crown ether complexes were formed and isolated by treatment with potassium tert-butoxide with 18-crown-6 ethers shown in Scheme 3.6.1.^[56] This demonstrates the reactivity of the potassium tert-butoxide towards the 18-crown-6 in THF solutions.

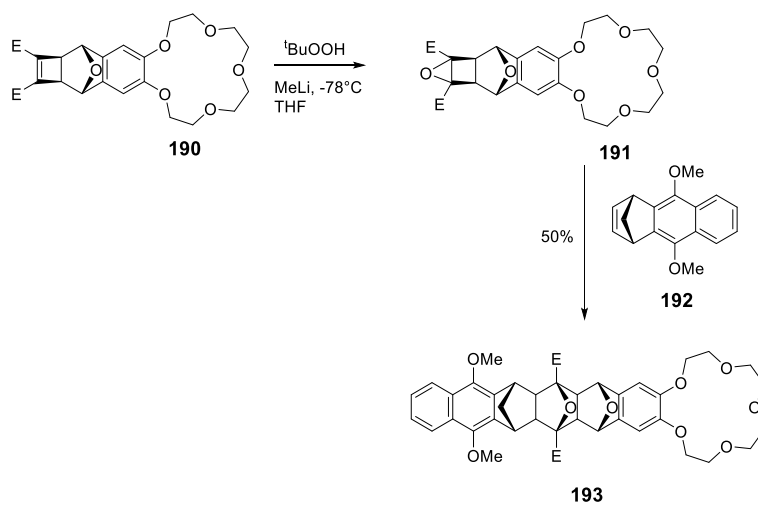


Scheme 3.6.1 Synthesis of 18-crown-6 complex with potassium tert-butoxide.^[56]

Both Gokel and Kleeberg and co-workers have illustrated the use of potassium tert-butoxide with crown ethers, particularly 18-crown-6, increasing nucleophilicity over basicity in THF. However the nucleophilic epoxidation reactions require basicity explaining the results obtained in section 3.5. Thus, alternative epoxidation conditions were required.

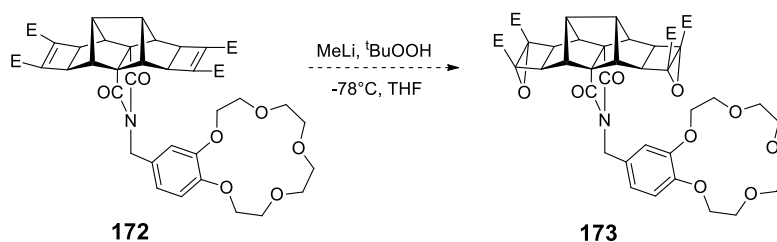
3.7 Epoxidation Reagents for Synthesis of Methylene Linked Polynorbornyl Blocks

In 1997 Warrener and co-workers reported the ACE coupling of crown ether substituted frameworks shown in Scheme 3.7.1. The nucleophilic epoxidation reactions were carried out with $t\text{BuOOH}$ and MeLi . The strong base MeLi has a much stronger pK_a of 48^[57] (for CH_4) than that of the now commonly used $t\text{BuOK}$ pK_a of 19 (for $t\text{BuOH}$)^[58] which should produce higher concentrations of $t\text{BuOO}^-$ in solution, increasing the rate of epoxidation.



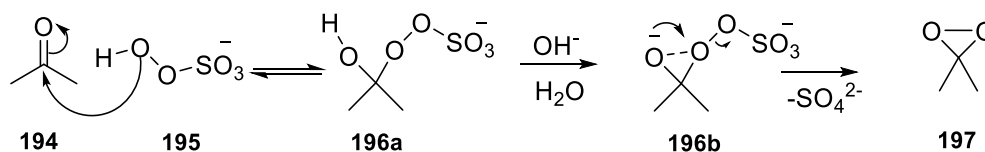
Scheme 3.7.1 Initial epoxidation conditions following the development of ACE coupling.^[35]

These conditions were applied to the synthesised crown block **172** from Section 3.6.2. A variety of sources of methyl lithium (MeLi) reagents were employed. Experiments with MeLi solutions and reagents such as; 1.6 M in diethyl ether, 3M in diethoxymethane and 1.5 M MeLi : lithium bromide complex were unsuccessful with complete degradation of **172** (Scheme 3.7.2) observed *via* ^1H NMR spectroscopy. From the NMR spectrum it would appear that the degradation was more specific to the aromatic and methylene unit moieties implying that the activated methylene carbon is a continuing problem in the formation of the epoxide for ACE coupling. The use of 1.5 equivalents of MeLi may cause a problem by reacting with the active methylene moiety resulting in degradation. The methyl lithium could deprotonate the active methylene moiety and cause reaction with the tert-butyl hydroperoxide resulting in decomposition.



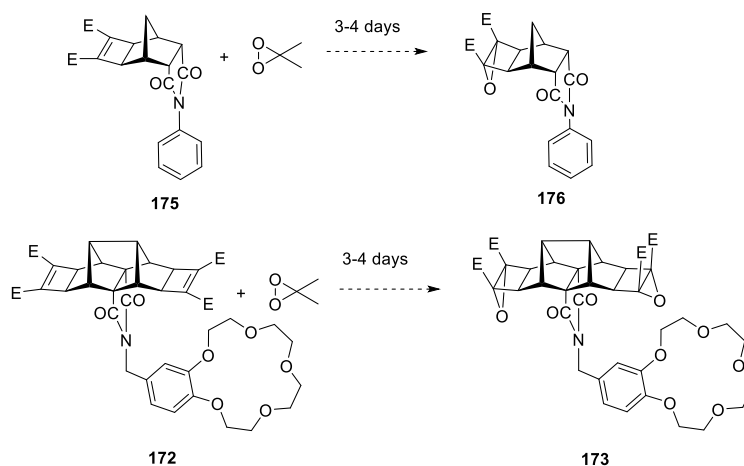
Scheme 3.7.2 General nucleophilic epoxidation conditions unsuccessful in the formation of diepoxide **173**.

Further investigations into epoxide formation led to the examination of a common reagent used with electron rich alkenes, dimethyldioxirane (DMDO).^[59–61] DMDO is generally used in the synthesis of epoxides, similar to that of *m*-CPBA.^[61] DMDO is largely prepared from a reaction of acetone with oxone (Scheme 3.7.3) in concentrations between 0.07-0.09 M.^[60] Reactions with DMDO can be carried out at room temperature and can lead to pure product due to the easy removal of acetone.^[60] DMDO is an electrophilic epoxidation reagent but it has been used with electron deficient alkenes under longer reaction times—generally 24 hr in comparison to 1 hr with electron rich alkenes.^[60]



Scheme 3.7.3 General mechanism for dimethyldioxirane (**197**) formation.

DMDO reactions were investigated with two different polynorbornyl blocks (**175** and **172** (Scheme 3.7.4)), which were allowed to react for periods of 24-48 hr. Upon workup, DMDO decomposes into acetone which is readily removed under reduced pressure. Analysis of the crude reaction material *via* ¹H NMR spectroscopy demonstrated no formation of the epoxidation products **176** and **173** with starting material and small baseline impurities dominating the spectra. The systems may have slightly degraded due to long reaction periods resulting in the baseline impurities, however the recovery of unreacted starting material demonstrated that DMDO was not reactive enough to effect the desired epoxidation in these systems.



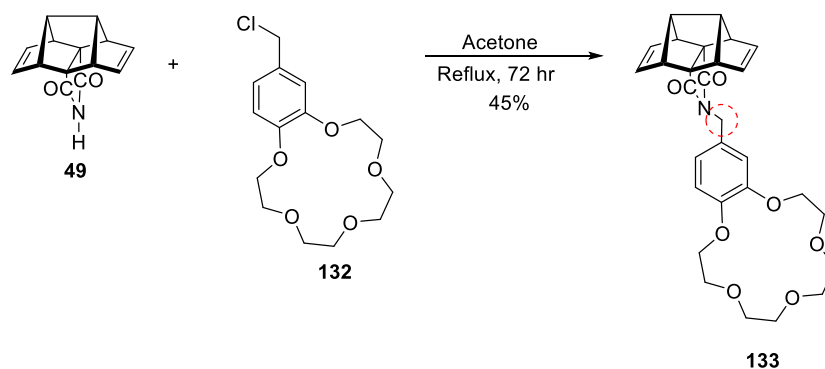
Scheme 3.7.4 Use of DMDO in the attempted epoxidation of electron deficient alkenes.

At this stage it was decided to halt further investigation with methylene systems and examine a directly linked block (between the polynorbornyl scaffold and aromatic). This system will be based around the crown aromatic being directly linked to the block imide.

Other strong bases which have been explored in this project in combination with $t\text{BuOOH}$ and electron deficient alkenes are n -butyllithium (pKa of conjugate acid = 50 for n -butane^[58]), LDA (pKa = 38 for iso-propane^[58]) and NaH (pKa = 35 for H_2 ^[58]). These conditions will be further explored in Chapter 4.

3.8 Conclusions

This chapter has described a new direction in the synthesis of polycyclic block systems with crown ethers attached for cation transportation. The work herein involved the synthesis and attachment of benzo-15-crown-5 to the polycyclic block with one methylene unit between the imide of the polycyclic block and the aromatic crown ether as depicted in Scheme 3.8.1 below.



Scheme 3.8.1 Formation of the fused Hedaya block **133** containing a single carbon linker between the crown and imide.

Additional synthesis was further explored for the coupling of these blocks together through a variety of different coupling reactions. As identified, both trifluoromethyl and *s*-tetrazine coupling were ineffective coupling processes and therefore the more commonly used ACE coupling reaction was examined.

Several limitations were identified for the formation of epoxides using a variety of reagents. It was recognised from the numerous reagents used for the nucleophilic epoxidation that both the presence of a crown ether and the activated methylene unit inhibited the formation of the epoxide. This was also demonstrated with the use of model compounds free of crown ethers, methylene units and with additional Boc and benzyl protected imides.

Further development of the ACE coupling reactions with crown ethers will be explored in the following chapter, in which different synthetic methods for the development of an artificial ion channel will be described.

REFERENCES

- [1] F. Otis, C. Racine-Berthiaume, N. Voyer, *J. Am. Chem. Soc.* **2011**, 6481–6483.
- [2] C. J. Fiscus, P. Pesavento, *Curr. Comm.* **1988**, 11, 111–117.
- [3] N. Zeighami, A. Boshra, A. Olliaey, *J. Phys. Theor. Chem.* **2013**, 10, 171–187.
- [4] F. Gámez, B. Martínez-Haya, S. Blanco, J. C. López, J. L. Alonso, *Phys. Chem. Chem. Phys.* **2012**, 14, 12912–12918.
- [5] V. Calderon, F. C. Garcia, J. L. De La Pena, E. M. Maya, J. M. Garcia, *J. Polym. Sci. Part A Polym. Chem.* **2006**, 44, 4063–4075.
- [6] S. J. Howell, D. Philp, N. Spencer, *Tetrahedron* **2001**, 57, 4945–4954.
- [7] O. P. Kryatova, A. G. Kolchinski, E. V Rybak-Akimova, *Tetrahedron* **2003**, 59, 231–239.
- [8] D. Margetic, M. Johnston, E. Tiekink, R. Warrener, *Tetrahedron Lett.* **1998**, 39, 5277–5280.
- [9] A. J. Lowe, F. M. Pfeffer, *Org. Biomol. Chem.* **2009**, 7, 4233–40.
- [10] G. Seitz, H. Wassmuth, *Chem. Zeitung* **1988**, 112, 80.
- [11] R. N. Warrener, D. N. Butler, W. Y. Liao, I. G. Pitt, R. A. Russell, *Tetrahedron Lett.* **1991**, 32, 1889–1892.
- [12] N. Vasil'ev, Y. Lyashenko, *Chem. Heterocycl. Compd.* **1987**, 4, 562.
- [13] G. Seitz, C. H. Gerninghaus, *Pharmazie* **1994**, 49, 102.
- [14] F. Thalhammer, U. Wallfahrer, J. Sauer, *Tetrahedron Lett.* **1988**, 29, 3231–3234.
- [15] D. Margetić, M. Eckert-Maksić, P. Trošelj, Ž. Marinić, *J. Fluor. Chem.* **2010**, 131, 408–416.
- [16] R. Warrener, P. Groundwater, I. Pitt, *Tetrahedron Lett.* **1991**, 1885–1888.
- [17] L. D. Van Vliet, T. Ellis, P. J. Foley, L. Liu, F. M. Pfeffer, R. A. Russell, R. N. Warrener, F. Hollfelder, M. J. Waring, *J. Med. Chem.* **2007**, 50, 2326–2340.
- [18] N. V. Vasil'ev, D. V. Romanov, T. D. Truskanova, K. a. Lyssenko, G. V. Zatonksy, *Mendeleev Commun.* **2006**, 16, 186–188.
- [19] R. N. Warrener, D. N. Butler, L. Liu, D. Margetic, R. A. Russell, *Chem. Eur. J.* **2001**, 7, 3406–3414.

- [20] P. Troselj, I. Dilovic, D. Matkovic-Calogivic, D. Margetic, *J. Hetero. Chem.* **2013**, *50*, 83–90.
- [21] N. Vasil'ev, D. V. Romanov, *J. Fluor. Chem.* **2007**, *128*, 740–747.
- [22] D. Butler, M. Shang, R. Warrener, *Tetrahedron Lett.* **2000**, *41*, 5985–5989.
- [23] R. Warrener, G. Elsey, R. Russell, E. Tiekink, *Tetrahedron Lett.* **1995**, *36*, 5275–5278.
- [24] R. Warrener, D. Margetic, E. Tiekink, R. Russell, *Synlett* **1997**, 196–198.
- [25] R. N. Warrener, D. Margetic, P. J. Foley, N. Butler, D. A. Winling, K. A. Beales, R. A. Russel, *Tetrahedron* **2001**, *57*, 571.
- [26] R. Warrener, D. Margetic, A. Amarasekara, D. Butler, I. Mahadevan, R. Russel, *Org. Lett.* **1999**, *1*, 199–202.
- [27] W. Dittmar, G. Heinrichs, A. Steigel, T. Troll, J. Sauer, *Tetrahedron Lett.* **1970**, *11*, 1623–1627.
- [28] D. Margetic, D. N. Butler, R. N. Warrener, *Synlett* **2013**, *24*, 2609–2613.
- [29] R. N. Warrener, D. Margetić, R. A. Russell, *Synlett* **1997**, 585.
- [30] M. Golić, M. R. Johnston, D. Margetić, A. C. Schultz, R. N. Warrener, *Aust. J. Chem.* **2006**, *59*, 899–914.
- [31] R. N. Warrener, R. A. Russell, D. N. Butler, *New Building BLOCK Techniques in Molecular Design*, **1998**.
- [32] R. N. Warrener, D. Margetic, R. A. Russel, *Synlett* **1998**, 585–587.
- [33] D. Boger, J. Panek, M. Patel, *Org. Synth.* **1992**, *70*, 79–88.
- [34] D. Boger, R. Coleman, J. Panek, *J. Org. Chem.* **1985**, *50*, 5377–5379.
- [35] R. Warrener, A. Schultz, *Chem. Commun.* **1997**, 1023–1024.
- [36] R. B. Murphy, D. T. Pham, S. F. Lincoln, M. R. Johnston, *Eur. J. Org. Chem.* **2013**, 2985–2993.
- [37] R. N. Warrener, A. C. Schultz, M. R. Johnston, *J. Org. Chem. Comm.* **1999**, *64*, 4218–4219.
- [38] A. Lowe, B. Long, F. Pfeffer, *J. Org. Chem.* **2012**, *77*, 8507–8517.
- [39] F. M. Pfeffer, T. Gunnlaugsson, P. Jensen, P. E. Kruger, *Org. Lett.* **2005**, *7*, 5357–5360.
- [40] R. Warrener, D. Margetic, *Org. Lett.* **1999**, *1*, 203–206.

- [41] A. J. Lowe, F. M. Pfeffer, *Chem. Commun.* **2008**, 1871–1873.
- [42] A. J. Lowe, F. M. Pfeffer, *Org. Biomol. Chem.* **2009**, *7*, 4233–4240.
- [43] R. Huisgen, *Angew. Chem. Int. Ed. Engl.* **1977**, *1785*, 572–585.
- [44] E. Ullman, J. Milks, *J. Am. Chem. Soc.* **1962**, *84*, 1315–1316.
- [45] E. Ullman, W. H. Jr, *J. Am. Chem. Soc.* **1966**, *1*, 4942–4960.
- [46] D. Arnold, L. Karnischky, *J. Am. Chem. Soc.* **1970**, *92*, 1404–1406.
- [47] W. Linn, *J. Am. Chem. Soc.* **1965**, 3665–3672.
- [48] R. C. Foitzik, A. J. Lowe, F. M. Pfeffer, *Tetrahedron Lett.* **2009**, *50*, 2583–2584.
- [49] T. Mitsudo, H. Naruse, T. Kondo, Y. Ozaki, Y. Watanabe, *Angew. Chem. Int. Ed. Engl.* **1994**, *33*, 580–581.
- [50] T. Mitsudo, K. Kokuryo, T. Shinsugi, Y. Nakagawa, Y. Watanabe, Y. Takegami, *J. Org. Chem.* **1979**, *44*, 4492–4496.
- [51] J. Clayden, N. Greeves, S. Warren, P. Wothers, *Organic Chemistry*, Oxford University Press, **2001**.
- [52] R. N. Warrener, *Eur. J. Org. Chem.* **2000**, 3363–3380.
- [53] K. H. Yoon, K. O. Kim, M. Schaefer, D. Y. Yoon, *Polymer (Guildf)*. **2012**, *53*, 2290–2297.
- [54] M. Breuning, T. Häuser, C. Mehler, C. Däschlein, C. Strohmman, A. Oechsner, H. Braunschweig, *Beilstein J. Org. Chem.* **2009**, *5*, 1–5.
- [55] S. A. DiBiase, G. W. Gokel, *J. Org. Chem.* **1978**, *43*, 447–452.
- [56] C. Kleeberg, *Z. Anorg. Allg. Chem.* **2011**, *637*, 1790–1794.
- [57] M. B. Smith, *Organic Synthesis*, Academic Press, San Diego, **2011**.
- [58] J. Hornback, *Organic Chemistry*, Thomson Brooks Cole, Belmont, **2006**.
- [59] A. Waldemar, S. Chantur R., Z. Cong-Gui, in *Org. React.* (Ed.: L. Overman), John Wiley And Sons, Inc., Wurzburg, **2002**, pp. 219–516.
- [60] R. W. Murray, M. Singh, *Org. Synth.* **1997**, *74*, 91–96.
- [61] H. M. C. Ferraz, R. M. Muzzi, T. D. O. Vieira, H. Viertler, *Tetrahedron Lett.* **2000**, *41*, 5021–5023.

CHAPTER 4

SYNTHESIS OF A RIGID SYSTEM BASED ON A DIRECT ATTACHMENT

4.1 Introduction

The studies outlined in Chapter 3 revealed difficulties surrounding the nucleophilic epoxidation of polynorbornyl systems with crown ethers and activated methylene units. To overcome these issues alternative methods will be detailed here in Chapter 4. In particular, the removal of all carbon units between the polynorbornyl scaffold and the crown ether substituent **197** was investigated (Scheme 4.1.1).

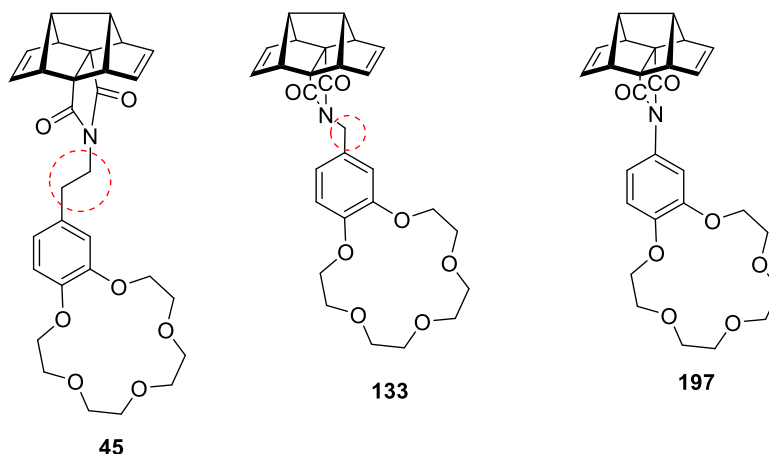
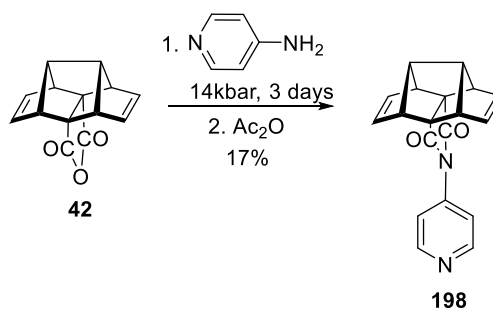


Figure 4.1.1 Polynorbornyl scaffolds with appended crown ethers with ethylene, methylene and a direct attachment.

To achieve the directly linked system **197**, aromatic amino crown ether derivatives were required due to the fact that aryl halides are unreactive towards nucleophilic substitution^[1] for example with imides. This occurs more readily when strong electron donating groups are in the *para* and *meta* positions. In comparison electron withdrawing groups situated in the *ortho* or *para* positions to the halogen, activate the ring towards nucleophilic attack.^[1]

The synthesis of polynorbornyl systems with appended aromatic derivatives through reaction of an anhydride have been deemed less reactive with the *bis*-oxa framework.^[2] This has also been demonstrated with the Hedaya polynorbornyl system by Warrener *et al.*, as shown in Scheme 4.1.1, with an overall yield of 17%.^[3]



Scheme 4.1.1 Preparation of **198** through initial amic acid formation followed by ring closure to the imide.^[3]

The low reactivity towards imide formation may be due to the direction of nucleophilic attack on the anhydride as well as the nucleophilicity of aniline. The optimal angle for attack on the carbonyl is the Bürgi–Dunitz angle of approximately 107° .^[4] This would suggest that the nucleophile needs to pass close to the double bond. Therefore more sterically hindered substrates will have less reactivity towards amic acid formation and furthermore the imide. Modelling suggests that with the Hedaya block the carbon-carbon bridgehead bond slightly pushes the alkene outwards and upwards which could allow for better access of aromatic amines to the anhydride group as shown in Figure 4.1.2.

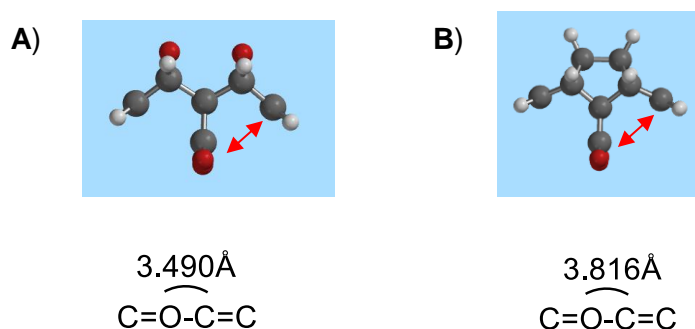


Figure 4.1.2 Variations in the positions and direction of olefinic protons on both polycyclic blocks **A)** *bis-oxa anhydride* **B)** Hedaya anhydride.

4.2 Molecular Modelling of the Polynorbornyl Scaffold with a Direct Attachment to the Benzocrown Ether

In addition to the designs outlined in Chapters 2 and 3 for the ethylene and methylene linkers, here a new model is outlined based upon a direct link between the polynorbornyl scaffold and the aromatic of the benzocrown. Modelling of the coupled polynorbornyl blocks is shown in Figure 4.2.1. As previously discussed, the attachment of the aromatic crown to the polynorbornyl block, occurs through

the imide, coupled to subsequent blocks (crown ethers and esters from coupling reactions were removed for the ease of modelling).

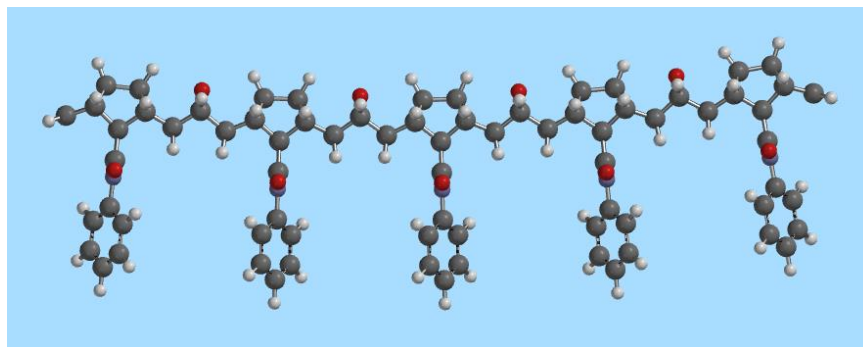


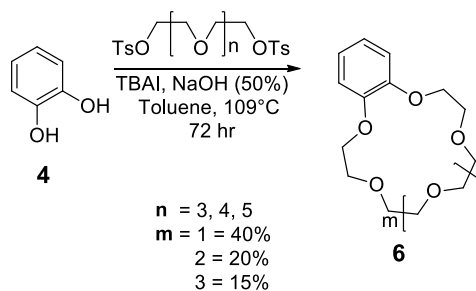
Figure 4.2.1 Proposed polycyclic norbornyl linear framework with direct link for channel transportation, crown ethers and esters were removed for ease of modelling (Spartan 10').

The direct link between the imide and the benzocrown ether allows for relative alignment of the crown ethers and equal spacing. Although a slight twist in the aromatic ring relative to the imide can be observed, there is still free rotation around the Ar-C-N bond. The relative distance between the crown relay sites is similar to that previously measured between $\sim 6.5\text{-}8.0$ Å with an overall length of 35 Å. Thus, the outlined scaffold would appear to be an appropriate ion channel target and therefore the synthesis of this system was initiated.

4.3 Aromatic Amine Crown Ether Preparation

The preparation of aromatic amino crown ethers have been explored extensively.^[5-8] Initial synthetic methods in this study involved the preparation of varying sized benzocrown ethers (15-crown-5, 18-crown-6, 21-crown-7) following the procedures outlined by Jiang *et al.* with minor modifications.^[9] This method for preparing crown ethers follows the PTC procedure outlined in Chapter 1.

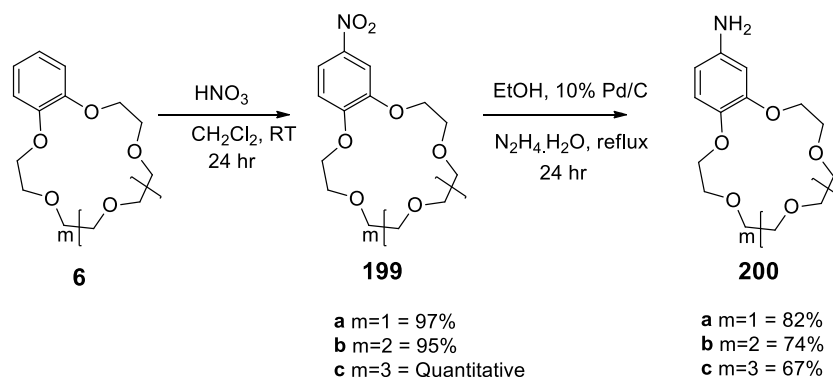
Benzocrown ethers were prepared from the corresponding di(*p*-toluenesulfonates) previously prepared from their corresponding glycols in moderate yields shown in Scheme 4.3.1.



Scheme 4.3.1 Preparation of benzocrown ethers *via* phase transfer conditions.

This was achieved in a two phase mixture with toluene, aqueous sodium hydroxide solution and tetrabutyl ammonium iodide (TBAI) as the transfer catalyst. In addition, the iodide may also assist in the formation of the crown ether by reacting with the *bis*-tosylate to produce the reactive iodoalkyl species. The reaction mixture required vigorous stirring for the di(*p*-toluenesulfonate) to react with catechol, due to the reaction mixture's viscosity. On most occasions the reaction mixture was left for longer time periods (>16 h) than specified by Jiang *et al.*, in order to obtain greater yields following hot hexane extractions. Depending on the size of the crown ether, the yields varied, with the smaller crown ethers being obtained in higher yield: 15-crown-5 (40-50%), 18-crown-6 (20-35%), 21-crown-7 (15-20%). The ^1H and ^{13}C NMR spectra of the corresponding crown ethers were consistent with reported literature values.^[9-11]

A number of different reaction pathways and conditions exist for the nitration and subsequent reduction of nitro compounds to amines.^[5-8,12,13] One method in particular that was considered was that of Cheema *et al.*^[14] The nitrated crown ethers were synthesised as shown in Scheme 4.3.2. The crown ethers were subjected to nitric acid (60 %) in CH_2Cl_2 for 24 hr. Removal of excess nitric acid with subsequent water washings afforded the substituted crown ethers, **199** in excellent yields.



Scheme 4.3.2 Preparation of amino crown ethers through nitration (with HNO_3) of benzo crown ethers followed by reduction to the corresponding aniline.^[15,16]

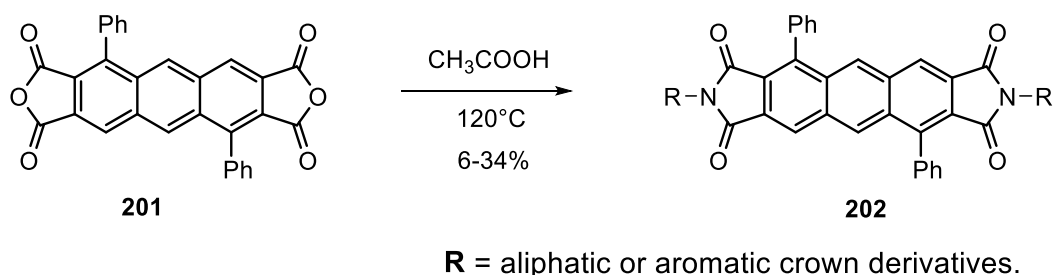
The ^1H NMR spectrum of the nitrated crown ethers indicated splitting of the aromatic signals. Coupling between protons on substituted aromatic rings were observed *via* the splitting patterns in the aromatic region of the ^1H NMR spectrum. The couplings observed were consistent with a tri-substituted aromatic ring. This was observed for all the nitro crown ethers synthesised.

Reduction of the nitro group on the benzocrown ethers was achieved through a catalytic transfer hydrogenation reaction over Pd/C with hydrazine in ethanol under reflux for 24 h. On completion the Pd/C was removed *via* filtration through celite® and the remaining ethanol solution concentrated *in vacuo*. Similar splitting patterns were observed for the amino crown compound resonances within the ^1H NMR spectrum. However the aromatic proton resonances had shifted upfield. Nitro groups are electron withdrawing and therefore proton shifts are observed downfield when reduction occurs. This was consistent for all the amino crown ethers synthesised. The amino crown ethers were now ready to be attached to anhydride-functionalised polynorbornyl blocks.

4.4 Linking of the Backbone with Crown Ether with Model *endo*-Carbic Anhydride

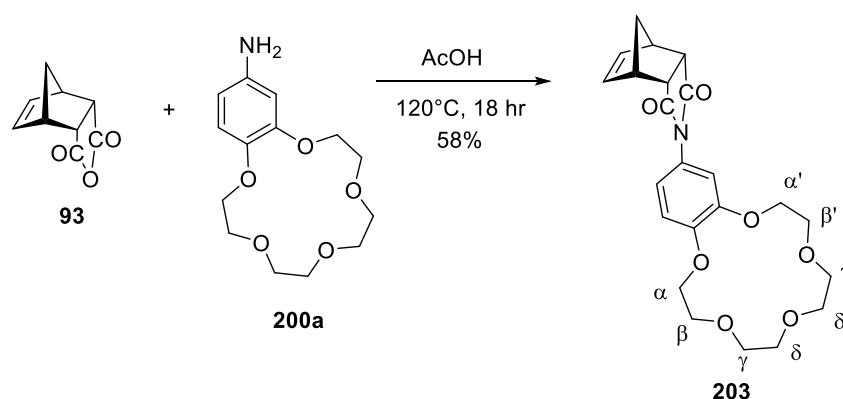
Discussions of aryl amine attachments to anhydride derivatives were explored in Chapter 2 with dopamine. Previously the reaction of amines like dopamine with polynorbornyl anhydrides were carried out in chloroform, where the amic acid most often precipitated, requiring further ring closing conditions with NaOAc and Ac_2O .

However in this scenario the linking of the aryl amine crown with the polynorbornyl block **42** using these procedures was unsuccessful in producing the fused product. Other solvent conditions were explored such as; DMF, DMSO, dioxane, and ACN, however all proved futile. A literature search of various reaction conditions with aryl amines and anhydrides was instigated. This revealed a synthetic procedure outlined by Meador *et al.*^[17] This procedure utilises different aromatic dianhydrides to prepare numerous N-substituted anthryl diimides in acetic acid at high temperatures as shown in Scheme 4.4.1.



Scheme 4.4.1 Attachment by Meador and co-workers of aliphatic and aromatic amino crown ethers to dianhydride, **201** to afford the disubstituted crown system, **202**.^[17]

This procedure was then adapted to our model system, where *endo*-carbic anhydride **93** was dissolved in acetic acid with the aryl amine **200a** shown in Scheme 4.4.2. Once the reactants had dissolved the reaction mixture was heated under reflux or at 120°C for 24 h. On completion, the acetic acid was removed *in vacuo* and the crude mixture purified *via* a silica plug with ethyl acetate as the mobile phase. It is important to note that a significant excess of the aryl amine **200a** was required to produce **203** in moderate yield (58%).



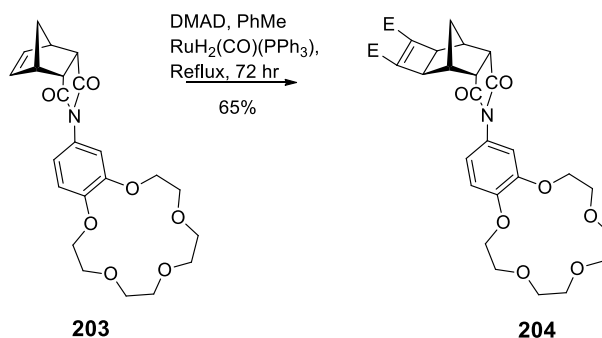
Scheme 4.4.2 Preparation of fused polycyclic crown ether system **203** through amic acid and imide formation between anhydride **93** and aniline crown ether **200a**.

Compound **203** was characterised *via* ^1H and ^{13}C NMR spectroscopy, infrared spectroscopy and mass spectrometry. The ^1H NMR spectrum gave insight into the linking of the aryl amine with the polynorbornyl system. Typical splitting patterns for 1,3,4-substituted aromatics were observed.

The polynorbornyl olefin protons resonated at 6.23 ppm. The $-\text{OCH}_2$ protons of the crown ethers appeared as three separate multiplet resonances α - protons were observed at 4.08-4.12 ppm, β - protons at 3.88-3.86 and γ - protons at 3.72-3.71 ppm consistent for a 15-crown-5 ether. The norbornyl block consisted of one *endo* and one *exo* proton set, at resonances at 3.47 and 3.38-3.37 ppm. Through COSY the chemical shifts of the *endo* and *exo* protons of the norbornyl scaffold were determined. The protons *exo* resonated at 3.38-3.37 ppm and do not correlate with any other protons other than the *endo* protons. Protons that were closest to the olefin resonated at 3.47 ppm with strong correlations between *endo* and *exo* protons, olefin and bridgehead protons.

The ^{13}C NMR spectrum reinforced the structure of **203** with important resonances consistent with carbonyl of the imide at 177.1 ppm as well as the olefin resonance at 134.7 ppm. Crown ether carbon atoms resonated further upfield between 71-69 ppm. Several signals were observed for the crowns which indicate that each carbon of the crown ether was in a slightly different environment. This was observed for most crown ether compounds reported in this thesis as described previously. High resolution mass spectroscopic data was consistent with the structure of **203** with m/z calculated for $\text{C}_{23}\text{H}_{27}\text{NO}_7$ 452.1685, found 452.1668 $[\text{M}]^+$.

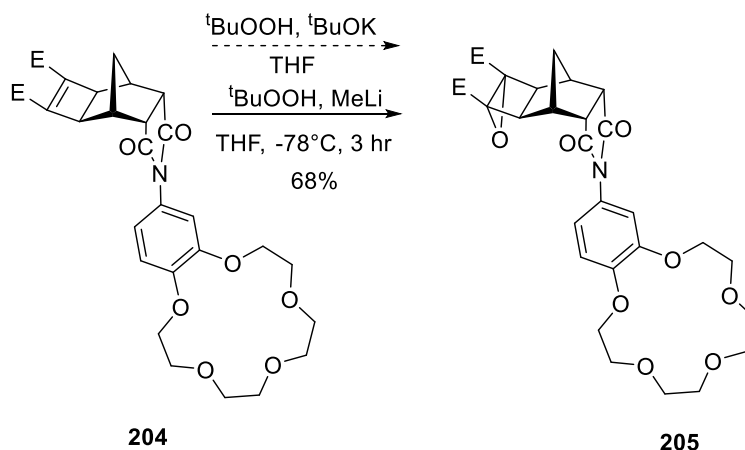
The successful synthesis of **203** focussed attention on the preparation of the Mitsudo adduct **204** (Scheme 4.4.3), an intermediate required on the way towards suitable functionality for the process of coupling blocks together. In this experiment the adduct **203** was mixed with the Ru(0) catalyst and DMAD in toluene, and heated under reflux for 72 hr. Upon workup and purification **204** was isolated as a light brown product in 65% yield.



Scheme 4.4.3 Preparation of cyclobutene 1,2-diester **204** via general Mitsunobu conditions.

NMR spectroscopic and HRMS data was consistent with the structure of **204**. This was supported by the disappearance of the olefinic resonance observed for the starting material at 6.23 ppm and the addition of the new methyl ester resonance at 3.77 ppm. Furthermore bridgehead resonances in the starting material observed at 2.85 ppm were shifted upfield to 2.48 ppm. These chemical shifts are consistent with the addition of the cyclobutene 1,2-diester to the diene. The ^{13}C NMR chemical shifts also supported the formation of the cycloaddition to the diene. The HRMS data was consistent with the structure of $\text{C}_{29}\text{H}_{33}\text{NO}_{11}$; calculated 572.2132, found 572.2126 $[\text{M}+\text{H}]^+$.

The next step in the synthetic sequence was the synthesis of epoxide **205**. Various nucleophilic epoxidising reagents were used as previously discussed in Chapter 3 to afford **205** in moderate yields. The successful reagents in the preparation of epoxide **205** were both MeLi in a 1.6M diethyl ether solution as well as freshly prepared LDA, combined with t-butylhydroperoxide. Similar strong bases investigated were; n-butyllithium and NaH, which were both unsuccessful. All metal ion tert-butoxides were thought to potentially coordinate to the crown ether (i.e. sodium tert-butoxide) as indicated for potassium tert-butoxide in previous systems (see Chapter 3). As noted in Scheme 4.4.4 the common nucleophilic epoxidation reagent potassium tert-butoxide did not facilitate the epoxide formation.



Scheme 4.4.4 Preparation of mono epoxide **205** via the first established nucleophilic epoxidation conditions ($t\text{BuOOH}$, MeLi).

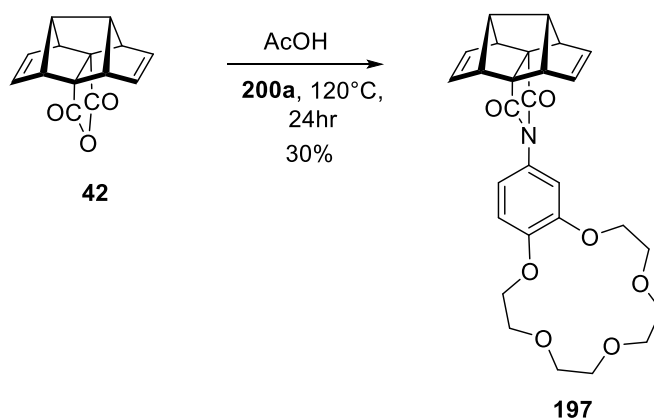
Of the successful reagents, LDA gave unreproducible results. Therefore MeLi was used throughout this work when available, and LDA was only employed when MeLi was unavailable. It is important to note that these reactions tended to be inconsistent, and the epoxide formation was irregular. This was due to a number of factors, such as decreased reactivity of supplied materials.

The epoxide **205** proved difficult to purify *via* column chromatography and was used as the crude product in subsequent ACE coupling reactions. This system was later used in the extension of new extended polynorbornyl frameworks for ion channel analysis.

Having successfully synthesised a model norbornyl system containing the functionality needed (i.e. crown ether and cyclobutene epoxide) attention was directed to the Hedaya block.

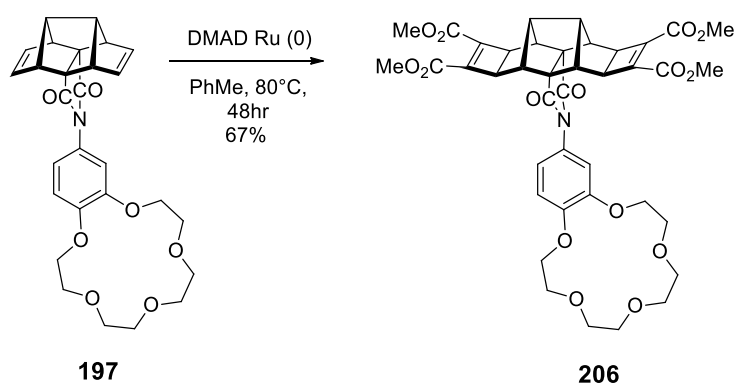
4.5 Amalgamation of the Backbone with Crown Ether using Anhydride, **42**.

The previously employed reaction conditions for the model system were used to join the polynorbornyl anhydride **42** to the crown ether (Scheme 4.5.1). Initially the anhydride **42** was dissolved in acetic acid along with amino benzocrown **200a** and heated under reflux for 24 hours. The reaction mixture was then purified *via* column chromatography to afford **197** in moderate yield (30%). NMR spectroscopy and mass spectroscopic data was consistent for compound **197**. The HRMS data was consistent with the structure of $\text{C}_{28}\text{H}_{29}\text{NO}_7$; calculated 491.1944, found 491.1939 $[\text{M}]^+$.



Scheme 4.5.1 Preparation of fused polycyclic crown ether system **197** through amic acid and imide formation between anhydride **42** and aniline crown ether **200a**.

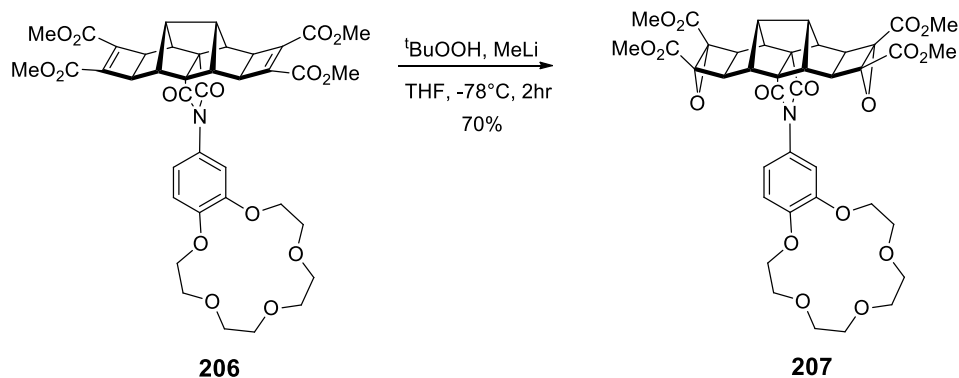
The subsequent Mitsudo reaction was employed as previously mentioned to prepare the cyclobutene 1,2-diester with DMAD and a ruthenium catalyst. The resulting Mitsudo product **206** was purified *via* column chromatography and analysed *via* NMR spectroscopy and mass spectrometry. The ^1H NMR spectrum for **206** showed distinctive differences to that of the starting material. The main differences observed were the addition of a new proton resonance at 3.77 ppm which represents that of the methyl esters and the loss of the olefinic resonance at 6.10 ppm. In the ^{13}C NMR spectrum there was an additional observed carbonyl (C (O) OCH₃) resonance at 160 ppm. Further analysis of **206** *via* HRMS was consistent with the structure C₄₀H₄₁NO₁₅; calculated 775.2476, found 775.2471 [M]⁺.



Scheme 4.5.2 Preparation of cyclobutene 1,2-diester **206** *via* general Mitsudo conditions.

The impact of the nucleophilic epoxidising reagents was also identified as an issue with the system described here. As described previously the general reaction conditions of potassium tert-butoxide and tert-butyl hydroperoxide on

this system in comparison to literature systems disrupts the crown ether, block and methylene carbons.^[18,19] The nucleophilic epoxide formation in this system used the conditions established for the model system **205** (Scheme 4.4.4) and used in this reaction to form **207** in 70% yield. The epoxide formation was verified by HRMS which was consistent with the structure $C_{40}H_{41}NO_{17}$; calculated 807.2374, found 807.2369 $[M]^+$.

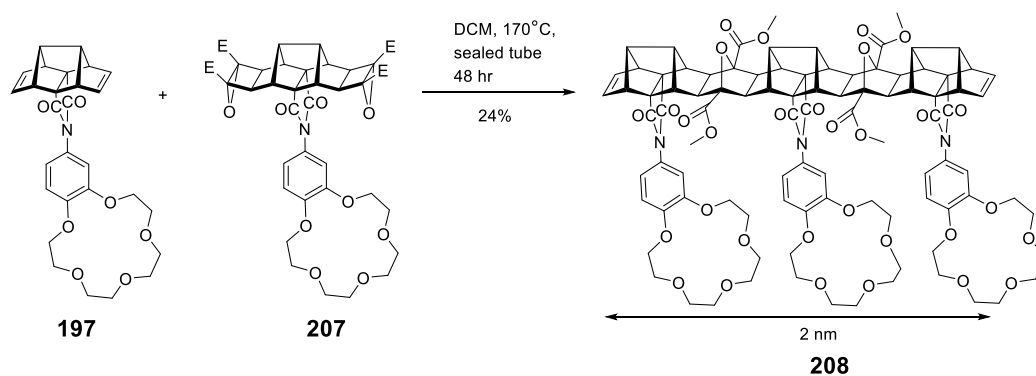


Scheme 4.5.3 Preparation of di-epoxide **207** via the nucleophilic epoxidation conditions (^tBuOOH, MeLi).

The epoxide **207** proved difficult to purify *via* column chromatography and was used as made in subsequent coupling reactions. The diepoxide **207** is a key molecule and this system was further used in the extension reactions to form new extended polynorbornyl frameworks (ACE reactions) for ion channel analysis.

4.6 ACE Coupling Reactions to form Tricrown A

The ACE coupling reaction was used to fuse block **197** with **207** so as to afford an extended polynorbornyl system (Scheme 4.6.1). The product **208** was initially isolated from a reaction mixture produced by heating **197** with **207** in a sealed tube at 180°C *via* column chromatography to afford **208** in poor yield (17 %). Subsequent reactions were performed under microwave conditions at 160-170°C in DCM to allow for the synthesis of tricrown A, **208** in slightly improved yield (24%).



Scheme 4.6.1 ACE coupling reaction between *bis*-alkene **197** and diepoxide **207** to afford the fused framework **208**.

This tricorn system **208** is a key molecule and its synthesis and isolation are a significant milestone. Thus, there is a significant need to characterise extensively since it is a major molecule that will be used in transport studies.

The polynorbornyl portions of tricorn A was modelled using the Spartan modelling software, Figure 4.6.1. The model indicated that the polynorbornyl backbone was in a linear orientation with the appended crown ethers aligned perpendicular with the attachment at the imide (when the crowns are modelled). The modelling of tricorn A has given an insight into how the sections in the molecule may align, more specifically the crown ethers in reference to NMR spectroscopy assignment. Free rotation around the imide (N-C-Phenyl) gives rise to the end blocks being in a similar environment, but different to that of the aromatic crown ether on the central block.

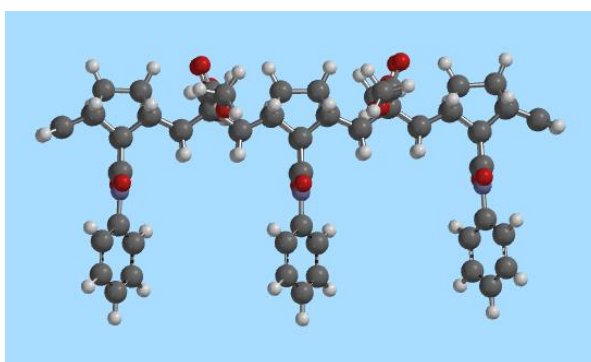


Figure 4.6.1 Molecular model of tricorn A (Crown ethers removed for ease of modelling) using Spartan modelling 10' software.

Armed with an appreciation of the model of **208** a variety of NMR spectroscopic experiments were performed (1D and 2D) to assign the complete configuration of tricorn A. The NMR spectral assignment of all proton resonances (labelled alphabetically) is shown in Figure 4.6.2.

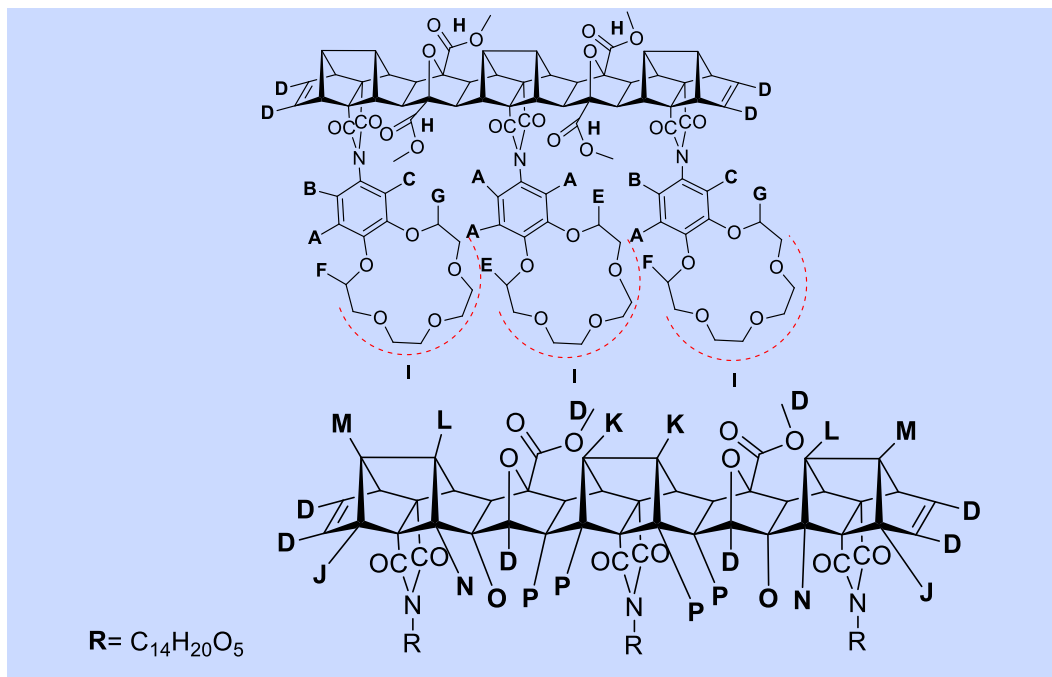


Figure 4.6.2 Complete assignment of tricrown A protons that will be observed in the NMR spectra.

The tricrown A 1H NMR spectrum in Figure 4.6.3 below gives rise to a set number of resonances indicating symmetry across the molecule (horizontally) and through the molecule (vertically). There are a number of important resonances which will be discussed in detail as defined areas of the spectrum are examined more closely.

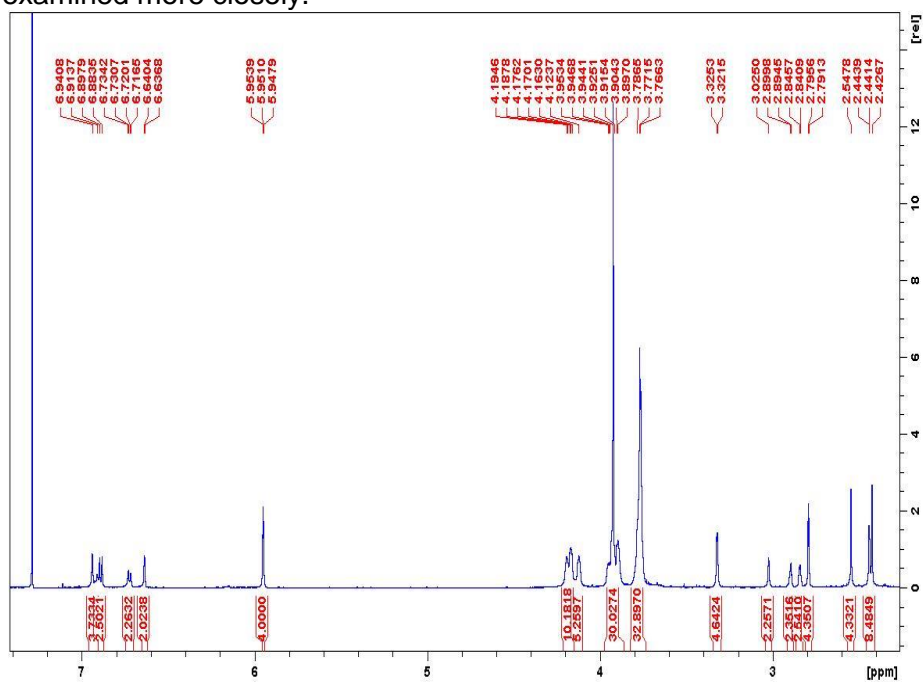


Figure 4.6.3 Tricrown A 1H NMR spectrum (600 MHz), (overall spectrum).

The aromatic and olefinic region of tricrown A is shown in Figure 4.6.4. In this section of the ^1H NMR spectrum there are two proton resonances which are overlapped, labelled (A).

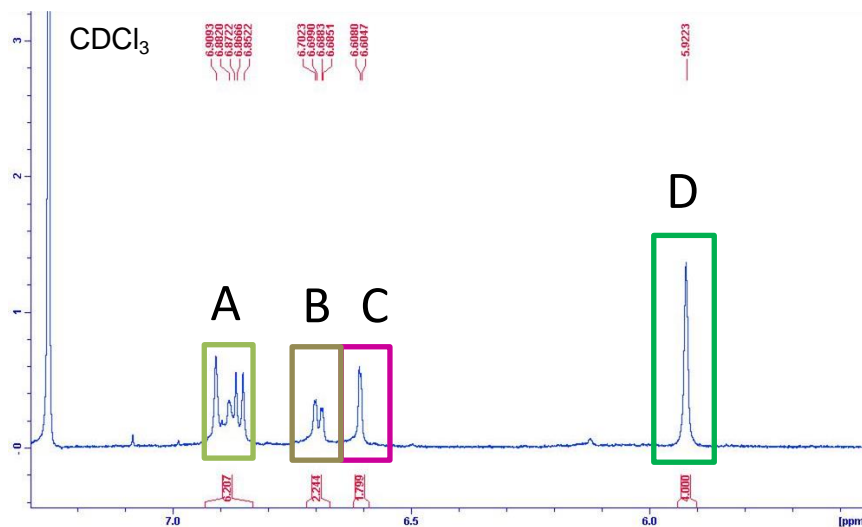


Figure 4.6.4 Tricrown A, aromatic and double bond region of the ^1H NMR spectrum.

As mentioned previously the two outside polynorbornyl crown blocks are in different chemical environments to that of the central block, signal overlay (**A**) is one indication in this system. It has been determined from the various NMR spectroscopy experiments that **A** correlates to the central block aromatic proton resonances, as well as the ortho protons on the outside block (see Figure 4.6.2), which is usually evident by splitting and larger J values for ortho positioned protons. Although in this spectrum it is difficult to determine the J values of all ortho protons on the aromatic rings of the central block, however the proton coupling constants from the outside blocks can be calculated, $J = 8.6$ Hz.

Protons labelled **B**, the doublet-of-doublets are split by both **A**, ortho, ($J = 8.4$ Hz) and **C**, meta, ($J = 1.98$ Hz). The protons of **C** are split by **B**, meta, ($J = 1.98$ Hz). Furthermore assignment **D** correlates to the olefin proton resonance at either end of the molecule at 5.9 ppm, and integrates for 4H.

Moving upfield, towards the crown ether assignment **E**, **F**, **G** as shown in Figure 4.6.5, three different environments for the crown ether protons are evident but with the same integration (4H for α proton). The α protons on the central crown ether are equivalent (**E**), whereas the α protons on the outside crown ethers are

non-equivalent (**F**, **G**). This results in three α proton signals integrating for 4H each.

Both **H** and **I** correspond to the esters from the ACE reaction and the remaining β and γ protons from the crown ether. Moving further upfield the *endo* protons have been assigned **O** and **P**, bridge protons **J** and **N** and the bridgehead protons **M**, **L** and **K**, via 2D NMR spectroscopy (COSY, NOESY) and are listed on the molecular structure in Figure 4.6.2.

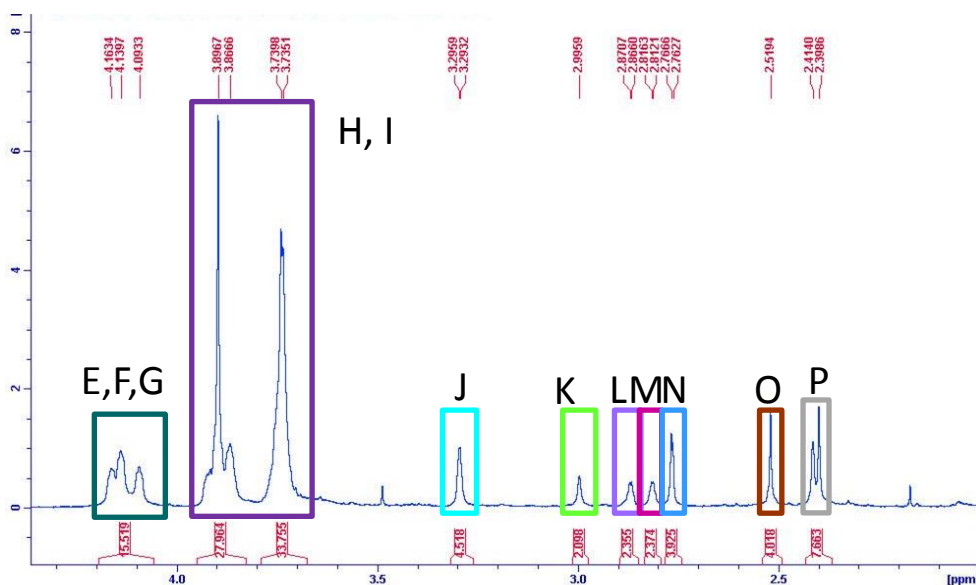


Figure 4.6.5 Tricrown A crown ether, *endo* and bridgehead proton resonances assigned.

The ^{13}C NMR spectrum also gives insight into the structure of tricrown A, shown in Figure 4.6.6 with assignments in Figure 4.6.7 (colour coded). Structural assignment of the key functional groups are shown in Figures 4.6.8-10.

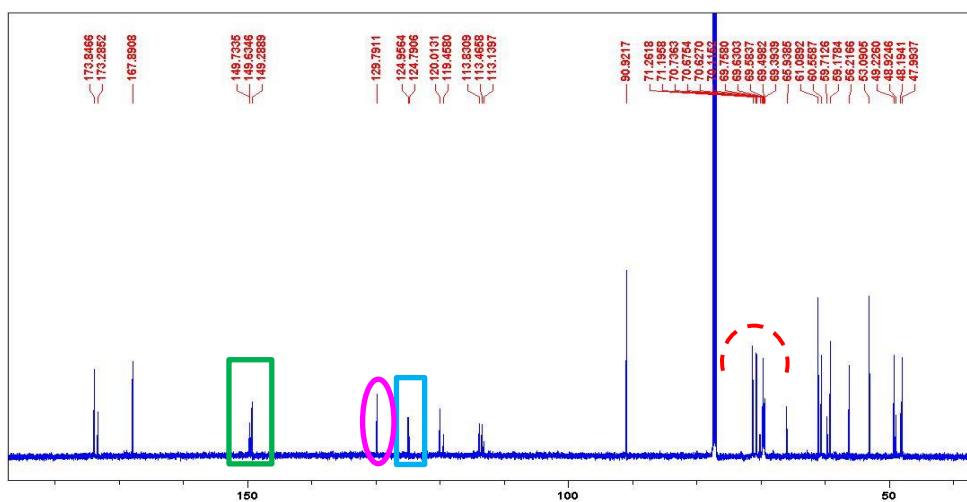


Figure 4.6.6 Tricrown A ^{13}C NMR spectrum.

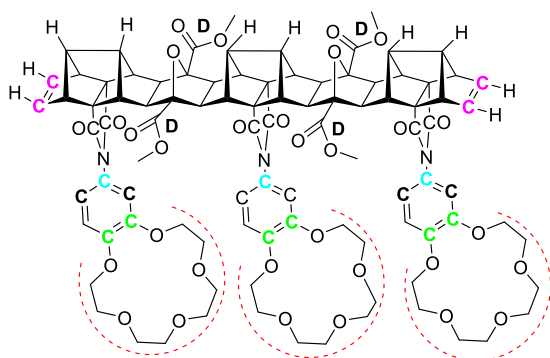


Figure 4.6.7 Tricrown A ^{13}C NMR spectroscopy assignment. (Highlighted carbons are assigned on ^{13}C NMR spectra Figure 4.6.6.

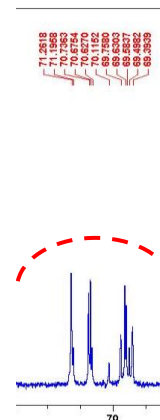


Figure 4.6.8 Tricrown A ^{13}C crown ether NMR spectroscopy shifts.

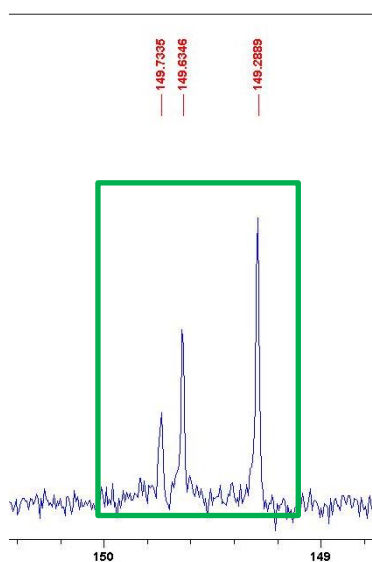


Figure 4.6.9 Tricrown A ^{13}C aromatic carbon 3, 4 position NMR spectroscopy shifts.



Figure 4.6.10 Tricrown A ^{13}C aromatic NMR spectroscopy shifts.

In Figure 4.6.8 there are multiple carbon resonances which correlate to the carbon atoms of the crown ethers (71-69 ppm). The majority of the carbon atoms of the crown ether are slightly different from each other resulting in multiple resonances being observed.

In addition (Figure 4.6.10) shows the carbon of the aromatic bonded to the imide (blue, Figure 4.6.7) to have two resonance signals. These carbon shifts are in a 2:1 ratio which confirms that the outside ends are the same but different to the central. In Figure 4.6.9, there are three carbon resonances which correlate to the carbon atoms on the aromatic ring to which the ether chains are attached (green,

Figure 4.6.7). At first it was not clear why three peaks were observed if the two outside blocks were in the same environment but different to the central (2:1). From the spectra it would indicate a 3:2:1 ratio where the three carbons that are para to the aromatic, imide bond (Ar-N) have the same chemical shift. But there is a difference for the three meta carbons, where the central block is different to the two outside blocks. This may be due to the way the various aromatic rings are positioned within the structure resulting in this ratio between the carbon atoms being observed.

Further characterisation was performed *via* HRMS which further reinforced the identity of **208**. The HRMS indicated a singly charged ion $[M+Na]^+$ observed at 1813.6219 (expected 1813.6160), doubly charged ion $[M+2Na]^+$ observed at 918.3032 (expected 918.3040) as well as triply charged ion $[M+3Na]^+$ observed at 619.5276 (expected, 619.8658) shown in Figure 4.6.11. This pattern of ions gives insight into the behaviour of the system with the three crown ethers complexing with sodium in the mass spectrometer. This is an encouraging finding as it shows that tricrown A has the potential to promote sodium transport.

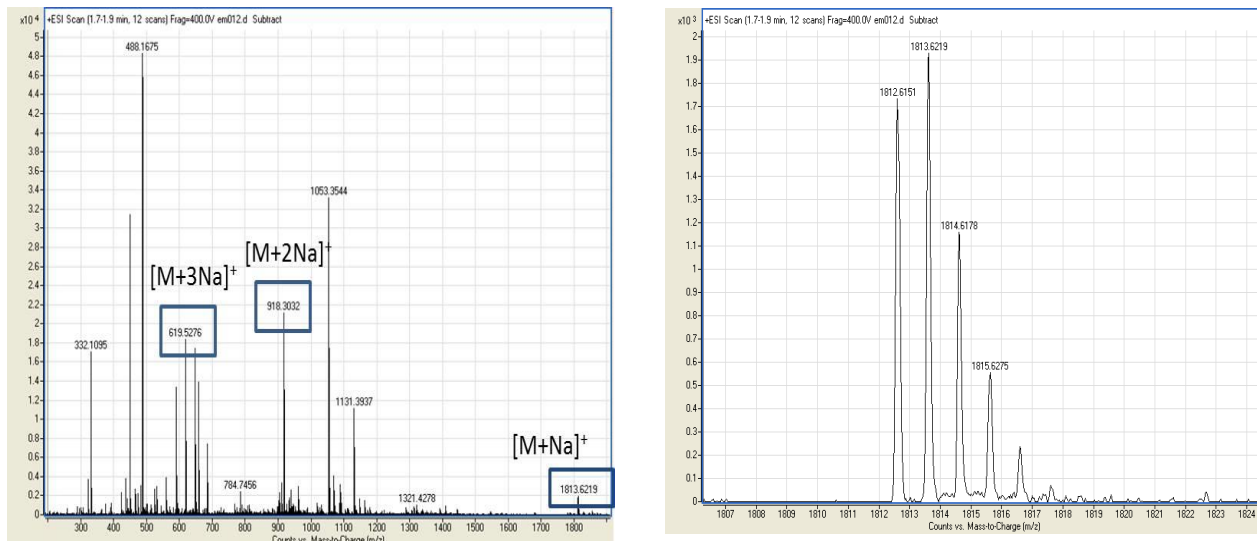
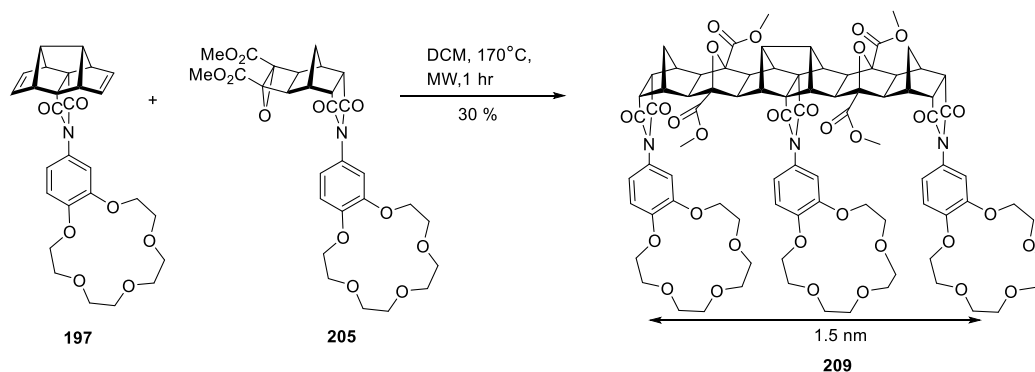


Figure 4.6.11 Tricrown A HRMS chromatogram with close up of the molecular ion.

4.7 ACE Coupling Reactions to form Tricrown B

The successful synthesis of tricrown A (**208**) led to investigations into variations in the tricrown systems. One system in particular, tricrown B pictured below (Figure 4.7.1) was synthesised through similar reaction conditions and pathways mentioned previously. Tricrown B was synthesised from the aforementioned

monoepoxide **205** in ACE reaction with the olefins of **197** under microwave conditions at 170°C for 1hr to produce tricrown B **209**, in moderate yield (30 %).



Scheme 4.7.1 ACE coupling reaction between *bis*-alkene **197** and epoxide **205** to afford the fused framework **209**.

Both ^1H , ^{13}C NMR spectra and HRMS spectroscopy were used to confirm the structure of tricrown B and its successful synthesis and these will be discussed below.

Molecular modelling of tricrown B (Figure 4.7.1) gives insight into the spacing of the crowns and the overall conformation of the system. One key aspect identified in this model is the orientation of the imide in the end blocks. These *endo* imides in tricrown B in comparison to tricrown A are pointed slightly inwards and this is supported by NMR spectroscopy, in particular by the variations in the aromatic chemical shift values.

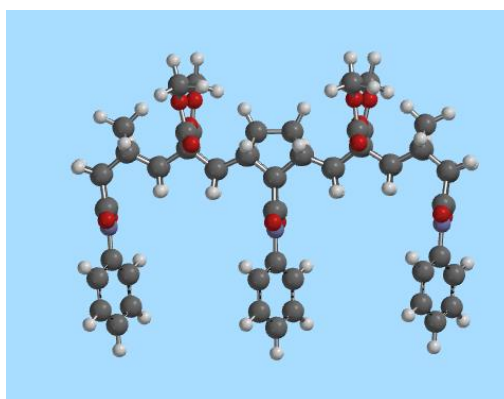


Figure 4.7.1 Tricrown B synthesis from ACE coupling reaction of epoxide **205** and *bis*-alkene **197** modelled using Spartan 10' (crown ethers removed for ease of modelling).

Tricrown B was characterised *via* ^1H , ^{13}C and 2D NMR spectroscopy experiments as a result of which the relative positions of the proton resonances were determined. In Figure 4.7.2 the structure of tricrown B is shown and the assignment of the protons indicated.

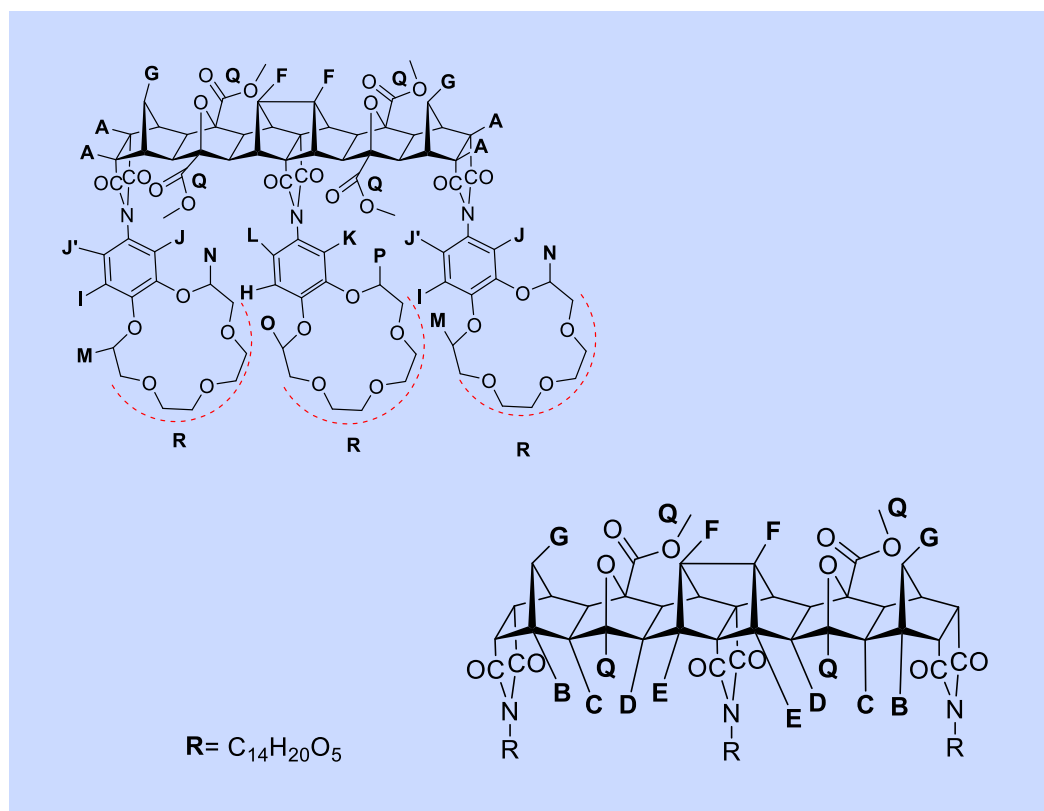


Figure 4.7.2 Tricrown B ^1H NMR spectrum assignment.

Figure 4.7.3 shows the overall spectra which will be broken down into smaller portions to assist with peak assignments.

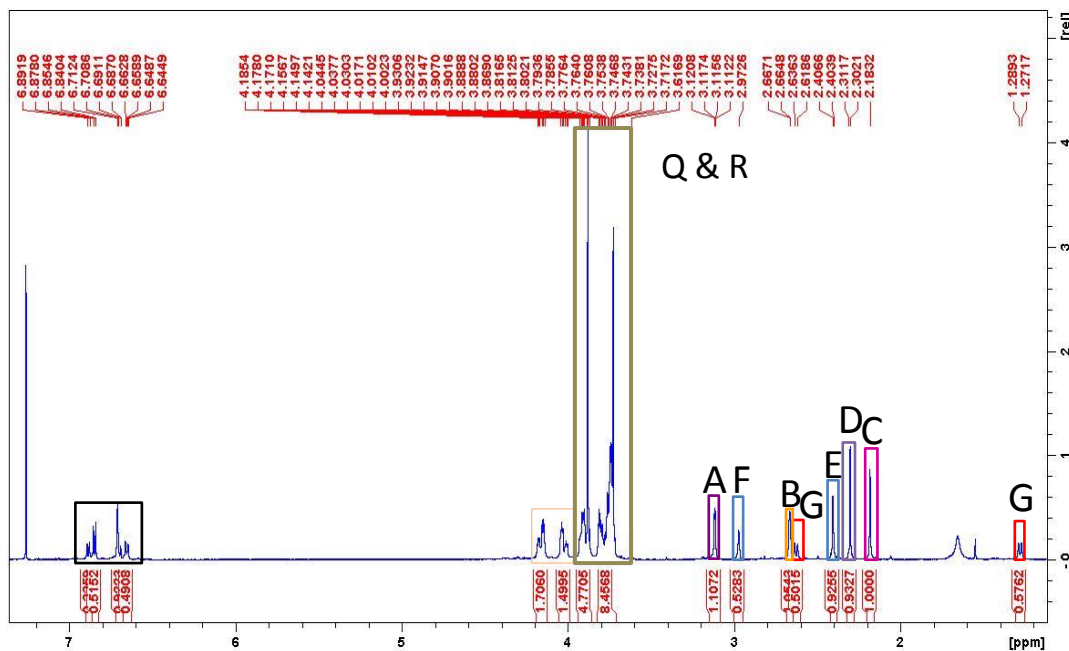


Figure 4.7.3 Complete tricrown B ^1H NMR spectrum.

As discussed previously for the aromatic region assignment for tricrown A, here tricrown B is more defined (Figure 4.7.4). It was observed that the outside blocks are different to the central block in a similar manner to tricrown A and this was consistent with NMR spectroscopic characterisation.

It has been determined that **H** (Figure 4.7.2) correlates (*via* nOe) to the central aromatic ring protons and **I** correlates to the protons on the outside rings, this is usually evident by splitting and larger J coupling values for ortho positioned protons. In this spectrum the J coupling values for both **H** and **I** are able to be calculated (**H** J = 8.4 Hz, **I** J = 8.5 Hz). Outside protons labelled **J'**, the doublet of doublets are split by both **I**, ortho, (J = 8.5 Hz) and **J**, meta, however overlap of signals is observed in this spectra and therefore no J coupling values can be determined for the outside proton resonances (**J'** and **J** labelled). On the central aromatic, **L** is split by both **K** (meta, J = 2.4 Hz) and **H** (ortho, J = 8.4 Hz) consistent with splitting patterns previously seen. The central block aromatic proton resonance for **K** is split by **L** (meta, J = 2.4 Hz) shown in Figure 4.7.4.

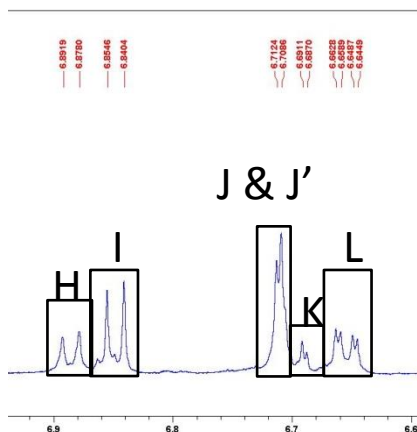


Figure 4.7.4 Tricrown B ^1H NMR spectrum of the aromatic region.

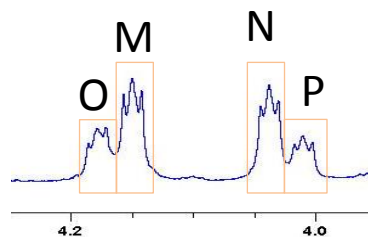


Figure 4.7.5 Tricrown B ^1H NMR spectrum of the α crown ether region.

Another indication that there is a 2:1 (outside to central) system also occurring in tricrown B is evident in the crown ether region shown in Figure 4.7.5. Here resonances were assigned to **O** and **P** on the central crown ethers of the molecule and **M** and **N** to the outside crowns based on integration. The central positioning of the crown ether must have changed the chemical environments of the ethers enough to produce these changes in shifts when compared to those seen in tricrown A.

Both **Q** and **R** (Figure 4.7.3) correspond to the esters from the ACE reaction and the remaining β and γ protons from the crown ether. Moving further upfield the *endo* protons have been assigned **C** and **D**, *exo* protons **A**, bridge protons **B** and **E** and the bridgehead protons **G** and **F**, *via* 2D NMR spectroscopy (COSY, NOESY) and are listed on the molecular structure in Figure 4.7.2.

Further characterisation was performed *via* mass spectrometry which indicated a doubly charged ion $[\text{M}+2\text{Na}]^+$ observed at 855.7852 (expected, 855.7872), however no triply charged ion $[\text{M}+3\text{Na}]^+$ was observed. The molecular ion $[\text{M}+\text{Na}]^+$ was observed at 1688.5843 (expected 1688.5847) shown below in Figure 4.7.6. The lack of $[\text{M}+3\text{Na}]^+$ was unexpected based on the tricrown A results, and may reflect the closer proximity of the outside crowns to the central crowns as a results of the more inward facing imide group of the outside blocks.

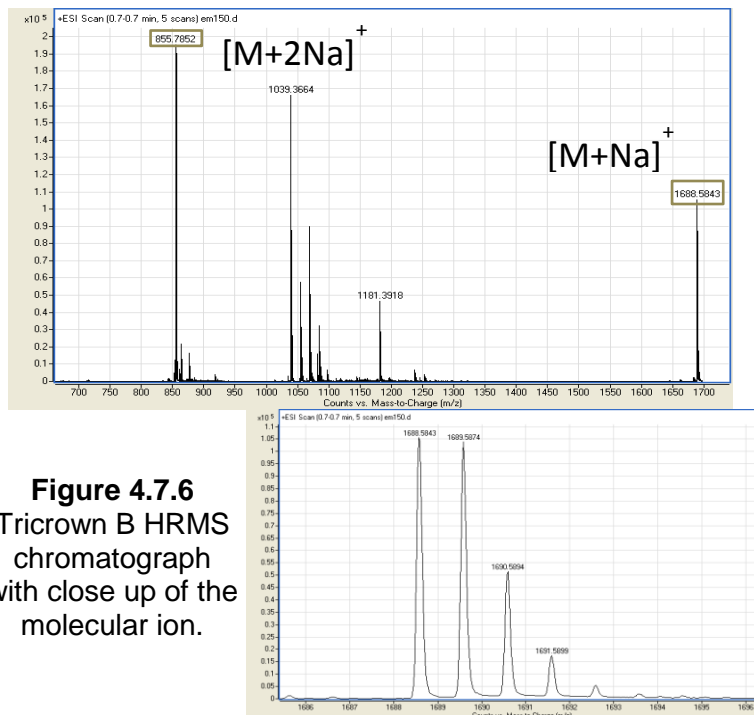
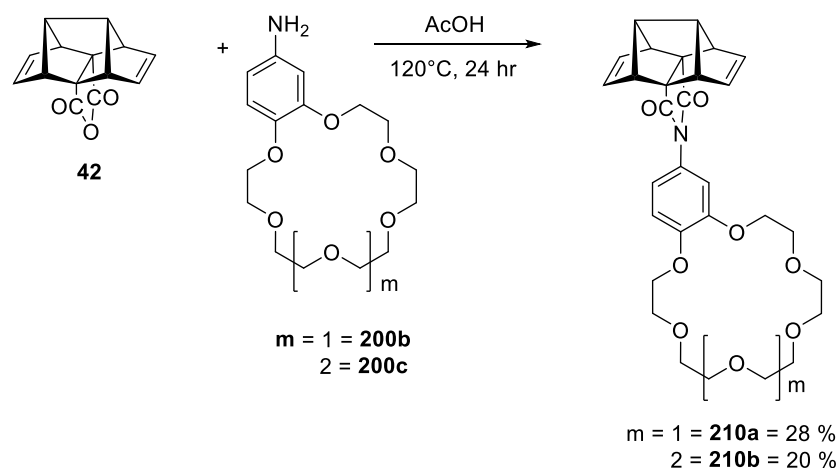


Figure 4.7.6
Tricrown B HRMS
chromatograph
with close up of the
molecular ion.

4.7.1 Tricrown Systems with Varying Crown Ether Sizes

Following on from the successful synthesis of both tricrown A (**208**) and tricrown B (**209**) with the use of 15-crown-5 ethers, it was decided to extend these systems to frameworks which incorporated larger crown ethers. This was done so as to allow variations in the size of crown ethers across the ion channel. Therefore, allowing for either all of the same sized crown ethers across the molecule or different sized crown ethers to the central crowns as larger entry portals to the ion channel, facilitating transport.

To achieve these tricrown systems, the monomer units containing the different crown ethers were required. The first framework to be synthesised was that containing the 18-crown-6 ether.



Scheme 4.7.1.1 Preparation of fused polycyclic crown ether system **210a**, **210b** through amic acid and imide formation between anhydride **42** and amino crown ethers **200b** and **200c**.

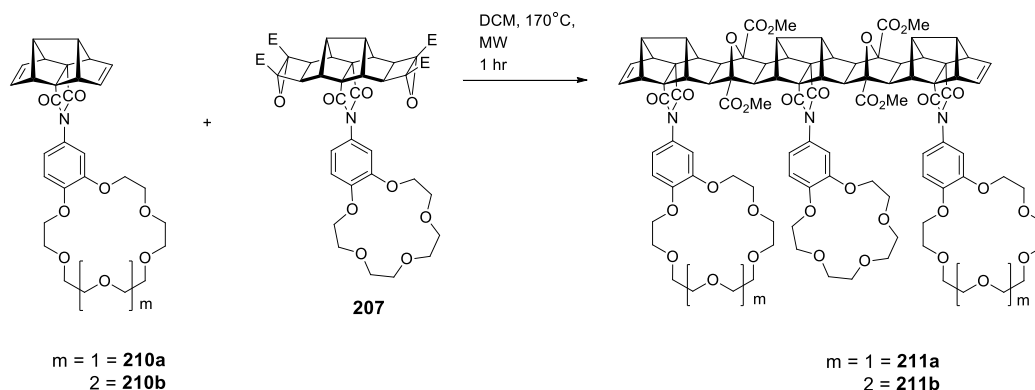
The fused block **210a** was synthesised as previously described for similar systems (AcOH at 120°C) and was characterised *via* NMR spectroscopy and HRMS. The ^1H NMR spectrum gave insight into the linking of the 18-crown-6 aryl amine and the polycyclic system. Aromatic resonances typical of a tri-substituted aromatic were observed i.e. the protons situated ortho to one another produced large J coupling ($J = 8.5$ Hz) and meta gave small J values ($J = 2.3$ Hz). The polynorbornyl olefin protons resonated at 6.59 ppm, followed upfield with the crown ether resonances between 4.10-3.70 ppm. The HRMS data was consistent with the structure of **210a**; calculated for $\text{C}_{30}\text{H}_{33}\text{NO}_8\text{Na}$ 535.2104, found 558.2094 $[\text{M}+\text{Na}]^+$.

In the meantime the 21-crown-7 fused polycyclic framework **210b** was also synthesised as depicted in Scheme 4.7.1.1. This structure was also characterised by NMR and HRMS. The ^1H NMR spectrum contained very similar resonances to that observed for the 18-crown-6 analogue, with additional resonances for extra crown ether protons in 21-crown-7. The HRMS data was consistent with the structure of **210b** calculated for $\text{C}_{32}\text{H}_{37}\text{NO}_9\text{Na}$ 602.2366, found 602.2366 $[\text{M}+\text{Na}]^+$.

Now being in possession of the polycyclic block appended with the different crown ethers (namely 15-crown-5, 18-crown-6, 21-crown-7) these could be combined with the 15-crown-5 epoxide **207** previously synthesised.

By way of example, following the procedure for ACE coupling reactions carried out with the assistance of microwave heating, attempts to synthesise the tricrown

systems of both the 18-crown-6 and 21-crown-7 (blocks **210a** and **210b**) were made with the diepoxide of **207** (Figure 4.7.1.2).



Scheme 4.7.1.2 Preparation of tricrown with 21-crown-7 ethers on the outside of 15-crown-5 ether through ACE coupling reaction under microwave conditions.

Initial NMR analysis of the crude tricrown mixtures indicated both compounds **211a** and **211b** were successfully synthesised due to multiple *endo* proton resonances and new double bond resonances as would be expected in the products. However attempted purification of the 18-crown-6 tricrown **211a** *via* column chromatography was unsuccessful and all of the product was lost on the silica gel.

In regards to the 21-crown-7 tricrown system **211b**, before attempting purification *via* column chromatography a sample of the crude reaction mixture was analysed *via* MS to confirm its presence (Figure 4.7.1.1). The results from the MS were consistent with the tricrown structure **211b**; calculated for $C_{104}H_{115}N_3O_{35}Na$ 1965.7311, found 1989.7184 $[M+Na]^+$. However similar issues were encountered when various purification methods were used, i.e. trituration, column chromatography, recrystallisation, i.e. loss of material.

Successful MS characterisation of **211b** shows that the building block/coupling approach is feasible to construct polycyclic frameworks appended with various sized crown ethers with a high degree of structural control.

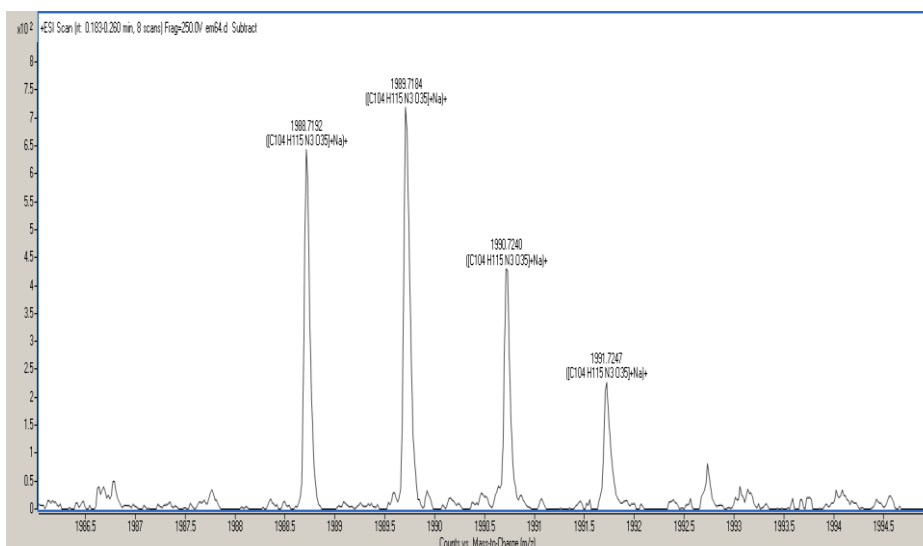


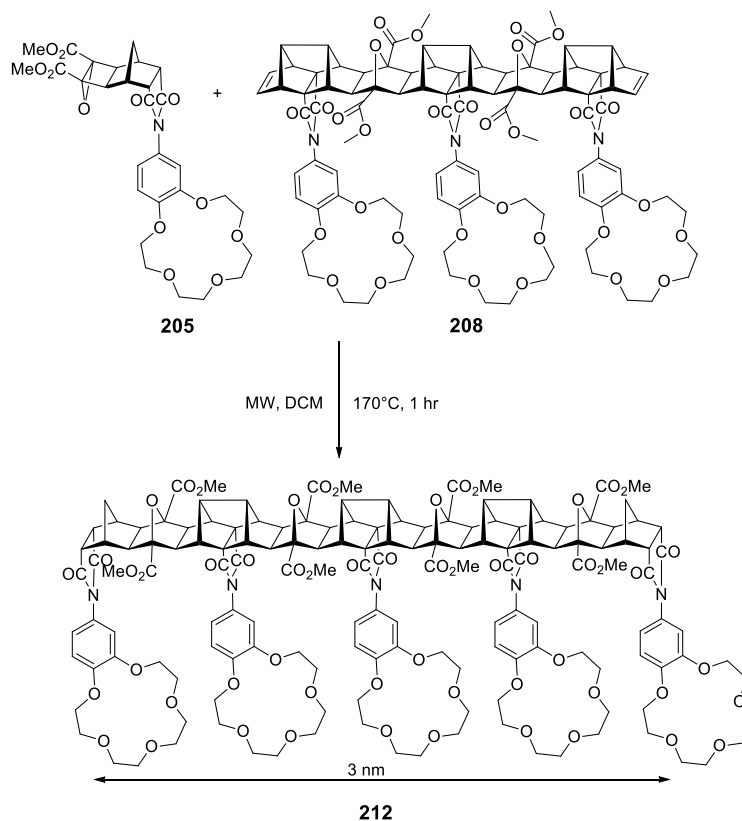
Figure 4.7.1.1 Tricrown **211b** MS chromatogram of molecular ion.

This area investigated has only been touched on and there is potential for it to be explored further in relation to the development of new crown ether systems or other cation or anion binding sites. In addition a more economical and simple purification process should be formulated to allow more straightforward access to these molecules.

4.8 Extension of Tricrown A to a Pentacrown System

In addition to the attempted synthesis of new tricrown systems as outlined in section 4.7.1 the tricrown A system was further extended to the pentacrown system with end caps similar to that of tricrown B. The pentacrown system was synthesised to extend the length of the molecule to be similar to that of the lipid bilayer (~40 Å). Most artificial ion channels described in the literature span the bilayer to act through a channel transport mechanism (hopping through the crown ethers) as opposed to an ion carrier mechanism. However, difficulties in both synthesis and purification were encountered for the pentacrown channel described below. The pentacrown system was synthesised through an ACE coupling reaction with tricrown A **208** and *endo* crown epoxide **205** (Scheme 4.8.1): **208** and **205** were heated *via* microwave irradiation in DCM at 170°C for 1 hour. Analysis of the crude reaction mixture showed a number of aromatic peaks, olefinic peaks and new ester resonances. Based on past experience these shifts indicated that the reaction had proceeded successfully.

However, difficulties in pentacrown purification were encountered. In particular, trituration, chromatography (silica, alumina), and recrystallisation were all unsuccessful in obtaining pure product. The impure nature of the product hampered ^1H NMR spectral characterisation and furthermore ion channel analysis. Although the pentacrown **212** was impure a sample was analysed by HRMS.



Scheme 4.8.1 Synthesis of a proposed artificial ion channel **212** using tricrown **208**, incorporating end block assembly and extension using an ACE reaction.

Characterisation of the pentacrown system $\text{C}_{154}\text{H}_{165}\text{N}_5\text{O}_{55}$ was through HRMS with a doubly charged ion observed $[\text{M}+2\text{Na}]^+$ at 1505.5041 (expected 1505.0134), however triply charged ion was observed $[\text{M}+3\text{Na}]^+$ at 1011.3318 (expected 1011.0089) shown in Figure 4.8.2.

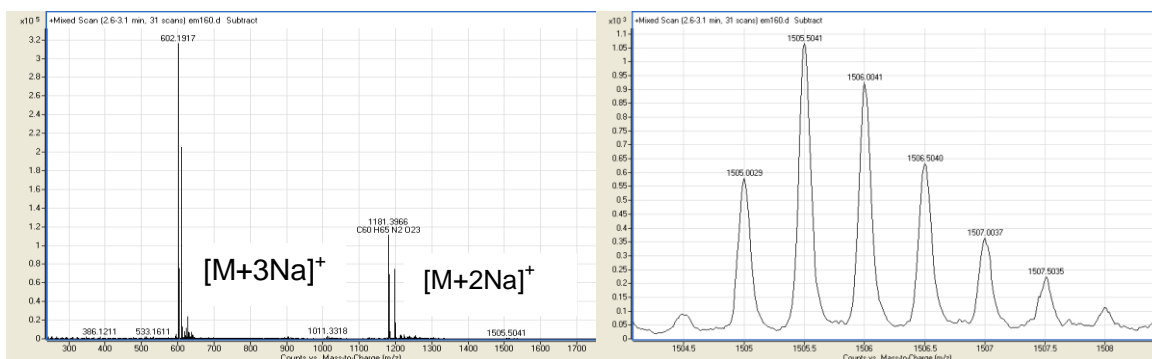


Figure 4.8.2 Pentacrown HRMS chromatogram with close up of the molecular ion.

Molecular modelling (Figure 4.8.1) of the pentacrown system gives insight into the overall conformation of the molecule (crown ethers have been removed for ease of modelling). Similar to the tricrown B system, *endo* block **205** fused to the ends causes these blocks to shift downwards and point the aromatic slightly more inwards than would be expected if the block **197** had been used in all of the segments of the polycyclic moiety. However, it can be seen that the alignment is good for all aromatics and with the crown ether attached, would provide a direct route for ions to cross the bilayer. The overall length of the system modelled was approximately 3 nm which has increased slightly from the previous tricrown systems (tricrown A, 2 nm and tricrown B, 1.5 nm).

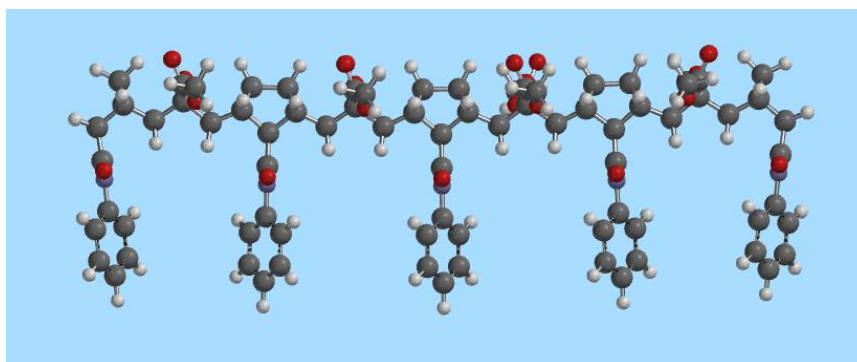


Figure 4.8.1 Molecular modelling of pentacrown system synthesised from the ACE coupling reaction of epoxide **205** and tricrown A **208** modelled using Spartan 10' (crown ethers removed for ease of modelling).

4.9 End Block Functionality and Potential Pathways for Additional Pentacrown Systems

As previously outlined in the introduction, the success of an artificial ion channel is based upon preparing systems that have similar lengths to the thickness of the bilayer rather than proceed through a carrier mechanism. Ideally this would include a characteristic non-polar interior with polar anchoring groups at either end to help incorporate the system into the lipid bilayer. Therefore investigations towards different end group block functionalities to integrate hydrophilicity and increased length into the synthetic ion channel system were explored through a number of polycyclic norbornyl systems (Figure 4.9.1).

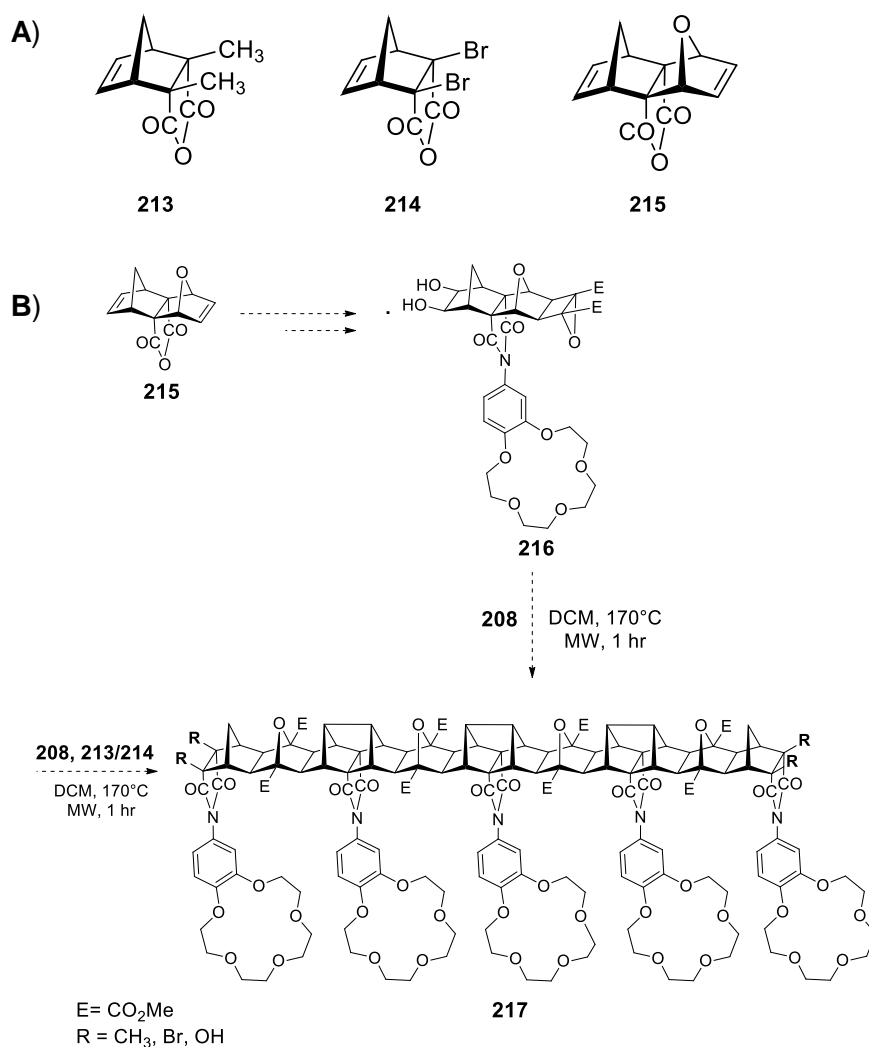
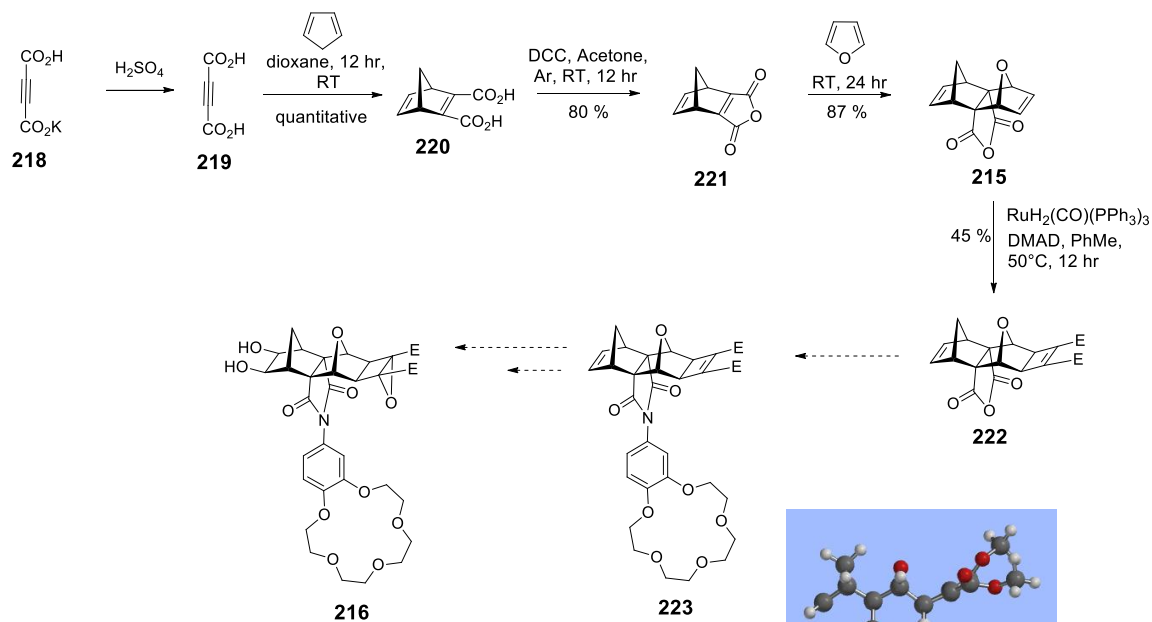


Figure 4.9.1 A) Various polycyclic molecules for potential *endo* groups **B)** Polycyclic system, **215** for chain extension to the pentacrown motif **217**.

The systems that were of synthetic interest were those that could be attached to the previously synthesised tricrown A. In general the concept was to have a norbornyl skeleton appended with functional groups suitable for ACE coupling to tricrown A, anhydride group for crown ether attachment and a third functional element to allow for the inclusion of polar anchoring groups. Thus three potential blocks were identified that differed in regards to the third functional element; **213** methyl, **214** bromo and **215** oxanorbornyl. The methyl groups could be functionalised or exchanged with hydrophilic groups through a possible radical bromination. The bromine groups could be displaced in a nucleophilic substitution and the oxanorbornyl by reaction of olefinic groups. Thus these three compounds were investigated for synthesis for block extension.

For example the synthesis of block **213** (Figure 4.9.1) allows for the attachment of the amino crown ether through the anhydride. Additional synthetic work as mentioned previously allows access to the epoxide which gives rise to the fused pentacrown system through the ACE reaction with alkenes. This was also the approach used for both **214** and **215** polycyclic norbornyl blocks.

The polycyclic norbornyl block **213** and **214** have been previously synthesised in low to moderate yields.^[20,21] However, repeating these synthetic procedures gave compounds that were difficult to purify, with numerous impurities and by-products present. After repeated and frustrating attempts at purification, attention was turned to block **215**. The compound **215** (Scheme 4.9.1) is a polycyclic norbornyl system with both norbornyl and oxanorbornyl fused rings. This block was investigated due to the potential isolation of an asymmetrically functionalised system, allowing for functionality to be installed on one side of the system. For example, one side may undergo the Mitsunobu reaction more quickly than the other. Therefore synthesis of block **215** (Scheme 4.9.1) was initiated.



Scheme 4.9.1 Attempted synthesis of end block **223** for potential channel extension.

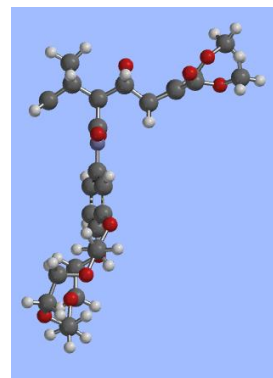


Figure 4.9.2 Molecular model of the proposed non-symmetrical system **223**

Block **220** was synthesised through already established methods^[22,23] with initial formation of the *bis*-acid **220** followed by ring closure with DCC^[24] to the anhydride **221** (80%). Once purified, anhydride **221** was stirred in furan^[22] at room temperature. The unreacted furan was removed affording block **215** in moderate yield (87%). Block **215** was characterised *via* ¹H NMR with a new alkene resonance being observed at 5.11-5.10 ppm and splitting of the bridge proton signals on the norbornyl block into two doublets observed at 3.07-3.05 and 1.82-1.80 ppm. The HRMS was consistent with the structure; calculated for C₁₃H₁₀O₄, 230.0574, found 230.0574 [M]⁺.

Block **215** was further functionalised through the Mitsunobu reaction with DMAD to produce one of potentially three products; reaction at both alkenes, reaction at norbornyl alkene or reaction at oxanorbornene. However in this instance only one product was isolated and purified to afford **222** in moderate yield (45% yield). The

product was characterised *via* ^1H NMR with the disappearance of the alkene resonance observed at 5.11-5.10 ppm from the oxanorbornyl alkene and new ester resonances at 3.77-3.76 ppm.

This system was unique in that the cyclobutene 1,2-diester adds to the oxanorbornyl side specifically. This was important due to the potential retro Diels Alder reactions which could occur if **215** was heated at high temperature without the cyclobutene ring attached (the product of a Mitsudo reaction) which has been shown for the *bis-oxa* system^[2] referred to in Chapter 2, Section 2.4. These systems are known to lose furan upon heating at elevated temperatures.^[2]

NMR spectroscopic analysis *via* both 1D and 2D experiments suggested the product of the Mitsudo reaction correspond to **222**. Further evidence that the structure isolated was **222** came from X-ray crystallography (see Figure 4.9.3). The X-ray crystal structure was obtained by Rebecca Norman (Flinders University) using Adelaide University's X-ray Crystallography equipment. It was observed that the cyclobutene 1,2-diester did in fact add to the oxanorbornene side of the asymmetric molecule.

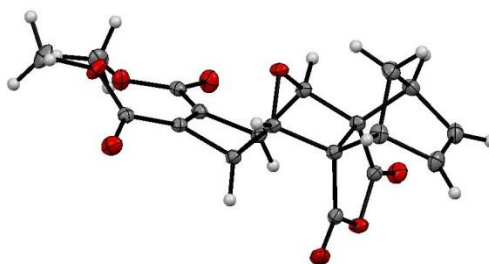
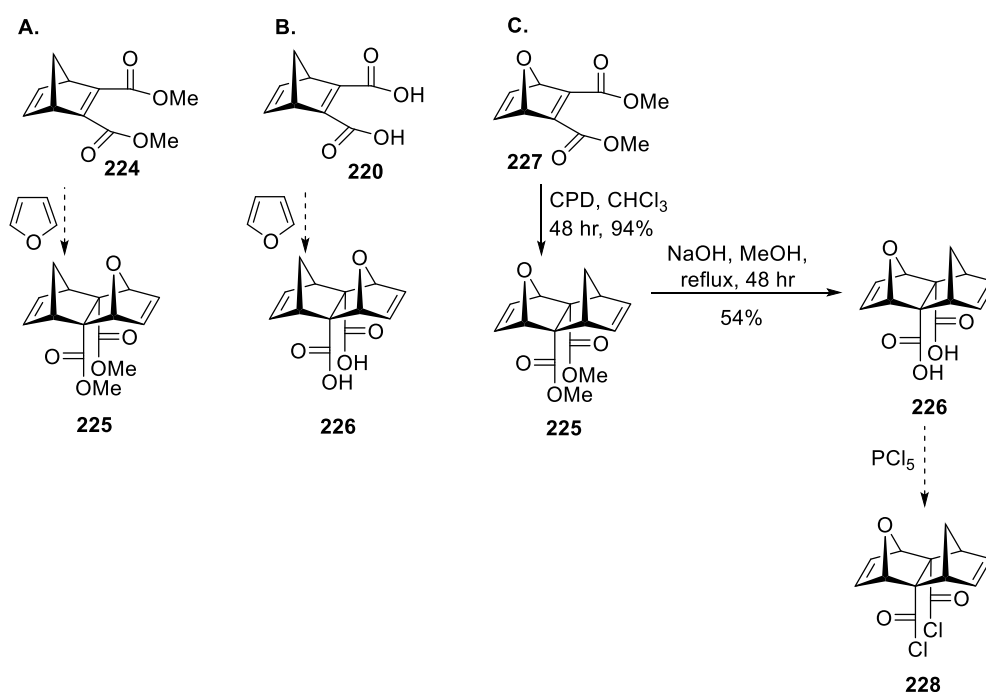


Figure 4.9.3 X-ray crystal structure of synthesised polycyclic block **222**.

This allowed for **222** to participate in the following reactions at elevated temperatures with aromatic amines without concern for a retro Diels Alder reaction occurring. Unfortunately, however, additional reactions towards **223** (Scheme 4.9.1) involving the addition of the aromatic crown amine were unsuccessful, which suggests that the reactivity of the anhydride was quite low. There was also additional bulk added to the system with the cyclobutene ring resulting in *endo* protons pointing downwards. This reaction was attempted at various temperatures in varying solvents however no reaction was observed to take place. Thus, it would appear that *endo* protons on one side only are sufficient to limit anhydride reactivity with aromatic amines. Other reactions which

were investigated were that of **215** with the aromatic crown amine (**200a**), although the conditions need to be monitored carefully so that the retro Diels Alder reaction and loss of furan did not occur. It was found that this reaction mixture could not be heated at temperatures above 70°C. Again no product was evident under these conditions.

The aforementioned acid chlorides discussed in Chapter 2 were of significance in this system due to the non-reactivity of the anhydride in the previous asymmetric block with aromatic amines. A number of different pathways were explored to synthesise the *bis*-acid **226** (Scheme 4.9.2), which could then be treated with phosphorus pentachloride or thionyl chloride to obtain the *bis*-acyl chloride **228**.



Scheme 4.9.2 Attempted synthesis of required blocks for acid chloride synthesis **228**.

Pathway **A** was first investigated with the synthesis of **224** from a reaction between DMAD and CPD in DCM for 24 hr in 73% yield. The product was consistent with ¹H NMR where an alkene resonance was observed at 6.91 ppm and an ester resonance at 3.77 ppm. Furthermore HRMS was consistent with the structure calculated for C₁₁H₁₂O₄Na 231.0633, found [M+Na]⁺, 231.0636.

Block **224** was further treated with furan at room temperature for 24 to 48 hr, however the furan did not show any reactivity towards the norbornyl system and therefore an alternative pathway was examined.

Pathway **B** was subsequently investigated with the potential to eliminate steps within the synthesis with the already established *bis*-acid from **220** which had previously been synthesised. However this pathway also shows that when **220** was treated with furan at RT, no formation of a fused norbornyl, oxanorbornyl system **226** was observed under these conditions.

Lastly pathway **C** was examined which is essentially a reversal of pathway **A** with oxanorbornyl ring synthesised first. Initially the synthesis of oxanorbornyl block **227** was investigated through a sealed tube reaction, with DMAD and furan heated at 80°C for 24 hr under an argon atmosphere to afford **227** in 70% yield. The product was characterised *via* NMR spectroscopy with new alkene resonance at 7.22 ppm and ester resonance at 3.82 ppm. Furthermore HRMS was consistent with the structure calculated for C₁₀H₁₀O₅Na 233.0426, found [M+Na]⁺, 233.0429.

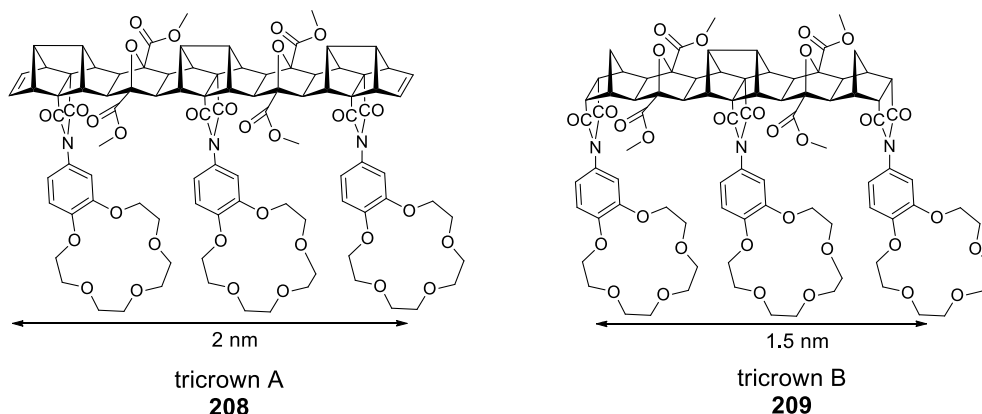
Block **227** was further treated with CPD in chloroform (stirred at RT) under argon for 48 hr whereupon the product **225** was isolated in 94% yield. The product was characterised *via* ¹H NMR spectroscopy with two alkene resonances at 6.60 ppm and 6.17 ppm. A linear isomer is evident with the CH₂ bridge protons shifted significantly apart (doublets observed at 2.46 and 1.62 ppm) similar to that in the synthesis of **222**. These shifts give insight into whether the linear product was formed over a bent system. Furthermore HRMS was consistent with the structure calculated for C₁₅H₁₆O₅Na 299.0895, found [M+Na]⁺, 299.0904.

Block **225** was treated with sodium hydroxide solution (20%) in MeOH under reflux for 48 hr to afford, following acidic work up, the *bis*-acid **226** in 54% yield. The product was characterised *via* ¹H NMR spectroscopy with the disappearance of the ester resonance at 3.67 ppm. Furthermore HRMS was consistent with the structure calculated for C₁₃H₁₂O₅ 247.0606, found [M-H]⁻, 247.0605.

Following the successful isolation of *bis*-acid **226** the *bis*-acylchloride synthesis was attempted with phosphorus pentachloride and thionyl chloride. However all attempts at synthesising and isolating the *bis*-acylchloride **228** were unsuccessful. The *bis*-acyl chloride block **228** has not been previously reported, which may suggest its instability. The stability of this system may be similar to that of the Hedaya diene system discussed in Chapter Two. Thus the generation of the fused block-crown system **223** was unsuccessful with several synthetic strategies all proving to be problematic.

4.9.1 Conclusions

This chapter has explored a new direction in the synthesis of new polycyclic systems with appended crown ethers. The area of focus within this chapter investigated the use of aromatic amines with anhydride systems to afford new polycyclic crown ether frameworks as depicted in Scheme 4.9.1.1.



Scheme 4.9.1.1 Synthesised fused polycyclic crown ether systems **208** and **209** prepared for ion channel analysis.

These new polycyclic frameworks were then used to further extend the system to incorporate three crown ethers side by side through the synthetic procedure referred to as ACE coupling to afford tricrown systems A and B.

Due to the success of both tricrown A and B, new tricrown blocks were explored with variations in crown ether sizing, *i.e.* 18-crown-6 and 21-crown-7. Although initial NMR results showed successful synthesis, difficulties in purification were observed and no compounds isolated.

It was further explored within this study to extend the polycyclic framework beyond three crowns coupled together to a pentacrown system. Again NMR appeared to indicate successful synthesis yet problems were encountered in purification. In addition to the pentacrown, various pathways for variations in end group functionality were explored for ease of incorporation of the end molecule into the lipid bilayer. However these again were fraught with synthetic problems.

Analysis of the successfully synthesised compounds tricrowns A and B will be explored in the following chapter, through various analytical techniques, for their ability to act as ion channels.

REFERENCES

- [1] J. Clayden, N. Greeves, S. Warren, P. Wothers, *Organic Chemistry*, Oxford University Press, **2001**.
- [2] S. P. Gaynor, M. J. Gunter, M. R. Johnston, R. N. Warrener, *Org. Bio. Mol. Chem.* **2006**, *4*, 2253–2266.
- [3] M. Golić, M. R. Johnston, D. Margetić, A. C. Schultz, R. N. Warrener, *Aust. J. Chem.* **2006**, *59*, 899–914.
- [4] I. Fleming, *Molecular Orbitals and Organic Chemical Reactions*, John Wiley And Sons Ltd, West Sussex, **2009**.
- [5] A. Czech, B. P. Czech, R. A. Bartsch, *J. Heterocycl. Chem.* **1988**, *25*, 1841–1843.
- [6] G. M. Dykes, D. K. Smith, *Tetrahedron* **2003**, *59*, 3999–4009.
- [7] M. Azechi, K. Yamabuki, K. Onimura, T. Oishi, *Polym. J.* **2010**, *42*, 632–639.
- [8] J. S. Yang, C. Y. Hwang, M. Y. Chen, *Tetrahedron Lett.* **2007**, *48*, 3097–3102.
- [9] X. Jiang, X. Yang, C. Zhao, L. Sun, *J. Phys. Org. Chem.* **2009**, *22*, 1–8.
- [10] C. Zhang, S. Li, J. Zhang, K. Zhu, N. Li, F. Huang, *Org. Lett.* **2007**, *9*, 5553–5556.
- [11] T. Bogaschenko, S. Basok, C. Kulygina, A. Lyapunov, N. Lukyanenko, *Synthesis (Stuttg.)* **2002**, 2266.
- [12] C.-G. Hwang, K. Sang-Ho, O. J. Hoon, M.-R. Kim, S.-H. Choi, *J. Ind. Eng. Chem.* **2008**, *14*, 864–868.
- [13] R. Cacciapaglia, S. D. Stefano, L. Mandolini, *J. Am. Chem. Soc.* **2003**, *125*, 2224–2227.
- [14] S. Cheema, S. S. Langford, S. Cheung, N. M. Beart, P. J. Macfarlane, K. *tGents and Methods for the Treatment of Disorders Associated with Oxidative Stress*, **2003**, WO03/099762.
- [15] E. Zhang, Y. Liu, S. Dong, F. Su, Y. Jiang, *Huaxue Shiji* **1985**, *7*.
- [16] J. C. Lee, *Synthesis of Novel Crown Ether Compounds and Ionomer Modification of Nafion*, **1992**.
- [17] M. A. Meador, D. S. Tyson, A. Carbaugh, *PSME Prepr.* **2008**, *98*, 130–131.
- [18] C. Kleeberg, *Z. Anorg. Allg. Chem.* **2011**, *637*, 1790–1794.
- [19] S. A. DiBiase, G. W. Gokel, *J. Org. Chem.* **1978**, *43*, 447–452.

- [20] S. Tiede, A. Berger, D. Schlesiger, D. Rost, A. Lühl, S. Blechert, *Angew. Chem. Int. Ed. Engl.* **2010**, *49*, 3972–3975.
- [21] R. M. Carman, B. R. P. C. Derbyshire, A. K. A. Hansford, R. Kadirvelraj, W. T. Robinson, *Aust. J. Chem.* **2001**, *54*, 117–126.
- [22] P. D. Bartlett, G. L. Combs, A. X. T. Le, W. H. Watson, J. Galloy, M. Kimura, *J. Am. Chem. Soc.* **1982**, *104*, 3131–3138.
- [23] J. Hendrickson, V. Singh, *Tetrahedron Lett.* **1983**, *24*, 431–434.
- [24] K. Maruyama, T. Hitoshi, S. Kawabata, *J. Org. Chem.* **1985**, *50*, 4742–4749.

CHAPTER 5

MONOMER AND TRICROWN TRANSPORT ANALYSIS

5.1 Introduction

In this chapter discussions will be centred on using the various monomer crown ether blocks and tricrown molecules synthesised in chapter 4 as artificial ion transport systems. Ion channels can be analysed via a variety of different analytical techniques such as, black lipid membrane (BLM),^[1] fluorescence spectroscopy with labelled unilamellar vesicles,^[2,3] circular dichroism,^[4] electrochemical impedance spectroscopy (EIS)^[5-7] and sodium and/or proton NMR spectroscopy.^[8,9]

Within this study EIS, ¹H NMR spectroscopy, BLM and calcein release fluorescent spectroscopy was used to study alkali metal complexation, ion transport and membrane disruption for the crown ether systems outlined in Figure 5.1.1.

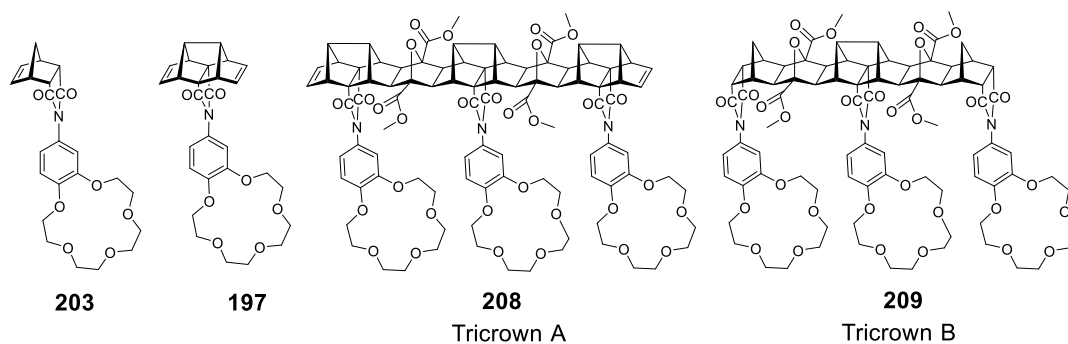


Figure 5.1.1 Polycyclic crown ether systems synthesised for analysis of transport properties.

5.2 Electrochemical Impedance spectroscopy of Polycyclic Crown Ether Compounds

Electrochemical impedance spectroscopy (EIS) is an analytical technique used to investigate electrochemical reactions, relating to the transport properties of materials as well as porous electrodes and surfaces.^[10] The foundations for EIS were established between 1880 to 1900 by the mathematician Oliver Heaviside.^[10,11] Heaviside was instrumental in the development of telegraphy and electrical circuit theory. He defined impedance spectroscopy and the terms, 'impedance', 'admittance', 'reactance' and operational calculus. These terms and principles were further developed over decades to form the basis of EIS today.^[12]

Impedance is a measure of an electrical circuit containing the linear elements, resistance (R), capacitance (C) and inductance (L). Overall the impedance is a measure of a circuit's ability to resist the flow of electrons and can be calculated using equations similar to the one outlined below.^[13,14]

$$Z = \frac{E_t}{I_t} + \frac{E_0 \sin(\omega t)}{I_0 \sin(\omega t + \phi)} = Z_0 \frac{\sin(\omega t)}{\sin(\omega t + \phi)} \quad (5.1)$$

The impedance of a system is measured by applying an alternating current (AC) potential to an electrochemical cell. An AC signal is a sinusoidal response. A pseudo-linear response is generated from a small excitation signal, a sinusoidal potential. This allows for a shift in phase at the same frequency, a sinusoid (Figure 5.2.1).^[14]

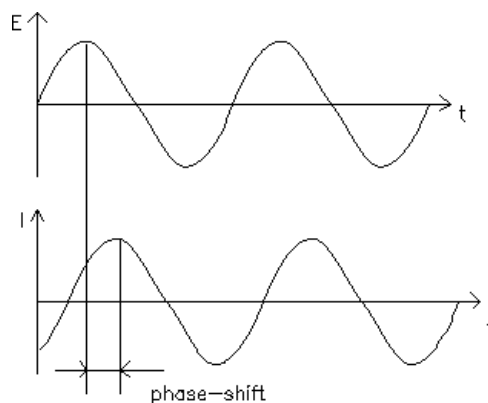


Figure 5.2.1 Linear sinusoidal current response.^[14]

The impedance of a system is measured over a range of frequencies and is commonly graphically expressed with either Bode (used in this thesis) and/or Nyquist plots (Figure 5.2.2).^[13,14] The Bode plot expresses the impedance (electrical resistance) and phase angle over a range of frequencies. In comparison, the Nyquist plot is a frequency response function of a linear system and relays information relating to the stability of a system.

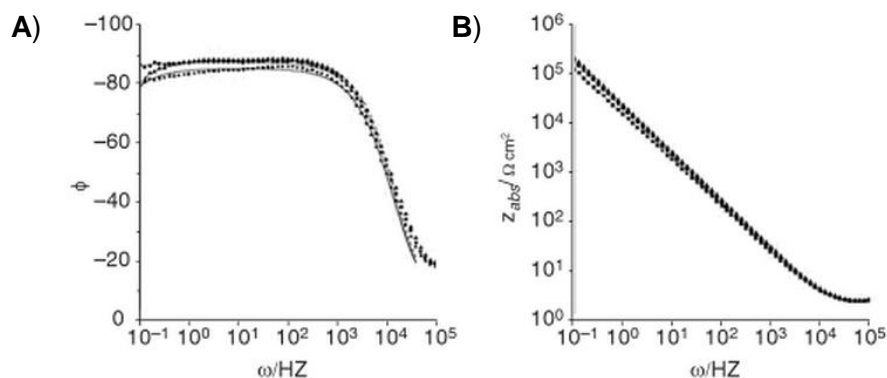


Figure 5.2.2 A) Example of a Nyquist plot B) Example of Bode plot for the impedance behaviour at a double layer oxidised gold electrode.^[15]

The EIS experiments which will be discussed in detail were undertaken at Flinders University by Jakob Andersson.

In this study the impedance of a system using tethered bilayer membranes^[16] (tBLMs) as shown in Figure 5.2.3 was measured and visualised using Bode plots. Tethered bilayer membranes have phospholipids attached directly to an electrode surface, and these are combined with unattached phospholipids to create a bilayer membrane (see below). Then the various crown ether molecules were incorporated into the membrane and impedance measured again to determine transport properties of various alkali metals. This transport is thus a reflection of the transportation properties of the embedded crown molecules in the tBLM.

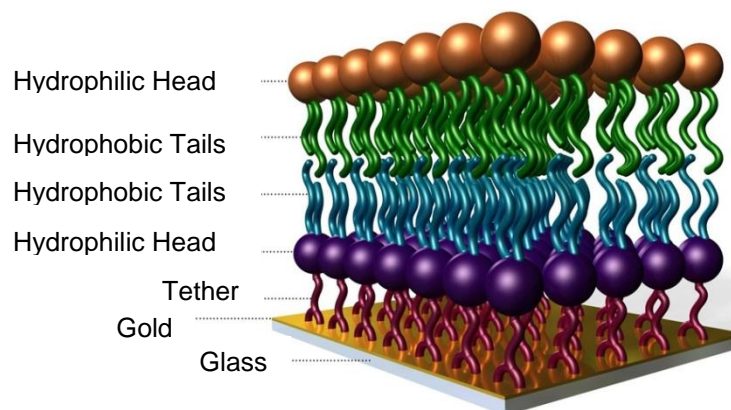


Figure 5.2.3 Tethered bilayer membrane used in the EIS studies of the synthesised crown ether systems.

The bilayers used in this study were formed from their monomers (phospholipids) and analysed to ensure bilayer formation in each separate experiment then fit to an equivalent circuit (Figure 5.2.3). The monolayers were prepared from DPTL

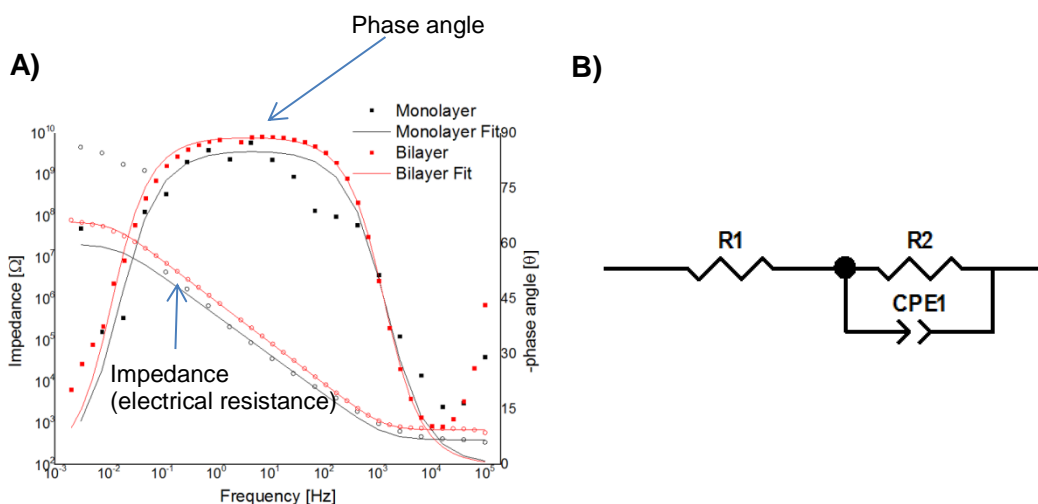
(2,3-di-*O*-phytanyl-*sn*-glycerol-1-tetraethyleneglycol-D,L- α -lipoic acid ester) followed by the addition of vesicles in an electrolyte solution, most commonly NaCl. Vesicles then unravel to form a bilayer with a tethered monolayer on the electrode surface. The capacitance decreases and the resistance increases as the membrane is increasing in thickness from monolayer to bilayer. The bilayer is fitted to an equivalent electrical circuit using resistive elements (R_1 , R_2) and capacitive elements (CPE1-T, CPE1-P). Typical data is shown in Table 5.2.1 which shows the resistance of monolayer R_2 to be $2.11 \times 10^7 \text{ M}\Omega$ and once the bilayer has formed this increases to $7.20 \times 10^7 \text{ M}\Omega$. The capacitance (CPE1-T) decreases from the monolayer at $4.35 \times 10^{-7} \text{ F}$ to $1.8 \times 10^{-7} \text{ F}$ for the bilayer. Shown in Figure 5.2.4 are the Bode plots showing impedance (LH axis) and phase angle (RH axis), both of which change with frequency (x-axis) observed for the monolayer and bilayer formation. This data was then fitted to an equivalent circuit as shown in Figure 5.2.4B consisting of two resistive elements and one capacitive element.

Note that for each experiment a new bilayer is formed and therefore is unique to each individual experiment. Therefore characterisation of this new bilayer is required each time one is produced.

Once the bilayers have formed, experiments with the artificial crown ethers can take place followed by ion transport measurements. Crown ethers (in CH_3CN) were introduced into the aqueous solution above the bilayer and allowed to stand for 12-24 hrs to allow the crown ether to become embedded into the membrane. Effective ion transport was observed by a decrease in the resistive element of the bilayer as ions are transported more easily.

Table 5.2.1 Resistance and capacitance data for the formation of both monolayer and bilayers in the study of artificial ion channels.

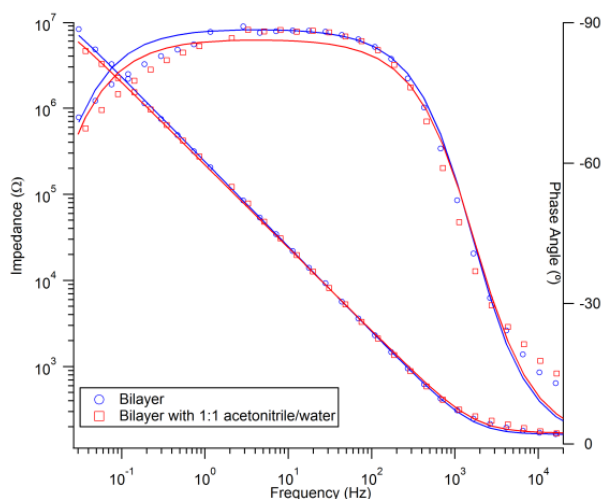
	Monolayer	Bilayer
R1 (Ω)	399.7	700.7
R2 (MΩ)	2.11×10^7	7.20×10^7
CPE1-T (F)	4.35×10^{-7}	1.86×10^{-7}
CPE1-P (F)	0.95	0.99

**Figure 5.2.4** **A)** Bode plot of impedance vs frequency vs phase angle for the formation of both monolayer and bilayer. **B)** Resultant equivalent circuit from fitting of EIS data. (Solid lines refer to model fitted to the data).

Before crown ethers systems were introduced into the bilayers a solvent study using acetonitrile was investigated. The crown ether materials are generally soluble in acetonitrile but this solvent is not commonly used to introduce compounds to the tBLM. This study gave insight into whether the solvent had any impact on the bilayer and its stability. As depicted in Table 5.2.2 and from the plot in Figure 5.2.5 there is little effect of the solvent acetonitrile on the bilayer. Therefore introduction of the synthesised artificial ion channels solvated in acetonitrile should not disrupt the bilayer. Note that when a computer model is fitted to the collected data an error in that data is determined. The size of those errors is dependent on the computer model fit to the experimental data and can therefore range quite significantly.

Table 5.2.2 Electrical data on the effect of acetonitrile on the bilayer

	Impedance (M Ω)	Error %	Capacitance (F)	Error %
Bilayer	2.03×10^7	22	6.82×10^{-7}	3
Bilayer/acetonitrile	1.70×10^7	13	7.77×10^{-7}	3

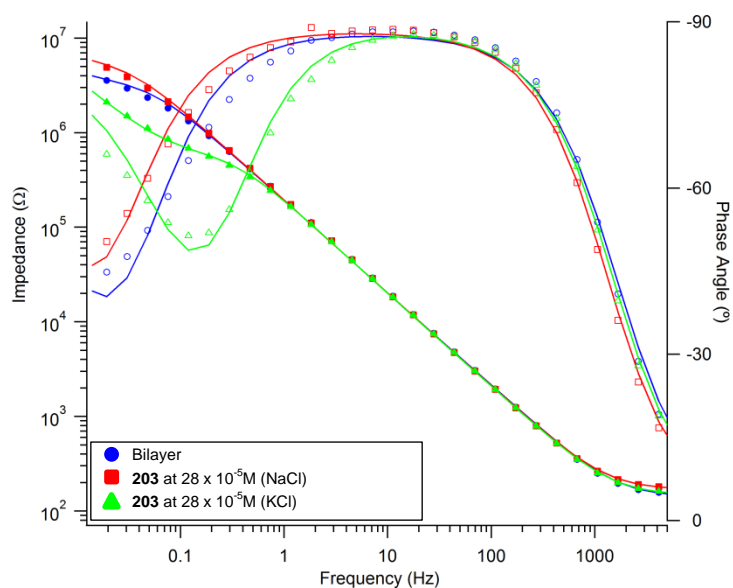
**Figure 5.2.5** Bode plot showing that acetonitrile has little effect on the bilayer.

Following these results initial crown ether testing was undertaken. Both monomer systems **203** and **197** were investigated initially before moving to the tricrown systems.

The *endo* monomer unit **203** was tested via EIS with both sodium (NaCl) and potassium (KCl) electrolytes at a concentration of 100 mM. Initially the *endo* monomer was analysed at higher concentrations before investigations at lower concentrations were undertaken. In all experiments, unless stated otherwise, 20 μ L of **203** stock solution (14 mM) was added to the tethered bilayer at a concentration of 28×10^{-5} M. It is not known whether or not all of the crown ether was embedded within the bilayer. However for comparative purposes the initial concentrations of the crown ethers in solution will be discussed. The experiment concluded that at this concentration (28×10^{-5} M) the *endo* monomer can facilitate the transport of ions across the membrane shown from the data (Table 5.2.3) and Bode plot (Figure 5.2.6). The plot indicates a decrease in impedance for the KCl electrolyte indicating transport of potassium ions.

Table 5.2.3 Electrical data of the *endo* monomer **203** with NaCl and KCl.

	Impedance (M Ω)	Error (%)	Capacitance (μ F)	Error (%)
Bilayer	3.0	8.6	1	3.5
203 at 28×10^{-5} M in NaCl	4.5	10	1.1	5.4
203 at 28×10^{-5} M in KCl	0.4	4.7	1.1	2.4

**Figure 5.2.6** Bode plot of *endo* monomer **203** in EIS with NaCl and KCl at a concentration of 28×10^{-5} M.

However when 10 μ L of a less concentrated stock solution of *endo* monomer (3.5 mM) was used with an overall concentration of 3.49×10^{-5} M there was minimal to no transport observed for both KCl and NaCl electrolytes. Increasing the concentration of monomer **203** (7×10^{-5} M and 14×10^{-5} M) showed very small changes in the resistive element. This is easily identified for KCl in the plot, Figure 5.2.7, where there is very little change in impedance suggesting minimal transport. The NaCl electrolyte was also studied at these concentrations indicating no transport but has been removed from the plot for ease of view of the KCl electrolyte.

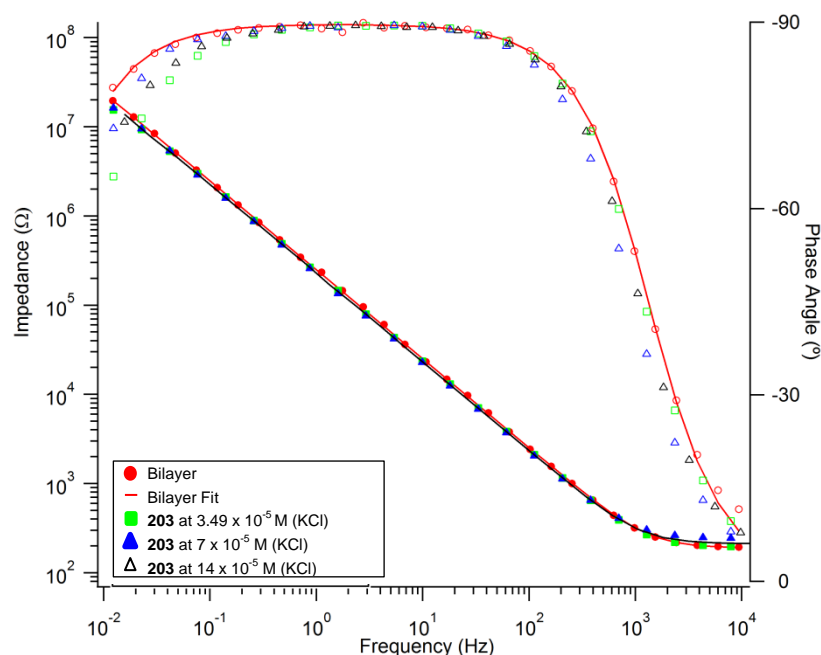


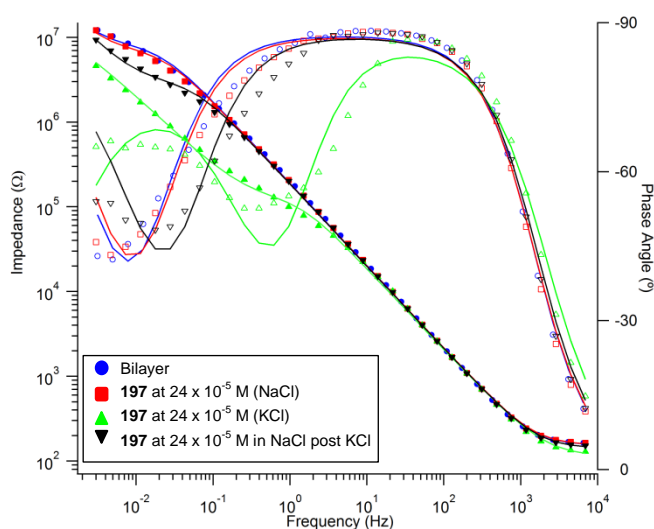
Figure 5.2.7 Bode plot of the *endo* crown ether with concentrations between $3.5 - 14 \times 10^{-5}$ M with the KCl electrolyte.

From these results it can be concluded that the **203** shows substantial transport at a concentration of 28×10^{-5} M. However at concentrations lower than 28×10^{-5} M the *endo* monomer **203** facilitates minimal to no transport. Therefore it is possible that when higher concentrations (28×10^{-5} M and above) are used there is potential aggregation of the monomers occurring within the bilayer or the monomer has increased potential to carry a larger amount of potassium ions across the bilayer. These results are also predicted for the Hedaya monomer **197** at similar concentrations which have also been examined via EIS.

Under similar conditions to **203**, the Hedaya monomer crown ether system **197** was analysed *via* EIS with both sodium and potassium electrolytes. Initially the Hedaya monomer was analysed at higher concentrations before investigations at lower concentrations. In all experiments unless stated otherwise $20 \mu\text{L}$ of **197** stock solution (12.2 mM) was added to the tethered bilayer at a concentration of 24×10^{-5} M. The results of the experiment indicated that at this concentration (24×10^{-5} M) the Hedaya monomer can facilitate the transport of ions across the membrane shown in the electrical data (Table 5.2.4) and the Bode plot (Figure 5.2.8). The plot indicated a decrease in impedance for the KCl electrolyte indicating transport of potassium ions.

Table 5.2.4 Electrical data for **197** with both NaCl and KCl electrolytes at a concentration of 24×10^{-5} M.

	Impedance (MΩ)	Error (%)	Capacitance (μF)	Error (%)
Bilayer	6.9	15	1.0	10
197 at 24×10^{-5} M (NaCl)	6	15	1.1	8
197 at 24×10^{-5} M (KCl)	0.1	6	1.2	5
197 at 24×10^{-5} M (NaCl post KCl)	2.4	11	1.1	4

**Figure 5.2.8** Bode plot of **197** with NaCl and KCl at concentration of 24×10^{-5} M.

Note the NaCl impedance after the introduction of KCl is reduced this is due to no Milli-Q water rinse between electrolyte solutions. When a Milli-Q water rinse is used the impedance recovers - this has been shown to be the case in further EIS experiments.

An additional experiment was undertaken in this case where the NaCl electrolyte was added to the bilayer post KCl electrolyte. As shown in Table 5.2.4 the impedance and capacitance have not fully recovered to the aforementioned NaCl values. This indicates that there is some residual KCl, due to the lack of Milli-Q water washing between the change in electrolyte solutions. When a Milli-Q water rinse is used the impedance recovers. This has been shown to be the case in EIS experiments (shown in Figure 5.2.14).

However when 10 μL of a less concentrated stock solution of **197** (3.0 mM) was used with an overall concentration of 3.0×10^{-5} M there was minimal to no transport observed for both KCl and NaCl electrolytes (Figure 5.2.9). Increasing the concentration of **197** (6.1×10^{-5} M and 12.2×10^{-5} M) showed very small changes in the resistive element. This is easily identified for the KCl in the plot, Figure 5.2.9, where there is very little change in impedance suggesting minimal transport. The NaCl electrolyte was also studied at these concentrations indicating no transport but has been removed from the plot for ease of view of the KCl electrolyte.

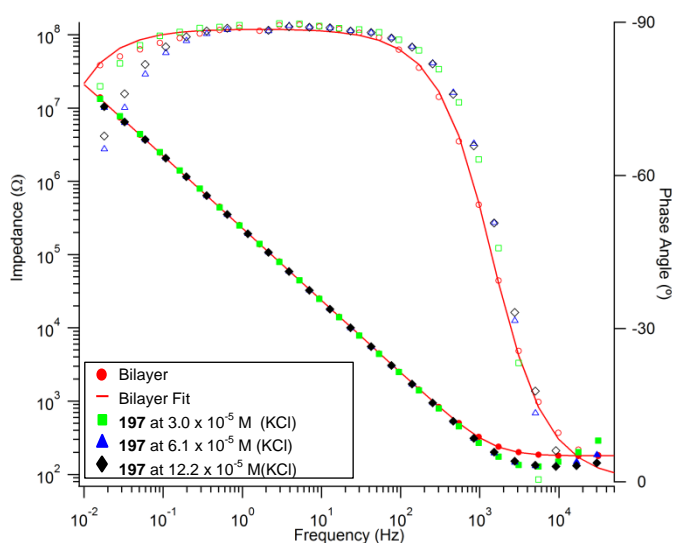


Figure 5.2.9 Bode plot of the lower concentrations of **197** with the KCl electrolyte.

However the initial bilayer measurements and NaCl electrolyte measurements were compared, plotted (Figure 5.2.10) to give an indication that there was no sodium ion transport occurring at these concentration levels of monomer.

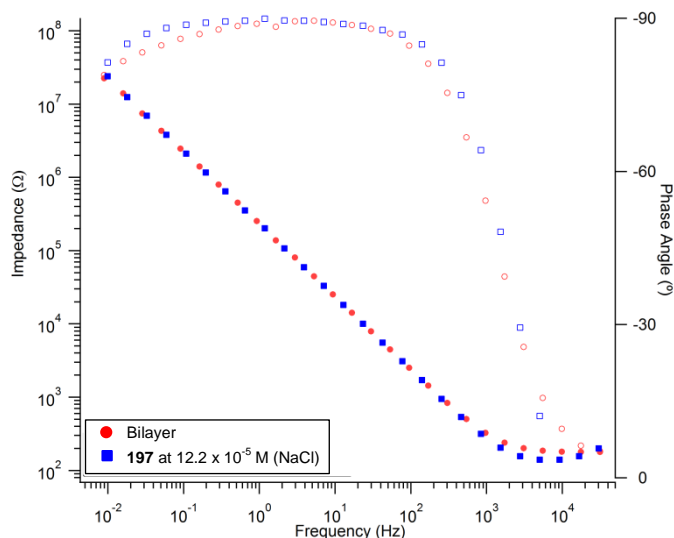


Figure 5.2.10 Bode plot of the NaCl electrolyte with **197** at a concentration of 12.2×10^{-5} M.

Therefore it can be concluded from these results that both the *endo* and Hedaya monomers at concentrations at or above 24×10^{-5} M can substantially transport potassium ions. However at concentrations lower than 24×10^{-5} M there is very minimal to no transport observed for either potassium or sodium ions. This suggests that at higher concentrations either monomer can facilitate substantial transport possibly via aggregation of monomers or increased potential to carry larger quantities of potassium ions across the bilayer.

Following on from the in-depth investigation of the transport properties of monomer systems **203** and **197**, attention was now focussed on the tricrown systems. Firstly tricrown A **208** was investigated followed closely by tricrown B **209**. In all experiments unless stated otherwise 20 μ L of **208** stock solution (3.35 mM) was added to the tethered bilayer at a concentration of 6.7×10^{-5} M.

The initial studies of tricrown A via EIS were undertaken to determine whether it could potentially transport sodium and or potassium ions, which was then followed by a concentration dependency evaluation and an examination of cycling various electrolytes past the bilayer. Initial studies suggested there to be minimal to no transport of sodium as depicted from the data in Table 5.2.5 and the plot in Figure 5.2.11.

Table 5.2.5 Electrical data for tricrown A with NaCl and KCl electrolytes.

	Acetonitrile	208 with NaCl	208 with KCl
R1 (Ω)	714.1	650.5	720
R2 ($M\Omega$)	7.38×10^7	2.11×10^7	1.64×10^3
CPE1-T (F)	1.81×10^{-7}	1.90×10^{-7}	6.55×10^{-7}
CPE1-P (μF)	1	1	1
R3 ($M\Omega$)	-	-	3.16×10^6
CPE2-T (F)	-	-	4.53×10^{-7}
CPE2-P (F)	-	-	9.60×10^{-1}

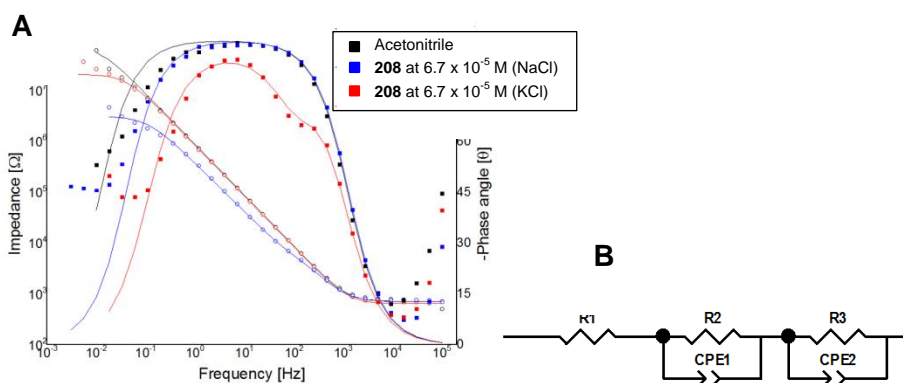


Figure 5.2.11 A) Bode plot of the tricrown A with NaCl and KCl electrolytes, **B)** The equivalent circuit the data for this experiment is fit to when modelled now including the spaced region R3.

However when the electrolyte solution was changed from NaCl to KCl the initial circuit used for fitting the data had to be changed because ions were reaching the spacer region (below the bilayer) and must be treated like another parallel circuit (Figure 5.2.11B). The KCl electrolyte had a significant impact on the impedance with a strong decrease in the resistive element R2 from 7.38×10^7 M Ω to 1.64×10^3 M Ω in the KCl solution (Table 5.2.5). The resistive element R3 models the spacer and adsorbed ions and only appears once the KCl electrolyte is used.

Using tricrown A, already embedded in the bilayer, the electrolyte solution was changed from KCl to NaCl and furthermore to tetramethylammonium chloride (TMAC). Upon changing the KCl to NaCl electrolyte, ions were still permitted to traverse the membrane. This was thought to be due to residual potassium ions left behind in the system. Further testing has identified this to be the case when the KCl solution is removed with washings of Milli-Q water and NaCl electrolyte

added, the resistive values were typical of NaCl measurements. Furthermore the addition of TMAC did not permit the ions to traverse the membrane with the impedance recovering to that similar to the bilayer. This is due to the fact that TMAC is a substantially larger ion and does not fit within the crown ethers (Refer to Appendix 1 for the Bode plot for this data).

Further studies have identified that initial formation and addition of the tricrown A (6.7×10^{-5} M) in the KCl electrolyte solution has an immediate impact on the impedance with a significant decrease evident (Table 5.2.6, Figure 5.2.12).

Note there is a large error in the data fitting for the impedance of **208** in the KCl electrolyte (Table 5.2.6), however there is still a significant difference between the bilayer and KCl electrolyte impedance identifying potassium ion transport.

Table 5.2.6 Electrical data for the introduction of tricrown A into a KCl electrolyte solution.

	Monolayer	Bilayer	208 at 6.7×10^{-5} M NaCl	208 at 6.7×10^{-5} M KCl
Impedance (MΩ)	1.50	38.48	53.86	1.20
Error %	53	7	4	46

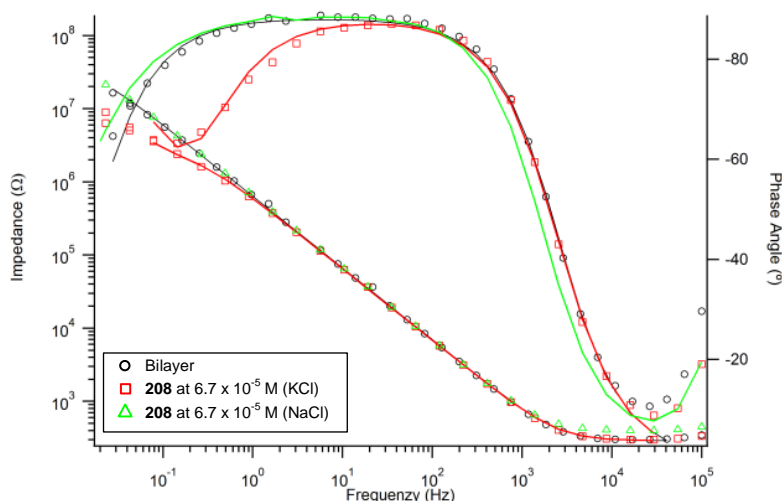


Figure 5.2.12 Bode plot of the tricrown A introduced into the bilayer in a KCl electrolyte solution followed by the NaCl electrolyte.

Investigations were also undertaken to examine the switchability of the ion transport. To examine this, the electrolyte solutions above the bilayer were changed between NaCl and KCl several times. After three repetitions of NaCl

and KCl electrolyte solutions the results still indicated potassium ion transport with little to no effect for sodium ion transport.

The effect of changes in crown ether concentrations was also examined. Preliminary results for changes in concentration of the tricrown A were observed with NaCl, KCl and TMAC electrolytes. The results for the KCl electrolyte are depicted in the plot, Figure 5.2.13.

The NaCl and TMAC electrolytes have been removed from the data for ease of viewing since there was little to no activity with these electrolytes. However it should be noted that the NaCl electrolyte impedance showed lower impedance at tricrown concentration (13.4×10^{-5} M) than other concentrations. To ascertain if this was from defects in the bilayer or from impurities, TMAC electrolyte was introduced to try and recover impedance. The impedance did recover with the TMAC electrolyte and this therefore suggested possible impurities in the NaCl electrolyte present rather than a bilayer defect. The trend for all other NaCl experiments (3.35×10^{-5} M, and 6.7×10^{-5} M) indicated no transport observed with the impedance recorded at similar levels to the bilayer.

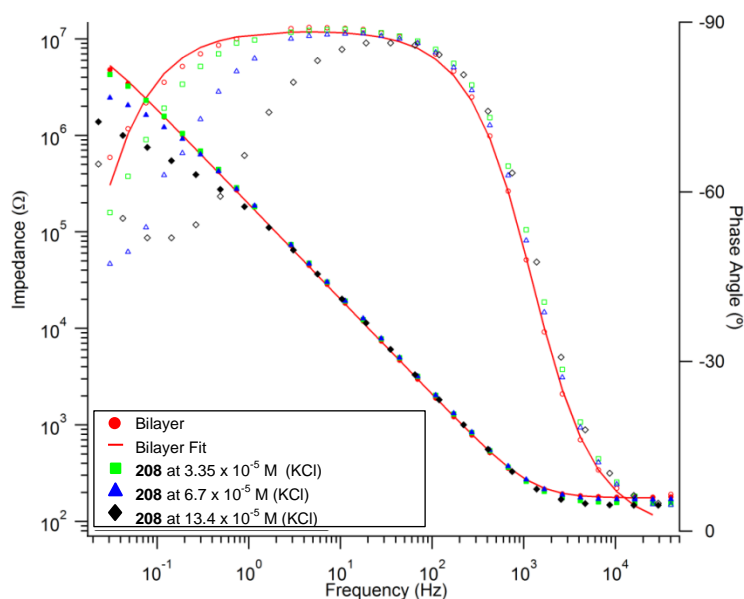


Figure 5.2.13 Bode plot of the concentration gradient of tricrown A with KCl.

As depicted from the plot in Figure 5.2.13, at 3.35×10^{-5} M of tricrown A there is very minimal to no transport. When the amount of tricrown A is doubled (6.7×10^{-5} M) there is a small amount of transport observed with a visible decrease in the impedance. However when 13.4×10^{-5} M of the tricrown A is monitored there is a significant decrease in impedance, suggesting substantial transport of potassium

across the bilayer. These results are summarised in Table 5.2.7, which suggest that reasonable transport of potassium ions for tricrown A are only observed at and above a crown concentration of 6.7×10^{-5} M. This proposes possible aggregation of more than one tricrown molecule in the bilayer to transport potassium ions via a carrier or channel mechanism.

Table 5.2.7 Summary of the KCl electrolyte impedance on tricrown **208** at varying concentrations.

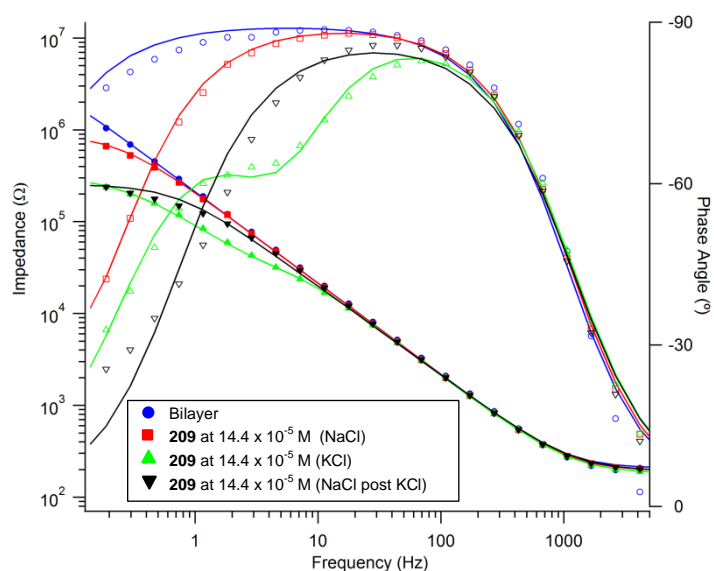
Concentration of 208 (M)	KCl electrolyte (100mM) Impedance (M Ω)
Bilayer	11.4
3.35×10^{-5}	11.5
6.7×10^{-5}	2.7
13.4×10^{-5}	0.5

Following on from the successful results for the transport of potassium for tricrown A, tricrown B **209** was investigated for similar effects. Firstly 10 μ L of **209** 3.6 mM stock solution with an overall concentration of 3.6×10^{-5} M was examined and found to show no reduction in impedance. Even after 7.2×10^{-5} M of **209** solution was added only a small reduction in impedance was observed for KCl (2.5 M Ω) as shown in Table 5.2.8. However after the addition of **209** at a concentration of 14.4×10^{-5} M a significant decrease in impedance (0.014 M Ω) was observed as shown in the electrical data (Table 5.28) and the Bode plot (Figure 5.2.14). This suggests that the transport of potassium ions are concentration dependent and may have possible implications regarding the transport mechanism.

In this experiment the impedance recovery of the NaCl electrolyte post KCl was not complete, but as discussed earlier this can be amended by flushing the system with Milli-Q water for impedance recovery.

Table 5.2.8 Electrical data for tricrown B with increasing increments in both NaCl and KCl electrolytes.

Electrolyte	Concentration (M) of 209	Impedance (M Ω)	Error (%)	Capacitance (μ F)	Error (%)
NaCl	Bilayer	4.1	52.5	1.1	31.7
	3.6×10^{-5}	5.0	25.5	1	13.1
	7.2×10^{-5}	same as bilayer		same as bilayer	
	14.4×10^{-5}	0.8	6.7	0.8	2.2
KCl	3.6×10^{-5}	1.8	34.9	1	15.6
	7.2×10^{-5}	2.5	15.8	1.1	8.7
	14.4×10^{-5}	0.014	20.4	1.2	13.6

**Figure 5.2.14** Bode plot of **209** at a concentration of 14.4×10^{-5} M followed by subsequent changes in electrolyte solutions.

Introduction of other ions such as lithium, TMAC and CaCl_2 showed no transport or at best minimal transport, compared to the significant reduction of impedance under the KCl electrolyte (Figure 5.2.15). The red data set (taken after Milli-Q rinse) also shows that impedance recovery occurs. As seen in previous examples if KCl is present the impedance does not recover unless the bilayer was washed thoroughly with Milli-Q water.

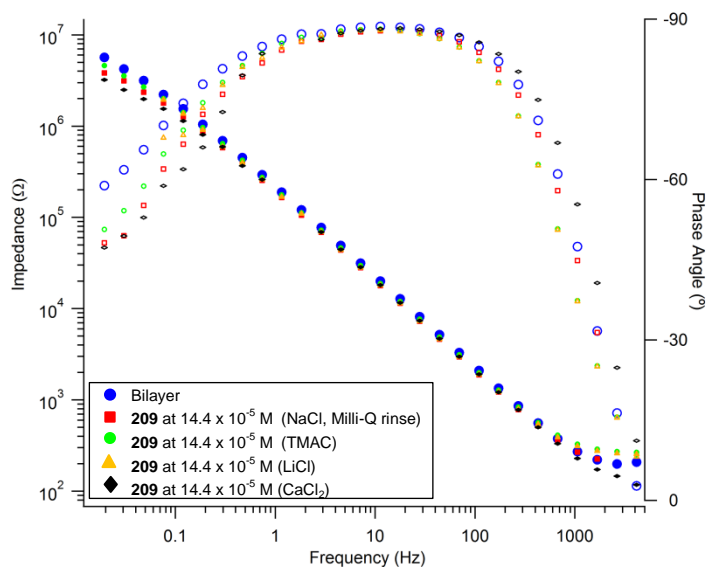


Figure 5.2.15 Bode plot for the introduction of other electrolytes to the bilayer with tricrown B (14.4×10^{-5} M).

Therefore it can be concluded from these results that a higher concentration of **209** is required to observe a reduction in impedance when transporting potassium ions. From the other ions examined, no decrease in impedance was observed and therefore those ions were unable to be transported across the bilayer. These results were similar to those of tricrown A **208** however a lower concentration (14.4×10^{-5} M) of crown ether was required to observe transport. This may be relevant to the estimated length of the two systems and the transport mechanism, whether it be related to aggregation, channelling or carrier capabilities.

In summary (Table 5.2.9) shows higher concentrations of monomer crown ethers **203** and **197** are required to observe reductions in impedance and therefore transport across the tBLM. For both tricrown A and B (**208** and **209**) a lower concentration of crown ether is required to observe reductions in impedance allowing ions to traverse the tBLM. These values outlined in Table 5.2.9 are the concentrations at which significant ion transport was observed.

Table 5.2.9 Summary of the concentrations of crown ether compounds required to have any effect on the impedance of the tBLM.

Crown Ether Compound	Concentration in KCl electrolyte (M)
203	28×10^{-5}
197	24×10^{-5}
208	6.7×10^{-5}
209	14.4×10^{-5}

Therefore it can be concluded that all monomer and tricrown compounds can facilitate the transport of potassium ions however at the specified concentrations in Table 5.2.9. The mechanism in which this occurs is however still unclear from these results whether ions transport through a channel or carrier approach. In Table 5.2.10 there are four potential models in which transport for potassium ions with the polycyclic compounds synthesised in Chapter 4 can occur with respect to the results outlined in Table 5.2.9.

Table 5.2.10 Potential variations in models for the transport of ions across a tBLM in EIS.

Model	Polycyclic Compound			
	203	197	208	209
1	12 unit aggregation	12 unit aggregation	Monomer	Dimer
2	12 unit aggregation	12 unit aggregation	Dimer	Dimer
3	All monomer carriers			
4	Monomer	Monomer	Dimer	Dimer

All of these models are dependent on how these polycyclic crown compounds embed within the tBLM. For example, tricrown A **208** may embed more efficiently than that of tricrown B **209** therefore a lower concentration of **208** is required for transport to be observed. The most probable models to occur would be three, and four with monomers **203** and **197** acting as singular ion carriers. The larger systems **208** and **209** could either act as singular ion carriers or form a dimer to act as a channel. It is very unlikely that aggregation of the monomer units would occur within the bilayer, as when analysed in solution no aggregation was observed via NMR spectroscopy.

5.3 ^1H NMR Titrations of Synthesised crown ether Systems

NMR spectroscopy is one technique used to determine binding constants between a host (crown ether) and guest (Na and or K ions).^[17-21] The advantage of NMR titrations is that they give information about changes in chemical environments during complexation. In this research the binding constants between a crown ether (15-crown-5) compounds synthesised and sodium, potassium ions were examined.

The complexation between sodium ions and samples of benzo-15-crown-5, *endo* 15-crown-5 **203**, and Hedaya 15-crown-5 **197** were investigated using titration techniques.

The NMR titrations were carried out using sodium perchlorate (NaClO_4) as the source of sodium ions and this was titrated against a known concentration of crown solution. In this titration the crown concentration decreased as sodium perchlorate solution (1M, CH_3CN) was added, increasing sodium ion concentration. The titrations were conducted multiple times, with variations in NaClO_4 (anhyd.) samples and acetonitrile (anhyd.) to eliminate possible errors.

The first crown ether examined was benzo-15-crown-5 and the results from the initial titrations for both the aromatic and crown ether proton resonances show small shifts from the initial crown resonances, Figure 5.3.1. In particular, downfield shifts were observed for all resonances with the largest changes occurring for the aromatic protons ($\Delta\delta$ 0.1 ppm) and the α -crown ether protons ($\Delta\delta$ 0.1 ppm). These types of shifts were observed for all of the compounds titrated with NaClO_4 in acetonitrile (see below).

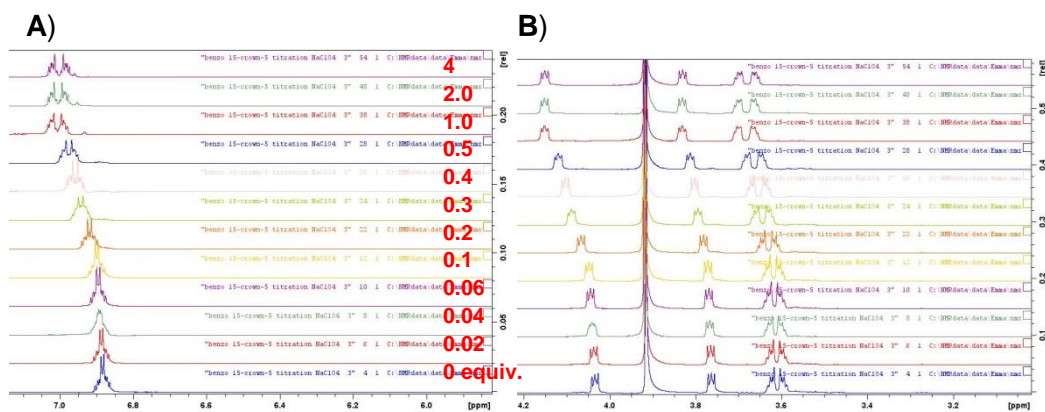


Figure 5.3.1 Visual representation of the ^1H NMR shifts of benzo-15-crown-5 upon addition of NaClO_4 . **A)** Aromatic crown ether proton chemical shifts, **B)** The α -crown ether proton chemical shifts.

Initial visual analysis of the data via Excel, (plotting chemical shift change against sodium concentration) suggested the formation of 1:1 complex. However when the data was modelled using HYPNMR 2008 a 1:1($[\text{Na}].[\text{Crown}]$) binding complex was observed as well as an additional 1:2 ($[\text{Na}].[\text{Crown}]_2$) complex, shown in Figure 5.3.2. Previous literature titration studies^[19], for the binding of benzo-15-crown-5 (B15C5) with NaClO_4 monitored via ^{23}Na NMR spectroscopy in acetonitrile (plotting chemical shift change against sodium concentration) have found a 1:1 binding complex and $\log \beta$ (where $\log \beta = \log K_a$) value of 4.^[6] The $\log \beta$ value for sodium ion analysed via various analytical techniques in various solvents and using different sodium salts can be between 0.5 and 7.^[22]

The HYPNMR fit shown in Figure 5.3.2 is based upon two aromatic and four crown ether resonances. The results for fitting the titration data using HYPNMR in Figure 5.3.2, where $\log \beta_{1:1}$ value for the 1:1 complex ($\text{Na}:\text{Crown}$) was 2.23 ± 0.08 . The $\log \beta_{1:2}$ value for the 1:2 complex of ($\text{Na}:(\text{Crown})_2$) was 4.21 ± 0.04 . The 1:1 β value is intermediate of the range reported in the literature (0.5–7),^[22] but the 1:2 complex is not usually discussed. These results were converged in 1 iteration with a sigma value of 2.031. These sigma values are used to assess the goodness of the fit with sigma values close to 1 being considered a good fit to the corresponding model.

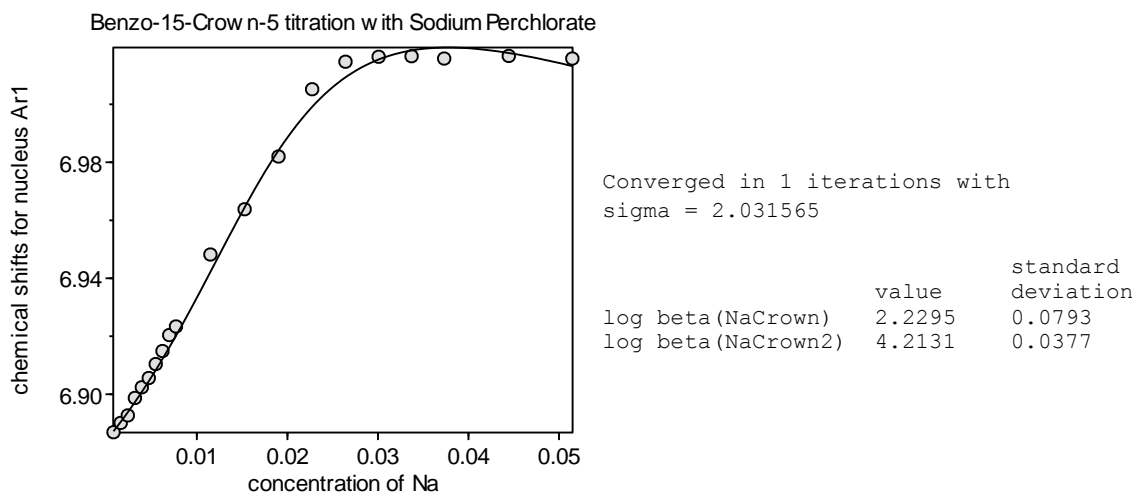


Figure 5.3.2 Plot of the aromatic proton resonance of benzo-15-crown-5 against $[\text{Na}^+]$ from sodium perchlorate.

Dilution studies were also conducted on benzo-15-crown-5 to eliminate dimerisation of the crown ethers as a potential factor responsible for the shifts observed. No dimerisation was observed within the NMR spectra, with no chemical shift changes observed over the concentration range 0.39M -0.039 M.

Following on from the results of the benzo-15-crown-5 titrations the new polycyclic 15-crown-5 systems were investigated. The first system to be examined was that of the *endo* block **203** and which gave results as depicted in Figure 5.3.3. The results for this monomer in comparison to the benzo-15-crown-5 were similar in that both a 1:1 and a 1:2 model fitted the ^1H NMR data. The HYPNMR fit for the monomer used one aromatic and three crown ether resonances.

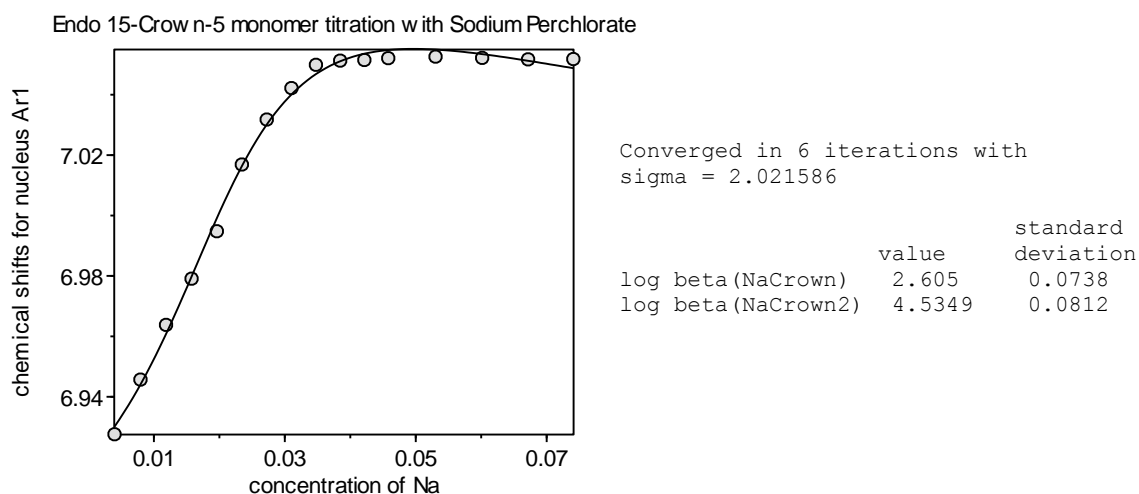


Figure 5.3.3 Plot of changes in chemical shift for aromatic proton resonances for the *endo* 15-crown-5 monomer against $[Na^+]$ from sodium perchlorate.

In this case fitting the data using HYPNMR yielded a $\log \beta_{1:1}$ value for the 1:1 complex (Na:Crown) of 2.605 ± 0.07 and a $\log \beta_{1:2}$ value for the 1:2 complex (Na:(Crown)₂) of 4.53 ± 0.08 . These results were converged in 6 iterations with a sigma value of 2.022.

As can be determined from the results of the *endo* 15-Crown-5 monomer **203** the same trend as the benzo-15-Crown-5 with both a 1:1 and 1:2 complex was forming in solution with similar binding constants being observed. This would imply that the norbornyl scaffold has minimal influence on the crown complexation behaviour.

Table 5.3.1 Binding constants observed for **203** and B15C5 with NaClO₄.

Compound	Na:Crown	Na:(Crown) ₂
203	2.60	4.53
B15C5	2.22	4.21

In addition to the *endo* monomer **203** the Hedaya monomer **197** was also titrated with NaClO₄ and a similar trend in chemical shift changes was observed as shown in Figure 5.3.4. The HYPNMR fit for **197** used one aromatic and three crown ether resonances.

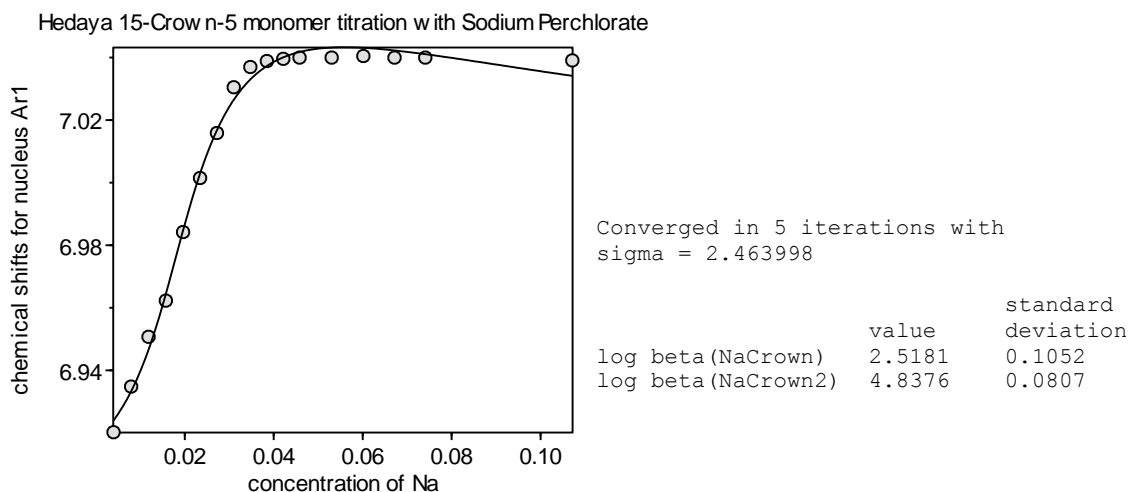


Figure 5.3.4 Plot of changes in chemical shift for aromatic proton resonances for **197** against $[\text{Na}^+]$ from sodium perchlorate.

HYPNMR fitting of the data produced a $\log \beta_{1:1}$ value for the 1:1 complex (Na:Crown) of 2.52 ± 0.10 . The $\log \beta_{1:2}$ value for the 1:2 complex of (Na:(Crown)₂) was 4.84 ± 0.08 . These results converged in 5 iterations with a sigma value of 2.46. As with *endo* crown, Hedaya monomer behaved in a similar manner to the benzo-15-crown-5 again. This indicates that the polycyclic scaffold does not interfere with the Na^+ complexation.

From the three sets of crown ether based compounds titrated with NaClO_4 in all scenarios both 1:1 and 1:2 complexes were observed. Attention was then turned to the tricrown molecules. Preliminary titrations were investigated for tricrown A using ^{23}Na NMR. However the spectra were not as easily interpreted as the mono crown systems. In particular the ^{23}Na resonance broadened considerably during the titration (as well as minor changes in chemical shift). Note, there were no ^1H NMR titrations undertaken due to the complexity of the ^{23}Na results. This indicated an exchange between various chemical environments and for the formation of 2:1 and 3:1 complexes. Variations in possible equilibrium complexes are shown in Figure 5.3.5.

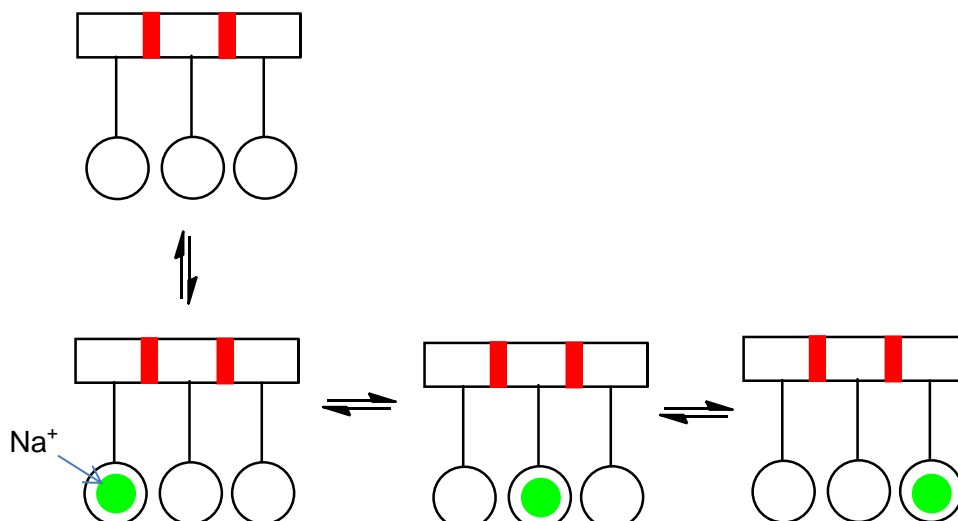


Figure 5.3.5 Possible equilibrium exchange of Na^+ ions with tricrown A **208** at low equivalents.

In an attempt to simplify the spectra, variable temperature (VT) NMR was examined at both high (60°C) and low temperature (-50°C). However, there were limitations in solvents and the solubility of the tricrown system and therefore limited data was obtained. The examination of these tricrown systems by NMR requires further investigation in the future.

5.3.1 NMR Titrations with Potassium Salts

Following on from the titration studies with sodium ions and in conjunction with the EIS results showing selectivity for the potassium ion, titration studies using potassium ions were investigated using potassium hexafluorophosphate and subsequently potassium thiocyanate.

Both monomer units (**203** and **197**) were examined with the potassium salt, potassium hexafluorophosphate. Initially the *endo* monomer **203** was titrated with potassium hexafluorophosphate with the data depicted in Figure 5.3.1.1 being observed. The plot (Figure 5.3.1.1) shows the changes in an aromatic resonance throughout the titration, however similar trends are observed for all proton peaks.

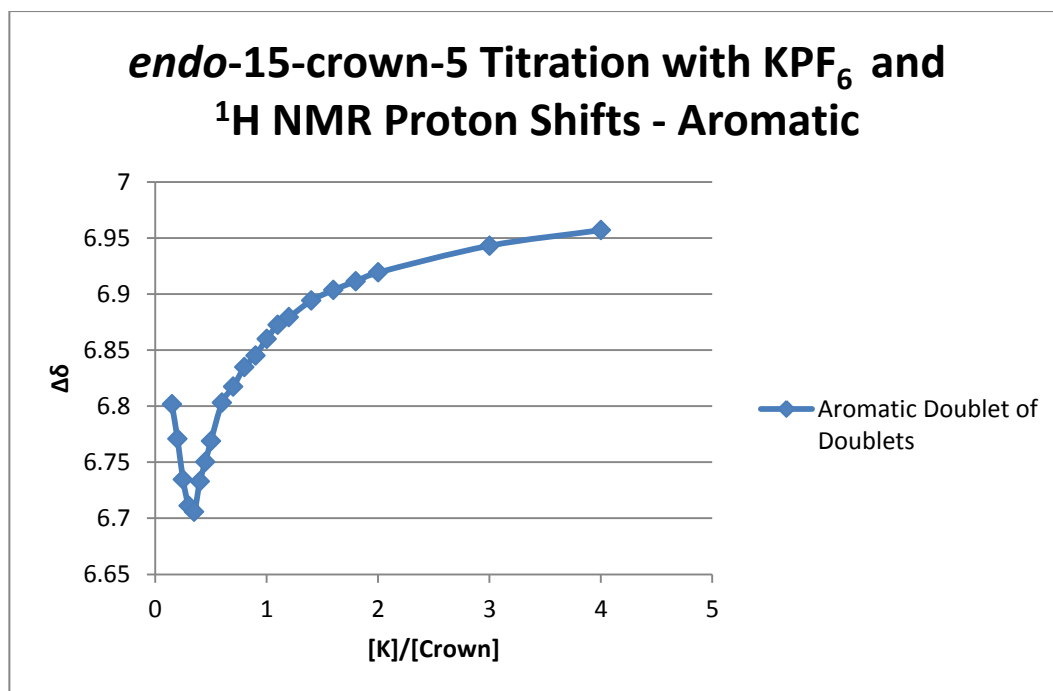
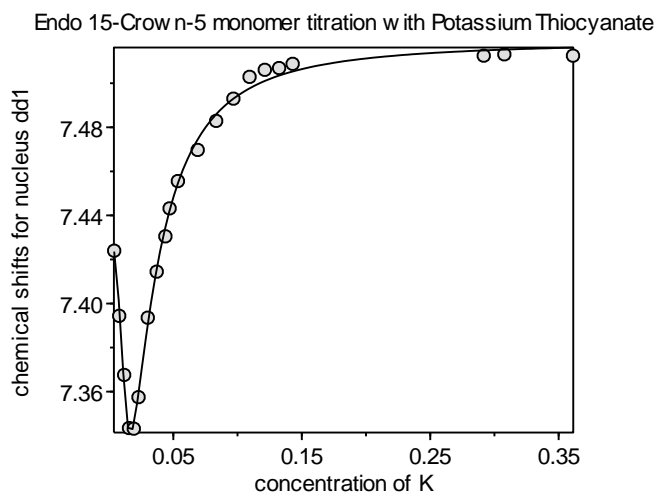


Figure 5.3.1.1 Plot of change in chemical shift of aromatic resonance versus [K]/[crown].

This data is quite unusual with a large inflection at 0.3 equivalents of potassium to crown ether since benzo-15-crown-5 forms 2:1 type sandwich complexes with potassium ions. Due to the unusual results a common salt, used in potassium NMR binding studies was utilised, potassium thiocyanate. However when numerous titrations were conducted using KSCN, similar results to those seen with potassium hexafluorophosphate were obtained indicating the reproducibility of the experiment. These results were analysed using HYPNMR 2008 in an attempt to fit a reasonable model to the system. However, these results have been difficult to assess. It was clear from the HYPNMR fitting that a 1:1 and a 1:2 model were not going to fit the data adequately, therefore variations in potassium to crown complexes were investigated. Using various models to fit to the data it became apparent that a 1:3 (K:crown) complex was required in the model to adequately fit the data. However even with the inclusion of a 1:3 species the data was unable to be refined by HYPNMR without large errors being present for the $\log \beta$ values even though visually the fit appears good (Figure 5.3.1.2). This suggests that more data is needed to be gathered at either end of the titration to assist the program in fitting the model. This was not undertaken due to time constraints.



Converged in 17 iterations with sigma = 3.989990

	value	standard deviation	Comments
1 log beta(KCrown)	2.9066	excessive	relative error on beta = 55%
2 log beta(KCrown2)	5.2562	excessive	relative error on beta = 65%
3 log beta(KCrown3)	7.703	excessive	relative error on beta = 85%

Figure 5.3.1.2 Plot of change in chemical shifts for aromatic proton resonance for the *endo* 15-Crown-5 monomer against $[K^+]$ from potassium thiocyanate.

To further assess the unusual complex properties between the synthesised *endo* 15-Crown-5 monomer **203** and the potassium ions, the second monomer, Hedaya monomer **197** was investigated with potassium thiocyanate in an NMR titration.

The results for the Hedaya monomer titration with the potassium thiocyanate salt revealed similar results to the previous *endo* system **203** with a large inflection observed at 0.3 equivalents of $[K^+]/[crown]$. However, in a similar manner to *endo* monomer **203** a 1:1, 1:2 and the 1:3 (K:Crown) model do not fit the data alone as depicted in Figure 5.3.1.3A.

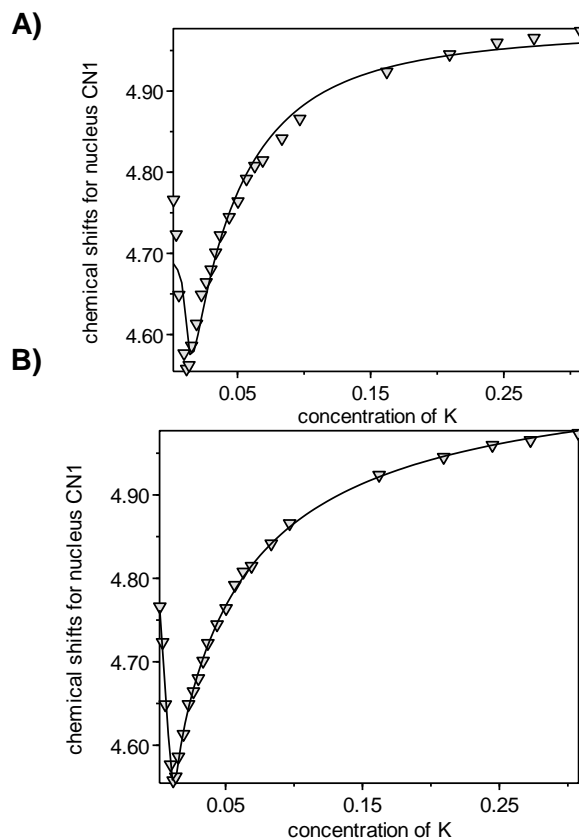


Figure 5.3.1.3 Plot of change in chemical shifts for crown ether proton resonances for the Hedaya 15-Crown-5 monomer against $[K^+]$ from potassium thiocyanate. **A)** 1:1, 1:2, 1:3 model, **B)** 1:1, 1:2, 1:3, 1:4 model.

Further models were examined and the best model which looked to fit the data was a 1:1, 1:2, 1:3 and 1:4 (potassium:crown) complexes, which is depicted in Figure 5.3.1.3B. In a similar manner to *endo* crown, visually the model fits the data well, however on all occasions the HYPNMR program has not been able to properly refine the model to obtain $\log \beta$ values for each complex formed. This suggests that either the models outlined above which have been attempted at refinement are not consistent with the data, or more data is needed at the extremities of the titration.

In considering the actual structure of the various complexes between the crown monomers and the potassium ion, it would seem that involvement of the carbonyl (C=O) interaction with a potassium ion is needed. This is due to the cavity size of the benzo-15-crown-5 ether not being able to complex with potassium ions. However literature examples of imide derivatised crown ethers have not reported such interactions.^[23,24]

In future studies the removal of the carbonyl groups in all systems could lead to an understanding of whether the lone pair of electrons on each carbonyl contributes to potassium ion complexation (see future directions, Chapter 6).

In summary both sodium and potassium ions have shown to complex with the crown ether systems. The sodium complexation is formed with both a 1:1 and 1:2 complex ($\text{Na}:(\text{Crown})_2$). However when titrations with potassium are conducted numerous complexes are formed and at this stage an overall binding fit is unable to be produced due to the complexity of the data. Further analysis with these systems as well as the tricrown systems is needed.

5.4 Black Lipid Membrane Analysis of Polycyclic Crown Ether Compounds

Another technique used to analyse ion channels within membranes is often referred to as planar bilayer conductance or black lipid membrane (BLM) studies. This technique employs two chambers filled with buffer solutions referred to as *cis* and *trans*. In a typical setup the *cis*-chamber is connected to an input electrode and the *trans*-chamber to a reference electrode as depicted in Figure 5.4.1

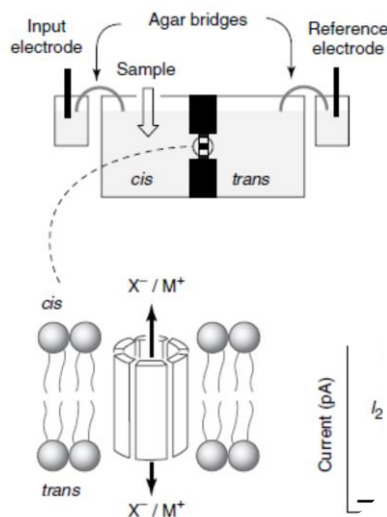


Figure 5.4.1 BLM setup based on a standard configuration.^[8]

In between the two chambers, *cis* and *trans*, the lipid bilayer or BLM is assembled across a micrometer sized hole. The artificial bilayer is formed from phosphatidylethanolamine and phosphatidylcholine in an alkane hydrocarbon solvent commonly decane. The solution is then applied to the micrometer hole to form a bilayer where it can then separate the two chambers. The transfer of ions

between both chambers does not occur without the presence of ion channels or pores in the membrane, as the BLM is essentially an insulator which preventing the passage of ions between the two chambers.

Artificial ion channels and/or pores can then be added to either chamber and a repulsive voltage is applied to the system to drive them towards the BLM. Once the voltage has been applied the current is then measured as a function of time and an output of the results is obtained (Figure 5.4.2). Results are usually random or stochastic in nature, as the ion channel opens and closes.

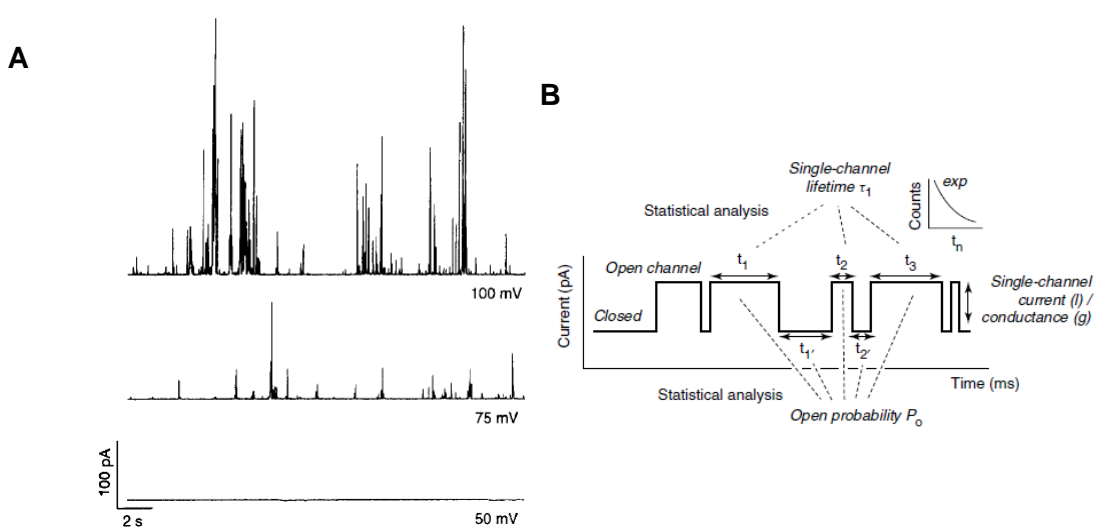


Figure 5.4.2 A) Single channel recording output from the BLM under different voltage conditions (50, 75 and 100mV). The ion channel activity was expressed over 2s detected via pA currents. B) Close up schematic of the BLM output with analysis of single channel conductance.^[8]

In this study, the effect of compounds **203**, **197**, **208**, **209** (Figure 5.1.1), on measured current through a BLM was examined by Professor Derek Laver and associates, University of Newcastle, Australia.

These compounds (approx. 1 mg) were prepared for BLM studies by initial solubilisation in chloroform. Before addition to the artificial lipid bilayers the crown compounds ($\sim 3\text{-}5 \times 10^{-3}$ M) of the stock chloroform solutions were dried under a stream of nitrogen and diluted in acetonitrile ($\sim 3\text{-}5 \times 10^{-6}$ M). Once the solutions were diluted, 10 μL of these solutions were added to the *cis* or *trans* baths. The baths were stirred and a voltage applied until channel activity was evident. If no channel activity was observed *via* this method, the chloroform stock

solutions (20 μL) were directly added to the lipid mixture (100 μL in chloroform) before forming the bilayer, to improve solubility within the system.

The results obtained showed that only **209** (tricorn B) induced electrical an electrical readout, and these were very weak, as shown in Figure 5.4.3.

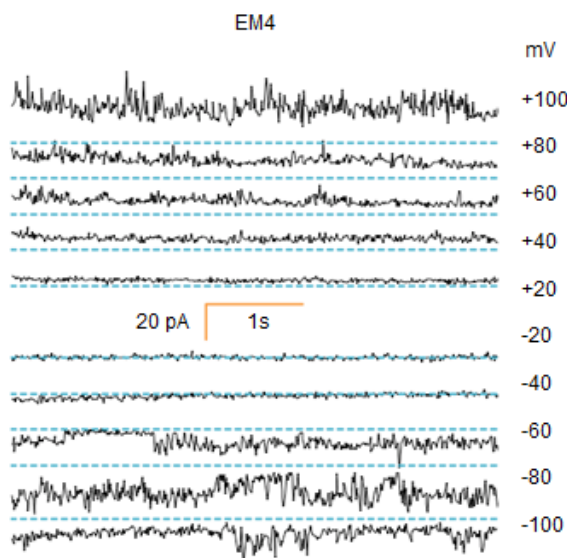


Figure 5.4.3 Stochastic activity of tricrown B **209** using KCl electrolyte.

In this instance there was no selectivity towards K, Na and or Cs ions. The BLM traces were similar with each ion present for this compound. However literature has suggested that if there is failure to detect currents from these ion channels it does not necessarily mean that they do not exist.^[8] There are a number of reasons by which this is possible, for example having the incorrect lipid composition of the BLM as well as insufficient partitioning into the BLM.

In a similar manner to Figure 5.4.3, none of the other crown compounds **203**, **197** and **208** showed any significant activity. It may also be due to the crown concentrations being below the limit for activity to be observed. Therefore observing no stochastic activity for the other three crown ether materials does not suggest that there is no transport, and a much more in depth study would be required to ascertain whether these systems transport ions. This would require multiple variables within the BLM to be adjusted and also a study of sample solubility and introduction into the set-up. As these studies were outsourced, these variables were not investigated in this instance but should form the basis of future BLM work.

5.5 Calcein Release from POPC Vesicles

A further characterisation of the crown ethers embedded into membranes was carried out using calcein release studies. These were undertaken to ascertain if the crowns were forming pores in the membrane allowing ion transport or causing disruption of the membrane. The release of calcein (a fluorescent dye) would indicate diffusion and disruption of the membrane. Therefore ideally no calcein release from the membrane should be observed. In this study the four previous compounds both monomers (**203** and **197**) and tricrowns (**208** and **209**), were examined for calcein release by Professor Phillip Gale and associates (Soton). The results from this study are detailed below.

Initially the vesicles were prepared with calcein and monitored before crown compounds were added. The fractional calcein release from POPC (1-palmitoyl-2-oleoyl-sn-glycero-3-phosphatidylcholine) vesicles was monitored over the course of 1 hour. The crown ethers were added as a solution of acetonitrile at $t = 0.5$ minutes and the vesicles were lysed with detergent at $t = 60.5$ minutes to calibrate the experiment to 100% calcein release. The results from these experiments are depicted in Figure 5.5.1.

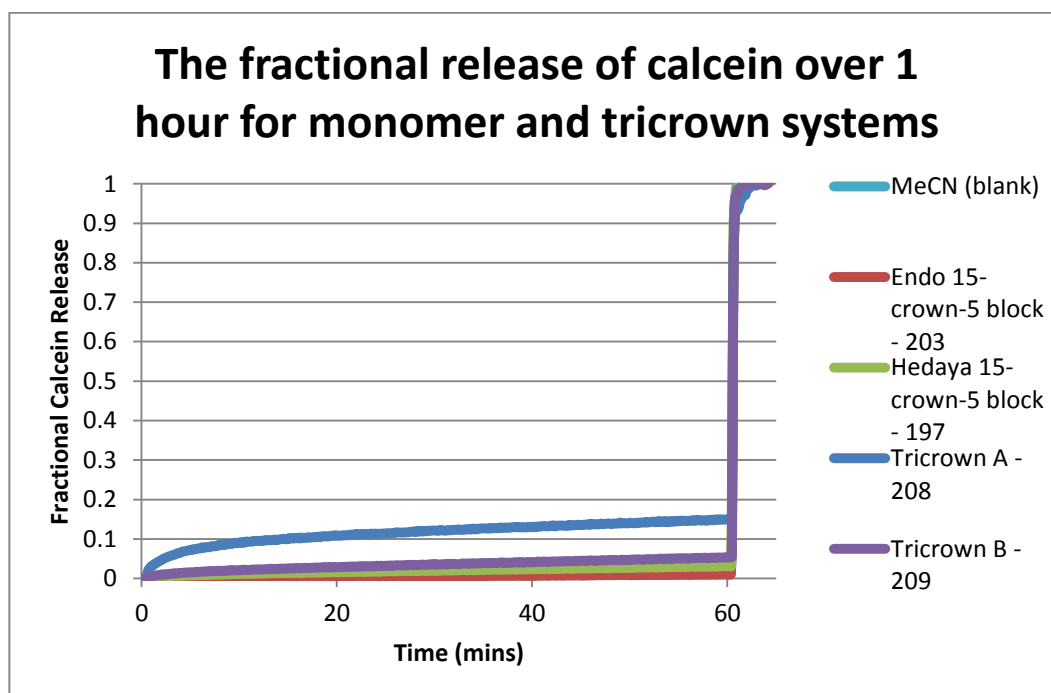


Figure 5.5.1 Fractional release of calcein for crown ether systems over 1 hour. Systems were lysed at 60 minutes allowing calibration to 100% release.

After 1 hour it can be observed that samples **203**, **197** and **209** show little to no calcein release from the vesicle. However sample **208** shows a small release (~15%) of the fluorescent dye indicating disruption of the membrane by the crown ether.

Due to the small release observed for **208** and **209** these vesicles with the crown ethers embedded were left for a longer period of time (12 hours), the results of which are shown in Figure 5.5.2.

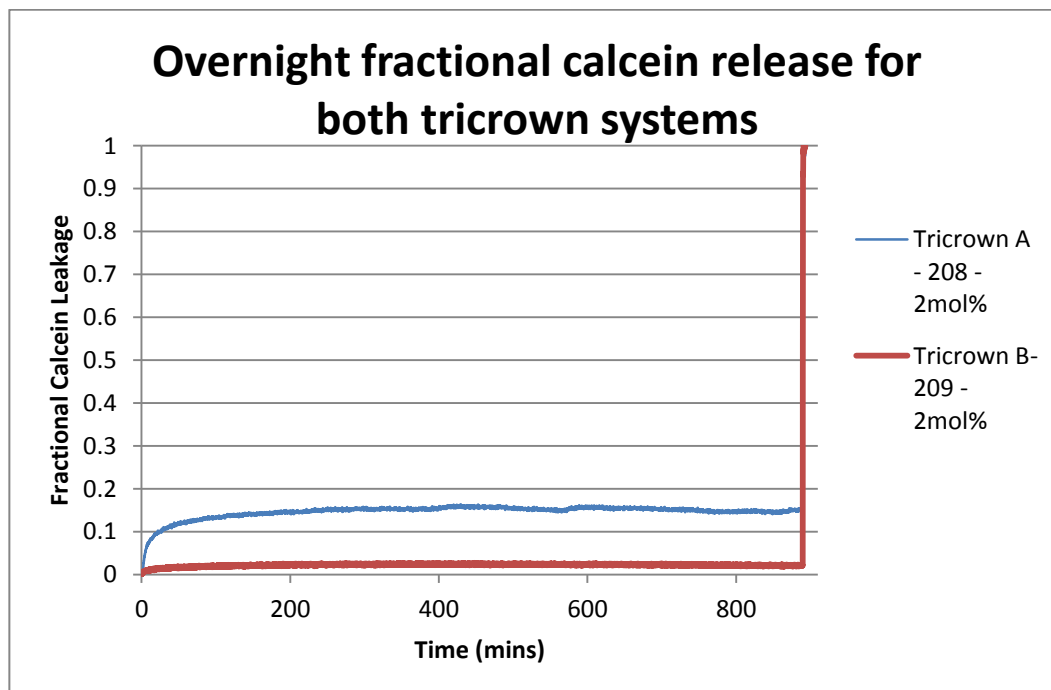


Figure 5.5.2 Fractional release of calcein for crown ether systems (**208**, **209**) overnight. Systems were lysed allowing calibration to 100% release.

The results from the 12 hour experiment have identified that the fractional release of calcein by **208** was 15% and that for **209** was 2%. The results suggest that there is some lytic activity occurring possibly by formation of a pore large enough to allow the flow of calcein through it. However it may be due to an initial disruption of the membrane as it embeds within the bilayer, because the amount of calcein release is kept constant over time, not increasing. It is unclear to why we don't see these results in EIS for membrane disruption with all ions analysed showing transportation across the membrane. These results need to be considered when examining the ion transport behaviour observed by EIS in Section 5.2.

Conclusions

Synthesised polynorbornyl crown ether blocks were analysed via EIS, NMR, BLM and calcein release techniques. The four blocks analysed via EIS indicated selective potassium ion transport that varied with concentration. In particular, both the *endo*-block **203** and the Hedaya block **197** showed that above 12×10^{-5} M potassium ion transport was observed. In comparison to the tricrown systems potassium transport was observed when tricrown A **208** was above 6.7×10^{-5} M and tricrown B **209** was above 14.4×10^{-5} M. This indicates that a higher concentration of monomer units is required for any potassium transport to be observed.

The mechanism for transport is still to be confirmed, possible models were outlined in Section 5.2 with the most likely being that these systems act as potassium ion carriers rather than potassium ion channels. Further channel analysis is required to identify whether these systems are acting as carriers rather than ion channels.

Preliminary NMR studies with both sodium and potassium ions were investigated for *endo* **203** and Hedaya **197** monomers. The monomers showed a 1:1 and 1:2 complex formation between monomer 15-crown-5 and sodium ions. However the potassium ion complexation studies were much more difficult to assess and fit to appropriate models, which may require further assessment and investigation in the future. In particular formation of 1:3 and 1:4 (K:Crown) stoichiometric complexes in addition to 1:1 and 1:2 were seen to improve the data fit.

BLM studies identified under the conditions outlined, that only one crown block, tricrown B showed stochastic activity, however no selectivity between ions was observed. These results are contrary to EIS results and may be as a result of insufficient material becoming embedded in the lipid membrane. Further concentration studies are required as undertaken for EIS investigations.

Calcein release studies indicated pore forming activity for two systems namely, tricrown A **208** and tricrown B **209**. Pore formation and or membrane disruption was much more evident with tricrown A over a period of 12 hours with calcein release of 15% in comparison to tricrown B at 2%.

What is clear is that these systems have the ability to selectively transport potassium ions either via a carrier or aggregated channel forming approach. It is quite unusual considering that 15C5 is supposed to selectively target sodium ions. However there is potential for these systems to leak ions across the membrane through unidentified pore formation after extended periods of time.

REFERENCES

- [1] G. W. Gokel, S. Negin, *Adv. Drug Deliv. Rev.* **2012**, *64*, 784–96.
- [2] N. Sakai, D. Gerard, S. Matile, *J. Am. Chem. Soc.* **2001**, *123*, 2517–2524.
- [3] F. Otis, C. Racine-Berthiaume, N. Voyer, *J. Am. Chem. Soc.* **2011**, 6481–6483.
- [4] P. L. Boudreault, N. Voyer, *Org. Biomol. Chem.* **2007**, *5*, 1459–1465.
- [5] A. Han, A. B. Frazier, *Lab Chip* **2006**, *6*, 1412–1414.
- [6] S. Alonso-Romanowski, L. M. Gassa, J. R. Vilche, *Electrochim. Acta* **1995**, *40*, 1561–1567.
- [7] J. Kendall, B. Johnson, P. Symonda, G. Imperato, R. Bushby, J. Gwyer, C. Van Berkel, S. Evans, L. Jeuken, *Eur. Cells Mater.* **2010**, *20*, 136.
- [8] S. Matile, N. Sakai, in *Anal. Methods Supramol. Chem.* (Ed.: C. Schalley), Wiley-VCH, Weinheim, **2012**, pp. 711–742.
- [9] M. Ouellet, F. Otis, N. Voyer, M. Auger, *Biochim. Biophys. Acta* **2006**, *1758*, 1235–1244.
- [10] D. D. MacDonald, *Electrochim. Acta* **2006**, *51*, 1376–1388.
- [11] “Oliver Heaviside,” can be found under <http://www-history.mcs.st-andrews.ac.uk/Biographies/Heaviside.html>, **2003**.
- [12] B. Y. Chang, S. M. Park, *Annu. Rev. Anal. Chem.* **2010**, *3*, 207–229.
- [13] A. Lasia, *Electrochemical Impedance Spectroscopy and Its Applications*, **2002**.
- [14] “Basics of Electrochemical Impedance Spectroscopy,” can be found under <http://www.gamry.com/application-notes/EIS/basics-of-electrochemical-impedance-spectroscopy/>, **2009**.
- [15] E. Barsoukov, J. R. Macdonald, *Impedance Spectroscopy: Theory, Experiment, and Applications*, John Wiley And Sons Inc, New Jersey, **2005**.
- [16] A. Junghans, I. Köper, *Langmuir* **2010**, *26*, 11035–11040.
- [17] E. Karkhaneei, M. K. Zebarjadian, M. Shamsipur, *J. Incl. Phenom.* **2006**, *54*, 309–313.
- [18] E. Karkhaneei, A. Afkhami, M. Shamsipur, *J. Coord. Chem.* **1996**, *39*, 33–42.
- [19] A. Popov, J. Lin, *J. Am. Chem. Soc.* **1981**, *103*, 3773–3777.

- [20] P. Szczygiel, M. Shamsipur, K. Hallenga, A. I. Popov, *J. Phys. Chem.* **1987**, *91*, 1252.
- [21] K. Hirose, in *Anal. Methods Supramol. Chem.* (Ed.: C.A. Schalley), Wiley-VCH, Weinheim, **2012**, pp. 27–66.
- [22] M. I. Reed, K. Pawlak, J. S. Bradshaw, *Chem. Rev.* **1991**, *91*, 1721–2085.
- [23] M. A. Meador, D. S. Tyson, A. Carbaugh, *PSME Prepr.* **2008**, *98*, 130–131.
- [24] X. Wang, J. Hu, T. Liu, G. Zhang, S. Liu, *J. Mater. Chem.* **2012**, *22*, 8622.

CHAPTER 6

CONCLUSIONS AND FUTURE DIRECTIONS

The studies outlined in this thesis present the various stages of design and successful synthesis for a polycyclic norbornyl crown ether block which can be extended to larger systems for transport studies. The initial developments in this study allowed the fusion of crown ether molecules to polycyclic norbornyl systems that are linear and have a high aspect ratio. Initial investigations centred on the use of an ethylene linking chain between crown and polycyclic moiety, **45**. However with synthetic difficulties unable to be overcome, attention was shifted to a methylene linker as shown for **133**. This proved equally problematic and finally the study progressed towards block **197** with a direct attachment, which could be extended with minimal complications.

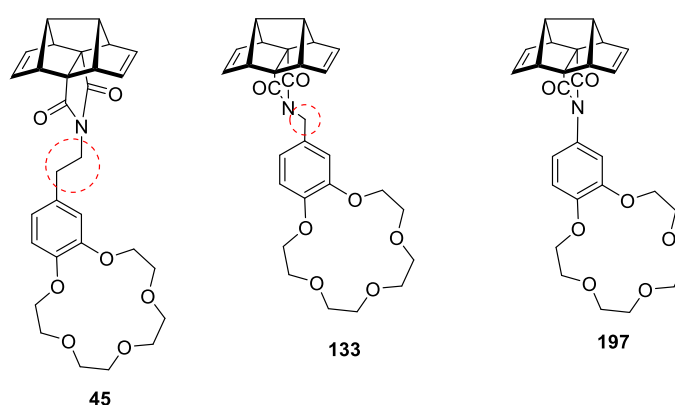


Figure 6.1 Polynorbornyl scaffolds with appended crown ethers with ethylene, methylene and direct attachment.

The successful synthesis of monomers (**203**, **197**) and tricrowns (**208**, **209**) through amic acid imide reactions and ACE coupling, led to preliminary transport studies using a variety of analytical techniques. Analysis *via* EIS indicated selectivity for potassium ions over Na⁺ for all monomers and tricrown molecules (tricrown B over Na⁺, TMAC, Li⁺, Ca²⁺), with potassium transport occurring when the concentration of the monomers **203** and **197** was greater than 12 x 10⁻⁵ M. The concentration for observed changes in impedance and transport of potassium ions for tricrown A **208** was found to be greater than 7 x 10⁻⁵ M and for tricrown B **209** to be greater than 14 x 10⁻⁵ M. These results are unusual given the preference for 15-crown-5 to complex with sodium ions.

Preliminary NMR binding studies with both sodium and potassium ions in acetonitrile solutions were undertaken with *endo* **203** and Hedaya **197** monomers, as described in Chapter 5. The results showed that these monomers were able to form both 1:1 and 1:2 complexes with sodium ions.

The literature log β value for the sodium ion analysed via various analytical techniques in various solvents and using different sodium salts can be between 0.5 and 7.^[22] The values reported for **203** and **197** fit within this range. To the best of our knowledge there are no reported literature values for the log β of the 1:2 complex. In addition the results of the potassium ion complexation studies were much more difficult to interpret and fit appropriate models.

BLM studies identified that under the conditions outlined, only one crown block, tricrown B showed stochastic activity and there was no selectivity between ions. In addition, the calcein release studies undertaken showed pore forming activity for two systems, tricrown A **208** (15% release) and tricrown B **209** (2% release) over a 12 hour period. This suggests that instead of channel or carrier activity the compounds may form pores, however this does not give insight into selectivity observed for these systems in EIS.

From the various techniques used for ion channel analysis in this project the mechanism of cation transport promoted by both the monomer and tricrown systems is still unclear. Further investigations using other transport techniques will be required to ascertain the appropriate mechanism by which ions cross the lipid bilayer.

The positive outcomes in relation to the synthesis of these tricrown systems led to preliminary (Chapter 4, Section 4.7.1) investigations of other tricrown systems with variations in crown ether sizes. In particular, tricrowns **211a**, **211b** containing 18-crown-6 and 21-crown-7 polycyclic blocks were synthesised (Figure 6.2). Further investigations within this area are required to maximise purification of these systems to enable additional transport studies to be undertaken. Furthermore the purification processes for the extended systems synthesised such as the pentacrown system **212** also need to be fully investigated.

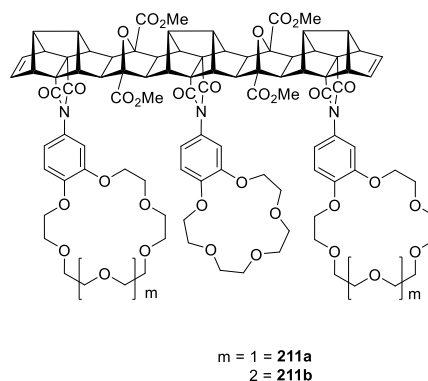


Figure 6.2 Tricrown with 21-crown-7 and 18-crown-6 ethers on the outside of the central 15-crown-5 ether synthesised through an ACE coupling reaction under microwave conditions.

Building on from the already discussed routes for possible tricrown and pentacrown extensions discussed in Chapter 4 new directions for chain extension may be investigated. For example the lateral extension of the already synthesised tricrown systems with hydrocarbon chains or glycol chains which may be a possibility for future work. To achieve this, diol formation at the alkenes is required with for example, osmium tetroxide followed by a subsequent Williamson ether formation. This would allow for an extended polycyclic block (Figure 6.3) to be at a length consistent with the bilayer thickness.

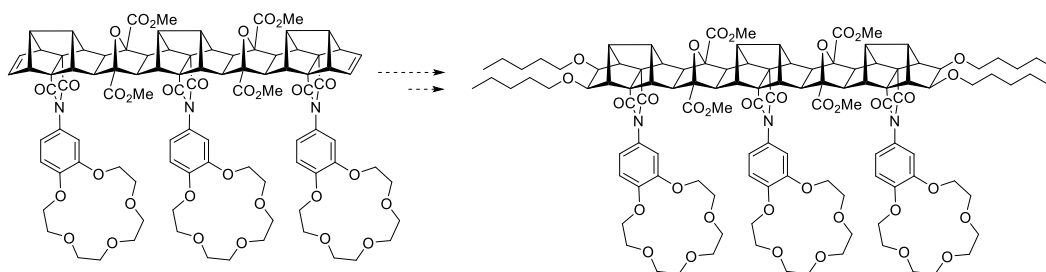


Figure 6.3 Functionalisation of synthesised tricrown A system with hydrocarbon chains.

In addition to the testing of both monomers and tricrown systems discussed in Chapter 5, further analysis *via* patch clamp methods would be highly desirable. The patch clamp approach is another technique used in the analysis of ion channels to study their structure and function through electrophysiological measurements. In conjunction with the patch clamp analysis, further EIS studies based on a concentration dependence could be important in determining a specific transport mechanism. Furthermore deuteration of the tricrown and monomer units (ANSTO Deuteration facility) for analysis via neutron scattering

may lead towards the understanding of how the crown compounds are positioned within the bilayer and therefore confirm a possible transport mechanism.

An additional aspect that requires further analysis is related to the monomer units and their complexation with potassium ions using ^1H NMR spectroscopy. Reduction and removal of the carbonyl groups and further investigation of the potassium ion complexation may give insight into whether the lone pair of electrons on the oxygen atoms of the carbonyl groups play a role in the binding of potassium ions. Furthermore synthesis of new blocks as shown in Figure 6.4, may also give insight into potassium ion complexation with the crown ether completely removed and the instalment of methoxy groups. These compounds (Figure 6.4) will give insight into the complexation of potassium ions with variations in polycyclic blocks.

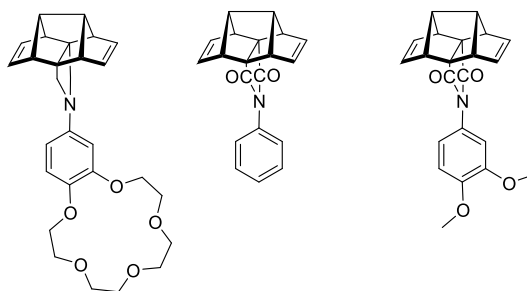


Figure 6.4 Variations in monomer units for the investigation of possible potassium ion complexation.

Finally, it must be emphasised that the use of these rigid polycyclic norbornyl blocks with the functionalisation of crown ethers can be adapted and manipulated to synthesise new and unique structures with variations in ionophores, shapes and lengths. These structures may not only be utilised in ion channel applications but for new applications in synthetic supramolecular chemistry.

CHAPTER 7

EXPERIMENTAL

7.1 General Experimental Details

All NMR spectra were recorded on a Bruker Avance (III) 600 spectrometer at 600 MHz (^1H) and 150 MHz (^{13}C) using Topspin 3 software unless otherwise stated. All spectra were recorded at 293K, and in deuterated solvents as indicated. Chemical shifts (δ) are reported as parts per million (ppm) and referenced to deuterated solvent peaks. Spin multiplicities are indicated by: s, singlet; bs, broad singlet; d, doublet; t, triplet; q, quartet; m, multiplet; dd, doublet of doublets. Peaks were assigned with the aid of homonuclear (^1H - ^1H) correlation spectroscopy (COSY) and (^1H - ^1H) nuclear Overhauser effect spectroscopy (NOESY), heteronuclear correlation spectroscopy (^1H - ^{13}C) HMQC.

DMAD^[1] and Ruthenium catalyst $[\text{RuH}_2(\text{CO})(\text{PPh}_3)_3]$ ^[2] were synthesised via previously reported procedures. All other products were purchased from Sigma Aldrich and AK Scientific Inc. DCM was distilled from CaH and THF was distilled from sodium benzophenone ketyl immediately before use. All other reagents were purified according to Perrin^[3], with dried solvents stored over molecular sieves (4Å).

Thin layer chromatography (TLC) was performed on pre-coated sheets of Merck Kieselgel silica gel 60 F₂₅₄ and visualised under UV light (254 nm) or using KMnO_4 stain. Column chromatography was carried out at atmospheric pressure using Grace Davison Discovery Sciences, Davisil silica gel (60 Å, 40–63 μm).

Melting points were obtained using Sanyo Gallenkamp melting point apparatus.

Microwave reactions were performed in a CEM Discover S-Class microwave in reaction vessels (10 mL) loaded with combined starting materials (0.25g) in solvent (<3 mL). The microwave was operated in variable power (dynamic) mode with the following parameters: power 435 W, pressure limit 300 bar, temperature 170 °C, stirring high, air/nitrogen cooling off. Ramp time to 170 °C was 5 min. The sample was held at this temperature for a further 60 min.

Molecular modelling of molecular geometry was calculated at a semi-empirical (AM1) level with the Spartan '10 software package.

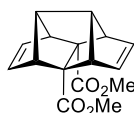
HRMS data was obtained using positive ion electrospray ionisation (ESI-MS) at CSIRO Manufacturing, Melbourne, Australia; Monash University, Melbourne, Australia, and Flinders Analytical, Flinders University, Adelaide, Australia.

7.2 Experimental Procedures

Systematic nomenclature has been used where possible, but larger more complicated structures are referred to by common abbreviated names e.g.

Tricrown A.

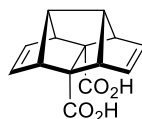
Dimethyl 3, 3a, 3b, 4, 6a, 7a-Hexahydro-3,4,7-metheno-7H-cyclopenta[*a*]pentalene-7,8-dicarboxylate



34

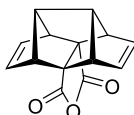
NaH (14.5 g, 60 % paraffin oil) was washed with hexane (50 mL) and which was removed via syringe before THF (dry, 100 mL) was added and the mixture cooled to 0°C. CPD (freshly cracked, 25 g, 0.38 mol) in THF (dry, 30 mL) was added dropwise over 45 min with the mixture slowly turning deep purple. The mixture was stirred for an additional 20 min before being cooled to -78°C, whereupon I₂ (48 g, 0.19 mol) in THF (dry, 100 mL) was added dropwise over 45 min, with stirring for an additional 10 min at -78°C. Dropwise addition of DMAD (28.5 g, 0.20 mol) in THF (40 mL) to the mixture occurred over 25 min before additional stirring for 15 min and warming to RT for 3 hr before storing at 5°C overnight. Residual THF was removed under reduced pressure whereupon the slurry was washed well with Et₂O (300 mL) and filtered over a bed of celite. The organic fractions were combined, solvent removed *in vacuo* and redissolved in MeOH (250 mL) at 0°C. Slow addition of KOH (22.8 g, 0.40 mol) in H₂O (50 mL) was carried out followed by stirring for 1.5 hr. The reaction mixture was warmed to RT, filtered over celite and diluted with H₂O (300 mL). The aqueous phase was extracted with hexane (4 x 200 mL), with combined organics washed with H₂O (2 x 200 mL), dried (Na₂SO₄) and concentrated *in vacuo* to afford an orange oil (crude). The oil was subjected to column chromatography (5% CHCl₃: hexane); (5% Et₂O: hexane); (20% EtOAc: hexane) to afford orange oil which solidified on standing (2.61 g, 8-11% yield). MP 60-62°C, lit. MP 61-62°C^[4];

¹H NMR (600 MHz, CDCl₃) δ 6.06 (4H, s), 3.58 (6H, s), 3.30-3.31 (4H, m), 2.53-2.52 (2H, m); ¹³C (150 MHz) δ 172.9, 132.8, 69.6, 64.5, 58.9, 51.7; HRMS-ESI calcd for C₁₆H₁₆O₄Na, 295.0946, found 295.0939 [M+Na]⁺.

3, 3a, 3b, 4, 6a, 7a-Hexahydro-3, 4, 7-metheno-7H-cyclopenta[a]pentalene-7,8-dimethanol**64**

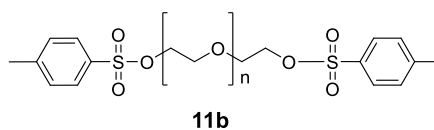
Hedaya diene (3.6 g, 13.2 mmol) was dissolved in methanol (66 mL) along with NaOH solution (10%, 66 mL) and the solution was heated under reflux for 2 hr. Upon cooling the methanol was removed *in vacuo*. The resulting water phase was acidified with concentrated HCl (37%) and the resulting bis-acid precipitated. The precipitate was removed by filtration and washed well with water and dried *in vacuo* to afford a beige solid, **64**, 1.4 g, 43% yield, mp > 225°C (dec), lit. MP >235-240°C (dec)^[5].

¹H NMR (600 MHz, CDCl₃) δ 6.09 (4H, s), 3.34-3.33 (4H, m), 2.53-2.52 (2H, m); ¹³C (150 MHz) δ 179.4, 132.8, 70.3, 64.4, 58.8.; MS-ESI calcd for C₁₄H₁₁O₄, 243.07, found 243.06 [M-H]⁻.

Pentacyclo[6.4.0.0^{2,10}.0^{3,7}.0^{4,9}]dodeca-5,11-diene-8,9-dicarboxylic anhydride**42**

A solution of Bis-acid (0.764 g, 3.12 mmol) in acetic anhydride (10 mL) was heated under reflux for 1 hr. The residual solvent was removed via distillation (20mm/Hg, 40°C) to afford beige crystalline solid, **42** (0.393 g, 44 %). MP 174 – 175°C, lit. MP 175-176°C^[6].

¹H NMR (600 MHz, CDCl₃) δ 6.16 (4H, s), 3.60-3.59 (4H, m), 2.92-2.91 (2H, m); ¹³C (600 MHz) δ 170.1, 132.7, 69.1, 65.3, 64.0.; HRMS-ESI calcd for C₁₄H₁₁O₃, 227.0708, found 227.0709 [M+H]⁺.

General procedure for synthesis of Poly(ethylene glycol) bis(tosylates)^[7]

Poly(ethylene glycol) (0.22 mol) and toluene-*p*-sulfonyl chloride (0.67 mol) was dissolved in THF (500 mL) whilst stirred vigorously for 10 mins. The reaction mixture was cooled to 0°C and a solution of KOH (1.46 mol) in water (170 mL) was added dropwise over 1 hr. The reaction was warmed to RT and stirred for an additional 10 hr. The suspension was poured into a mixture of CH₂Cl₂ (200 mL) and ice-water (200 mL). The aqueous phase was extracted with CH₂Cl₂ and the organic phases were combined and dried over anhydrous MgSO₄. The residual solvent was removed *in vacuo* and the product purified via column chromatography (Et₂O: EtOAc, 1:2, silica) to isolate the PEG ditosylate. Characterisation identical to literature values.

Tetraethylene glycol di(p-toluenesulfonate) (n = 2)^[7]

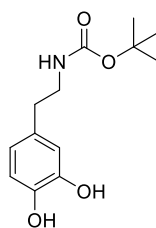
(100.7 g, 91 %), ¹H NMR (600 MHz, CDCl₃) δ 7.78 (4H, d, J = 8.2 Hz) 7.34 (4H, d, J = 8.2 Hz) 4.15 (4H, t, J = 4.8 Hz) 3.68 (4H, t, J = 4.8 Hz) 3.57-3.53 (8H, m), 2.44 (6H, s). ¹³C (150 MHz) δ 144.9, 133.1, 129.9, 128.0, 70.8, 70.6, 69.4, 68.8, 68.0, 21.7; HRMS-ESI calcd for C₂₂H₃₀O₉S₂Na, 525.1229, found 525.1215 [M+Na]⁺.

Pentaethylene glycol di(p-toluenesulfonate) (n = 3)^[7]

(10.7g, 94 %), ¹H NMR (600 MHz, CDCl₃) δ 7.79 (4H, d, J = 8 Hz), 7.34 (4H, d, J = 8 Hz) 4.16-4.14 (4H, m), 3.68-3.67 (4H, m), 3.59 (4H, s), 3.58 (8H, s), 2.44 (6H, s).

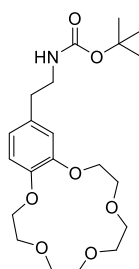
Hexaethylene glycol di(p-toluenesulfonate) (n = 4)^[7]

(8.9g, 85%), ¹H NMR (600 MHz, CDCl₃) δ 7.79 (4H, d, J = 8.2 Hz) 7.33 (4H, d, J = 8.2 Hz), 4.16-4.14 (4H, m), 3.68-3.67 (4H, m), 3.61-3.60 (8H, m), 3.57-3.54 (8H m), 2.44 (6H, s); ¹³C (150 MHz, CDCl₃) δ 144.9, 133.2, 130., 128.1, 70.8, 70.7, 70.6, 70.6, 69.4, 68.8, 21.8. HRMS-ESI calcd for C₂₆H₃₈O₁₁S₂Na, 613.1753, found 613.1744 [M+Na]⁺.

N-[2-(3,4-dihydroxyphenyl)ethyl]-, 1,1-dimethylethylester**66**

NaHCO₃ (8.3 g, 98.2 mmol) and Boc₂O (11.5 g, 52.7 mmol) were combined with dopamine hydrochloride (5 g, 32.6 mmol) in a solution of THF:H₂O (1:1, 200 mL) and stirred at 0°C for 30 min. The mixture was warmed to RT and stirred for an additional 16 hours. The turbid solution was extracted with ether (2 x 150 mL) and the aqueous layer acidified to pH 4-5 by slow addition of citric acid (aq.) at 0°C. The aqueous phase was extracted with DCM (2 x 150 mL) and the organic phases were combined, dried (Na₂SO₄), and concentrated *in vacuo*. The residue was subjected to distillation and recrystallization (THF, Hexane) to afford a white powder, 2.0g, 30% yield. MP 144- 146°C. ¹H NMR and ¹³C NMR matched literature values.^[8]

¹H (400 MHz, CDCl₃) 6.62 (1H, d, J = 7.6 Hz), 6.58 (1H, dd, J= 2, 7.6 Hz), 6.46 (1H, d, J= 2 Hz), 3.15-3.11 (2H, m) 2.56-2.52 (2H, m), 1.37 (9H, s); ¹³C (150 MHz, CDCl₃) 158.4, 146.1, 144.6, 132.1, 121.0, 116.8, 116.3, 79.9, 43.3, 36.6, 28.7; MS-ESI calcd for C₁₃H₁₉NO₄, 253, found 252 [M-H]⁻.

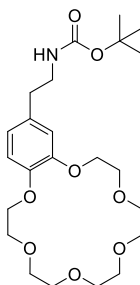
4-(2'-Boc)-ethyl-monobenzo-15-crown-5**67a**

Boc protected Dopamine (1 g, 3.95 mmol) in CH₃CN (dry and deoxygenated) with K₂CO₃ (5.46 g, 39.5 mmol 10 equiv.) was stirred for 1 hr at RT under N₂. Tetraethylene glycol di(p-toluenesulfonate) (1.98g, 3.95 mmol) in CH₃CN (25 mL) was added dropwise over 1 hr before the mixture was heated under reflux for 6 days. The K₂CO₃ was removed via filtration and the solids washed with CH₃CN

and the solvent removed *in vacuo*. The residue was redissolved in DCM and washed with brine, H₂O and dried over Na₂SO₄ to afford **67a** without further purification as a white powder, 0.697g, 41% yield. MP 79- 81°C.

¹H NMR (600 MHz, CDCl₃) δ 6.80 (1H, d, J = 8.4Hz), 6.71-6.70 (2H, m), 4.13-4.10 (4H, m), 3.91-3.89 (4H, m), 3.69-3.68 (8H, m), 3.33-3.32 (2H, m), 2.72-2.69 (2H, m), 1.46 (9H, s); ¹³C NMR (150 MHz, CDCl₃) δ 155.8, 149.1, 147.6, 132.15, 121.4, 114.5, 114.3, 79.2, 71.0, 70.7, 70.5, 69.7, 69.6, 69.1, 68.9, 41.8, 35.6, 28.4; HRMS-ESI calcd for C₂₁H₃₃NO₇Na, 434.2155, found 434.2149 [M+Na]⁺.

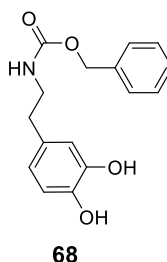
4-(2'-Boc)-ethyl-monobenzo-18-crown-6



67b

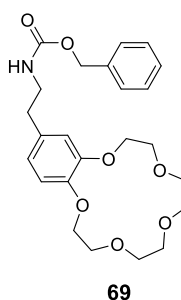
Boc protected Dopamine (250 mg, 1 mmol) in CH₃CN (25 mL, dry and deoxygenated) with K₂CO₃ (1.39 g, 10 equiv.) was stirred for 1 hr at RT under N₂. Pentaethylene glycol di(p-toluenesulfonate) (0.55 g, 1 mmol) in CH₃CN (25 mL) was added dropwise over a 1 hr before the mixture was heated under reflux for 5 days. The K₂CO₃ was removed via filtration and the solids washed with CH₃CN and the solvent removed *in vacuo*. The residue was redissolved in DCM and washed with brine, H₂O and dried over Na₂SO₄ to afford **67b** without further purification as a white powder, 0.287g, 64% yield. MP 80- 82°C.

¹H NMR (600 MHz, CDCl₃) δ 6.81-6.79 (1H, m), 6.71-6.70 (2H, m), 4.14-4.11 (4H, m), 3.87-3.86 (4H, m), 3.70-3.69 (4H, m), 3.68-3.67 (4H, m), 3.65-3.64 (4H, m), 3.33-3.32 (2H, m), 2.72-2.69 (2H, m), 1.43 (9H, s); ¹³C NMR (150 MHz, CDCl₃) δ 155.8, 148.8, 147.3, 132.0, 121.3, 114.4, 114.0, 79.1, 70.6, 69.5, 69.2, 68.9, 41.8, 35.6, 28.4; MS-ESI calcd for C₂₃H₃₇NO₈Na, 478, found 478 [M+Na]⁺.

***N*-[2-(3, 4-Dihydroxyphenyl)ethyl]carbamic acid benzyl ester**

To a solution of dopamine hydrochloride (0.95 g, 5 mmol) in H₂O (8 mL) at 0°C was added solid NaOH (0.5 g, 12.5 mmol) and the solution stirred until all material was dissolved. DCM (8 mL) was added and whilst stirring rapidly, CBz-Cl (0.84 mL, 6.0 mmol) was added dropwise. The mixture was warmed to RT overnight. The reaction mixture was diluted with DCM (10 mL) and poured into H₂O (10 mL). The organic and aqueous phases were separated and the DCM layer washed with brine (20 mL) and dried over Na₂SO₄. The solvent was removed *in vacuo* and orange brown wax was recovered and purified *via* column chromatography (EtOAc: Hexane, 2:1) to afford **68**, 472 mg, 30%. ¹H NMR and ¹³C NMR matched literature values.^[9]

¹H NMR (600MHz) δ 7.40-7.36 (5H, m), 6.80 (1H, d, J = 5.2 Hz), 6.69-6.67 (1H, m), 6.61-6.59 (1H, m), 5.11 (2H, s), 3.44-3.41 (2H, m), 2.71- 2.69 (2H, m). MS-ESI calcd for C₁₆H₁₇NO₄, 287, found 286 [M-H]⁻.

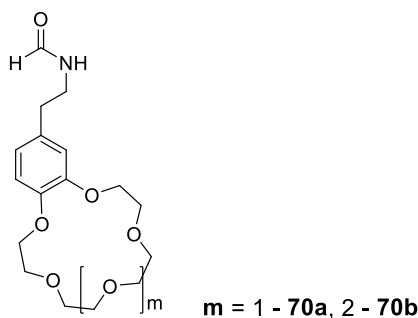
4-(2'-Cbz)-ethyl-monobenzo-15-crown-5

CBz-DOPA (419 mg, 1.46 mmol), was dissolved in CH₃CN (25 mL, dry and deoxygenated) along with K₂CO₃ (2.0 g, 10 equiv.) and was stirred for 1 hr at room temperature under N₂ atmosphere. Tetraethylene glycol di(p-toluenesulfonate) (0.73 g, 1.46 mmol) in CH₃CN (10 mL) was added dropwise over 1 hr before the mixture was heated under reflux for 5 days. The K₂CO₃ was removed *via* filtration and the solids washed with CH₃CN and the solvent removed *in vacuo*. The residue was redissolved in DCM and washed with brine,

H₂O and dried over Na₂SO₄ to afford without further purification a beige wax, 0.188g, 30%.

¹H NMR (600MHz) δ 7.35-7.34 (6H, m), 6.79-6.78 (1H, m), 6.71-6.70(2H, m), 5.10 (2H, s), 4.11-4.09 (4H, m) 3.89-3.87 (4H, m) 3.76-3.74 (8H, m) 3.42- 3.41 (2H, m) 2.75 -2.74 (2H, m); HRMS-ESI calcd for C₂₄H₃₁NO₇Na, 468.1998, found 468.2002 [M+Na]⁺.

4-(2'-Formidyl)-ethyl-monobenzo-15-crown-5 and 4-(2'-Formidyl)-ethyl-monobenzo-18-crown-6 (m = 1, 2)^[10]



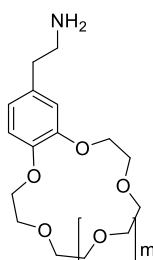
Dopamine hydrochloride (1.61 g, 8.5 mmol) was heated in DMF (300 mL) under N₂ at 100-110^oC for 1 hour. Sodium methoxide in methanol 25% (5.8 mL, 26 mmol) was added followed by dropwise addition of bis[chloro] PEG (n= 2, 3) (26 mmol) in DMF (20 mL, dry, deoxygenated) over 1 hour at 100-110^oC. Sodium chloride precipitation started within 5-10 mins. The reaction was allowed to continue for 12 hours at 100-110^oC under an N₂ atmosphere. After cooling the DMF was removed *in vacuo*. The residue was taken up in distilled water (100 mL) and extracted with DCM (3 x 75 mL). The combined organic phases were dried over molecular sieves (4Å) and solvent the removed *in vacuo* to afford an amber oil. The material was purified on a column (neutral alumina, Et₂O to MeOH) to afford a viscous yellow oil, which crystallised on standing. Trituration with Et₂O and recrystallization from ethyl acetate gave 15-Crown-5 derivative in (33 %, 0.958 g), or 18-Crown-6 derivative in (20 % 0.65 g).

70a 15-Crown-5 derivative – MP 130-131^oC^[10]; ¹H NMR (400 MHz, CDCl₃): δ 8.12 (1H, s), 6.81-6.79 (1H, m), 6.72-6.70 (2H, m), 5.60 (1H, br. S ,NH), 4.11-4.10 (4H, m), 3.91-3.90 (4H, m), 3.75-3.73 (8H, m), 3.58 (2H, m), 2.75 (2H, t, 4.8 Hz, 4.8 Hz).

70b 18-Crown-6 derivative – MP 94-96^oC; ¹H NMR (600 MHz, CDCl₃): δ 8.10 (1H, s), 6.75 (3H, m), 5.7 (1H, br. S ,NH), 4.11-4.09 (4H, m), 3.91-3.89 (4H, m),

3.67-3.67 (8H, m), 3.56-3.55 (2H, m), 2.76 (2H, m); ^{13}C NMR (150 MHz, CDCl_3): δ 161.2, 149.1, 147.7, 131.3, 121.3, 121.3, 114.7, 114.4, 70.8, 70.7, 70.6, 69.6, 69.1, 39.2, 35.0; HRMS-ESI calcd for $\text{C}_{19}\text{H}_{29}\text{NO}_7\text{Na}$, 406.1842, found 406.1830 $[\text{M}+\text{Na}]^+$.

2,3-(4'- β -Aminoethylbenzo)-1,4,7,10,13-pentaoxa-2-cyclopentadecene and 2,3-(4'- β -Aminoethylbenzo)-1,4,7,10,13, 16-hexaoxa-2-cyclooctadecene ($m = 1, 2$)^[10]



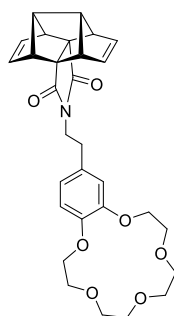
$m = 1 - 43a, 2 - 43b$

Formidyl protected dopamine (2.8 mmol) was hydrolysed by heating under reflux in a solution of 1:1 hydrochloric acid/methanol (5%, 50 mL) upon cooling. The mixture was brought to pH of 13 with KOH solution (20%) and extracted with DCM (4 x 50 mL). The combined organic solutions were dried over Na_2SO_4 and the solvent was removed *in vacuo*. Dopamine 15-Crown-5 and 18-Crown-6 were recrystallised from cyclohexane to afford 15-Crown-5 derivative (60 %, 0.52 g) and 18-Crown-6 derivative (40%, 0.40 g).

43a 15-Crown-5 derivative – MP 74-75°C^[10]; ^1H NMR (600 MHz, CDCl_3) δ 6.81 (1H, m), 6.72 (2H, m), 4.11 (4H, m), 3.90 (4H, m), 3.75 (8H, m), 2.93 (2H, t, J = 4.5, 4.5 Hz), 2.67 (2H, t, J = 4.5, 4.5 H); ^{13}C NMR (150 MHz) δ 149.3, 147.7, 133.2, 121.6, 114.9, 114.5, 71.2, 70.7, 69.8, 69.4, 69.2, 43.7, 39.7.

43b 18-Crown-6 derivative - ^1H NMR (600 MHz, CDCl_3) δ 6.80 (1H, d, 8.52 Hz), 6.71-6.70 (2H, m), 4.16-4.14 (4H, m), 3.92-3.89 (4H, m), 3.75-3.74 (4H, m), 3.72-3.67 (4H, m), 3.66-3.63 (4H, m), 3.33-3.32 (2H, m), 2.72-2.69 (2H, m); ^{13}C NMR (150 MHz) δ 148.8, 143.4, 133.2, 121.2, 114.4, 114.0, 70.6, 69.6, 69.5, 69.2, 68.6, 41.8, 35.6.

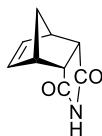
Hedaya block dopamine 15-crown-5



45

A solution of Dopamine 15-crown-5 **43a** (50 mg, 0.16mmol) and Hedaya anhydride **42** (36 mg, 0.16mmol) in CHCl_3 (2 mL) were stirred at RT for 96 hours. The solvent was removed *in vacuo* and the residue redissolved in acetic anhydride (5 mL), sodium acetate (26.3 mg, 2 equiv.) was added and the solution heated at 60°C for a further 96 hours. Upon completion the acetic anhydride was removed *in vacuo* and the residue redissolved in CHCl_3 . The organic phase was washed with brine, water and dried over Na_2SO_4 . Residual CHCl_3 was removed *in vacuo* before purification via column chromatography (DCM/MeOH (10 %) to $\text{CHCl}_3/\text{MeOH}$ (10 %) to afford **45** as a yellow oil, 29 mg, 34%.

^1H NMR (600 MHz, CDCl_3): δ 6.74 (1H, d, $J = 8.04$ Hz), 6.67-6.66 (2H, m, Ar-H), 5.89 (2H, s, alkene), 4.12-4.11 (4H, m), 3.89-3.88 (4H, m), 3.74-3.70 (8H, m), 3.60 (2H, t, $J = 7.68$ Hz), 3.41-3.40 (4H, m), 2.85 (2H, s), 2.68 (2H, t, $J = 7.80$ Hz); ^{13}C NMR (150 MHz, CDCl_3): δ 175.3, 132.1, 131.0, 128.3, 125.6, 121.8, 114.6, 113.9, 70.0, 66.9, 64.4, 62.2, 39.4, 34.3, 33.6, 30.4, 22.5; HRMS-ESI calcd. for $\text{C}_{30}\text{H}_{33}\text{NO}_7\text{Na}$, 542.2155, found 542.2146 $[\text{M}+\text{Na}]^+$.

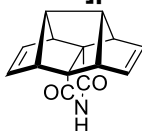
Bicyclo[2.2.1]hept-5-ene-2,3-dicarboximide^[11]

91

A solution of *endo*-carbic anhydride (1.0 g, 6.1 mmol) and NH_4OAc (1.4 g, 18.2 mmol) dissolved in acetic acid (20 mL) was stirred at 140°C for 4 days. The solvent was removed *in vacuo* and the residue diluted with water and extracted with EtOAc (4 x 10 mL). The combined organic phases were dried over MgSO_4 and concentrated under reduced pressure to afford a white crystalline solid, 0.83 g, 84%. MP $170\text{-}173^\circ\text{C}$, lit. MP $170^\circ\text{C}\text{-}172^\circ\text{C}$ ^[11].

^1H NMR (600 MHz, CDCl_3) δ 8.00 (1H, s), 6.20 (2H, s), 3.39-3.38 (2H, m), 3.11-3.30 (2H, m), 1.74 (1H, d, $J = 8.7$ Hz), 1.52 (1H, d, $J = 8.7$ Hz); ^{13}C NMR (150 MHz, CDCl_3) δ 177.9, 134.7, 52.4, 47.4, 45.0; GCMS-Cl calcd for $\text{C}_9\text{H}_9\text{NO}_2 - 163$, found 9.08 min 164 $[\text{M}+\text{H}]^+$.

3-Azahexacyclo[7.6.0.0^{1,5}.0^{5,12}.0^{6,10}.0^{11,15}]pentadeca-7,13-diene-1,2-dione^[12]

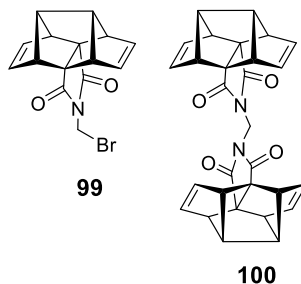


49

Following the Vazquez method, a mixture of diacid **64** (0.20 g, 0.82 mmol) and urea (0.25 g, 4.16 mmol) was heated slowly to 135°C. When the mixture melted, it was heated to 180°C for 30 minutes before being cooled to room temperature. Water (50 mL) was added, and the suspension was extracted with CH_2Cl_2 (6 x 30mL). The combined organic extracts were washed with brine (1 x 45 mL), dried with anhydrous Na_2SO_4 , filtered and concentrated *in vacuo* to dryness to give imide **49** as a white solid, 74 mg, 40%, MP > 245⁰ (dec), lit. MP >245°C (dec)^[12].

^1H NMR (600MHz, CDCl_3) δ 6.09 (4H, t, $J = 1.92$ Hz), 3.47 (4H, s), 2.88 (2H, s); ^{13}C NMR (150 MHz) δ 175.41, 132.39, 68.50, 64.0, 62.57; IR (ATR) $\nu - 3179$ cm^{-1} (N-H, stretch), 1750 cm^{-1} , 1707 cm^{-1} (C=O,stretch).

Hedaya mono bromo and dimer blocks



99

100

Vazquez imide **49** (70 mg, 0.31 mmol) was added to a solution containing dibromomethane (270 mg, 1.55 mmol) and K_2CO_3 (64 mg, 0.61 mmol) in acetone (7 mL) and the resulting solution heated under reflux for 7 hours. The K_2CO_3 was removed by filtration and the filtrate concentrated under reduced pressure. The residue was purified via column chromatography (hexane:ethyl acetate (1:1), silica) to afford monomer **99** (15 mg, 15.2 %) and dimer **100** (72 mg, 48.8%).

99 Monomer - ^1H NMR (600MHz, CDCl_3) δ 6.03 (4H, s), 5.05 (2H, s), 3.54 (4H, s), 2.89 (2H, s); ^{13}C NMR (150 MHz, CDCl_3) δ 173.5, 132.3, 67.3, 64.6, 62.9, 30.3.; HRMS-ESI calcd for $\text{C}_{15}\text{H}_{12}\text{BrNO}_2\text{Na}$ 339.9949, found 339.9961 $[\text{M}+\text{Na}]^+$.

100 Dimer - ^1H NMR (600MHz, CDCl_3) δ 5.95 (4H, s), 4.93 (1H, s), 3.45 (4H, s), 2.84 (2H, s); ^{13}C NMR (150 MHz, CDCl_3) δ 173.6, 132.1, 66.9, 64.4, 62.9, 40.9; HRMS-ESI calcd for $\text{C}_{29}\text{H}_{22}\text{N}_2\text{O}_4\text{Na}$ 485.1477, found 485.1483 $[\text{M}+\text{Na}]^+$.

***N*-Aminobicyclo[2.2.1]hept-2-ene-*endo*-5,*endo*-6-Dicarboximide^[13]**

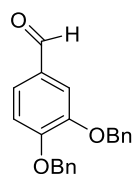


101

To a dispersion of *endo* carbic anhydride (0.492 g, 3 mmol) in benzene (1.5 mL) was added with stirring hydrazine hydrate, (0.198 g, 0.19 mL, 3 mmol, 60-65%). Stirring was continued at room temperature for 2 hr. The precipitate was removed by filtration and washed with cold isopropanol. Compound **101** was recrystallised from isopropanol in 40% yield, MP 147-148 $^{\circ}\text{C}$, lit. MP 146-147 $^{\circ}\text{C}$ ^[14].

^1H NMR (600 MHz, CDCl_3): δ 6.10 (2H, s), 4.10 (2H, s), 3.40 (2H, s), 3.26 (2H, s), 1.77 (1H, d, $J = 5.9$ Hz) 1.62 (1H, d, $J = 5.9$ Hz); ^{13}C NMR (150 MHz, CDCl_3): δ 175.1, 134.8, 52.2, 44.9, 44.4; HRMS-ESI calcd for $\text{C}_9\text{H}_{10}\text{N}_2\text{O}_2\text{Na}$ 201.0640, found 201.0643 $[\text{M}+\text{Na}]^+$.

3, 4-(Dibenzylhydroxy)benzaldehyde

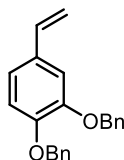


110

Benzyl bromide (0.24 mL, 2.0 mmol) was added to a solution of 3, 4-dihydroxybenzaldehyde (138 mg, 1.0 mmol) and K_2CO_3 (288 mg, 2.1 mmol) in acetone (10 mL). The reaction mixture was heated under reflux for 20 hr. Acetone was removed, and the remaining residue was diluted with diethyl ether (25 mL). The ether was washed with water (2 x 10 mL), dried (Na_2SO_4), and concentrated under reduced pressure to afford the product as an off white solid (2.30g, Quantitative yield). MP 88-91 $^{\circ}\text{C}$, lit.MP 90-91 $^{\circ}\text{C}$ ^[15].

^1H NMR (600MHz, CDCl_3) δ 9.81 (1H, s), 7.49-7.31 (12H, m), 7.02 (1H, d, $J = 8.4$ Hz), 5.26 (2H, s), 5.22 (2H, s); ^{13}C NMR (150MHz, CDCl_3) δ 190.9, 154.3, 149.3, 136.6, 136.3, 130.4, 128.8, 128.7, 128.2, 128.1, 127.4, 127.2, 126.8, 113.1, 112.3, 71.0, 70.9; HRMS-ESI calcd for $\text{C}_{21}\text{H}_{18}\text{O}_3\text{Na}$ 341.1154, found 341.1158 $[\text{M}+\text{Na}]^+$.

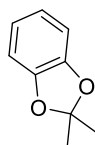
3,4-Bis(benzyloxy)styrene



118a

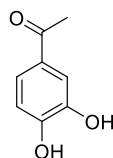
To a suspension of methyltriphenylphosphonium iodide (500 mg, 1.23 mmol) in THF (anhyd, 15 mL) under an argon atmosphere, *n*-BuLi solution (0.70 mL, 1.11 mmol, 1.6 M in hexanes) was slowly added via a syringe maintaining the bath temperature between -25°C and -20°C . The solution was left stirring for 30 min to ensure the production of the ylide. The resulting orange coloured ylide solution was then transferred dropwise via syringe to a well stirred solution of the aldehyde (392 mg, 1.00 mmol) dissolved in THF (anhyd.) at -25°C to -20°C under an argon atmosphere. The reaction mixture was then left stirring to reach room temperature gradually over 0.5 h, and then was rapidly quenched by addition of 2-3 mL water. The reaction solution was extracted with ether (3 x 25 mL) and the residue obtained after work-up was chromatographed on silica gel (EtOAc/MeOH (2 - 5%)) to afford a viscous oil, 130 mg, 33% yield.

^1H NMR (600MHz, CDCl_3) δ 7.43-7.53 (4H, m), 7.37-7.41 (4H, m), 7.34-7.36 (2H, m), 7.11 (1H, d, $J = 2.0$ Hz), 6.97 (1H, dd, $J = 2.0, 8.3$ Hz), 6.93 (1H, d, $J = 8.3$ Hz), 6.66 (1H, dd, $J = 10.8, 17.6$ Hz), 5.62 (1H, d, $J = 17.6$ Hz), 5.21 (4H, d, $J = 10.8$ Hz), 5.18 (1H, d, $J = 10.8$ Hz); ^{13}C NMR (150 MHz, CDCl_3) δ 149.1, 148.9, 137.3, 137.3, 136.4, 131.5, 128.6, 127.9, 127.8, 127.4, 127.3, 120.2, 114.8, 112.6, 112.2, 71.4, 71.3; GCMS-Cl calcd for $\text{C}_9\text{H}_9\text{NO}_2$ 316.2, found 13.9 min 316.2 $[\text{M}]^+$.

1,2-Isopropylidenedioxybenzene^[16]**127**

A mixture of catechol (5.5 g, 50 mmol) and P₂O₅ (1.42 g, 5 mmol) in toluene (25 mL) was heated at 75°C. Acetone (7.35 mL, 100 mmol) was added to the suspension dropwise over 3 h. After the addition had been started, four portions of P₂O₅ (1.42 g, 5 mmol) were added to the reaction mixture every 30 min. In total 8.5 g of P₂O₅ was used. After the addition of the acetone, the mixture was stirred at 75°C for a further 1 h. The residue was washed with NaOH (30 mL, 25% aq.) and the organic layer was separated, washed with water and concentrated *in vacuo* to give an oil, from which **127** was obtained by distillation (77-80°C @ 22.3 mm/Hg) as a colourless liquid 3.54g, 47 % yield.

¹H NMR (600 MHz, CDCl₃) 6.78-6.73 (4H, m), 1.68 (6H, s); ¹³C NMR (150 MHz, CDCl₃) 147.4, 121.1, 117.5, 108.6, 25.9.

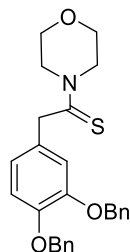
3,4-dihydroxyacetophenone^[17]**125**

2-chloro-3,4-dihydroxyacetophenone (2.5 g, 13.5 mmol) and activated zinc powder (2.5 g, 13.5 mmol) was suspended in THF (60 mL) and acetic acid (15 mL) and the solution stirred vigorously over 2 days at RT. The remaining zinc powder was removed *via* filtration and the THF removed *in vacuo* with the residue being redissolved in EtOAc (50 mL). The organic layer was washed with water (3 x 50 mL) and dried over Na₂SO₄. The solvent was removed *in vacuo* and purified *via* column chromatography (Hex: EtOAc, 1:1) to give an off white powder (quantitative yield, 2.0g). MP 120-123°C, lit. 120-121°C.^[17]

¹H NMR (600 MHz, CDCl₃) 7.65 (1H, d, J = 1.86 Hz), 7.50 (1H, dd, J = 1.92, 8.3 Hz), 6.94 (1H, d, J = 8.3 Hz), 2.56 (3H, s); ¹³C NMR (150 MHz, CDCl₃) 197.8,

149.3, 143.6, 130.5, 123.6, 114.9, 114.7, 26.3; GCMS-Cl calcd for C₈H₈O₃ 152, found 9.8 min 152 [M]⁺.

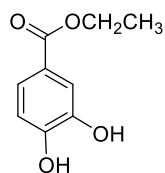
Wilgerodt Kindler - Morpholide



131

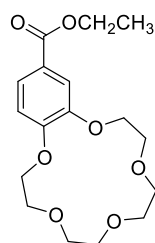
To 3,4-dihydroxyacetophenone (286 mg, 0.86 mmol) was added Sulphur (70 mg, 2.15 mmol) and morpholine (150 μ L, 1.72 mmol) and the solution heated under reflux for 5 hrs. DCM (2 mL) and H₂O were added to the cooled reaction mixture and the DCM layer separated. The aqueous layer was extracted with DCM (2 x 5 mL). The combined DCM layers were washed with HCl solution (10%, 5 mL) and water (5 mL). The organic layer was dried over Na₂SO₄ and concentrated *in vacuo* to afford brown residue which was purified *via* column chromatography (Hexane:EtOAc, 1:1) to afford beige solid. MP > dec 220°C.

¹H NMR (600 MHz, CDCl₃) 7.44 (4H, d, J = 7.74 Hz), 7.37-7.34 (4H, m), 7.31-7.29 (2H, m), 6.96-6.95 (1H, m), 6.96 (1H, d, J = 8.22 Hz), 6.77-6.76 (1H, m), 5.17 (2H, s), 5.16 (2H, s), 4.25 (2H, t, J = 4.8 Hz), 4.20 (2H, s), 3.60 (2H, t, J = 4.8 Hz), 3.46 (2H, t, J = 4.8 Hz), 3.23 (2H, t, J = 4.8 Hz); ¹³C NMR (150 MHz, CDCl₃) 200.1, 149.1, 148.3, 137.3, 137.2, 128.8, 128.9, 128.6, 128.5, 127.9, 127.5, 127.2, 120.76, 115.5, 114.7, 71.5, 71.1, 66.4, 66.2, 50.8, 50.3, 50.2; HRMS-ESI calcd for C₂₆H₂₇NO₃SNa 456.1609, found 456.1609 [M+Na]⁺.

Ethyl 3, 4-dihydroxybenzoate**134**

3, 4-dihydroxybenzoic acid (10 g, 65.0 mmol) was dissolved in ethanol (40 mL) along with H₂SO₄ (conc. 5 mL) and the solution heated under reflux for 3 hr. Upon cooling, ethanol was removed *in vacuo* and the residue was redissolved in EtOAc (40 mL). The organic phase was washed with NaHCO₃ (10%) solution, H₂O, and dried over Na₂SO₄. The solvent was removed *in vacuo* to produce the ethyl ester as a white solid, 10.8 g, 91 % yield. MP 131-134°C, lit. MP 132-134°C.^[18]

¹H NMR (600 MHz, CDCl₃) δ 9.58 (2H, bs, C-OH), 7.29-7.39 (2H, m), 6.79-6.81 (1H, m), 4.21 (2H, q, J = 7.1 Hz), 1.27 (3H, t, J = 7.1 Hz); ¹³C NMR (150 MHz, CDCl₃) δ 165.7, 150.4, 145.1, 121.9, 121.8, 116.6, 115.3, 60.1, 14.3; HRMS-ESI calcd for C₉H₁₀O₄Na 205.0477, found 205.0483 [M+Na]⁺.

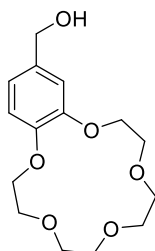
4-Ethoxycarbonyl-benzo-15-Crown-5^[19]**135**

K₂CO₃ (8.4 g, 60.8 mmol) was added with stirring to DMF (150 mL). The mixture was heated to 150°C and 3,4-dihydroxybenzoate (5.0 g, 27.4 mmol) and tetraethylene glycol dichloride (6.4 g, 27.7 mmol) were added dropwise. The reaction was maintained at 150°C over 24 hr. The reaction mixture was cooled and the DMF removed *in vacuo*. The crude material was extracted with DCM (2 x 50 mL) and the organic phase was washed with H₂O, dried over Na₂SO₄ and concentrated to dryness. The residue was extracted repeatedly with hot hexane to afford **135** as a white powder, 2.8 g, 40% yield, MP 65-68°C, lit. MP 65±1°C^[19]

¹H NMR (600 MHz, CDCl₃) δ 7.66 (1H, dd, J = 1.96, 8.4 Hz), 7.53 (1H, d, J = 8.4 Hz), 6.85 (1H, d, J = 8.4 Hz), 4.36 (2H, q, J = 7.1 Hz), 4.17-4.20 (4H, m), 3.90-

3.93 (4H, m), 3.76 (8H, m), 1.37 (3H, t, $J = 7.1$ Hz); ^{13}C NMR (150 MHz, CDCl_3) δ 166.5, 153.2, 148.5, 124.0, 123.3, 114.6, 112.1, 71.3, 70.5, 70.4, 69.5, 69.4, 69.1, 68.7, 14.5; HRMS-ESI calcd for $\text{C}_{17}\text{H}_{24}\text{O}_7\text{Na}$ 363.1420, found 363.1409 $[\text{M}+\text{Na}]^+$.

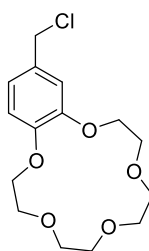
4-Hydroxymethylbenzo-15-Crown-5^[20]



136

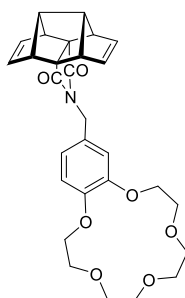
Compound **135** (1.5g, 44 mmol) in anhydrous THF (60 mL) was added dropwise to a slurry of LiAlH_4 (0.42 g, 110 mmol, 2.50 eq) in anhydrous THF (50 mL) whilst stirring vigorously under an N_2 atmosphere. Subsequently the reaction mixture was heated under reflux overnight. The reaction was cooled and water (10 mL) was added. The reaction mixture was poured cautiously onto ice water and treated with a few drops of conc. HCl. The water /THF solution was filtered through celite and the THF was removed *in vacuo*. The aqueous phase was extracted with DCM (3 x 30 mL), dried MgSO_4 and vacuum concentrated to afford a yellow oil, 1.23 g, 90% yield.

^1H NMR (600 MHz, CDCl_3) δ 6.94-6.83 (3H, m), 4.59 (2H, s), 4.15-4.11 (4H, m), 3.91-3.89 (4H, m), 3.74 (8H, m); ^{13}C NMR (150 MHz, CDCl_3) δ 149.8, 149.3, 134.3, 120.0, 114.0, 113.1, 71.4, 70.6, 69.7, 69.2, 68.9, 65.3; HRMS-ESI calcd for $\text{C}_{15}\text{H}_{22}\text{O}_6\text{Na}$ 321.1314, found 321.1321 $[\text{M}+\text{Na}]^+$.

4-Chloromethylbenzo-15-Crown-5^[20]**132**

Triethylamine (0.60 g, 5.88 mmol, 0.82 mL) was added to **136** (1.6 g, 5.35 mmol) in DCM (32 mL) and the resulting mixture was cooled to -5°C . Thionyl chloride (0.96 g, 8.02 mmol, 0.58 mL) in DCM (10 mL) was added dropwise whilst under a N_2 atmosphere. The resulting reaction was kept at -5°C for a further 45 minutes before stirring at room temperature for 3 hrs. The reaction mixture was washed with H_2O (100 mL), saturated aqueous NaHCO_3 (100 mL), 2M HCl (100 mL) and H_2O (2 x 100 mL) and dried over MgSO_4 . The solvent was removed *in vacuo* affording the crude product as a colourless oil which was purified via crystallisation (hexane: diethyl ether (50:5 v/v)) at -15°C to give **132**, 0.775g, 45% yield.

^1H NMR (600 MHz, CDCl_3) δ 6.88-6.90 (2H, m), 6.79-6.80 (1H, m), 4.52 (2H, s), 4.14-4.10 (4H, m), 3.88-3.90 (4H, m), 3.75 (8H, m); ^{13}C NMR (150 MHz, CDCl_3) δ 149.4, 149.3, 130.5, 121.8, 114.5, 113.7, 71.2, 70.54 69.6, 69.9, 69.1, 46.7.

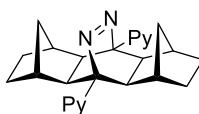
Hedaya Block Methylene Linker**133**

Compound **42** (70 mg, 0.22 mmol) and **132** (70 mg, 0.22 mmol) along with K_2CO_3 were placed in acetone (3 mL) and the solution heated under reflux for 7 hours and cooled. K_2CO_3 was removed by filtration, the residue concentrated and

purified via column chromatography hexane:ethyl acetate (1:4) to afford a colourless oil **133** 1.6g , 45% yield. MP 148-151°C.

^1H NMR (600 MHz, CDCl_3) δ 6.76-6.69 (3H, m), 5.92 (4H, s), 4.41 (2H, s), 4.06-4.05 (4H, m), 3.87-3.85 (4H, m), 3.72-3.70 (8H, m), 3.44 (4H, s), 2.85 (2H, s); ^{13}C NMR (150 MHz, CDCl_3) δ 175.2, 148.6, 148.2, 132.2, 129.8, 121.3, 113.8, 113.3, 70.4, 70.2, 68.6, 69.9, 64.5, 62.3, 60.5, 41.8; HRMS-ESI calcd for $\text{C}_{29}\text{H}_{31}\text{O}_7\text{Na}$ 528.1998, found 528.1995 $[\text{M}+\text{Na}]^+$.

Norbornene s-Tetrazine

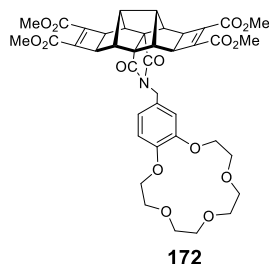


Py = 2-pyridyl

150c

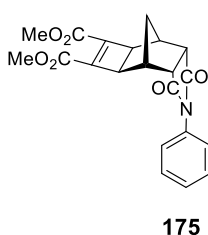
Norbornene (100 mg, 1.06 mmol) was dissolved in DCM (<2 mL) along with 2-pyridyl s-tetrazine (125 mg, 0.53 mmol) with 3 drops of TEA. The reaction was stirred at room temperature for 2 hours, where a colour change from purple to yellow occurred. The reaction solution was subjected to high pressure (14 kbar) for 48 hours. The reaction mixture was diluted with CH_2Cl_2 (10 mL) and washed with water, dried (Na_2SO_4) and concentrated *in vacuo* to afford an off white product without purification (150 mg, 40% yield). MP > dec 200°C.

^1H NMR (600MHz, CDCl_3) 7.71-7.68 (4H, m), 7.29-7.28 (2H, m), 7.24-7.22 (2H, m), 2.68 (4H, s), 1.33-1.31 (4H, m), 1.11-1.09 (4H, m), 1.02-1.01 (1H, m), 1.02-1.00 (4H, m), 0.40 (2H, d, J = 12 Hz); HRMS-ESI calcd for $\text{C}_{26}\text{H}_{30}\text{N}_4$ 397.2392, found 397.2387 $[\text{M}+\text{H}]^+$.

Hedaya Cyclobutene Diester Methylene Linked Benzo-15-crown-5

Compound **133** (100.0 mg, 0.42 mmol) was added, along with DMAD (118.9 mg, 0.84 mmol) and Ru Catalyst (20 mol%, 76.0 mg, 8.4 mmol), to toluene (5 mL) and the resulting solution heated at 80^oC for 12 hours. Toluene was removed *in vacuo* and the residue redissolved in chloroform. The product was separated via column chromatography (4% THF in CHCl₃) to afford a white solid, (85 mg, 54% yield). MP 145-147^oC.

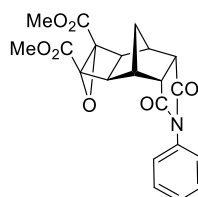
¹H NMR (600 MHz, CDCl₃) δ 6.90-6.88 (2H, m), 6.75-6.73 (1H, m), 4.52 (2H, s), 4.12-4.09 (4H, m), 3.88-3.86 (4H, m), 3.76 (12H, s), 3.74-3.76 (8H, m) 3.00 (4H, s), 2.85 (4H, s), 2.48 (2H, s); ¹³C NMR (150MHz, CDCl₃) δ 173.8, 160.8, 148.9, 148.7, 141.4, 129.5, 121.8, 114.7, 113.5, 71.1, 70.4, 69.5, 68.9, 68.7, 60.4, 53.2, 52.2, 44.8, 42.2, 41.3; HRMS-ESI calcd for C₄₁H₄₃NO₁₅Na 812.2530, found 812.2527 [M+Na]⁺.

endo-Cyclobutene Diester Block

Compound **174** (100.0 mg, 0.42 mmol) was added, along with DMAD (118.9 mg, 0.84 mmol) and RuH₂CO(P(Ph)₃)₃ catalyst (20 mol%, 76.0 mg, 8.4 μmol), to DMF (5 mL) and the solution was heated at 80^oC for 12 hours. DMF was removed *in vacuo* and the residue redissolved in chloroform. The product was separated via column chromatography (4% THF in CHCl₃) to afford white solid, (116 mg, 53% yield). MP 205-207^oC.

^1H NMR (600MHz, CDCl_3) δ 7.47-7.44 (2H, m), 7.406-7.38 (1H, m), 7.21-7.20 (2H, m), 3.77 (6H, s), 3.40-3.39 (2H, m), 2.99 (2H, s), 2.94-2.93 (2H, m), 1.81 (1H, d, $J = 12$ Hz), 1.55 (1H, d, $J = 12$ Hz); ^{13}C NMR (150MHz, CDCl_3) δ 176.0, 160.8, 141.3, 131.7, 129.4, 129.0, 126.7, 52.2, 47.63, 42.7, 36.8, 34.4; HRMS-ESI calcd for $\text{C}_{21}\text{H}_{19}\text{NO}_6\text{Na}$ 404.1110, found 404.1100 $[\text{M}+\text{Na}]^+$.

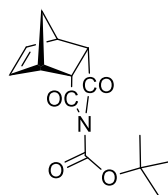
endo-epoxide Block



176

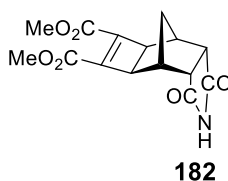
Cyclobutene **175** (200 mg, 0.52 mmol) was dissolved in THF (30 mL). Tert-butyl hydroperoxide (590 mg, 200 μl , 0.65 mmol) was added at room temperature and stirred for 10 minutes before the addition of K-tert butoxide (29 mg, 0.26 mmol, 0.5 eq) at 0°C. The reaction was allowed to proceed for 4 hr before being quenched with sodium bisulfite solution (10%). The reaction mixture was diluted with chloroform and the organic phase separated. The organic phase was washed with brine, water, dried (Na_2SO_4) and concentrated under vacuum to afford a beige residue, 145 mg, 70% yield.

^1H NMR (600 MHz, CDCl_3) 7.17-7.16 (2H, m), 7.43-7.38 (1H, m), 7.48-7.45 (2H, m), 3.76 (6H, s), 3.36-3.35 (2H, m), 3.29-3.28 (2H, m), 2.55 (2H, s), 2.13 (1H, d, $J = 12$ Hz), 1.75 (1H, d, $J = 12$ Hz); ^{13}C NMR (600 MHz, CDCl_3) 175.6, 163.7, 131.4, 129.2, 128.7, 126.5, 63.8, 52.6, 45.8, 45.6, 39.2, 36.8; HRMS-ESI calcd for $\text{C}_{21}\text{H}_{19}\text{O}_7\text{N}$ 397.1162, found 397.1159 $[\text{M}]^+$.

endo-Boc Protected Block**180**

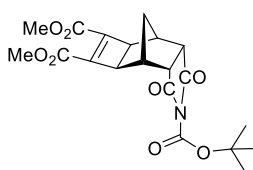
A solution of the imide **91** (0.5 g, 2.7 mmol), Boc₂O (0.75g, 3.4 mmol), and DMAP (1-2mg) in CH₂Cl₂ (20 mL) was stirred for 16 hr at RT. Water (5 mL) was added and the mixture was extracted with CH₂Cl₂ (2 × 30 mL). The combined organic layers were washed with brine (30 mL) and dried over MgSO₄. Evaporation of the solvent under reduced pressure afforded a beige solid, 450 mg, 64 % yield. MP 177-179°C.

¹H NMR (600 MHz, CDCl₃) 6.16 (2H, bs), 3.38-3.37 (2H, m), 3.27-3.26 (2H, m), 1.67-1.65 (1H, m), 1.46-1.45 (10H, m); ¹³C NMR (600 MHz, CDCl₃) 173.8, 146.4, 134.8, 85.9, 52.4, 46.2, 45.7, 27.8; HRMS-ESI calcd for C₁₄H₁₇O₄N 263.1158, found 163.0628 [M-BOC+2H]⁺.

endo-Cyclobutene Imide Block**182**

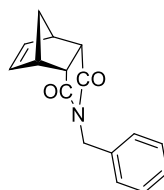
A solution of **91** (120 mg, 0.74 mmol), RuH₂(CO)(PPh₃) (30 mg, 0.03 mmol, 0.2 %) and DMAD (0.19 mL, 2.1 mmol) in toluene was heated under reflux overnight. The reaction mixture was cooled, filtered (Whatman No. 1) and the solvent removed under reduced pressure. The crude material thus obtained was subjected to column chromatography using 4-20% THF/CHCl₃ as eluent yielding **182**, 50mg, 36% yield. MP 161-163°C.

¹H NMR (600 MHz, CDCl₃) 1.41 (1H, d, J = 7.6 Hz), 1.68 (1H, d, J = 7.6 Hz), 2.75 (2H, s), 2.88 (2H, s), 3.23-3.22 (2H, m) 3.69 (6H, s); ¹³C NMR (150 MHz, CDCl₃) δ 177.7, 160.7, 141.1, 52.0, 48.9, 42.5, 35.9, 34.4; GCMS-Cl calcd for C₁₅H₁₅NO₆ 305, found at 14.1 min, 306 [M+H]⁺.

endo-Cyclobutene Boc Protected Imide Block**183**

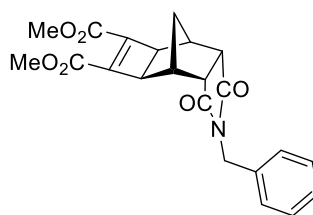
A solution of imide (50 mg, 0.27 mmol), Boc₂O (87 mg, 0.40 mmol) and DMAP (1-2mg) in CH₂Cl₂ (10 mL) was stirred for 16 hr at RT. Water (5 mL) was added and the mixture was extracted with CH₂Cl₂ (2 × 10 mL). The combined organic layers were washed with brine (20 mL) and dried over MgSO₄. Evaporation of the solvent under reduced pressure afforded a brown viscous oil 35 mg, 45% yield.

¹H NMR (600 MHz, CDCl₃) 3.76 (6H, s), 3.26-3.25 (2H, m), 2.99 (2H, s), 2.87 (2H, s), 1.76 (1H, d, J= 11.4 Hz), 1.55 (9H, s), 1.45 (1H, d, J= 11.4 Hz); ¹³C NMR (150 MHz, CDCl₃) 172.7, 160.5, 145.9, 140.9, 86.4, 47.5, 42.2, 38.9, 36.7, 33.9, 27.6; HRMS-ESI calcd for C₂₀H₂₃O₈N 405.1424, found 305.0894 [M-BOC+2H]⁺.

endo-N-Benzylbicyclo[2.2.1]hept-2-ene-5,6-dicarboximide**185**

Compound **91** (500 mg, 3.0 mmol) was allowed to react with K₂CO₃ (1.6 g, 12 mmol) and BnBr (0.36 mL, 3.0 mmol) in acetone (20 mL) with stirring under reflux conditions for 24 hours. Acetone was removed under reduced pressure and the residue redissolved into ether, washed with water, brine and dried over Na₂SO₄. The solvent was removed under reduced pressure to afford **185**, 385 mg, 74 % yield. MP 87-89°C.

¹H NMR (600 MHz, CDCl₃) 7.29-7.25 (5H, m), 5.91 (2H, m), 4.51 (2H, s), 3.39-3.38 (2H, m), 3.28-3.27 (2H, m), 1.71 (1H, d, J = 8.7 Hz) 1.54 (1 H, d, J= 8.7 Hz); ¹³C NMR (150 MHz, CDCl₃) 147.6, 136.1, 134.5, 129.0, 128.5, 127.9, 52.3, 45.8, 45.1, 42.1; GCMS-Cl calcd for C₁₆H₁₅NO₂ 253, found 9.8 min 254 [M+H]⁺.

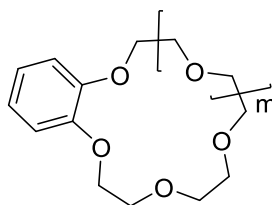
endo-Cyclobutene Benzyl Protected Imide Block**186**

Compound **182** (50 mg, 0.16 mmol) was allowed to react with K_2CO_3 (113 mg, 0.82 mmol) and BnBr (0.02 mL, 0.16 mmol) in acetone (4 mL) with stirring under reflux conditions for 24 hours. Acetone was removed under reduced pressure and the residue redissolved into ether, washed with water, brine and dried over Na_2SO_4 . The solvent was removed under reduced pressure to afford **186** as semi-solid, 48mg, 74 % yield.

1H NMR (600MHz, $CDCl_3$) 7.41-7.33 (2H, m), 7.31-7.28 (3H, m), 4.62 (2H, s), 3.77 (6H, s), 3.24-3.23 (2H, m), 2.84 (2H, s), 2.56 (2H, s), 1.72 (1H, d, $J = 7.6$ Hz), 1.46 (1H, d, $J = 7.6$ Hz); ^{13}C NMR (150MHz, $CDCl_3$) 176.6, 160.7, 141.2, 135.9, 129.1, 128.8, 128.3, 52.1, 47.5, 42.4, 42.4, 36.4, 34.4, 33.7.

3,3-Dimethyl-1,2-dioxirane (DMDO)^[21]**197**

To a solution of water (63.5 mL) and acetone (48 mL) was added $NaHCO_3$ (14.5 g) with vigorous stirring at 5-10°C. Oxone (30 g, 197 mmol) was added in 5 portions over 3 minutes. Three minutes after the last addition, a moderate vacuum (80-100 Torr) was applied. The cold bath was removed and a -78°C bath was placed under the receiving flask. The dimethyl dioxirane was collected at -78°C in acetone. The acetone solution was dried with K_2CO_3 and stored in the freezer over molecular sieves 4Å. The approximate concentration and yield of dimethyldioxirane was between 0.09M-0.11M, ca 5% yield.

Benzocrown ethers (m = 1, 2, 3) [7]**6a, 6b, 6c**

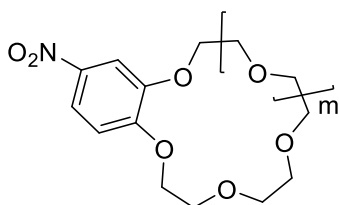
General procedure:

To a stirred solution of catechol (3.3 g, 30 mmol) and Bu_4NI (2.8 g, 7.5 mmol) in toluene (180 mL) was added aq. NaOH (60 mL, 50%) at 50–60 °C. The mixture was stirred at this temperature for a further 30 min, whereupon a solution of tetraethylene glycol di(p-toluenesulfonate) (15.1 g, 30 mmol) in toluene (180 mL) was added. The resulting mixture was vigorously stirred at under reflux for 16 h. The organic layer was separated and washed with water (3 x 150 mL), brine (100 mL), and dried over anhydrous MgSO_4 . The solvent was removed under reduced pressure to afford a semisolid. Further purification was performed by recrystallization from hexane to afford the benzocrown ether as white crystalline solid.

6a 15-Crown-5 - 3.2g, 40%, MP 79-81°C, lit. MP 78-80 °C^[22]; ^1H NMR (600 MHz, CDCl_3) 6.92-6.87 (4H, m), 4.15-4.13 (4H, m), 3.92-3.91 (4H, m), 3.77 (8H, m); ^{13}C NMR (150 MHz, CDCl_3) 149.2, 121.5, 114.2, 71.1, 70.6, 69.7, 69.1; HRMS-ESI calcd for $\text{C}_{14}\text{H}_{20}\text{O}_5$ 268.1311, found 268.1305 $[\text{M}]^+$.

6b 18-Crown-6 – 1.2g, 20%, MP 41-44°C, lit. 43-44°C^[23]; ^1H NMR (600 MHz, CDCl_3) 6.89-6.88 (4H, m), 4.16-4.15 (4H, m), 3.93-3.92 (4H, m), 3.71-3.78 (8H, m), 3.68-3.66 (4H, m); ^{13}C NMR (150 MHz, CDCl_3) 149.2, 121.6, 114.6, 71.0, 70.9, 70.9, 70.8, 70.7, 70.4, 70.3, 69.8, 69.7, 69.3; HRMS-ESI calcd for $\text{C}_{16}\text{H}_{24}\text{O}_6\text{Na}$ 335.1471, found 335.1472 $[\text{M}+\text{Na}]^+$.

6c 21-Crown-7 – 0.952g, 15%, MP 130-132°C lit. MP 134-135^[24]; ^1H NMR (600 MHz, CDCl_3) 6.94-6.89 (4H, m), 4.19-4.17 (4H, m), 3.91-3.89 (4H, m), 3.75-3.74 (4H, m), 3.68-3.67 (4H, m), 3.66-3.65 (8H, m); ^{13}C NMR (150 MHz, CDCl_3) 148.43, 122.0, 114.10, 70.1, 69.9, 69.8, 69.8, 69.4, 68.3, 66.8; ; HRMS-ESI calcd for $\text{C}_{18}\text{H}_{28}\text{O}_7\text{K}$ 395.1472, found 395.1476 $[\text{M}+\text{K}]^+$.

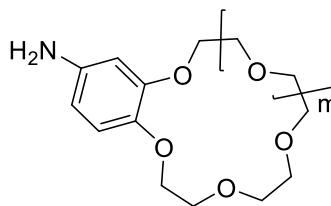
4-Nitrobenzo crown ethers (m = 1, 2, 3)**199a, 199b, 199c****General Procedure:**

Concentrated nitric acid (0.30 mL) was added to a stirring solution of benzocrown ether (0.80 mmol) in DCM (15 mL). The solution was allowed to stir at room temperature for 24 hours. The organic layer was washed with water (3 x 30 mL), dried over sodium sulphate, filtered and the solvent removed under reduced pressure to afford the oily product which solidified on standing.

199a 15-Crown-5 - 0.285g, 97%, MP 96-98°C, lit. MP 94-96^[25]; ¹H NMR (600 MHz, CDCl₃) δ 7.89 (1H, dd, J = 2.6, 8.9 Hz), 7.72 (1H, d, J = 2.6 Hz), 6.87 (1H, d, J = 8.9 Hz), 4.22-4.19 (4H, m), 3.94-3.92 (4H, m), 3.77-3.74 (8H, m); ¹³C NMR (150 MHz, CDCl₃) δ 154.72, 148.71, 141.54, 118.21, 111.32, 108.44, 71.23, 70.33, 70.25, 69.13, 69.11, 69.07, 68.96; HRMS-ESI calcd for C₁₄H₁₉NO₇ 313.1162, found 313.1156 [M]⁺.

199b 18-Crown-6 - 0.25 g, 95%, MP 71-73°C, lit MP 70-72°C^[26]; ¹H NMR (600 MHz, CDCl₃) δ 7.88 (1H, dd, J = 2.6, 8.9 Hz), 7.71 (1H, d, J = 2.6 Hz), 6.87 (1H, d, J = 8.9 Hz), 4.22-4.20 (4H, m), 3.93-3.91 (4H, m), 3.75-3.73 (8H, m), 3.70-3.67 (4H, m); ¹³C NMR (150 MHz, CDCl₃) δ 154.3, 148.4, 141.5, 118.0, 111.24, 108.06, 70.9, 70.8, 70.7, 70.6, 70.5, 70.4, 69.2, 69.1, 69.0, 68.9; HRMS calcd for C₁₆H₂₃NO₈Na 380.1321, found 380.1304 [M+Na]⁺.

199c 21-Crown-7 - 0.450g, quantitative, MP 66-68°C, lit. MP 67-68°C^[26]; ¹H NMR (600 MHz, CDCl₃) δ 7.91 (1H, dd, J = 2.6, 8.9 Hz), 7.77 (1H, d, J = 2.6 Hz), 6.92 (1H, d, J = 8.9 Hz), 4.26-4.24 (4H, m), 3.97-3.96 (4H, m), 3.82-3.80 (4H, m), 3.76-3.75 (4H, m), 3.70-3.68 (8H, m); ¹³C NMR (150 MHz, CDCl₃) δ 154.4, 148.5, 141.5, 118.0, 111.6, 108.5, 71.4, 71.3, 71.1, 71.0, 70.6, 70.5, 69.5, 69.4, 69.3; HRMS calcd for C₁₈H₂₉NO₇Na, 440.1323 found 440.1302 [M+Na]⁺.

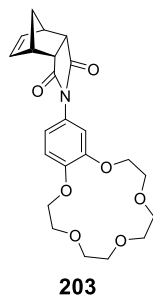
4-Aminobenzo crown ethers (m = 1, 2, 3)**200a, 200b, 200c****General Procedure:**

Benzocrown ether (0.40g, 1.40 mmol) was dissolved in absolute ethanol and hydrogenated with hydrazine hydrate over palladium on carbon (10%). The reaction was heated under reflux for 24 hours, filtered over celite and the solvent removed under reduced pressure. Water was added and the residue extracted with DCM, with combined organic extracts dried over Na_2SO_4 , filtered and concentrated to afford a yellow oil.

200a 15-Crown-5 – 0.30 g, 82%; ^1H NMR (600 MHz, CDCl_3) 6.71 (1H, d, $J = 8.4$ Hz), 6.26 (1H, d, $J = 2.6$ Hz), 6.20 (1H, dd, $J = 2.6, 8.4$ Hz), 4.07-4.03 (4H, m), 3.88-3.85 (4H, m), 3.74-3.73 (8H, m), 3.40 (2H, bs, (N-H)); ^{13}C NMR (150 MHz, CDCl_3) 150.4, 141.8, 141.6, 117.2, 107.3, 102.5, 70.9, 70.8, 70.7, 70.6, 70.4, 69.9, 69.5, 68.5, 53.6; HRMS calcd for $\text{C}_{14}\text{H}_{21}\text{NO}_5$ 283.1420, found 283.1414 $[\text{M}]^+$.

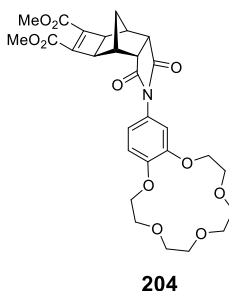
200b 18-Crown-6 – 0.27g, 74%; ^1H NMR (600 MHz, CDCl_3) δ 6.71 (1H, d, $J = 8.4$ Hz), 6.28 (1H, d, $J = 2.6$ Hz), 6.20 (1H, dd, $J = 2.6, 8.4$ Hz), 4.10-4.07 (4H, m), 3.86-3.75 (4H, m), 3.74-3.72 (8H, m), 3.71-3.67 (4H, m); ^{13}C NMR (150 MHz, CDCl_3) δ 150.2, 141.7, 141.6, 117.0, 107.4, 102.8, 70.8, 70.7, 70.6, 70.3, 70.2, 70.0, 69.7, 69.8; HRMS calcd for $\text{C}_{16}\text{H}_{25}\text{NO}_6\text{Na}$ 350.1580, found 350.1567 $[\text{M}+\text{Na}]^+$.

200c 21-Crown-7 – 0.25g, 67%; ^1H NMR (600 MHz, CDCl_3) δ 6.73 (1H, d, $J = 8.4\text{Hz}$), 6.28 (1H, d, $J = 2.6\text{Hz}$), 6.21 (1H, dd, $J = 2.6, 8.4$ Hz), 4.11-4.07 (4H, m), 3.91-3.86 (4H, m), 3.78-3.76 (4H, m), 3.71-3.68 (4H, m), 3.67-3.66 (8H, m); ^{13}C NMR (150 MHz, CDCl_3) δ 150.3, 141.7, 141.5, 117.5, 107.4, 102.8, 71.2, 71.1, 71.0, 70.9, 70.6, 70.5, 70.2, 69.8, 69.0; HRMS calcd for $\text{C}_{18}\text{H}_{29}\text{NO}_7\text{Na}$ 394.1842, found 394.1843 $[\text{M}+\text{Na}]^+$.

endo-Benzo 15-Crown-5 Block

A mixture of **93** (50mg, 0.30 mmol) and compound **200a** (130mg, 0.46 mmol) were added to acetic acid (2 mL) and heated under reflux for 18 hours. The resulting mixture was cooled to room temperature and the solvent removed *in vacuo*. The residue was redissolved in chloroform and washed with water. The chloroform was removed under reduced pressure and the residue subjected to column chromatography, EtOAc: MeOH (4%) to afford a white amorphous solid **203** (76 mg, 58 %). MP 131-133°C;

^1H NMR (600 MHz, CDCl_3) δ 6.86 (1H, d, $J = 8.5$ Hz), 6.67 (1H, dd, $J = 2.34, 8.4$ Hz), 6.62 (1H, d, $J = 2.34$ Hz), 6.23-6.22 (2H, m), 4.11-4.08 (4H, m), 3.88-3.86 (4H, m), 3.72-3.71 (8H, m), 3.47-3.46 (2H, m), 3.38-3.37 (2H, m), 1.76 (1H, d, $J = 8.82$ Hz), 1.59 (1H, d, $J = 8.82$ Hz); ^{13}C NMR (150 MHz, CDCl_3) δ 177.1, 149.4, 149.3, 134.7, 125.1, 119.8, 113.9, 112.9, 71.3, 71.2, 70.6, 70.6, 69.5, 69.5, 69.3, 69.3, 52.4, 45.8, 45.6; HRMS calcd for $\text{C}_{23}\text{H}_{27}\text{NO}_7$ 452.1685, found 452.1668 $[\text{M}]^+$.

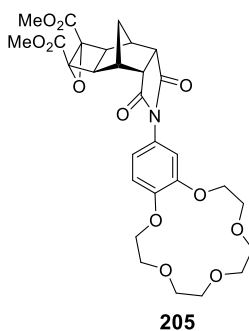
endo-Benzo 15-Crown-5 Cylcobutene Diester Block

A solution of **203** (200 mg, 0.74 mmol), $\text{RuH}_2(\text{CO})(\text{PPh}_3)$ (225 mg, 0.2 mol%) and DMAD (0.31 mL, 2.1 mmol) in toluene (10 mL) was heated under reflux for 72 hr. The reaction mixture was cooled, filtered and the solvent removed under reduced pressure. The crude material obtained was subject to column chromatography

using 4-20% THF/CHCl₃ as eluent to afford brown semi-solid, 245mg, 65% yield. MP 84-86°C.

¹H NMR (600 MHz, CDCl₃) 6.94 (1H, d, J = 8.5Hz), 6.79 (1H, dd, J = 2.3, 8.5 Hz), 6.78 (1H, d, J = 2.3 Hz), 4.17-4.14 (4H, m), 3.93-3.90 (4H, m), 3.80 (6H, s), 3.76-3.72 (8H, m), 3.39-3.38 (2H, m), 2.96 (2H, s), 2.95 (2H, m), 1.82 (1H, d, J = 11.5 Hz), 1.56 (1H, d, J = 11.5 Hz); ¹³C NMR (150 MHz, CDCl₃) 176.2, 160.8, 141.3, 125.6, 124.7, 119.7, 113.8, 112.7, 99.8, 71.2, 70.5, 69.5, 69.2, 68.1, 52.2 47.5, 42.6, 36.7, 34.3, 31.08, 30.4, 25.7; HRMS-ESI calcd for C₂₉H₃₄NO₁₁, 572.2132, found 572.2126 [M+H]⁺.

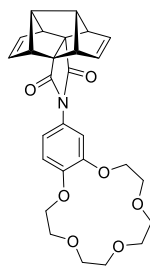
endo-Benzo 15-Crown-5 Mono Epoxide Block



Compound **204** (50 mg, 0.087 mmol) was dissolved in THF (2 mL) under a nitrogen atmosphere and the solution cooled to -78°C. ^tBuOOH (30 μl, 0.11 mmol, 1.4 eq) was added and the solution allowed to stir for 10 mins at which point MeLi (65 μl, 1.5 eq) was added. Stirring was continued for 20 mins before warming the solution to room temperature for 2.5 hrs. DCM (10 mL). Sodium bisulfite solution (10%) was added to the reaction mixture and the organic phase was separated washed with water, and dried over Na₂SO₄. The solvent was removed under reduced pressure to afford the crude epoxide as a brown semi-solid (35 mg, 68 %).

¹H NMR (600MHz, CDCl₃) 6.90 (1H, d, J = 8.5 Hz), 6.71 (1H, d, J = 8.5 Hz), 6.65 (1H, s), 4.14-4.10 (4H, m), 3.90-3.89 (4H, m), 3.81 (6H, s), 3.76-3.72 (8H, m), 3.42-3.39 (2H, m), 3.33-3.31 (2H, m), 2.58-2.55 (2H, m), 2.18 (1H, d, J = 11.5 Hz), 1.79 (1H, d, J = 11.5 Hz); HRMS calcd for C₂₉H₃₃NO₁₂ 587.2003, found 587.1997 [M]⁺.

Hedaya Benzo 15-Crown-5 Block

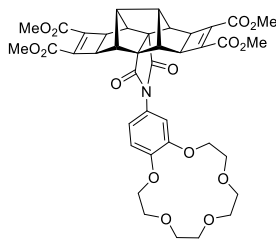


197

Under N_2 , a solution of Hedaya anhydride **42** (1.70 g, 7.5 mmol) and 4-aminobenzo-15-crown-5 **200a** (3.19 g, 11.26 mmol) in glacial acetic acid (10 mL) was stirred at under reflux conditions for 24 hr. The reaction mixture was cooled to room temperature and the residual solvent was removed *in vacuo*. The residue was redissolved in $CHCl_3$ and washed with water (2 x 20 mL). Drying (Na_2SO_4) and concentration *in vacuo* gave a purple/brown mixture. Column chromatography (1:5 ethyl acetate /chloroform) was performed on the residue to give a white solid (1.07 g, 30 %). MP 128-130°C.

1H NMR (600 MHz, $CDCl_3$) δ 6.84 (1H, d, $J = 8.5$ Hz), 6.62 (1H, dd, $J = 2.34, 8.4$ Hz), 6.56 (1H, d, $J = 2.34$ Hz), 6.10-6.09 (4H, m), 4.11-4.07 (4H, m), 3.87-3.84 (4H, m), 3.73-3.69 (8H, m), 3.55-3.52 (4H, m), 2.91-2.89 (2H, m); ^{13}C NMR (150 MHz, $CDCl_3$) δ 174.8, 149.3, 149.1, 132.3, 125.2, 120.2, 113.7, 113.4, 71.1, 70.6, 70.5, 69.5, 69.4, 69.3, 69.2, 66.7, 64.5, 62.6. HRMS calcd for $C_{28}H_{29}NO_7$ 491.1944, found 491.1939 $[M]^+$. IR (ATR) - 1705 (C=O), 1264 (Ar-O), 1120 (C-O-C), 1053 (C-O), 870 (Ar-H), 805 (Ar-H).

Hedaya Benzo 15-Crown-5 Cyclobutene Diester Block



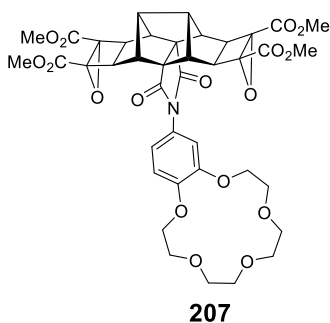
206

A solution of **197** (0.60 g, 1.22 mmol), DMAD (0.42 mL (0.48g), 3.42 mmol), and $[RuH_2(CO)(PPh_3)_3]$ (0.45 g, 0.48 mmol, 40 mol%) in toluene (10 mL) was heated under reflux for 48 hr under a nitrogen atmosphere. The reaction mixture was cooled to room temperature and the residual solvent was removed *in vacuo*.

Column chromatography (4-20% THF/CHCl₃) performed on the residue gave the cyclobutene adduct **206** as an orange/brown powder (0.63 g, 67 %). MP 120-123°C.

¹H NMR (600 MHz, CDCl₃) δ 6.90 (1H, d, J= 8.5 Hz), 6.69 (1H, dd, J=2.2, 8.5 Hz), 6.62 (1H, d, J= 2.2 Hz), 4.15-4.12 (4H, m), 3.88-3.90 (4H, m), 3.77 (12H, s), 3.74-3.73 (8H, m), 3.16-3.15 (4H, m), 3.12-3.11 (4H, m), 2.56-2.55 (2H, m); ¹³C NMR (150 MHz, CDCl₃) δ 173.5, 160.7, 149.7, 141.5, 124.8, 120.0, 113.7, 113.1, 71.2, 71.2, 70.6, 70.5, 69.4, 69.2, 68.06, 60.3, 53.6, 52.2, 44.9, 41.5. HRMS calcd for C₄₀H₄₁NO₁₅ 775.2476, found 775.2471 [M]⁺; IR (ATR) – 1709 (C=O), 1261 (Ar-O), 1204 (C-OCH₃), 1120 (C-O-C), 1058 (C-O).

Hedaya Benzo 15-Crown-5 Diepoxide Block

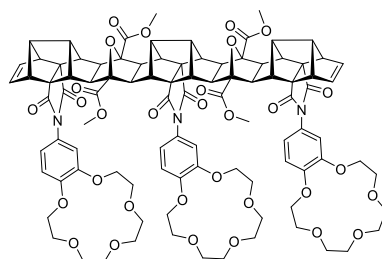


207

A solution of **206** (80 mg, 0.10 mmol) in THF (4 mL) was stirred under a blanket of N₂, cooled to -78°C, and anhydrous *tert*-butyl hydroperoxide in toluene (3.3 M, 87 μl, 2.9 mmol, 2.8 equiv.) was added. After stirring for 10 minutes, anhydrous MeLi in diethyl ether (1.6M, 3.1 mmol, 193 μl, 3 equiv.) was added and the solution stirred for 20 minutes, then warmed to RT over 1.5 hr. The mixture was diluted with DCM (10 mL) and sodium sulfite (10% aqueous solution, 2 mL) added with subsequent stirring for 30 minutes. The organic layer was separated, washed with water (2 x 5 mL), then dried (Na₂SO₄) and concentrated *in vacuo*. The product was obtained as a brown oil (59 mg, 70%), which was used without further purification.

¹H NMR (600 MHz, CDCl₃) δ 6.88 (1H, d, J= 8.5 Hz), 6.60 (1H, dd, J = 2.2, 8.5 Hz), 6.53 (1H, d, J= 2.2 Hz), 4.13-4.11 (4H, m), 3.90-3.89 (4H, m), 3.89 (12H, s), 3.73-3.75 (8H, m), 3.44-3.43 (4H, m), 3.02-3.01 (2H, m), 2.73-2.72 (4H, m); HRMS calcd for C₄₀H₄₁NO₁₇ 807.2374, found 807.2369 [M]⁺.

Tricrown A

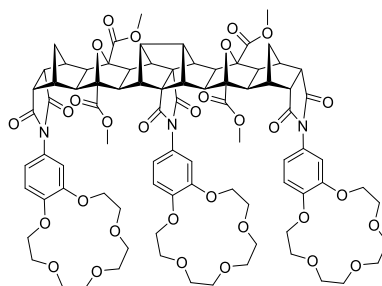


208

Compound **207** (32 mg, 0.04 mmol) and compound **197** (119 mg, 0.24 mmol) were dissolved in DCM (3 mL) and subjected to microwave irradiation (See General Procedure for microwave) for 1 hr. The solvent was removed *in vacuo* and the residue purified *via* column chromatography (4- 20% methanol/ CHCl_3) to afford **208** as a beige solid (17.4 mg, 24 %). MP dec $>225^\circ\text{C}$.

^1H NMR (600 MHz, CDCl_3) δ 6.89-6.85 (5H, m), 6.69 (2H, dd, $J = 1.98, 8.4$ Hz), 6.61 (2H, d, $J = 1.98$ Hz), 4.16-4.09 (12H, m), 3.89-3.86 (24H, m), 3.74-3.73 (24H, m) 3.30-3.29 (4H, m), 3.01- 2.98 (2H, m), 2.87-2.86 (2H, m), 2.81-2.82 (2H, m), 2.76- 2.75 (4H, m), 2.51-2.50 (4H, m), 2.41-2.39 (8H, m). ^{13}C NMR (150 MHz, CDCl_3) δ 173.7, 173.1, 167.7, 149.4, 149.0, 132.2, 132.1, 129.6, 128.5, 128.4, 124.8, 124.6, 119.8, 119.3, 113.5, 113.1, 90.8; HRMS calcd for $\text{C}_{96}\text{H}_{99}\text{N}_3\text{O}_{31}$ 1813.6219, found 1813.6194 $[\text{M}]^+$.

Tricrown B

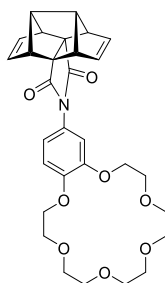


209

Compound **197** (20 mg, 0.02 mmol) and **205** (22 mg, 0.05 mmol) were dissolved in DCM (3 mL) and subjected to microwave irradiation (See General Procedure for microwave) for 1 hr. The solvent was removed *in vacuo* and the residue purified *via* column chromatography (4- 20% methanol/ CHCl_3) to afford **209** as a beige solid (12.5 mg, 30 %). MP dec $>225^\circ\text{C}$.

^1H NMR (600 MHz, CDCl_3) δ 6.89 (1H, d, $J = 8.4$ Hz), 6.85 (2H, d, $J = 8.4$ Hz), 6.71-6.70 (4H, m), 6.68-6.67 (1H, m), 6.66-6.64 (1H, m), 4.17-4.16 (2H, m), 4.15-4.14 (4H, m), 4.04-4.03 (4H, m), 4.02-4.00 (2H, m), 3.91-3.86 (16H, m), 3.80-3.73 (32H, m), 3.11 (4H, bs), 2.97-2.96 (2H, m), 2.67-2.66 (4H, m), 2.63 (2H, d, $J = 10.8$ Hz), 2.41 (4H, bs), 2.30 (4H, bs), 2.18 (4H, bs), 1.28 (2H, d, $J = 10.8$ Hz); ^{13}C NMR (150 MHz, CDCl_3) δ 176.0, 173.0, 167.6, 149.82, 149.80, 149.7, 149.5, 124.9, 124.8, 119.4, 119.0, 114.4, 114.3, 113.3, 112.6, 90.5, 71.3, 70.7, 70.3, 69.7, 69.5, 59.7, 56.0, 53.0, 50.0, 48.94, 48.91, 48.1, 41.8, 37.8; HRMS calcd. for $\text{C}_{86}\text{H}_{95}\text{N}_3\text{O}_{31}$, 1688.5847 found 1688.5843 $[\text{M}]^+$.

Hedaya Benzo-18-crown-6 Block

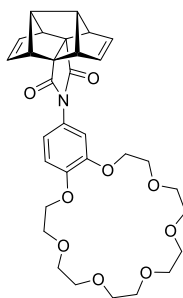


210a

Under N_2 , a solution of Hedaya anhydride **42** (0.80 g, 3.5 mmol) and 4-aminobenzo-18-crown-6 **200b** (1.72 g, 5.25 mmol) in glacial acetic acid (5 mL) was stirred under reflux for 24 hr. The reaction mixture was cooled to room temperature and the residual solvent was removed *in vacuo*. The residue was re-dissolved in CHCl_3 and washed with water (2 x 20 mL), dried (Na_2SO_4) and concentrated *in vacuo* to give a purple/brown mixture. Column chromatography (1:5 ethyl acetate / CHCl_3) performed on the residue gave a beige wax/oil (0.54 g, 28%).

^1H NMR (600 MHz, CDCl_3) δ 6.86 (1H, d, $J = 8.5$ Hz), 6.64 (1H, dd, $J = 2.3, 8.5$ Hz), 6.59 (1H, d, $J = 2.3$ Hz), 6.12-6.11 (4H, m), 4.13-4.12 (4H, m), 3.90-3.88 (4H, m), 3.75-3.74 (4H, m), 3.70-3.69 (4H, m), 3.69-3.68 (4H, m), 3.56-3.55 (4H, m), 2.93-2.92 (2H, m); ^{13}C NMR (150 MHz, CDCl_3) δ 174.9, 149.3, 149.1, 132.4, 125.4, 120.3, 114.2, 113.6, 71.0, 70.9, 70.8, 69.6, 69.4, 66.8, 64.6, 62.8; HRMS-ESI calcd for $\text{C}_{30}\text{H}_{33}\text{NO}_8\text{Na}$ 558.2104, found 558.2094 $[\text{M}+\text{Na}]^+$.

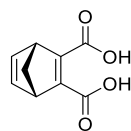
Hedaya Benzo-21-crown-7 Block



210b

Under N_2 , a solution of Hedaya anhydride **42** (1.0 g, 4.4 mmol) and 4-aminobenzo-21-crown-7 **200c** (2.4 g, 6.6 mmol) in glacial acetic acid (10 mL) was stirred under reflux conditions for 24 hr. The reaction mixture was cooled to room temperature and the residual solvent was removed *in vacuo*. The residue was redissolved in $CHCl_3$ and washed with water (2 x 20 mL), dried (Na_2SO_4) and concentrated *in vacuo* to give a purple/brown mixture. Column chromatography (1:5 ethyl acetate / $CHCl_3$) performed on the residue gave a beige wax/oil (0.52 g, 20 %).

1H NMR (600 MHz, $CDCl_3$) δ 6.86 (1H, d, $J = 8.5$ Hz), 6.63 (1H, dd, $J = 2.2, 8.5$ Hz), 6.58 (1H, d, $J = 2.2$ Hz), 6.11-6.10 (4H, m), 4.13-4.10 (4H, m), 3.90-3.87 (4H, m), 3.76-3.75 (4H, m), 3.71-3.70 (4H, m), 3.65-3.64 (8H, m), 3.55-3.54 (4H, m), 2.92-2.91 (2H, m); ^{13}C NMR (150 MHz, $CDCl_3$) δ 174.8, 149.1, 148.9, 132.6, 125.3, 120.3, 113.8, 113.6, 71.1, 70.6, 69.6, 66.7, 64.5, 64.0, 63.1, 62.7; HRMS calcd for $C_{32}H_{37}NO_9Na$ 602.2366, found 602.2366 $[M+Na]^+$.

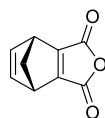
Norborna-2,5-diene-2,3-dicarboxylic Acid^[27]

220

Cyclopentadiene (1.85g, 28 mmol) was added dropwise to a stirring solution of acetylene dicarboxylic acid in 1,4-dioxane (10 mL). The reaction mixture was stirred under N_2 for 12 hr at RT. The solvent was removed *in vacuo* to afford a white solid, 5.02g, quantitative yield. MP 157 -159°C, lit. MP 158.2 – 159.2°C^[27].

^1H NMR (600 MHz, CDCl_3) δ 6.94 (2H, s), 4.21 (2H, s), 2.29 (1H, d, $J = 7.1$ Hz), 2.18 (1H, d, $J = 7.1$ Hz); ^{13}C NMR (150 MHz, CDCl_3) δ 167.1, 142.6, 73.2, 66.9, 54.3; HRMS calcd. for $\text{C}_9\text{H}_7\text{O}_4$, 179.0344 found 179.0337 $[\text{M}-\text{H}]^-$.

Norbornadiene-2,3-dicarboxylic Acid Anhydride^[28]

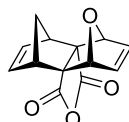


221

DCC (618 mg, 3 mmol) was dissolved in acetone (9 mL, anhyd.) under and Ar atmosphere. A solution of Norborna-2,5-diene-2,3-dicarboxylic acid (540 mg, 3 mmol) was added dropwise to the DCC solution with vigorous stirring until a white precipitate began to form. The mixture was continued to stir at RT overnight. The mixture was filtered and the filtrate concentrated *in vacuo* to afford a yellow oil which was purified *via* column chromatography (silica) with toluene as the eluent to afford pure product, 0.396 g, 80 % yield. MP 87-89°C lit. MP 86-89°C^[28].

^1H NMR (600 MHz, CDCl_3) δ 6.98 (2H, s), 4.0 (2H, s), 2.71 (2H, s); ^{13}C NMR (150 MHz, CDCl_3) δ 170.9, 159.6, 142.9, 78.3, 48.0; HRMS calcd. for $\text{C}_9\text{H}_7\text{O}_3$, 163.0390 found 163.0390 $[\text{M}+\text{H}]^+$.

Dimethyl bicyclo(2.2.1)-7-oxa-2,3-dien-2,3-dicarboxylic acid anhydride^[29]

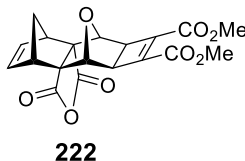


215

Norbornadiene-2,3-dicarboxylic acid anhydride (150 mg, 0.93 mmol) was dissolved in furan (7.5 mL, 0.1 mol) and stirred at RT for 24 hr under N_2 . The solvent was removed *in vacuo* and the residue purified *via* column chromatography (silica) with CHCl_3 as the eluent to afford white solid, 0.186 mg, 87 % yield. MP 145-148°C, lit. MP 146-147°C^[29].

^1H NMR (600 MHz, CDCl_3) δ 6.74-6.73 (2H, m), 6.51-6.50 (2H, m), 5.11-5.10 (2H, m), 3.32-3.33 (2H, m), 3.06 (1H, d, $J = 9.1$ Hz), 1.81 (1H, d, $J = 9.1$ Hz); ^{13}C NMR (150 MHz, CDCl_3) δ 170.5, 141.4, 139.9, 81.7, 72.2, 49.6, 46.7; HRMS calcd. for $\text{C}_{13}\text{H}_{10}\text{O}_4$, 230.0574 found 230.0574 $[\text{M}]^+$.

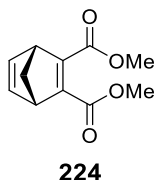
**Dimethyl bicyclo(2.2.1)-7-oxa-2,3-dien-2,3-dicarboxylic acid anhydride -
Cyclobutene**



A solution of **216** (180 mg, 0.78 mmol), $\text{RuH}_2(\text{CO})(\text{PPh}_3)_3$ (143 mg, 0.16 mmol) and DMAD (0.18 mL, 1.45 mmol, 1.8-2.0 equiv.) in toluene (4 mL) was heated at 50°C overnight. The reaction mixture was cooled, filtered (Whatman No° 1) and the solvent removed under reduced pressure. The crude material thus obtained was subject to column chromatography using 4-20% THF/ CHCl_3 as eluent to give **222**, 132 mg, 45% yield.

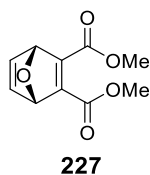
^1H NMR (600 MHz, CDCl_3) δ 6.41-6.42 (2H, m), 4.61-4.60 (2H, m), 3.77-3.76 (6H, bs), 3.35-3.34 (2H, bs), 3.24 (2H, bs), 2.93 (1H, d, $J = 9.3$ Hz), 1.58 (1H, d, $J = 9.3$ Hz); ^{13}C NMR (150 MHz, CDCl_3) δ 169.5, 160.2, 140.5, 139.2, 76.3, 70.9, 52.3, 49.4, 48.5, 45.4.

Norborna-2,5-diene-2,3-dicarboxylate ^[30]



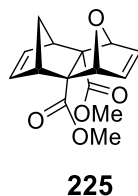
A solution of DMAD (2.8 mL, 22.7mmol) in DCM (40 mL) with freshly cracked cyclopentadiene (2 mL, 23.8 mmol) was stirred at RT for 24 h. The solvent was removed *in vacuo* and the resulting product used without further purification as viscous oil, 0.345 g, 73% yield.

^1H NMR (600 MHz, CDCl_3) δ 6.91-6.90 (2H, m), 3.93 (2H, m), 3.77 (6H, s), 2.28-2.27 (1H, m), 2.10-2.09 (1H, m) ; ^{13}C NMR (150 MHz, CDCl_3) δ 1165.6, 152.6, 142.5, 73.1, 53.6, 52.2 ; HRMS calcd for $\text{C}_{11}\text{H}_{12}\text{O}_4\text{Na}$ 231.0633, found 231.0636 $[\text{M}+\text{Na}]^+$.

7-oxanorborna-2,5-diene-2,3-dicarboxylate

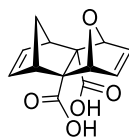
A solution of DMAD (1 mL, 8.16 mmol) in toluene (1 mL) and furan (0.9 mL, 12.24 mmol) was stirred at 80°C for 24 h in a sealed tube under an argon atmosphere. The solvent was removed *in vacuo*, and the resulting product was used without further purification as viscous oil, 1.2 g, 70% yield.

^1H NMR (600 MHz, CDCl_3) δ 7.22 (2H, s), 5.68 (2H, s), 3.82 (6H, s); ^{13}C NMR (150 MHz, CDCl_3) δ 163.4, 153.1, 143.4, 85.2, 52.5; HRMS calcd for $\text{C}_{10}\text{H}_{10}\text{O}_5\text{Na}$ 233.0426, found 233.0429 $[\text{M}+\text{Na}]^+$.

Dimethyl bicyclo(2.2.1)-7-oxa-2,3-dien-2,3-dicarboxylate^[31]

A solution of CPD (0.35 mL, 4.16 mmol) in CHCl_3 (1 mL) was added dropwise to **227** (0.88 g, 4.16 mmol) dissolved in CHCl_3 and the resulting solution stirred at RT for 48 hr under an argon atmosphere. The solvent was removed *in vacuo* and used without further purification, 1.07 g, 94% yield.

^1H NMR (600 MHz, CDCl_3) δ 6.60 (2H, s), 6.17 (2H, s), 4.58 (2H, s), 3.67 (6H, s), 3.18 (2H, s), 2.46 (1H, d, $J = 8.7$ Hz), 1.62 (1H, d, $J = 8.7$ Hz); ^{13}C NMR (150 MHz, CDCl_3) δ 173.8, 138.9, 136.0, 81.7, 69.2, 54.2, 52.3, 50.8; HRMS calcd. for $\text{C}_{15}\text{H}_{16}\text{O}_5\text{Na}$ 299.0895, found 299.0904 $[\text{M}+\text{Na}]^+$.

Dimethyl bicyclo(2.2.1)-7-oxa-2,3-dien-2,3-dicarboxylic acid**226**

A solution of NaOH (20 % in MeOH) was added to the diester **225** (0.5 g, 1.8 mmol) and the solution heated under reflux overnight. The solvent was removed *in vacuo* and the residue redissolved in ethyl acetate (10 mL) and washed with H₂O and brine. The solvent was dried (Na₂SO₄) and the solvent removed under reduced pressure to afford a white powder, 0.24g, 54% yield. MP 156-158°C.

¹H NMR (600 MHz, CDCl₃) δ 6.60 (2H, bs), 6.15 (2H, bs), 4.61 (2H, bs), 3.14 (2H, bs), 2.46 (1H, d, J = 8.64 Hz), 1.57 (1H, d, J = 8.64 Hz); ¹³C NMR (150 MHz, CDCl₃) δ 178.2, 140.4, 136.7, 82.9, 69.9, 54.2, 52.8; HRMS calcd. for C₁₃H₁₁O₅ 247.0606, found 247.0605 [M-H]⁻.

7.3 Analytical Procedures**EIS experimental (Jakob Andersson, Flinders University)**

All EIS measurements were carried out on an Autolab Impedance Spectrometer and all experimental data was modelled in Zview (published by Scribner Associates). The frequencies measured were between 100 kHz and 3 MHz. All introduced electrolyte concentrations (NaCl, KCl, LiCl, TMAC) were 100 mM unless otherwise specified. The crown ether compounds, Tricrown A, B and monomers were introduced into the system with an aliquot of 20 μl at a concentration of 6 mg/mL in acetonitrile unless otherwise stated. The initial monolayers were assembled by the insertion of ultraflat gold surface into a solution of 0.2 mM tethered-lipid in HPLC grade ethanol for 18-24 h. Bilayers were assembled by the introduction of 20 μL of 100 nM vesicles of phospholipids at a concentration of 2 mg/mL in MilliQ grade water incubated overnight at 25°C. Bilayers, with average area of 0.283 cm² were incubated with the corresponding Tricrown or monomer overnight.

Calcein Release Experimental (Phillip Gale, University of Southampton)

Fractional calcein release was monitored with 1-palmitoyl-2-oleoyl-sn-glycero-3-phosphocholine (POPC) vesicles over a period of 1 hour to 12 hours. The receptors were added as a solution in acetonitrile at $t = 0.5$ mins and the vesicles lysed with detergent at $t = 60.5$ mins to calibrate the experiment to 100% calcein release.

BLM Experimental (Derek Laver, University of Newcastle)

Tricrown A **208**, B **209** and monomers (**197**, **203**) (approx. 1mg) were prepared for BLM studies by the initial solubilisation in CHCl_3 . Before addition to the artificial lipid bilayers the 0.1 mL of the stock chloroform solutions were dried under a stream of nitrogen and diluted in acetonitrile (0.1 mL). Once the molecules were diluted 10 μL of these solutions were added to the *cis* or *trans* baths. The baths were stirred and a voltage applied until channel activity was evident. If no channel activity was observed *via* this method, the CHCl_3 stock solutions (20 μL) were directly added to the lipid mixture (100 μL in chloroform) before forming the bilayer, to improve solubility within the system.

endo-monomer and Hedaya Block NMR Titrations

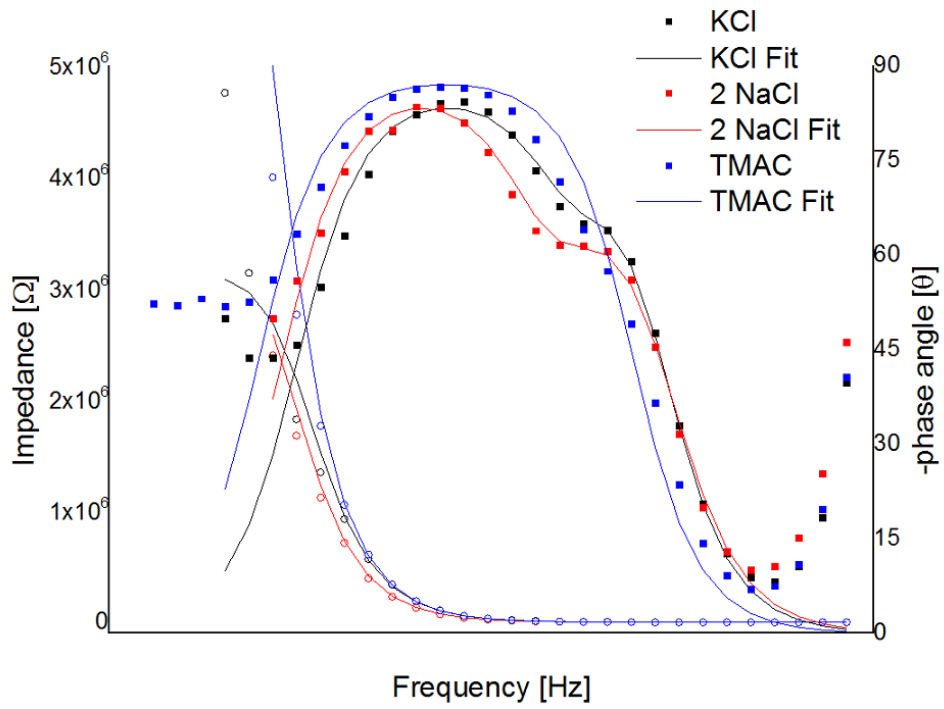
All titration experiments were run on a Bruker AV (III) 600 spectrometer at 600 MHz (^1H) using Topspin 3 software. All spectra were recorded at 293K, and in anhydrous acetonitrile, with reference insert of deuterated H_2O . Chemical shifts (δ) are reported as parts per million (ppm) and referenced to deuterated solvent peaks. Sodium and potassium salts (NaClO_4 , KSCN , KPF_6) were dissolved in anhydrous acetonitrile at a known concentration (1M unless otherwise stated). Crown ether compounds were dissolved in anhydrous acetonitrile at a known concentration (0.398M). Salt solutions were titrated against the crown solution, with each addition increasing the amount of alkali metal present. Binding constants were determined using the ^1H NMR data modelled using HYPNMR2008 by fitting appropriate models to the data.

REFERENCES

- [1] T. E. Lesslie, J. Bornstein, E. H. Huntress, *Org. Synth.* **1963**, *4*, 329–330.
- [2] N. Ahmad, J. J. Levison, S. D. Robinson, M. F. Uttley, *Inorg. Synth.* **1974**, *15*, 45–64.
- [3] D. D. Perrin, W. L. F. Armarego, D. R. Perrin, *Purification of Laboratory Chemicals*, Pergamon Press, Oxford, **1966**.
- [4] L. A. Paquette, M. J. Wyvratt, *J. Am. Chem. Soc.* **1974**, *96*, 4673–4674.
- [5] L. A. Paquette, M. J. Wyvratt, *J. Am. Chem. Soc.* **1974**, *42*, 4671–4673.
- [6] P. Camps, X. Pujol, S. Vázquez, *Org. Lett.* **2000**, *2*, 4225–4228.
- [7] X. Jiang, X. Yang, C. Zhao, L. Sun, *J. Phys. Org. Chem.* **2009**, *22*, 1–8.
- [8] I. M. Khalil, D. Barker, B. R. Copp, *J. Org. Chem.* **2016**, *81*, 282–289.
- [9] C. Fernández, O. Nieto, E. Rivas, G. Montenegro, J. a. Fontenla, A. Fernández-Mayoralas, *Carbohydr. Res.* **2000**, *327*, 353–365.
- [10] C. Detellier, H. D. H. Stover, *Synthesis (Stuttg.)* **1983**, 990–992.
- [11] S. Michaelis, S. Blechert, *Chem. Eur. J.* **2007**, *13*, 2358–2368.
- [12] M. Duque, C. Ma, E. Torres, J. Wang, L. Naesens, J. Juarez-Jimenez, P. Camps, F. Luque, W. DeGrado, R. Lamb, et al., *Med. Chem. (Los Angeles)* **2011**, *54*, 2646–2657.
- [13] M. Gul, N. Ocal, *Can. J. Chem.* **2010**, *88*, 323–330.
- [14] L. I. Kas'yan, I. N. Tarabara, Y. S. Bondarenko, S. V. Shishkina, O. V. Shishkin, V. I. Musatov, *Russ. J. Org. Chem.* **2005**, *41*, 1122–1131.
- [15] M. Chen, H. Chen, Y. Wang, H. Wang, Y. Nan, X. Zheng, R. Jiang, *Tetrahedron Asymmetry* **2011**, *22*, 4–7.
- [16] H. Iwagami, M. Yatagai, M. Nakazawa, H. Orita, T. Honda, Yutaka, Ohnuki, T. Yukawa, *Bull. Chem. Soc. Jpn.* **1991**, *64*, 175–182.
- [17] A. Tran, N. West, W. Britton, R. Payne, *ChemMedChem* **2012**, *7*, 1031–1043.
- [18] M. G. El-Ghazool, A. M. El-Lakany, M. I. Abour-Shoer, A. H. Aly, *Nat. Prod. Sci.* **2003**, *9*, 213–219.
- [19] V. Calderon, F. C. Garcia, J. L. De La Pena, E. M. Maya, J. M. Garcia, *J. Polym. Sci. Part A Polym. Chem.* **2006**, *44*, 4063–4075.
- [20] S. J. Howell, D. Philp, N. Spencer, *Tetrahedron* **2001**, *57*, 4945–4954.

- [21] M. Y. Ovchinnikov, D. V. Kazakov, S. L. Khursan, *Kinet. Catal.* **2012**, *53*, 42–53.
- [22] J. Małgorzata, L. Madej, *J. Chem. Eng. Data* **2010**, *55*, 1965–1970.
- [23] F. De Jong, D. N. Reinhoudt, A. Van Zon, G. J. Torny, E. M. Van de Vondervoort, *Recl. Trav. Chim. Pays-Bas* **1981**, *100*, 449–52.
- [24] C. Zhang, S. Li, J. Zhang, K. Zhu, N. Li, F. Huang, *Org. Lett.* **2007**, *9*, 5553–5556.
- [25] E. Zhang, Y. Liu, S. Dong, F. Su, Y. Jiang, *Huaxue Shiji* **1985**, *7*.
- [26] J. C. Lee, Synthesis of Novel Crown Ether Compounds and Ionomer Modification of Nafion, **1992**.
- [27] A. J. Lowe, G. a. Dyson, F. M. Pfeffer, *European J. Org. Chem.* **2008**, 1559–1567.
- [28] K. Maruyama, T. Hitoshi, S. Kawabata, *J. Org. Chem.* **1985**, *50*, 4742–4749.
- [29] P. D. Bartlett, G. L. Combs, A. X. T. Le, W. H. Watson, J. Galloy, M. Kimura, *J. Am. Chem. Soc.* **1982**, *104*, 3131–3138.
- [30] R. A. Valiulin, T. M. Arisco, A. G. Kutateladze, *J. Org. Chem.* **2013**, *78*, 2012–2025.
- [31] J. Hendrickson, V. Singh, *Tetrahedron Lett.* **1983**, *24*, 431–434.

APPENDIX



A.1 Bode plot of the bilayer recovery when TMAC is added to the tBLM with tricrown A.